

Reactions between nitrite and soil organic matter and their role in nitrogen trace gas emissions and nitrogen retention in soil

Jing Wei

Energie & Umwelt / Energy & Environment

Band / Volume 409

ISBN 978-3-95806-299-3

Forschungszentrum Jülich GmbH
Institut für Bio- und Geowissenschaften
Agrosphäre (IBG-3)

Reactions between nitrite and soil organic matter and their role in nitrogen trace gas emissions and nitrogen retention in soil

Jing Wei

Schriften des Forschungszentrums Jülich
Reihe Energie & Umwelt / Energy & Environment

Band / Volume 409

ISSN 1866-1793

ISBN 978-3-95806-299-3

Bibliografische Information der Deutschen Nationalbibliothek.
Die Deutsche Nationalbibliothek verzeichnet diese Publikation in der
Deutschen Nationalbibliografie; detaillierte Bibliografische Daten
sind im Internet über <http://dnb.d-nb.de> abrufbar.

Herausgeber und Vertrieb: Forschungszentrum Jülich GmbH
Zentralbibliothek, Verlag
52425 Jülich
Tel.: +49 2461 61-5368
Fax: +49 2461 61-6103
zb-publikation@fz-juelich.de
www.fz-juelich.de/zb

Umschlaggestaltung: Grafische Medien, Forschungszentrum Jülich GmbH

Druck: Grafische Medien, Forschungszentrum Jülich GmbH

Copyright: Forschungszentrum Jülich 2018

Schriften des Forschungszentrums Jülich
Reihe Energie & Umwelt / Energy & Environment, Band / Volume 409

D 5 (Diss., Bonn, Univ., 2018)

ISSN 1866-1793
ISBN 978-3-95806-299-3

Vollständig frei verfügbar über das Publikationsportal des Forschungszentrums Jülich (JuSER)
unter www.fz-juelich.de/zb/openaccess.



This is an Open Access publication distributed under the terms of the [Creative Commons Attribution License 4.0](https://creativecommons.org/licenses/by/4.0/), which permits unrestricted use, distribution, and reproduction in any medium, provided the original work is properly cited.

Acknowledgements

I would like to thank my supervisor Prof. Dr. Nicolas Brüggemann for all the kind support in the past years, I was inspired a lot by his patience, intelligence, and open-mindedness when working together with him. I am also very grateful to Prof. Dr. Harry Vereecken for such a great experience to work in IBG-3, and for all the nice discussions in my PhD reports. In addition, I would like to express my sincere gratitude to Prof. Dr. Wulf Amelung for being my second supervisor and offering constructive suggestions for my work. I am especially thankful to Dr. Wolfgang Tappe for the assistance in sterilization, to Holger Wissel for the support in analytical measurement, to Dr. Rüdiger Reichel and Muhammad Saiful Islam for their kind cooperation, to Maria Quade for helping to translate the abstract into German, to Dr. Kathrina Prost and all the other helpful colleagues for the happy moments together.

Furthermore, my thanks to Dr. Joachim Mohn and Prof. Dr. Heike Knicker for hosting me to work at EMPA, Switzerland and IRNAS, Spain, respectively, during my abroad stay. I got very promising results under their kind supervision, and enjoyed the life in Dübendorf and Seville with the kind accompany of the colleagues there.

I am very thankful to my family and my friends for their immense love and support. Finally, thanks a lot to the Chinese Education Ministry and Chinese Scholarship Council for financing my living in the last years.

Abstract

As a key intermediate of both nitrification and denitrification, nitrite (NO_2^-) is highly chemically reactive to soil organic matter (SOM), and it was proved previously that considerable amounts of nitrogen (N) trace gases, including nitrous oxide (N_2O) and nitrogen oxides (NO_x), were produced from the reactions of NO_2^- with SOM in chemical assays decades ago. However, the role of NO_2^- –SOM reactions in nitrogen trace gas emissions and nitrogen retention in soils has been neglected until recently. It is vital to identify and quantify major sources and sinks of nitrogen trace gases for the sake of the environment. On the other hand, better understanding of N_2O sources and nitrogen retention is also essential to improve the nitrogen use efficiency and soil fertility in agriculture. Therefore, this thesis aimed to gain a better understanding of the contribution of NO_2^- –SOM reactions to nitrogen trace gas emissions and nitrogen retention in soil.

Emissions of N_2O and carbon dioxide (CO_2) from the reactions of NO_2^- with lignin and lignin derivatives (4-hydroxybenzoic acid, 4-hydroxybenzaldehyde, 4-hydroxy-3-methoxybenzoic acid, 4-hydroxy-3-methoxybenzaldehyde, 4-hydroxy-3,5-dimethoxybenzoic acid, 4-hydroxy-3,5-dimethoxybenzaldehyde), as well as N_2O isotopic signatures, were studied in chemical assays at pH 3–6. Among the six tested lignin derivatives, the highest N_2O emission was found in the 4-hydroxy-3,5-dimethoxybenzaldehyde treatment, and the dependency of N_2O and CO_2 on pH varied according to the structures of the organic substances. Most interestingly, N_2O ^{15}N site preference (SP) varied largely from 11.9–37.4 ‰ depending on pH and structures of lignin derivatives, which was undistinguishable from other N_2O sources, such as nitrification, denitrification, and abiotic hydroxylamine oxidation. Furthermore, real-time N_2O isotopic characterization revealed that SP also shifted largely during the reaction of NO_2^- with lignin derivatives. Hyponitrous acid and nitramide pathways, which could be responsible for N_2O formation, were proposed to explain the shift of N_2O SP values.

Nitrite-driven N_2O and NO_x emissions in spruce forest soils and SOM fractions were investigated online and simultaneously with a quantum cascade laser and a chemoluminescence analyzer, respectively. 17–52 % and 3.3–7.1 % of NO_2^- was immediately transformed to NO_x and N_2O , respectively, when NO_2^- was applied into soils. Abiotic N_2O sources contributed 19.5–42.3 % of the total N_2O emission, and among four SOM fractions (dissolved organic matter, fulvic acid, humic acid, and humin), fulvic acid accounted for most of the abiotic N_2O emission from NO_2^- –SOM reactions. Since the SP values of N_2O from NO_2^- –SOM reactions were not distinguishable from that of microbial sources (denitrification and fungal denitrification for this experiment), end-member maps failed to distinguish abiotic from biotic N_2O sources, and application of a two-end-member mixing model

biased N₂O source apportioning by overestimating the contributions of both bacterial and fungal denitrification.

Nitrogen retention resulting from NO₂⁻-SOM reactions was investigated in forest, grassland, and agricultural soils using ¹⁵N-NO₂⁻, and about 6 % of ¹⁵N-NO₂⁻ was immobilized by SOM within 4 d. ¹⁵N enrichment in the fulvic acid fraction was dramatically higher compared with the humus. Solid-state CP/MAS-¹⁵N-NMR analysis revealed that nitro- and amide-N were the dominant products of abiotic N immobilization from NO₂⁻-SOM reactions.

The effect of lignin content and composition on N₂O emission, N retention, and mineral N pool dynamics were studied in agricultural soil after the application of organic soil amendments and ¹⁵N-labelled ammonium in a 114-d laboratory incubation experiment. Both N retention and N₂O emission were dramatically promoted by the combined application of N fertilizer and organic substances in the order: wheat straw > spruce sawdust > lignin. Moreover, both N retention and mineral N content were significantly ($P < 0.05$) correlated with lignin composition. For the first time, it was found that lignin composition regulated N partitioning of fertilizer in soil.

Finally, an open pump theory was suggested to explain the combined and cross-interacting biotic-abiotic interactions of carbon and nitrogen in soil. This theory suggests that NO₂⁻-SOM reactions could be a significant source of N trace gas emissions and N retention in soils. Notably, neither SP of N₂O generated nor N immobilized by NO₂⁻-SOM reactions is significantly distinct from biotic pathways, which makes it difficult to distinguish biotic and abiotic N₂O production and N retention pathways. Further research is needed to identify and quantify the contribution of abiotic processes to soil N cycling.

Zusammenfassung

Nitrit (NO_2^-) ist ein wichtiges Glied in der Nitrifikations- und Denitrifikationskette und verhält sich bei Kontakt mit den organischen Substanzen des Bodens (soil organic matter, SOM) hochreaktiv. Studien haben belegt, dass bedeutende Mengen von Stickstoffspurengasen wie Lachgas (N_2O) und andere Stickoxide (NO_x) aus den Reaktionen von Nitrit mit SOM hervorgehen. Dennoch wurde bisher die Rolle der NO_2^- -SOM Reaktionen in Bezug auf Stickstoffspurengas-Emissionen und die Retention von Stickstoff im Boden vernachlässigt. Jedoch ist es einerseits zum Schutz der Umwelt wichtig, die Hauptquellen und -senken von Stickstoffspurengasen zu identifizieren, und andererseits ist ein besseres Verständnis der N_2O -Quellen und der Stickstoff-Retention essentiell, um die Nutzungseffizienz von Stickstoff und stickstoffbasierten Bodendüngern in der Landwirtschaft zu verbessern. Das Ziel der vorliegenden Doktorarbeit war daher, zu einem besseren Verständnis der NO_2^- -SOM-Reaktionen und der Stickstoff-Retention im Boden zu erlangen.

Die Emissionen von N_2O und Kohlenstoffdioxid (CO_2), die bei der Reaktionen von Nitrit mit Lignin und Lignin-Derivaten (4-Hydroxybenzoesäure, 4-Hydroxy-3-methoxybenzoesäure, 4-Hydroxy-3-methoxybenzaldehyd, 4-Hydroxy-3,5-dimethoxybenzoesäure, 4-Hydroxy-3,5-dimethoxybenzaldehyd) auftreten, sowie die N_2O -Isotopenzusammensetzungen, wurden in einem pH-Wertbereich von 3 bis 6 untersucht. Unter den sechs getesteten Lignin-Derivaten wurde die höchste N_2O -Emission bei Reaktionen von Nitrit mit 4-Hydroxy-3,5-dimethoxybenzaldehyd gefunden. Die Beziehung zwischen N_2O und CO_2 und dem pH-Wert variierte je nach Struktur der organischen Substanzen. Interessanterweise zeigte sich in Abhängigkeit vom pH-Wert und der Struktur der Lignin-Derivate eine starke Variabilität der ^{15}N -Positionspräferenz im N_2O -Molekül (^{15}N site preference, SP) im Bereich von 11.9–37.4 ‰, welcher nicht unterscheidbar von anderen N_2O -Quellen wie Nitrifikation, Denitrifikation und der abiotische Hydroxylaminoxidation war. Außerdem offenbarte die Echtzeit- N_2O -Isotopen-Charakterisierung eine starke Verschiebung der SP während der Reaktion von NO_2^- mit den Lignin-Derivaten. Eine potentielle Ursache für diese Verschiebung könnten die unterschiedlichen chemischen Reaktionswege entweder über hyposalpetrige Säure oder Nitrylamid sein. Beides sind chemische Verbindungen, die einen wichtigen Anteil an der Bildung von N_2O haben.

Durch Nitrit verursachte N_2O - und NO_x -Emissionen in Fichtenwaldböden und deren SOM-Fractionen wurden online und simultan mit einem Quantenkaskadenlaser-Analysator und einem Chemilumineszenz-Analysator untersucht. 17–52 % und 3.3–7.1 % des Nitrits wurden nach Applikation von Nitrit in den Boden sofort in N_2O und NO_x umgewandelt. Abiotische N_2O -Quellen machten 19.5–42.3 % der totalen N_2O -Emissionen aus, und von den vier getesteten SOM-Fractionen (gelöste organische Substanz, Fulvinsäure, Huminsäure und Humin) verursachte Fulvinsäure die

höchsten abiotischen N_2O Emissionen. Die SP-Werte von in NO_2^- -SOM Reaktionen gebildetem N_2O ließen sich nicht von den mikrobiellen Quellen (Denitrifikation und pilzliche Denitrifikation) unterscheiden. Die Einordnung der gemessenen SP-Werte in Endglied-Darstellungen lieferten keine aussagekräftigen Resultate bei der Unterscheidung zwischen abiotischen und biotischen N_2O -Quellen. Die Anwendung eines Mischungsmodells mit zwei Endgliedern lieferte eine verfälschte Zuordnung der N_2O -Quellen durch eine Überschätzung des Beitrags sowohl der bakteriellen als auch der pilzlichen Denitrifikation.

Stickstoff-Retention infolge von NO_2^- -SOM Reaktionen wurde in Wald-, Grasland- und landwirtschaftlichen Böden unter Verwendung von ^{15}N - NO_2^- untersucht. Ungefähr 6% des applizierten ^{15}N - NO_2^- waren nach vier Tagen durch SOM immobilisiert. Die ^{15}N -Anreicherung in der Fulvinsäure-Fraktion war deutlich höher als in der Humus-Fraktion. Eine CP/MAS- ^{15}N -NMR Analyse zeigte, das Nitro- und Amid-N die vorherrschenden Produkte der abiotischen N-Immobilisierung durch NO_2^- -SOM-Reaktionen waren.

Der Einfluss von Ligningehalt und -zusammensetzung auf N_2O -Emissionen, N-Retention und mineralische N-Pool-Dynamik wurde in landwirtschaftlichen Böden untersucht. In einem 114-tägigen Bodeninkubationsexperiment wurden organische Bodenzusatzstoffe und ^{15}N -markiertes Ammonium appliziert. Sowohl die N-Retention als auch N_2O -Emissionen wurden deutlich durch die kombinierte Applikation von N Dünger und organischer Substanzen gefördert, wobei deren Wirkung in der Reihenfolge Weizenstroh > Fichtensägemehl > Lignin abnahm. Außerdem korrelierten die N-Retention und der mineralische N-Gehalt des Bodens signifikant ($P < 0.05$) mit der Ligninzusammensetzung.

Abschließend wurde eine Open-Pump-Theorie zur Erklärung der kombinierten und kreuzinteragierenden biotisch-abiotischen Wechselwirkungen von Kohlenstoff und Stickstoff entwickelt. Diese Theorie nimmt an, das NO_2^- -SOM-Reaktionen eine signifikante Quelle für Stickstoffspurengas-Emissionen und N-Retention in Böden sein könnten. Weder die SP-Werte von N_2O noch immobilisiertes N infolge von NO_2^- -SOM-Reaktionen unterscheiden sich von biotischen Reaktionspfaden, was eine Unterscheidung zwischen biotischer und abiotischer N_2O -Produktion und N-Retention unmöglich macht. Weitere Untersuchungen sind notwendig, um den Beitrag der abiotischen Prozesse im N-Kreislauf zu identifizieren und zu quantifizieren.

Contents

Acknowledgements	I
Abstract	II
Zusammenfassung.....	IV
Contents	VI
List of figures	X
List of tables.....	XVIII
List of abbreviations	XX
I.Introduction.....	1
I.1 Rationale and state-of-the-art.....	2
I.2 Objectives and outline of the thesis	4
II.Large variability of CO ₂ and N ₂ O emissions and of ¹⁵ N site preference of N ₂ O from reactions of nitrite with lignin and its derivatives at different pH	7
II.1 Introduction.....	8
II.2 Material and Methods.....	9
II.2.1 Chemicals.....	9
II.2.2 Quantification of N ₂ O and CO ₂ emissions	10
II.2.3 Analysis of N ₂ O isotopic signatures	10
II.2.4 Statistical analysis.....	11
II.3 Results	12
II.3.1 Response surfaces of N ₂ O and CO ₂ emissions.....	12
II.3.2 N ₂ O isotopic signatures	15
II.4 Discussion	16
II.4.1 Mechanisms involved in chemodenitrification	16
II.4.2 N ₂ O isotopic signatures	20
II.5 Conclusions.....	22
III.First real-time isotopic characterization of N ₂ O from chemodenitrification	24
III.1 Introduction.....	25
III.2 Materials and Methods	27
III.2.1 Laser spectroscopic analysis of N ₂ O isotopic composition.....	27
III.2.2 Experimental setup	27
III.2.3 Experimental procedure.....	28
III.2.4 Data analysis.....	29
III.3 Results	30
III.3.1 N ₂ O emissions and isotopic composition from reactions of NO ₂ ⁻ with lignin derivatives ..	30
III.3.2 N ₂ O emissions and isotopic signature from NO ₂ ⁻ reactions with soil	34

III.4 Discussion	34
III.4.1 Pathways of N ₂ O formation and impact on N ₂ O production rate	34
III.4.2 Differences in ¹⁵ N SP of N ₂ O depending on reaction conditions	36
III.4.3 Nitrite-related N ₂ O formation in soil	38
III.4.4 The application of N ₂ O isotopic species in source partitioning	39
III.5 Conclusions	40
IV. N ₂ O and NO _x emissions by reactions of nitrite with soil organic matter of a Norway spruce forest	42
IV.1 Introduction	43
IV.2 Materials and methods	45
IV.2.1 Soil sampling and analysis	45
IV.2.2 Soil organic matter fractionation	46
IV.2.3 NO _x and N ₂ O emissions	46
IV.2.4 Isotopic N ₂ O analysis	47
IV.2.5 Statistical analysis	47
IV.3 Results and discussion	48
IV.3.1 Soil NO _x and N ₂ O emissions	48
IV.3.2 NO _x and N ₂ O emissions from SOM fractions	59
IV.4 Conclusions	61
V. Abiotic nitrite retention in soils revealed by solid-state ¹⁵ N-NMR structure analysis	62
V.1 Introduction	63
V.2 Materials and Methods	64
V.2.1 Soils	64
V.2.2 Abiotic nitrite retention in soils	64
V.2.3 Solid-state ¹⁵ N-NMR spectroscopy	65
V.2.4 Statistical analysis	65
V.3 Results and discussion	66
V.3.1 Abiotic retention of NO ₂ ⁻	66
V.3.2 Structure of immobilized N	67
V.4 Conclusions	71
VI. Effect of lignin content and composition of organic soil amendments on nitrogen partitioning in agricultural soil	72
VI.1 Introduction	73
VI.2 Materials and Methods	74
VI.2.1 Materials	74
VI.2.2 Experimental setup	74
VI.2.3 Gas sampling and analysis	75
VI.2.4 Soil sampling and analysis	76
VI.2.5 Statistical analysis	77

VI.3 Results	77
VI.3.1 Soil N ₂ O and CO ₂ emissions.....	77
VI.3.2. Nitrogen partitioning in soils.....	78
VI.3.3 Influence of lignin content and composition on decomposition of OSA	81
VI.4 Discussion.....	83
VI.4.1 Transformation of fertilizer-N in soils	83
VI.4.2 Effect of lignin content and composition on N ₂ O emission	85
VI.4.3 Effect of lignin content and composition on mineral N content and N retention	86
VI.5 Conclusions	89
VII.Open-pump theory of biotic–abiotic C–N interactions in soil	90
VII.1 Introduction	91
VII.2 Soil N pump	92
VII.2.1 Drivers of the soil N pump	93
VII.2.2 Reactive N intermediates in the soil	95
VII.3 Soil C pump.....	98
VII.3.1 Drivers of the soil C pump	98
VII.3.2 Reactive C intermediates in soil	100
VII.3.3 Free organic radicals	100
VII.4 Role of abiotic C–N interactions in N trace gas formation and N retention	102
VII.4.1 N ₂ O and NO _x emissions	102
VII.4.2 Nitrogen retention	104
VII.5 Conclusions	105
VIII.Synopsis.....	106
VIII.1 Summary	107
VIII.2 Synthesis.....	109
VIII.2.1 N ₂ O emission and N ₂ O isotopic signatures	109
VIII.2.2 N sequestration.....	109
VIII.2.3 Role of lignin in N cycling	110
VIII.3 Perspectives	110
IX.Appendix	112
Appendix A: supplementary information for chapter II	113
Appendix B: supplementary information for chapter III	122
Methods	122
Results	122
Appendix C: supplementary information for chapter IV	131
CO ₂ emission.....	131
NO _x and N ₂ O emission	131
Appendix D: supplementary information for chapter VI.....	137

References 142

List of figures

- Fig. II.1.** Response surface plots of N₂O emission from the reaction of nitrite with lignin and lignin derivatives in dependence on pH and nitrite concentration. Red circle represents the measured value in each treatment.....13
- Fig. II.2.** Response surface plots of CO₂ emission from the reaction of nitrite with lignin and lignin derivatives in dependence on pH and nitrite concentration. Red circle represents the measured value in each treatment.....14
- Fig. II.3.** ¹⁵N site preference of N₂O from the reactions of nitrite with lignin and lignin derivatives at different pH (a) and nitrite concentrations (b). Each point is the mean value of three replicates. Capital letters represent significant differences (*P* < 0.05) between different pH and nitrite concentrations according to one-way ANOVA.....16
- Fig. II.4.** End-member maps of SP vs $\delta^{15}\text{N}^{\text{bulk}}$ (a) and $\delta^{18}\text{O}$ (b). The area in the dashed line represents chemodenitrification (SP values of 10 to 37 ‰, $\delta^{15}\text{N}^{\text{bulk}}$ values of -34 to -3 ‰, and $\delta^{18}\text{O}$ values of 13 to 35 ‰, data in this study and previously reported chemical assays) (Jones et al., 2015; Toyoda et al., 2005; Wei et al., 2017a). Nitrification is represented by SP values of 27 to 37 ‰, $\delta^{15}\text{N}^{\text{bulk}}$ values of -61 to -40 ‰, and $\delta^{18}\text{O}$ values of 40 to 50 ‰ (Sutka et al., 2006), fungal denitrification by SP values of 34 to 40 ‰, $\delta^{15}\text{N}^{\text{bulk}}$ values of -34 to -21.9 ‰, and $\delta^{18}\text{O}$ values of 30 to 40 ‰ (Sutka et al., 2008), bacterial denitrification by SP values of -11 to 1.4 ‰, $\delta^{15}\text{N}^{\text{bulk}}$ values of -34.8 to -8.8 ‰, and $\delta^{18}\text{O}$ values of 10 to 20 ‰ (Toyoda et al., 2005; Zou et al., 2014), and nitrifier denitrification by SP values of -13.6 to -5 ‰ and $\delta^{15}\text{N}^{\text{bulk}}$ values of -73 to -35 ‰ (Sutka et al., 2003). Black square, organosolv lignin; gray triangle, alkali lignin; blue symbols, H units; pink symbols, G units; violet symbols, S units; solid circles, acids; solid stars, aldehydes.....21
- Fig. III.1.** Schematic diagram of the setup used for real-time measurement of N₂O isotopic species by QCLAS.....31
- Fig. III.2.** Reaction of NO₂⁻ with organosolv lignin. (a) N₂O mixing ratio, (b) $\delta^{15}\text{N}^{\alpha}$, $\delta^{15}\text{N}^{\beta}$, and $\delta^{15}\text{N}^{\text{bulk}}$ of N₂O, (c) $\delta^{18}\text{O}$ of N₂O, and (d) N₂O ¹⁵N site preference.....32
- Fig. III.3.** Reaction of NO₂⁻ with 4-hydroxy-3,5-dimethoxybenzoic acid. (a) N₂O mixing ratio, (b) $\delta^{15}\text{N}^{\alpha}$, $\delta^{15}\text{N}^{\beta}$, and $\delta^{15}\text{N}^{\text{bulk}}$ of N₂O, (c) $\delta^{18}\text{O}$ of N₂O, and (d) N₂O ¹⁵N site preference.....32
- Fig. III.4.** Reaction of NO₂⁻ with 4-hydroxy-3,5-dimethoxybenzaldehyde. (a) N₂O mixing ratio, (b)

$\delta^{15}\text{N}^\alpha$, $\delta^{15}\text{N}^\beta$, and $\delta^{15}\text{N}^{\text{bulk}}$ of N_2O , (c) $\delta^{18}\text{O}$ of N_2O , and (d) N_2O ^{15}N site preference33

Fig. III.5. N_2O emission and its isotopic composition in grassland soil after NO_2^- application. (a) N_2O mixing ratio, (b) $\delta^{15}\text{N}^\alpha$, $\delta^{15}\text{N}^\beta$, and $\delta^{15}\text{N}^{\text{bulk}}$ of N_2O , (c) $\delta^{18}\text{O}$, and (d) N_2O site preference.....34

Fig. III.6. Proposed hyponitrous acid pathway (a) and nitramide pathway (b) of N_2O formation in the reactions of NO_2^- with lignin products. The reaction with 4-hydroxybenzoic acid is taken as an example.....35

Fig. III.7. Three dimensional end-member map of SP vs. $\delta^{15}\text{N}^{\text{bulk}}$, $\delta^{18}\text{O}$. Pink asterisks represent N_2O from chemical NO_2^- reduction by Fe^{2+} (Jones et al., 2015); black circles represent N_2O from the reaction of NO_2^- with trimethylamine-borane and hydroxylamine (Toyoda et al., 2005); blue triangles are delta values of N_2O from reactions of NO_2^- with lignin products at pH 3–5 for 24 h (Wei et al., 2017b); cyan squares denote N_2O isotope deltas measured in this study.....40

Fig. IV.1. Cumulative NO_x emission from unsterilized soil (a), sterilized soil (b), and NO emission from SOM fractions (c) after application of NO_2^- . DOM, dissolved organic matter fraction; FA, fulvic acid fraction; HA, humic acid fraction; HN, humin fraction. Lines are the fitting results of the Hill equation; each point is the mean value of three replicates; residues are the differences between the true values and calculated values.....50

Fig. IV.2. Paired t -test of NO_x emission (a), N_2O emission (b), initial NO_x emission rate (c), initial N_2O emission rate (d), NO/NO_x (e), and S/U (f). The box indicates the range of the 25 and 75 percentiles of the data, the line in the box is the median, and the notch lines indicate the 1.5 interquartile range. Each point is the mean value of three replicate, t and P values represent the results of a paired t -test. R_{NO_x} , initial NO_x emission rate, calculated by half of $\text{NO}_{x\text{max}}$ divided by $t_{1/2}$; $R_{\text{N}_2\text{O}}$, initial N_2O emission rate, calculated by half of $\text{N}_2\text{O}_{\text{max}}$ divided by $t_{1/2}$; S/U , the ratio of $\text{NO}_{x\text{max}}$ or $\text{N}_2\text{O}_{\text{max}}$ of sterilized soil to that of unsterilized soil; NO/NO_x , the proportion of NO in NO_x51

Fig. IV.3. Cumulative N_2O emission from unsterilized soil (a), sterilized soil (b), and SOM fractions (c) after NO_2^- application. DOM, dissolved organic matter fraction; FA, fulvic acid fraction; HA, humic acid fraction; HN, humin fraction. Lines are the fitting results of the Hill equation; each point is the mean value of three replicates; residues are the differences between the true values and calculated values.....52

Fig. IV.4. Paired t -test of isotope signatures of N_2O between sterilized and unsterilized soil. The box indicates the range of the 25 to 75 percentiles of the data, the line in the box indicates the median value, and the notch lines indicate the 1.5 interquartile range; t and P values represent the results of

a paired *t*-test. $\Delta^{15}\text{N}$ is the ^{15}N isotopic difference between the applied nitrite and the $\delta^{15}\text{N}^{\text{bulk}}$ of the N_2O produced; $\delta^{15}\text{N}^{\alpha}$ and $\delta^{15}\text{N}^{\beta}$ are the $\delta^{15}\text{N}$ values at the central and terminal position of N_2O , respectively; $\delta^{18}\text{O}$ is the ^{18}O isotopic signature of the N_2O produced, and SP is the ^{15}N site preference ($\text{SP} \equiv \delta^{15}\text{N}^{\alpha} - \delta^{15}\text{N}^{\beta}$).....54

Fig. IV.5. End-member map of SP vs. $\delta^{15}\text{N}^{\text{bulk}}\text{-N}_2\text{O}$ (a) and $\delta^{18}\text{O}\text{-N}_2\text{O}$ (b), and contribution of abiotic N_2O production (AB), fungal denitrification (FD) and denitrification (DN) to N_2O production calculated with a two-end-member mixing model (c). The left bars in (c) show the contribution of FD and DN when AB is neglected, while the right bars represent the relative contribution of all three sources.....56

Fig. IV.6. Redundancy analysis (RDA) based on total N_2O and NO_x emission, and characteristics of sterilized and unsterilized soils. TOC, total organic carbon; TN, total nitrogen; P, phosphate; G, guaiacyl units of lignin; S, syringyl units of lignin; H, *p*-hydroxyphenyl units of lignin; (Ad/Al)_G, acid-to-aldehyde ratio of vanillyl units; (Ad/Al)_S, acid-to-aldehyde ratio of syringyl units. (Ad/Al)_G and (Ad/Al)_S are indicators of the degree of lignin degradation.....58

Fig. V.1. Abiotic N retention of nitrite in agricultural, forest, and grassland soil (a) and $\delta^{15}\text{N}$ values of soil, fulvic acid, and humus in $^{15}\text{NO}_2^-$ amended soils (b). Stars indicate the $\delta^{15}\text{N}$ value is significantly ($P < 0.05$) different from the soil before HF treatment.....67

Fig. V.2. Solid-state CP/MAS ^{15}N -NMR spectra of forest humus (FOM) with or without $^{15}\text{NO}_2^-$ amendment under sterilized conditions. * signifies spinning side band.....69

Fig. V.3. Solid-state ^{15}N -NMR spectra of grassland humus (GOM), GOM amended with $^{15}\text{NO}_2^-$ and microbes (GOM+ NO_2^- +M), and GOM amended with $^{15}\text{NO}_2^-$ under sterilized conditions (GOM+ NO_2^-).....70

Fig. VI.1. Total CO_2 flux (a), total N_2O flux (b), fertilizer-derived N_2O flux (c), and contribution of fertilizer- N_2O to total N_2O flux (d). Nitrogen fertilizer was applied at day 0.....78

Fig. VI.2. Total and fertilizer-derived NH_4^+ (a-c) and NO_3^- (d-f), and N retention in the form of soil organic nitrogen (SON) (g) in different treatments during the experiment. Nitrogen fertilizer was applied at day 0.....79

Fig. VI.3. Nitrogen partitioning in wheat amended soils (black stars), spruce amended soils (down triangles), lignin amended soils (up triangles), and fertilizer control (circles). X, Y, and Z axis denotes N retention, the contribution of fertilizer-derived N_2O to total N_2O , and the proportion of mineral N

(NH ₄ ⁺ + NO ₃ ⁻) in total fertilizer-N, respectively.....	81
Fig. VI.4. Dependency of organic soil amendments (OSA) decomposition on lignin G unit (a), H unit (b), and S unit (c) (n = 36), and the lignin patterns of soils with the application of spruce sawdust, wheat straw, or alkali lignin (d).....	82
Fig. VI.5. Redundancy analysis (RDA) to explain the regulations of total lignin, lignin G/S/H units, nitrite, soil pH, and organic soil amendment (OSA) decomposition on fertilizer-N partitioning into ammonium, nitrate, soil organic nitrogen (SON), and N ₂ O. Circles, up triangles, down triangles, and stars represent fertilizer control, soil + lignin + fertilizer, soil + spruce + fertilizer, and soil + wheat + fertilizer treatments, respectively.....	84
Fig. VI.6. Correlations between lignin composition and immobilized fertilizer-N (n = 36) in SON (a–c), and immobilized fertilizer-N in organic soil amendment (OSA) (e–f).....	88
Fig. VII.1. Open pump theory of combined abiotic and biotic C–N interactions in soils. N pump refers to biological N transformation driven by N fixers, nitrifiers, denitrifiers, ammonifiers, and N assimilating plants and microbes, while C pump to the synthesis and decomposition of organic carbon driven by autotrophs and heterotrophs.....	92
Fig. VII.2 Biotic drivers and reactive nitrogen intermediates from N pump. AOB, Ammonium oxidizing bacteria; AOA, ammonia-oxidizing archaea; NOB, NO ₂ ⁻ -oxidizing bacteria; anammox, anaerobic ammonium oxidation; DNRA, dissimilatory NO ₂ ⁻ reduction to NH ₄ ⁺ ; BON, biological organic carbon in organisms; SON, soil organic nitrogen; DON, dissolved organic nitrogen.....	94
Fig. VII.3 Drivers of the C pump and C intermediates released. BOC, biologic organic carbon; SOC, soil organic carbon; DOC, dissolved organic carbon.....	98
Fig. VII.4 The structure of lignin with guaiacyl (G), syringyl (S), and <i>p</i> -hydroxyphenyl (H) units.....	99
Fig. VII.5 The M–OC wheel hypothesis, explaining the combined biotic and abiotic production of nitrogenous gases and soil organic nitrogen. Gray dot lines indicate abiotic reactions; M–OC, the complex of metal and organic radicals; SOM, soil organic matter; SON, soil organic nitrogen.....	101
Fig. A1. The structures of lignin and lignin derivatives.....	113
Fig. A2. N ₂ O and CO ₂ emissions from the reaction of 0.01 g organosolv lignin and 5 ml of 0.5 mM	

NO₂⁻ solution in water for 24 h. For sterilized treatment, the vials were sterilized at 170 °C for 6 h in an oven, and nitrite solution was sterilized by passing through a 0.2 μm filter. There was no significant difference ($P > 0.05$) between sterilized and unsterilized treatments.....114

Fig. A3. Linear regression of $\Delta^{15}\text{N}^{\text{bulk}}$ with $\delta^{15}\text{N}^{\alpha}$ and $\delta^{15}\text{N}^{\beta}$ (a), $\delta^{15}\text{N}^{\alpha}$ with site preference and $\delta^{15}\text{N}^{\beta}$ (b), and $\delta^{15}\text{N}^{\alpha}$ with $\delta^{15}\text{N}^{\beta}$ ($n = 41$).....114

Fig. A4. Paired t test to compare the differences of $\Delta^{15}\text{N}^{\text{bulk}}$ between organosolv and alkali lignin (a), 4-hydroxybenzoic acid and 4-hydroxybenzaldehyde (b), 4-hydroxy-3-methoxybenzoic acid and 4-hydroxy-3-methoxybenzaldehyde (c), and 4-hydroxy-3,5-dimethoxybenzoic acid and 4-hydroxy-3,5-dimethoxybenzaldehyde (d). The *box* indicates the range of the 25 and 75 percentiles of the data, *the line in the box* is the median, and the notch lines indicate the 1.5 interquartile rang.....115

Fig. A5. Paired t test to compare the differences of $\Delta^{18}\text{O}$ between organosolv and alkali lignin (a), 4-hydroxybenzoic acid and 4-hydroxybenzaldehyde (b), 4-hydroxy-3-methoxybenzoic acid and 4-hydroxy-3-methoxybenzaldehyde (c), and 4-hydroxy-3,5-dimethoxybenzoic acid and 4-hydroxy-3,5-dimethoxybenzaldehyde (d). The *box* indicates the range of the 25 and 75 percentiles of the data, *the line in the box* is the median, and the notch lines indicate the 1.5 interquartile rang.....116

Fig. A6. Paired t test to compare the differences of site preference between organosolv and alkali lignin (a), 4-hydroxybenzoic acid and 4-hydroxybenzaldehyde (b), 4-hydroxy-3-methoxybenzoic acid and 4-hydroxy-3-methoxybenzaldehyde (c), and 4-hydroxy-3,5-dimethoxybenzoic acid and 4-hydroxy-3,5-dimethoxybenzaldehyde (d). The *box* indicates the range of the 25 and 75 percentiles of the data, *the line in the box* is the median, and the notch lines indicate the 1.5 interquartile rang.....117

Fig. A7. Paired t test to compare the differences of $\delta^{15}\text{N}^{\alpha}$ between organosolv and alkali lignin (a), 4-hydroxybenzoic acid and 4-hydroxybenzaldehyde (b), 4-hydroxy-3-methoxybenzoic acid and 4-hydroxy-3-methoxybenzaldehyde (c), and 4-hydroxy-3,5-dimethoxybenzoic acid and 4-hydroxy-3,5-dimethoxybenzaldehyde (d). The *box* indicates the range of the 25 and 75 percentiles of the data, *the line in the box* is the median, and the notch lines indicate the 1.5 interquartile rang.....118

Fig. A8. Paired t test to compare the differences of $\delta^{15}\text{N}^{\beta}$ between organosolv and alkali lignin (a), 4-hydroxybenzoic acid and 4-hydroxybenzaldehyde (b), 4-hydroxy-3-methoxybenzoic acid and 4-

hydroxy-3-methoxybenzaldehyde (c), and 4-hydroxy-3,5-dimethoxybenzoic acid and 4-hydroxy-3,5-dimethoxybenzaldehyde (d). The box indicates the range of the 25 and 75 percentiles of the data, the line in the box is the median, and the notch lines indicate the 1.5 interquartile rang.....119

Fig. B1. Allan variance plot for N₂O isotopologue ratios R^α (green lines), R^β (red lines) and R^{18O} (purple lines) at 35 ppm of N₂O mixing ratio. R^α, R^β, and R^{18O} correspond to ¹⁴N¹⁵N¹⁶O / ¹⁴N¹⁴N¹⁶O, ¹⁵N¹⁴N¹⁶O / ¹⁴N¹⁴N¹⁶O and ¹⁴N¹⁴N¹⁸O / ¹⁴N¹⁴N¹⁶O, respectively.....123

Fig. B2. Stepwise regression of δ¹⁵N^α vs N₂O concentration (a), δ¹⁵N^β vs N₂O concentration (b), and δ¹⁸O vs N₂O concentration (c) for 12 to 45 ppm N₂O (dashed line) and 36 to 82 ppm N₂O (dotted line). The R² values were higher than 0.99 for all the *f_{low}* and *f_{high}*.....124

Fig. B3. Reaction of NO₂⁻ with 4-hydroxybenzoic acid. (a) N₂O mixing ratio, (b) δ¹⁵N^α, δ¹⁵N^β, and δ¹⁵N^{bulk} of N₂O, (c) δ¹⁸O of N₂O, and (d) ¹⁵N site preference of N₂O.....125

Fig. B4. Reaction of NO₂⁻ with 4-hydroxy-3-methoxybenzoic acid. (a) N₂O mixing ratio, (b) δ¹⁵N^α, δ¹⁵N^β, and δ¹⁵N^{bulk} of N₂O, (c) δ¹⁸O of N₂O, and (d) ¹⁵N site preference of N₂O.....125

Fig. B5. Reaction of NO₂⁻ with 4-hydroxy-3-methoxybenzaldehyde. (a) N₂O mixing ratio, (b) δ¹⁵N^α, δ¹⁵N^β, and δ¹⁵N^{bulk} of N₂O, (c) δ¹⁸O of N₂O, and (d) ¹⁵N site preference of N₂O.....126

Fig. B6. N₂O emission and its isotopic composition in forest soil after NO₂⁻ application. (a) N₂O mixing ratio, (b) δ¹⁵N^α, δ¹⁵N^β, and δ¹⁵N^{bulk} of N₂O, (c) δ¹⁸O of N₂O, and (d) ¹⁵N site preference of N₂O.....126

Fig. B7. N₂O emission and its isotopic composition in agricultural soil after NO₂⁻ application. (a) N₂O mixing ratio, (b) δ¹⁵N^α, δ¹⁵N^β, and δ¹⁵N^{bulk} of N₂O, (c) δ¹⁸O of N₂O, and (d) ¹⁵N site preference of N₂O.....127

Fig. B8. NO_x (NO and NO₂) and N₂O emissions from the reactions of NO₂⁻ with organosolv lignin (a), 4-hydroxybenzoic acid (b), 4-hydroxy-3-methoxybenzoic acid (c), 4-hydroxy-3,5-dimethoxybenzoic acid (d), 4-hydroxy-3-methoxybenzaldehyde (e), 4-hydroxy-3,5-dimethoxybenzaldehyde (f). Nitrite sodium solution was injected into the reaction chamber at 12:00 AM. The N₂O signal of 4-hydroxybenzoic acid, 4-hydroxy-3-methoxybenzoic acid, 4-hydroxy-3,5-dimethoxybenzoic acid, and 4-hydroxy-3-methoxybenzaldehyde treatments was below the detection limit of 0.1 ppb.....128

Fig. B9. Gas chromatography–mass spectrometry spectrum of the products from the reaction of nitrite with 4-hydroxy-3-methoxybenzoic acid. Three main products including 2-methoxyphenol (retention time: 12.42 min), vanillin (retention time: 20.87 min), and methyl vanillate (retention time: 23.64 min) were detected. The broad peak between 27–32 min denotes the reactant 4-hydroxy-3-dimethoxybenzoic acid.....129

Fig. B10. Gas chromatography–mass spectrometry spectrum of the products from the reaction of nitrite with 4-hydroxy-3,5-dimethoxybenzoic acid. Two main products including 2,6-dimethoxyphenol (retention time: 19.38 min) and 4-hydroxy-3,5-dimethoxybenzohydrazide (retention time: 29.42 min) were detected. The broad peak between 32–36 min denotes the reactant 4-hydroxy-3,5-dimethoxybenzoic acid.....130

Fig. C1. Sampling sites of Wüstebach catchment. The blue line is the river, the five sampling sites are labelled with red dots.....133

Fig.C2. Schematic diagram of the QCLAS-CLD system for the real-time determination of N₂O and NO_x emission from soils induced by nitrite.....133

Fig. C3. The real-time measurement of N₂O and NO_x emissions from unsterilized (a, b) and sterilized (c, d) soils.....134

Fig. C4. Real-time N₂O emission from biotic and abiotic sources. The biotic N₂O mixing ratio at each time point was calculated by the N₂O mixing ratio from unsterilized soil minus the N₂O mixing ratio from its corresponding sterilized soil at the same time point.....135

Fig. C5. NO_x emission from different soil organic matter fractions measured in real-time. DOM, dissolved organic matter fraction; FA, fulvic acid fraction; HA, humic acid fraction; HN, humin fraction; N, control treatment of 0.25 M nitrite solution at pH 3.4.....135

Fig. C6. N₂O emission from the different soil organic matter fractions measured in real-time. DOM, dissolved organic matter fraction; FA, fulvic acid fraction; HA, humic acid fraction; HN, humin fraction.....136

Fig. D1. Effect of lignin content on OSA decomposition (n = 36).....138

Fig. D2. Linear regression of OSA N content based on OSA decomposition (n = 36).....139

Fig. D3. Concentration of fertilizer derived DON in different treatments during the experiment. Nitrogen fertilizer was applied at day 0.....139

Fig. D4. Effect of N content, C/N ratio, and lignin content of OSA on cumulated N₂O emission.....140

Fig. D5. Effect of lignin content on N immobilization in OSA and soils (n = 36).....134

List of tables

Table II.1. Isotopic signatures of N ₂ O from the reactions of nitrite with lignin and lignin derivatives. The values were shown as mean ± standard deviation of three replicates.....	18
Table II.2. Pearson correlation coefficients of isotopic signatures of N ₂ O (n = 41).....	19
Table III.1. δ ¹⁵ N ^{bulk} , δ ¹⁸ O, and site preference values of N ₂ O from the reaction of NO ₂ ⁻ with organics and soils.....	33
Table IV.1. Isotopic signatures of N ₂ O from NO ₂ ⁻ -SOM fraction reactions.....	61
Table V.1. Peak areas as percentage of total ¹⁵ N for CP/MAS ¹⁵ N NMR spectra.....	68
Table VI.1. Pearson Correlations between immobilization of fertilizer-N in OSA, total fertilizer-N in organic soil amendment (OSA), OSA decomposition, and N retention in soils (n = 45).....	87
Table VI.2. Pearson Correlations between NO ₂ ⁻ content, soil pH, lignin composition, organic soil amendment (OSA) decomposition, and contents of fertilizer-derived NO ₃ ⁻ , NH ₄ ⁺ , N ₂ O, and SON (n = 36).....	87
Table VII.1. N ₂ O loss, NO _x loss, and N retention in various soils after N application.....	103
Table A1. Parameters of the mathematical equations for response surfaces of N ₂ O emission from nitrite reactions with lignin and lignin derivatives.....	120
Table A2. Parameters of the mathematical equations for response surface of CO ₂ emission from nitrite reactions with lignin and lignin derivatives.....	121
Table B1 Characteristics of the soil samples. The indicated precision is the standard deviation for replicate sample measurements (n = 3).....	122
Table B2. Experimental details for individual treatments.....	123
Table C1. Characteristics of five soil samples from the Wüstebach test sites.....	132
Table C2. Fitting results of Hill equation.....	132
Table D1. Pearson Correlations among total CO ₂ and N ₂ O emission rates, fertilizer-derived N ₂ O	

emission rate, $\delta^{15}\text{N-N}_2\text{O}$, and $\delta^{18}\text{O-N}_2\text{O}$ (n = 141).....137

Table D2. Pearson Correlations among total N_2O , NH_4^+ , and NO_3^- , and fertilizer-derived N_2O , NH_4^+ , and NO_3^- in soils (n = 90).....137

Table D3. Decomposition of OSA, total fertilizer-N in OSA, immobilized fertilizer-N in OSA, and immobilized/total fertilizer-N in OSA.....138

List of abbreviations

Al	aluminum
Anammox	anaerobic ammonium oxidation
ANOVA	one-way analysis of variance
AOA	ammonia-oxidizing archaea
AOB	ammonia-oxidizing bacteria
BOC	biologic organic carbon
BON	biologic organic nitrogen
C	carbon
CH ₄	methane
CH ₃ ONO	methyl nitrite
CLD	chemoluminescence analyzer
C/N	carbon-to-nitrogen ratio
DNRA	dissimilatory nitrate reduction to ammonium
CO ₂	carbon dioxide
DOC	dissolved organic carbon
DOM	dissolved organic matter
DON	dissolved organic nitrogen
cw-QCL	continuous wave quantum cascade laser
δ	the relative difference of isotope ratio from a reference
δ ¹⁵ N	the relative difference of ¹⁵ N to a reference
δ ¹⁵ N ^{bulk}	average of δ ¹⁵ N of N ₂ O
δ ¹⁵ N ^α	δ ¹⁵ N of the central nitrogen atom in N ₂ O
δ ¹⁵ N ^β	δ ¹⁵ N of the terminal nitrogen atom in N ₂ O
δ ¹⁸ O	the relative difference of ¹⁸ O to a reference
Δ	net isotope effect
Δ ¹⁵ N	net isotope effect of ¹⁵ N
Δ ¹⁸ O	net isotope effect of ¹⁸ O
EPR	electron paramagnetic resonance
Fe ²⁺	ferrous iron
Fe ³⁺	ferric iron
FA	fulvic acid
Fe	iron

G	guaiacyl unit of lignin
GC	gas chromatography
GHG	greenhouse gas
H	<i>p</i> -hydroxyphenyl unit of lignin
H ⁺	proton
HA	humic acid
H ₂ O	water
HN	humic acid
HNO	nitroxyl
HNO ₂	nitrous acid
HNO ₃	nitric acid
H ₂ N ₂ O ₂	hyponitrous acid
HQ	hydroquinone
ICP-OES	inductively coupled plasma optical emission spectroscopy
IN	inorganic nitrogen
IRMS	isotope ratio mass spectrometer
Lac	laccase
LiP	lignin peroxidases
MFC	mass flow controller
Mn	manganese
MnP	manganese peroxidases
<i>m/z</i>	mass-to-charge ratio
N	nitrogen
N _r	reactive nitrogen
N ₂	dinitrogen
NaNO ₂	sodium nitrite
NAR	nitrate reductase
NH ₂ OH	hydroxylamine
NH ₃	ammonia
NH ₄ ⁺	ammonium
NIR	nitrite reductase
NMR	nuclear magnetic resonance spectroscopy
N ₂ O	nitrous oxide
NO	nitric oxide
NO ₂	nitrogen dioxide

NO _x	the sum of NO and NO ₂
NO ⁺	nitrosonium cation
NO ₂ ⁻	nitrite
NO ₃ ⁻	nitrate
NOB	nitrite-oxidizing bacteria
NUE	nitrogen use efficiency
O ₂	oxygen gas
O _a	organic matter layer of soil
OC	organic carbon
OH	hydroxyl
ON	organic nitrogen
OSA	organic soil amendment
⁻ ONNO ⁻	hyponitrite
P	phosphate
pK _a	acid dissociation constant
PTFE	polytetrafluoroethylene
Q	quinone
QCLAS	quantum cascade laser absorption spectrometer
RDA	redundancy analysis
S	syringyl unit of lignin
SOC	soil organic carbon
SOM	soil organic matter
SON	soil organic nitrogen
SQ	semiquinone radicals
SQA	semiquinone radical anion
SP	site preference
TN	total nitrogen
TOC	total organic carbon
VSMOW	Vienna Standard Mean Ocean Water
WHC	water holding capacity

I. Introduction

1.1 Rationale and state-of-the-art

As one of the primary nutrients in ecosystems, nitrogen (N) is an essential element for living organisms to synthesize proteins and deoxyribonucleic acids. Most N exists in the form of dinitrogen (N_2), which is chemically unreactive and only biologically available to N fixers, therefore, agricultural soils are generally N-limited. To promote food production, N fertilizer produced by the industrial Haber-Bosch process has been widely used since the 1920s, and N fertilization increased to about 100 Tg N yr^{-1} in the 1990s (Gruber and Galloway, 2008). However, only 10–65 % of applied fertilizer-N could be used by crops and the rest is lost through N gas emissions and nitrate (NO_3^-) leaching, or immobilized by soil organic matter (SOM) (Cassman et al., 1998; Said-Pullicino et al., 2014). Consequently, global atmospheric N_2O concentration increased from a pre-industrial level of 270 ppb to 328 ppb in 2015 (WMO, 2016).

Nitrous oxide (N_2O) is the third most important greenhouse gas whose radiative forcing is almost 300 times higher on a weight basis than that of CO_2 in a 100-year timeframe (IPCC, 2013). It accounts for about 6 % of the global radiative forcing by long-live greenhouse gases (WMO, 2016). The atmospheric lifetime of N_2O is about 116 years (Prather et al., 2015), and it can be photolyzed to nitric oxide (NO) when transferred into the stratosphere, which further catalyzes the depletion of ozone. Hence, N_2O also represents currently the most important ozone-depleting source after successful emission reduction of chlorine- and bromine-containing halocarbons (Ravishankara et al., 2009). So it is currently the primary task to identify major N_2O sources and to develop corresponding mitigation strategies.

According to the “hole-in-the-pipe” model proposed by Firestone and Davidson (1989), N_2O is “leaking” as a by-product of nitrification and an intermediate of denitrification. During nitrification, ammonium (NH_4^+) is stepwise oxidized to hydroxylamine (NH_2OH), nitrite (NO_2^-), and NO_3^- by nitrifiers including ammonia-oxidizing bacteria (AOB), ammonia-oxidizing archaea (AOA), and NO_2^- -oxidizing bacteria (NOB) under aerobic conditions, and according to the common assumption N_2O is produced as a by-product of biotic NH_2OH oxidation (Sutka et al., 2003). In contrast, both NO_2^- and NO_3^- can be stepwise reduced to nitric oxide (NO), N_2O , and N_2 by NO_2^- or NO_3^- reducers during denitrification, while part of the NO and N_2O is emitted to the atmosphere (Bateman et al., 2004). According to the type of microbes conducting the reduction of NO_2^- and NO_3^- , denitrification can be classified into bacterial denitrification, fungal denitrification, and nitrifier denitrification. Bacterial denitrification is also frequently called denitrification, and denitrifying bacteria are widely distributed including the genera *Pseudomonas*, *Alkaligenes*, *Bacillus*, and others (Fillery, 1983). By contrast, denitrification conducted by fungi is defined as fungal denitrification. Meada et al. (2015) found that seventy strains out of 207 fungal isolates were able to produce N_2O , most of which were *Hypocreales*. Under microoxic or anoxic conditions, nitrifiers can also reduce NO_2^- to N_2O and N_2 ,

which is called nitrifier denitrification (Wrage et al., 2001). Both *Nitrosomonas* and *Nitrosospira* have been demonstrated to produce N_2O anaerobically through nitrifier denitrification. In addition, hybrid N_2O and N_2 can be produced through co-denitrification, namely by the microbe-mediated N-nitrosation of amino compounds by NO_2^- or NO (Spott et al., 2011; Spott and Stange, 2011).

Recently, N_2O production from abiotic NH_2OH oxidation and abiotic NO_2^- reduction has been receiving increasing attention. Hydroxylamine is not stable and can be quickly oxidized to N_2O by oxygen (O_2), ferric iron (Fe^{3+}), manganese dioxide (MnO_2), and NO_2^- (Heil et al., 2014). The N_2O emission from chemical oxidation of NH_2OH in soils is favored by alkaline pH and less soil organic carbon, approximate 50 % of NH_2OH was chemically oxidized to N_2O in cropland soils at pH 6.4, but only less than 5 % in acidic forest soil where soil organic carbon was much higher than cropland soils (Heil et al., 2015). The abiotic reduction of NO_2^- to N_2O , NO , and N_2 by transition metals or SOM is defined as chemodenitrification. Nitrogen trace gas emissions from chemodenitrification were found decades ago in the reactions of NO_2^- with ferrous iron (Fe^{2+}), lignin, humic acid, and fulvic acid (Stevenson and Harrison, 1966; Stevenson and Swaby, 1964; Wullstein and Gilmour, 1964), yet, the role of reactions of NO_2^- with SOM in N trace gas emission and N retention has been neglected till recently (Ma et al., 2015; Venterea, 2007).

N_2O isotopic signatures ($\delta^{15}N^{bulk}$, $\delta^{18}O$, site preference (SP) $\equiv \delta^{15}N^{\alpha} - \delta^{15}N^{\beta}$) have been considered as efficient tools for N_2O source partitioning until now (Toyoda and Yoshida, 1999). Compared with $\delta^{15}N^{bulk}$ and $\delta^{18}O$, SP is thought to be more specific to identify N_2O production pathways because SP from a certain source process was found stable and independent of the substrate (Toyoda and Yoshida, 1999; Toyoda et al., 2002). Microbial sources of nitrification and fungal denitrification, as well as chemical oxidation of NH_2OH denote a relatively high SP value of 27 to 40 ‰ (Heil et al., 2014; Rohe et al., 2014), while bacterial denitrification and nitrifier denitrification denote a low SP value ranging from -11 to 1.4 ‰ (Decock and Six, 2013). End-member maps of SP vs. $\delta^{15}N^{bulk}$ and SP vs. $\delta^{18}O$, as well as end-member mixing models, have been used to estimate the N_2O sources in an urban river (Toyoda et al., 2009), agricultural soil (Toyoda et al., 2011), and waste water treatment (Wunderlin et al., 2013). However, in spite of the fact that chemodenitrification accounts for significant N_2O emission under certain conditions, its N_2O isotopic signatures are rarely reported or considered in N_2O source partitioning (Ostrom et al., 2016; Zhu-Barker et al., 2015).

When NO is emitted to the atmosphere, it is rapidly oxidized to nitrogen dioxide (NO_2), and the sum of NO and NO_2 is called NO_x . In the troposphere, NO_x reacts with volatile organic compounds in the presence of sunlight to form photochemical smog, which endangers the lung function of human beings. When dissolved in atmospheric moisture, NO_x can form nitric acid (HNO_3) and eventually be deposited back to earth in the form of acid rain. In addition, NO_x reacts with ozone in stratosphere and leads to the depletion of the ozone layer (Medinets et al., 2015). Agriculture accounts for about

10 % of the global NO emission (IPCC, 2013). Liu et al. (2015) reported that NO emission corresponded linearly and positively with the increase of fertilization rates in calcareous soils, while alkaline pH limited NO emission. Nitrite is a key precursor of NO production in both biotic denitrification and abiotic chemodenitrification, while NH_2OH and amino compounds act as the direct precursor of NO in biotic nitrification (Medinets et al., 2015). Factors controlling soil NO emissions include N availability, soil moisture, soil temperature, pH, and vegetation (Delon et al., 2015; Pilegaard, 2013). Till now, the contribution of NO_2^- reactions with SOM to NO_x emissions from soils is still unknown.

When fertilizer is applied to soils, it is partly incorporated into SOM leading to N retention (Blesh and Drinkwater, 2014). It was found that N retention was significantly positively correlated with the total N loading in various ecosystems (Johnson et al., 2000; Saunders and Kalff, 2001). Biological N uptake accounted for the largest N retention in the case of NH_4^+ and NO_3^- , while abiotic reactions of NO_2^- with SOM led to a much higher N retention in the case of NO_2^- (Lewis and Kaye, 2012). Abiotic retention of both NH_4^+ and NO_2^- was positively related with the soil organic carbon (SOC) content (Fitzhugh et al., 2003b). However, abiotic N retention of NH_4^+ is facilitated by alkaline pH, and acidic pH favors the abiotic immobilization of NO_2^- in SOM (Broadbent, 1960; Nelson, 1967). The products of abiotic reactions of humus substances with NO_2^- include nitrosophenols, ketoximes, amides, nitriles, and heterocyclic N compounds (Rousseau and Rosazza, 1998; Thorn and Mikita, 2000), indoles, pyrroles, pyridines, amides, and aminohydroquinones in the case of NH_4^+ (Thorn and Mikita, 1992), and nitriles, amides, oximes, and hydroxamic acids in the case of NH_2OH (Thorn et al., 1992). However, the structure of in-situ immobilized N is rarely reported till now.

Because of its complexity, SOM is like a black box and except for some low-molecular-weight compounds, such as organic acids, sugars, amino acids, have been identified, most of the macromolecules are not yet chemically identified in detail (Kalbitz et al., 2000). ^{13}C -NMR analysis revealed that most of the humus substances, including humic acids, fulvic acids, and humin, are aromatic super-polymers with various functional groups like C=O, C=C and -OH (Stevenson, 1995; Zhang et al., 2015a). Lignin, the most abundant natural aromatic polymer, is generally regarded as the main source of stable SOM. During the degradation of lignin, highly reactive polyphenols, aromatic aldehydes and acids are formed in soils, which could be important participants in abiotic reactions with NO_2^- .

1.2 Objectives and outline of the thesis

The overall aim of the present thesis was to explore the role of abiotic NO_2^- -SOM reactions in N trace gas emissions and N retention. To this end, five laboratory studies were conducted to examine the emissions of N_2O , NO_x , and CO_2 , N_2O SP, and N retention from NO_2^- -SOM reactions in chemical

assays and soils. The aim of the first study (chapter II) was to quantify the N_2O and CO_2 production in chemical assays with NO_2^- and lignin derivatives, as well as to determine the variability of N_2O SP along pH and NO_2^- concentration gradients. In the second study (chapter III), the isotopic signatures of N_2O from NO_2^- -SOM reactions were determined for the first time in real-time in chemical assays and soils (forest, agriculture, and grassland). The third study (chapter IV) was designed to investigate NO_2^- -driven biotic and abiotic production of N_2O and NO_x in acidic forest soils, as well as the roles of different SOM fractions in abiotic N_2O emission. In the fourth study (chapter V), the structure of immobilized N from NO_2^- -SOM reactions was explored with solid-state ^{15}N -NMR analysis. And the fifth study (chapter VI) was aimed to examine the influence of combined application of N fertilizer with organic soil amendments (OSA) (wheat straw, spruce sawdust, and lignin) on N_2O and CO_2 emissions, as well as N retention in agricultural soils. Finally, an open-pump theory was proposed to explain the biotic release of reactive N and C intermediates into soil, the mechanisms of abiotic C-N interactions, and their role in N gas emission and N retention (chapter VII).

The addressed questions and work steps are outlined as follows:

1) How does the lignin structure affect N_2O and CO_2 emissions when reacting with NO_2^- ? What is the SP value of N_2O from reactions of NO_2^- with lignin products? And how do pH and NO_2^- concentration affect N_2O and CO_2 emissions and N_2O SP values?

N_2O and CO_2 emissions from reactions of NO_2^- with two lignin products (alkali lignin and organosolv lignin) and six lignin derivatives (4-hydroxybenzoic acid, 4-hydroxybenzaldehyde, 4-hydroxy-3-methoxybenzoic acid, 4-hydroxy-3-methoxybenzaldehyde, 4-hydroxy-3,5-dimethoxybenzoic acid, and 4-hydroxy-3,5-dimethoxybenzaldehyde) were measured at pH 3 to 6 and at NO_2^- concentrations from 0.1 to 0.5 mM. The SP of N_2O was also measured by isotope ratio mass spectrometry (IRMS). The chemodenitrification N_2O source was located on the end-member maps of SP vs. $\delta^{15}N^{bulk}$ and SP vs. $\delta^{18}O^{bulk}$ (cf. chapter II).

2) Does the ^{15}N SP of N_2O from NO_2^- -SOM reactions stay constant according to the common assumption that N_2O SP from a certain source remains relatively stable?

A quantum cascade laser absorption spectrometer (QCLAS) was used for real-time analysis of the N_2O isotopic signatures from chemical reactions of NO_2^- with lignin derivatives (organosolv lignin, 4-hydroxybenzoic acid, 4-hydroxy-3-methoxybenzoic acid, 4-hydroxy-3,5-dimethoxybenzoic acid, 4-hydroxy-3-methoxybenzaldehyde, and 4-hydroxy-3,5-dimethoxybenzaldehyde), and from NO_2^- -amended soils (forest, grassland, and agricultural soil). Hyponitrous acid and nitramide pathways were proposed to explain the possible reason for shifted SP values during the reaction (cf. chapter III).

3) How much do the abiotic reactions contribute to the total N_2O and NO_x emissions in acidic forest soils where NO_2^- is abundant? And which SOM fraction is the most reactive to NO_2^- , associated

with the highest N₂O and NO_x production?

To quantify the biotic and abiotic N₂O and NO_x emissions in NO₂⁻-amended soils, five acidic spruce forest soils were sampled from the O_a layer of the Wüstebach catchment, Eifel National Park, Germany. Sodium NO₂⁻ solution was applied to sterilized or live soils, and afterwards, N₂O and NO_x emissions were measured simultaneously with a QCLAS and a chemoluminescence detector. To explore the role of different SOM fractions in NO₂⁻-SOM reactions, one soil sample was fractionated into dissolved organic matter (DOM), fulvic acid, humic acid, and humin fractions, and N₂O and NO_x emissions from their reaction with NO₂⁻ at the original soil pH were measured. In addition, N₂O sources were partitioned according to the N₂O isotopic signatures (cf. chapter IV).

4) How much N can be immobilized by SOM through abiotic NO₂⁻-SOM reactions in soils? And what is the structure of immobilized N?

¹⁵N-labeled sodium NO₂⁻ was applied to sterilized forest and grassland soils. After 4 d of incubation, inorganic N was removed by extraction with 1 M KCl solution, and N retention was calculated according to the remaining ¹⁵N in the SOM. The mineral fraction in soils was removed by treatment with hydrogen fluoride, and then reacted with NO₂⁻ for a second time to enhance ¹⁵N-NMR signals. Finally, the structure of immobilized N was investigated using solid-state ¹⁵N-NMR (cf. chapter V).

5) How does OSA affect N₂O and CO₂ emissions in fertilized agricultural soils? What is the role of lignin in N₂O emission and N retention in fertilized soils?

Agricultural soil from Kiel, Germany, was amended with different organic substances (wheat straw, spruce sawdust, and lignin) and ¹⁵N-labeled fertilizer ((NH₄)₂SO₄), then incubated at room temperature for 114 d. Emissions of N₂O and CO₂, N₂O isotopic composition, lignin degradation, ¹⁵N-content of NH₄⁺ and NO₃⁻, N retention, and lignin composition were measured to explore the effects of lignin content and composition of OSA on N partitioning (cf. chapter VI).

6) What is the role of abiotic C–N interactions in N gas emission and N retention in soils? How do the biotic processes affect abiotic C–N interactions?

An open pump theory was developed and suggested to explain the combined action of biotic and abiotic processes in C–N interactions. This review revealed the mechanisms involved in the biotic formation and release of reactive C and N intermediates to the soil, as well as N₂O and NO_x emissions and N retention from abiotic C–N interactions (cf. chapter VII).

II. Large variability of CO₂ and N₂O emissions and of ¹⁵N site preference of N₂O from reactions of nitrite with lignin and its derivatives at different pH

Based on:

Wei, J., Zhou, M., Vereecken, H. , Brüggemann, N. (2017b). Large variability of CO₂ and N₂O emissions and of ¹⁵N site preference of N₂O from reactions of nitrite with lignin and its derivatives at different pH. *Rapid Communications in Mass Spectrometry* 31, 1333-1343.

II.1 Introduction

Nitrous oxide and CO₂ are two important greenhouse gases (GHG), their concentrations in the atmosphere increased to 328.1 ± 0.1 ppb and 400 ± 0.1 ppm in 2015, which was 21 % and 44 % higher compared with the pre-industrial levels, respectively (WMO, 2016). Terrestrial soils are the largest source of atmospheric CO₂ and N₂O, with an annual flux of about 120 Gt C and 10 Tg N, respectively (IPCC, 2013). While the biological sources of the two GHG are well established, i.e. respiration in the case of CO₂, and nitrification and denitrification in the case of N₂O, abiotic sources of N₂O and CO₂ in soil are neglected, but they could play a much larger role than currently assumed and need to be understood for predictions of soil GHG emissions in the future (Venterea, 2007). As a key intermediate of nitrification and denitrification, NO₂⁻ is chemically highly reactive, and can be easily reduced to nitric oxide (NO), N₂O, and N₂ by SOM and transition metals in soil, which is defined as chemodenitrification (Chalk and Smith, 1983). It has been shown that the abiotic reaction of NO₂⁻ with SOM, such as lignin derivatives, humic and fulvic acids, led to considerable production of N₂O and CO₂ (Stevenson et al., 1970), and the contribution of chemodenitrification to N₂O emission is recently receiving more and more attention (Venterea, 2007; Wei et al., 2017a).

As a three-dimensional biopolymer of high molecular weight, lignin is the most abundant aromatic compound on earth (Bahri et al., 2006). It is formed by radical polymerization of the guaiacyl (G) unit, syringyl (S) unit, and *p*-hydroxyphenyl (H) unit, which are derived from the precursor coniferyl alcohol, sinapyl alcohol, and *p*-coumaryl alcohol, respectively. The ratio of G:S:H units varies between plant species. For example, softwood lignin contains mainly G units, hardwood lignin is dominated by a mixture of G and S units, while grass lignin is mainly composed of G and H units (Bugg et al., 2011a). The monomeric phenylpropanoid units are connected by non-hydrolyzable C-O-C and C-C bonds, forming complex structures which contribute largely to the high resistance of lignin towards decomposition (Kiem and Kögel-Knabner, 2003). Therefore, it is generally thought that lignin contributes to the recalcitrant pool of SOM (Bahri et al., 2008), and the reactions of NO₂⁻ with lignin and lignin derivatives could control the N₂O and CO₂ emissions from chemodenitrification in soil.

In the linear N₂O molecule, the two nitrogen atoms align asymmetrically (N^β=N^α=O), and the intramolecular distribution of ¹⁵N is defined as ¹⁵N site preference (SP): $SP \equiv \delta^{15}N^{\alpha} - \delta^{15}N^{\beta}$ (Toyoda and Yoshida, 1999). It is thought that the N₂O SP value is independent of the $\delta^{15}N$ value of its precursors, for example NO₂⁻, NH₂OH, NH₄⁺, and NO₃⁻, and it remains constant for a certain pathway of N₂O formation (Toyoda et al., 2002). Thereby, the SP value of N₂O is widely regarded as a key element of N₂O source partitioning. Till now, the SP values of N₂O from fungal denitrification (Sutka et al., 2008), nitrifier denitrification (Sutka et al., 2006), denitrification (Sutka et al., 2006; Toyoda et al., 2005), autotrophic nitrification (Sutka et al., 2006; Sutka et al., 2003, 2004), and abiotic NH₂OH oxidation

(Heil et al., 2014; Toyoda et al., 2005) have been determined in pure cultures or chemical assays. Generally, the SP values of N₂O from above sources are classified into a lower range of -8.7 to 8.5 ‰ and a higher range of 19.7 to 40.0 ‰ for source partitioning, which represent N₂O_D (including denitrification and nitrifier denitrification) and N₂O_N (including nitrification, fungal denitrification and abiotic NH₂OH oxidation), respectively (Decock and Six, 2013). Based on the theory that SP values can be divided into two completely different ranges, end-member maps and two-end-member mixing models have been developed to estimate the contribution of possible sources to the total N₂O emission in both laboratory and field studies (Toyoda et al., 2011; Zhang et al., 2016).

However, the intramolecular ¹⁵N distribution of N₂O from chemodenitrification has never been systematically studied before, and the scanty reported SP values are not comparable with each other. For example, Jones et al. (2015) reported that SP values of N₂O from the chemical reduction of NO₂⁻ by iron minerals under anoxic conditions at pH 7 ranged from 10 to 22 ‰, which was in the middle of the SP values of N₂O_D and N₂O_N. In contrast, Samarkin et al. (2010) revealed very low SP values (-45 to 4 ‰) of N₂O from chemodenitrification in the Don Juan Pond, Antarctica, while Toyoda et al. (2005) found that the SP value of N₂O from the chemical reduction of NO₂⁻ by trimethylamine borane was 30 ‰, which was in the range of N₂O_N. Currently, there is no clear explanation for the contradictory SP values of chemodenitrification. Since chemodenitrification is an important N₂O source in certain soils, and since N₂O source partitioning could be strongly biased without taking the N₂O production from NO₂⁻-SOM reactions into account (Wei et al., 2017a), the N₂O isotope signatures from NO₂⁻-SOM reactions should be determined and compiled to allow for uniqueness of N₂O source partitioning using SP values.

Motivated by the above described research need, the CO₂ and N₂O emissions from chemical reactions of nitrite with lignin and its derivatives were measured at different NO₂⁻ concentrations and pH values, and the isotopic signatures of N₂O from these reactions were analyzed to update the current database of N₂O isotope signatures from different source processes.

II.2 Material and Methods

II.2.1 Chemicals

Sodium nitrite (NaNO₂, δ¹⁵N vs air N₂ = -18.00 ± 0.08 ‰, δ¹⁸O vs VSMOW = 10.09 ± 0.05 ‰, VWR, Germany) was used as the NO₂⁻-N source. Organosolv lignin (chemicalpoint, Germany) and alkali lignin (Sigma-Aldrich, Germany) were two lignin representatives. Organosolv lignin is extracted through a pulping technique, in which organic solvents are used, while alkali lignin is separated from the industrial black liquor by acid treatment (Johansson et al., 2014). Considering their different extraction procedures, organosolv lignin and alkali lignin were expected to show different reactivity to NO₂⁻. All following chemicals were obtained from VWR. 4-hydroxybenzoic acid and 4-

hydroxybenzaldehyde were chosen as two common H lignin units, 4-hydroxy-3-methoxybenzoic acid and 4-hydroxy-3-methoxybenzaldehyde corresponded to typical G lignin units, while 4-hydroxy-3,5-dimethoxybenzoic acid and 3,5-dimethoxy-4-hydroxybenzaldehyde represented S lignin units. The structures of lignin derivatives are shown in Fig. A1. Monopotassium phosphate and disodium phosphate were used to prepare 0.4 M buffer solutions at pH 3, 4, 5, and 6 to control the pH of the reaction assays.

II.2.2 Quantification of N₂O and CO₂ emissions

Sodium nitrite solutions (0.1, 0.3, and 0.5 mM) were prepared by diluting 20 mM of NaNO₂ solution with 0.4 M of phosphate buffer at pH 3, 4, 5, and 6, and they were immediately used after preparation. For the measurement of N₂O and CO₂ emissions, 0.06 mmol of lignin derivative (4-hydroxybenzoic acid, 4-hydroxy-3-methoxybenzoic acid, 4-hydroxy-3,5-dimethoxybenzoic acid, 4-hydroxybenzaldehyde, 4-hydroxy-3-methoxybenzaldehyde, or 4-hydroxy-3,5-dimethoxybenzaldehyde) or 0.01 g of lignin (organosolv or alkali) were put into 22.5-ml gas chromatography vials, then 5 ml of prepared NaNO₂ solution was added into the vials, and immediately afterwards the vials were crimped gas-tight. The mixtures were incubated for 24 h on a shaker at 200 rpm and 20°C. Then, N₂O and CO₂ concentrations in the headspace of the vials were measured with a gas chromatography equipped with an electron capture detector and flame ionization detector (GC-ECD/FID, Clarus 580, PerkinElmer, Rodgau, Germany). Control treatments, in which water instead of NaNO₂ solution was applied to the GC vials, were used for background correction, and all treatments were conducted in triplicate. Except for lignin, which was not soluble, the solubility of the aromatic acids and aldehydes increased with increasing pH, i.e., while a small amount of acids or aldehydes remained suspended in the NO₂⁻ solution at pH 3, all of the compounds were completely dissolved at pH 6. To test if biological processes were involved in the interactions, the N₂O and CO₂ emissions from sterilized and unsterilized treatments were compared, and no significant difference ($P > 0.05$) was found (Fig. A2). Therefore, only chemical reactions are considered in this experiment.

II.2.3 Analysis of N₂O isotopic signatures

For the determination of N₂O isotopic signatures, organic compounds were weighed into 100-ml serum flasks, then the flasks were crimped gas-tight and the headspace was evacuated and flushed with an N₂O-free gas mixture of helium and oxygen (80:20, v/v), afterwards 0.5–20 ml of NaNO₂ solution (0.5 or 0.3 mM) at pH 3, 4, or 5 was injected into the bottles. The ratios of organic compounds to NO₂⁻ remained the same as the measurement of N₂O emission, but the total amount was adjusted to reach an N₂O concentration of 0.3–0.6 ppm in the headspace. After 24 h of incubation at 20°C, N₂O in the headspace was analyzed with an isotope ratio mass spectrometer

(IRMS, IsoPrime 100, Elementar Analysensysteme, Hanau, Germany) coupled to an online pre-concentration unit (TraceGas, Elementar Analysensysteme). The headspace of the flasks was flushed with helium for 20 min to move out the N₂O sample gas. Water, CO₂, and any potential CO in the sample gas were removed by a water trap (a 6 mm × 200 mm borosilicate glass tube packed uniformly with magnesium perchlorate pellets), a CO₂ trap (a 9 mm × 200 mm glass tube packed with carbosorb), and a CO trap (a 6 mm × 200 mm glass tube packed with Sofnocat CO oxidation catalyst), respectively. Then the sample gas N₂O was cryogenically concentrated in a cold trap (trap 1) submerged in a Dewar with liquid nitrogen. The concentrated N₂O sample was remobilized again by heating trap 1, focused on a second cold trap (trap 2), and dried again with a Nafion membrane dryer before the sample was remobilized again and separated on a Poraplot column with the length of 30 m and the diameter of 0.32 mm. The mass-to-charge ratios (*m/z*) of N₂O at 44 (¹⁴N¹⁴N¹⁶O), 45 (¹⁴N¹⁵N¹⁶O, ¹⁵N¹⁴N¹⁶O, and ¹⁴N¹⁴N¹⁷O), and 46 (¹⁴N¹⁴N¹⁸O), as well as NO⁺ fragment ion of N₂O at 30 (¹⁴N¹⁶O⁺) and 31 (¹⁵N¹⁶O⁺), were measured simultaneously by the mass spectrometer. The values of δ¹⁵N^{bulk}, δ¹⁵N^α, and δ¹⁸O were calculated from the isotope ratios of *m/z* 44, 45, and 46, and a ¹⁷O correction was performed according to Kaiser et al. (2003). The δ¹⁵N^β value was calculated by δ¹⁵N^β = 2 · δ¹⁵N^{bulk} - δ¹⁵N^α, and SP = δ¹⁵N^α - δ¹⁵N^β. Pure N₂O (99.999 %, Linde, Munich, Germany) was used as reference gas for isotope analysis. The working standard gas (δ¹⁵N^α vs air-N₂ = 3.18 ± 0.23 ‰, δ¹⁵N^β vs air-N₂ = 1.42 ± 0.21 ‰, δ¹⁸O vs VSMOW = 39.35 ± 0.27 ‰) was calibrated in our lab against two secondary standard gases (Ref 1: δ¹⁵N^α vs air-N₂ = 15.70 ± 0.31 ‰, δ¹⁵N^β vs air-N₂ = -3.21 ± 0.37 ‰, δ¹⁸O vs VSMOW = 35.16 ± 0.35 ‰; Ref 2: δ¹⁵N^α vs air-N₂ = 5.55 ± 0.21 ‰, δ¹⁵N^β vs air-N₂ = -12.87 ± 0.32 ‰, δ¹⁸O vs VSMOW = 32.73 ± 0.21 ‰) provided by EMPA (Dübendorf, Switzerland) (Mohn et al., 2014). Each treatment was conducted in triplicate.

II.2.4 Statistical analysis

The N₂O and CO₂ concentrations in the headspace were first corrected by subtracting the background, and then the ideal gas law was applied to calculate the total emission:

$$E = \frac{(C_s - C_c) \times T_0 \times V}{T \times V_m}$$

E (nmole) denotes the total N₂O or CO₂ emission; *T*₀ (273.15 K) and *T* (293.15 K) denote the temperature for ideal gas and sample gas, respectively; *V*_{*m*} (22.4 L mol⁻¹) and *V* (17.5 ml) are the volume of one mole of ideal gas and the volume of sample gas, respectively; *C*_{*s*} and *C*_{*c*} (ppm) are concentrations of N₂O or CO₂ in treatments and their corresponding controls, respectively.

Response surface analysis of N₂O and CO₂ emissions from the reactions of NO₂⁻ with lignin products was conducted through polynomial regression with Design-Expert 10.0 (Stat-Ease,

Minneapolis, Minnesota, USA) on historical analysis mode. Due to the high ratio of maximum to minimum response, N₂O and CO₂ emission data were transformed by extracting the square root before the fitting process. OriginPro 2015 (OriginLab Corporation, Wellesley Hills, MA, USA) was used for one-way analysis of variance (ANOVA), paired *t*-test, Pearson correlation analysis and linear regression of N₂O isotopes.

II.3 Results

II.3.1 Response surfaces of N₂O and CO₂ emissions

Response surfaces of both N₂O and CO₂ emissions from the reactions of NO₂⁻ with organic substances were well fitted with the polynomial model with R² values higher than 0.89, and the differences between adjusted and predicted R² smaller than 0.1 (Table A1 and A2). Both the R² values were much higher than those (less than 0.8) of multiple regression. The highest N₂O emission occurred in the organosolv lignin and 4-hydroxy-3,5-dimethoxybenzaldehyde treatments, followed by alkali lignin, 4-hydroxybenzoic acid, and 4-hydroxy-3-methoxybenzaldehyde, while only a very small amount of NO₂⁻ was transformed into N₂O in the 4-hydroxybenzaldehyde, 4-hydroxy-3-methoxybenzoic acid, and 4-hydroxy-3,5-dimethoxybenzoic acid treatments (Fig. II.1). At pH 3, about 1.7 % of NO₂⁻ was transformed into N₂O in the organosolv lignin treatment, which was much higher than the 0.7 % in the alkali lignin treatment. The highest N₂O yield was about 2.2 % in the 4-hydroxy-3,5-dimethoxybenzaldehyde treatment with 0.5 mM sodium NO₂⁻ at pH 4. Among the lignin-derived aldehydes, the G and S units (represented by 4-hydroxy-3-methoxybenzaldehyde and 4-hydroxy-3,5-dimethoxybenzaldehyde, respectively) accounted for higher N₂O emission. In contrast, the H unit (represented by 4-hydroxybenzoic acid) accounted for the highest N₂O emission among lignin-derived acids.

In all the eight treatments with different carbon substances, N₂O emission declined nonlinearly with decreasing NO₂⁻ concentration, whereas the pH dependence of N₂O emission differed in response to the structure of the lignin derivatives. In the treatments with organosolv and alkali lignin, 4-hydroxybenzaldehyde, 4-hydroxy-3-methoxybenzoic acid, and 4-hydroxy-3-methoxybenzaldehyde, significant N₂O production occurred only at pH < 4. However, the highest N₂O production was observed at pH 5 in the 4-hydroxy-3,5-dimethoxybenzoic acid treatment, while at around pH 4 in the treatment with 4-hydroxy-3,5-dimethoxybenzaldehyde (Fig. II.1). The reaction of NO₂⁻ with 4-hydroxybenzoic acid continuously produced considerable amounts of N₂O from pH 3 to 5 (Fig. II.1c).

The highest CO₂ emission occurred in the 4-hydroxy-3,5-dimethoxybenzoic acid treatment, followed by the 4-hydroxy-3-methoxybenzoic acid, 4-hydroxy-3,5-dimethoxybenzaldehyde, and 4-hydroxybenzoic acid treatments, while the CO₂ emission in the 4-hydroxybenzaldehyde and 4-hydroxy-3-methoxybenzaldehyde treatments was much lower (Fig. II.2). The CO₂ emission was

always much higher from the reaction of NO₂⁻ with oxidized lignin units (i.e. lignin-derived acids) than their corresponding reduced lignin units (i.e. lignin-derived aldehyde).

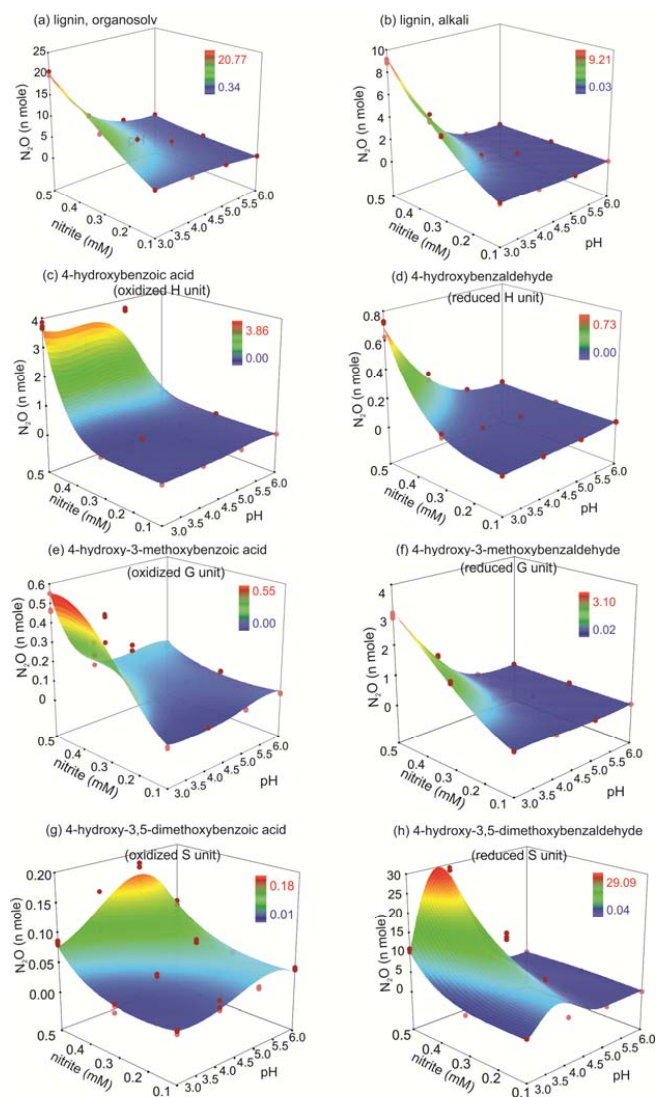


Fig. II.1. Response surface plots of N₂O emission from the reaction of NO₂⁻ with lignin and lignin derivatives in dependence on pH and NO₂⁻ concentration. Red circles represent the measured values in each treatment.

What is more, S lignin units, which were represented by 4-hydroxy-3,5-dimethoxybenzoic acid and 4-hydroxy-3,5-dimethoxybenzaldehyde, were associated with much higher CO₂ emission than the other lignin units (Fig. II.2). Similar to N₂O emission, CO₂ emission from the eight treatments decreased

nonlinearly with descending NO₂⁻ concentration, but the pH dependence of CO₂ emission varied according to the structure of the carbon substances. The highest CO₂ emission was found at pH 3 in the organosolv and alkali lignin, 4-hydroxy-3-methoxybenzaldehyde, and 4-hydroxy-3,5-dimethoxybenzaldehyde treatments, while at around pH 5 in the treatments of 4-hydroxybenzaldehyde and 4-hydroxy-3-methoxybenzoic acid. Pearson correlation analysis revealed that CO₂ emission was significantly ($P < 0.01$) positively correlated with N₂O emission.

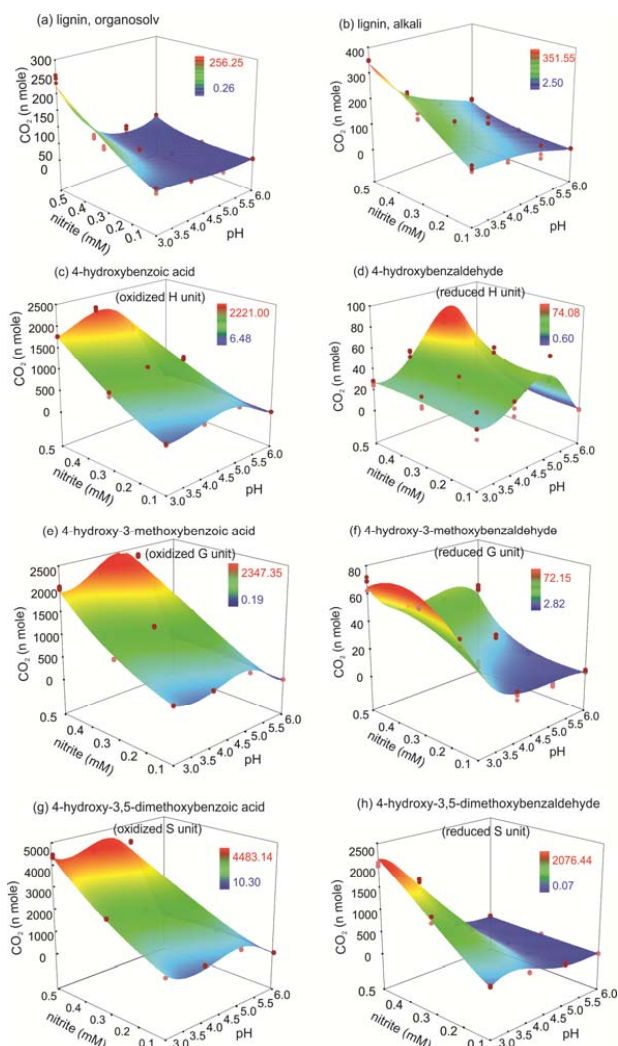


Fig. II.2. Response surface plots of CO₂ emission from the reaction of NO₂⁻ with lignin and lignin derivatives in dependence on pH and NO₂⁻ concentration. Red circles represent the measured values in each treatment.

II.3.2 N₂O isotopic signatures

Contrary to the assumption that the SP value of N₂O from a certain source process remains constant, the SP values of N₂O from chemodenitrification mediated by different lignin forms and lignin derivatives varied significantly in a range from 11.9 to 37.4 ‰ from pH 3 to 5 (Fig. II.3a). The SP values were significantly affected by pH ($P < 0.05$), but there was no constant trend in the eight treatments. The N₂O SP value was 21.1 ± 1.2 ‰ at pH 3, and increased to 29.5 ± 0.7 ‰ and 35.0 ± 1.9 ‰ at pH 4 and 5, respectively, in the 4-hydroxy-3-methoxybenzoic acid treatment (Fig. II.3a). Similarly, the SP values in the treatments of organosolv lignin and 4-hydroxybenzaldehyde also increased significantly ($P < 0.05$) from pH 3 to 5 (Fig. II.3a). By contrast, the SP value of N₂O from the reaction of NO₂⁻ with 4-hydroxybenzoic acid increased from 11.9 ± 1.7 ‰ at pH 3 to 34.2 ± 1.3 ‰ at pH 4, and decreased to 19.8 ± 1.5 ‰ at pH 5 (Fig. II.3a). In contrast to the significant changes of SP values at the different pH levels, no significant ($P > 0.05$) change of SP values was found when the concentration of sodium NO₂⁻ decreased from 0.3 to 0.5 mM (Fig. II.3b). The changes of SP values along pH did not only result from the shifts of $\delta^{15}\text{N}^{\alpha}$ values (-21.0 to 8.7 ‰), but also from $\delta^{15}\text{N}^{\beta}$ values (-48.0 to -16.5‰), both of which varied with increasing pH (Table II.1). Pearson correlation analysis showed that the $\delta^{15}\text{N}^{\alpha}$ values were positively correlated with the corresponding $\delta^{15}\text{N}^{\beta}$ values ($P < 0.01$), while the SP values were positively correlated with $\delta^{15}\text{N}^{\alpha}$ ($P < 0.01$), but negatively correlated with $\delta^{15}\text{N}^{\beta}$ ($P < 0.05$) (Table II.2, Fig. A3). The N₂O SP values were neither significantly ($P > 0.05$) different between organosolv and alkali lignin nor between reduced and oxidized lignin units (Fig. A6). However, both $\delta^{15}\text{N}^{\alpha}$ and $\delta^{15}\text{N}^{\beta}$ values were significantly different ($P < 0.05$) between organosolv lignin and alkali lignin, and between two G lignin units (Fig. A7 and A8).

The value of ¹⁵N net isotopic effect ($\Delta^{15}\text{N}^{\text{bulk}}$) was estimated by subtracting $\delta^{15}\text{N}\text{-NO}_2^-$ from $\delta^{15}\text{N}^{\text{bulk}}\text{-N}_2\text{O}$, while the ¹⁸O net isotopic effect ($\Delta^{18}\text{O}$) was calculated by subtracting $\delta^{18}\text{O}\text{-NO}_2^-$ from $\delta^{18}\text{O}\text{-N}_2\text{O}$ (Coplen, 2011). The values of $\Delta^{15}\text{N}^{\text{bulk}}$ and $\Delta^{18}\text{O}$ were affected by both pH and NO₂⁻ concentration. The highest $\Delta^{15}\text{N}^{\text{bulk}}$ value (11.4 ‰) was found in the reaction of NO₂⁻ with organosolv lignin at pH 3, and lowest (-16.4 ‰) in the reaction of NO₂⁻ with 4-hydroxy-3,5-dimethoxybenzaldehyde at pH 5 (Table II.1). Compared with the precursor NO₂⁻, N₂O was generally enriched in ¹⁵N in the treatments of organosolv lignin, 4-hydroxybenzoic acid, and 4-hydroxy-3-methoxybenzoic acid, where $\Delta^{15}\text{N}^{\text{bulk}}$ was positive, but depleted in the other treatments where negative $\Delta^{15}\text{N}^{\text{bulk}}$ values were observed (Table II.1). Paired *t*-test analysis revealed that $\Delta^{15}\text{N}^{\text{bulk}}$ was significantly ($P < 0.01$) different between organosolv and alkali lignin treatments, and between the treatments of reduced and oxidized S lignin units (Fig. A4).

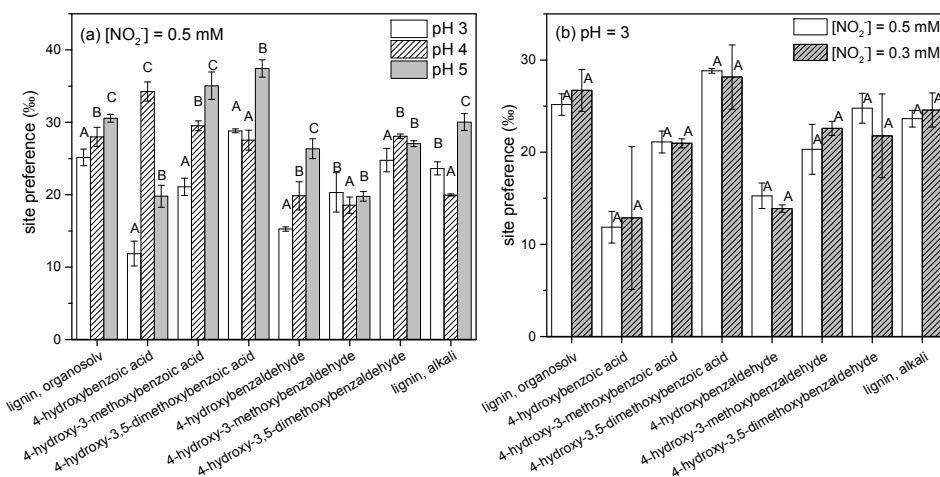


Fig. II.3. ¹⁵N site preference of N₂O from the reactions of NO₂⁻ with lignin and lignin derivatives at different pH (a) and NO₂⁻ concentrations (b). Each point is the mean value of three replicates. Capital letters represent significant differences ($P < 0.05$) between different pH and NO₂⁻ concentrations according to one-way ANOVA.

The highest and lowest $\Delta^{18}\text{O}$ value of 27.0 ‰ and 3.0 ‰, respectively, were observed in the reaction of NO₂⁻ with organosolv lignin at pH 3 and 4-hydroxybenzoic acid at pH 4 (Table II.1). By contrast with $\Delta^{15}\text{N}^{\text{bulk}}$, no significant difference ($P > 0.05$) was found between reduced and oxidized lignin units and the two lignin treatments (Fig. A5). The $\Delta^{15}\text{N}^{\text{bulk}}$ value was significantly ($P < 0.01$) positively correlated with both $\delta^{15}\text{N}^{\alpha}$ and $\delta^{15}\text{N}^{\beta}$, while no significant relationship was found between $\Delta^{18}\text{O}$ and any other isotopic signatures (Table II.2, Fig. A3a).

II.4 Discussion

II.4.1 Mechanisms involved in chemodenitrification

Nitrite is a highly reactive intermediate of both nitrification and denitrification. It has been shown that NO₂⁻ can react with various organic compounds, such as humic acid, fulvic acid and lignin-derived compounds, associated with the formation of N₂O, N₂ and CO₂ (Stevenson and Swaby, 1964). However, the activity of NO₂⁻ depends highly on the pH of the reaction system, but the knowledge how pH and NO₂⁻ concentration affect N₂O and CO₂ emission in reactions of NO₂⁻ with lignin and its derivatives is limited. The NO₂⁻ is relatively stable at neutral or higher pH, while at lower pH it can combine with H⁺ and form nitrous acid ($\text{H}^+ + \text{NO}_2^- \rightleftharpoons \text{HNO}_2$). The acid dissociation constant (pK_a) for this equilibrium is 3.29 at 25 °C, and at pH 3, 4, 5 and 6, the proportion of nitrous acid is 74, 16, 1.9 and 0.2 %, respectively (Allison, 1963; Porter, 1969). Since electrophilic attack of organic substances by the nitrosonium ion (NO⁺) derived from nitrous acid is a key step for the production of N₂O during chemodenitrification (Reactions [II.1–3]) (Austin, 1961), the N₂O emission decreased to almost zero

at pH 6 in our experiment. It can be concluded that chemodenitrification is most active in acidic soils where pH is under 6 if no catalysts or other strong reducing agents are present, and almost all lignin units can take part in chemical reactions with NO₂⁻ below pH 4, but the S lignin unit might be the main NO₂⁻-reactive lignin derivative between pH 4 and 6 (Fig. II.1).

The influence of plant litter on N₂O emission in agricultural soils has been studied previously (Frimpong and Baggs, 2010). In NO₂⁻-amended agricultural soils, N₂O emission was strongly and positively correlated with total SOC (Venterea, 2007), which is consistent with the current findings that reactions of SOM with NO₂⁻ lead to significant N₂O production. While commonly the considered factors were C-to-N ratio and (lignin + polyphenol)-to-N ratio, the influence of different lignin units has been neglected so far (Frimpong and Baggs, 2010; Garcia-Ruiz and Baggs, 2007; Millar and Baggs, 2004, 2005). According to our results, the reaction of NO₂⁻ with 4-hydroxy-3,5-dimethoxybenzaldehyde resulted in large N₂O emission, while only a small amount of N₂O was emitted from the reaction of NO₂⁻ with 4-hydroxy-3-methoxybenzaldehyde. The much higher N₂O emission from organosolv lignin than alkali lignin indicates that the structure of organosolv lignin favors N₂O formation in the reaction with NO₂⁻, e.g. the number of methoxy groups in the aromatic aldehyde rings might be higher, while it is lower in the aromatic acid rings. Therefore, the influence of different lignin units, i.e. the composition of SOM, on soil N₂O emissions should be considered in the future. During the degradation of lignin, the aromatic polymer is first hydrolyzed to aromatic aldehydes, and then the aldehydes are further oxidized to aromatic acids, thereby the lignin-derived acid-to-aldehyde ratios are generally used to indicate the degree of lignin decomposition (Hedges et al., 1988). Even though both 4-hydroxy-3,5-dimethoxybenzoic acid and 4-hydroxy-3,5-dimethoxybenzaldehyde are S units, the N₂O emission from 4-hydroxy-3,5-dimethoxybenzaldehyde was about 59 times higher than that from 4-hydroxy-3,5-dimethoxybenzoic acid at pH 3, hence, the contribution of each lignin unit to total chemodenitrification-derived N₂O emission might change during the process of lignin degradation. Since the N₂O production was much higher in 4-hydroxy-3-methoxybenzaldehyde and 4-hydroxy-3,5-dimethoxybenzaldehyde treatments than 4-hydroxybenzaldehyde, but much higher in 4-hydroxybenzoic acid than the other two acids, it is very likely that during the decomposition of lignin in soils, G and S aldehyde units are mainly responsible for the N₂O emission from abiotic NO₂⁻-lignin reactions at the beginning, while the H units contribute more to chemodenitrification-derived N₂O emission later when aldehydes are oxidized to aromatic acids. However more research is needed to explore the influence of lignin structure and degradation on N₂O and CO₂ emissions in laboratory and field studies.

Table II.1. Isotopic signatures of N₂O from the reactions of NO₂⁻ with lignin and lignin derivatives. The values were shown as mean ± standard deviation of three replicates.

	pH	[NO ₂ ⁻] (mM)	Δ ¹⁵ N ^{bulk a} (vs air-N ₂ , ‰)	Δ ¹⁸ O ^b (vs VSMOW, ‰)	δ ¹⁵ N ^a (vs air-N ₂ , ‰)	δ ¹⁵ N ^B (vs air-N ₂ , ‰)
C1 ^c	3	0.3	11.4 ± 0.1 ^{Cd}	27.0 ± 0.0 ^D	6.7 ± 0.2 ^C	-20.0 ± 0.0 ^C
	3	0.5	14.1 ± 0.5 ^D	24.8 ± 0.2 ^C	8.7 ± 1.0 ^D	-16.5 ± 0.6 ^D
	4	0.5	8.0 ± 0.1 ^B	17.9 ± 0.1 ^B	4.0 ± 0.6 ^B	-24.02 ± 0.7 ^B
	5	0.5	4.2 ± 0.1 ^A	14.7 ± 0.2 ^A	1.4 ± 0.2 ^A	-29.2 ± 0.3 ^A
C2	3	0.3	5.1 ± 1.3 ^{AB}	14.0 ± 1.8 ^B	-6.5 ± 2.7 ^A	-19.4 ± 5.1 ^A
	3	0.5	3.8 ± 0.8 ^A	13.0 ± 0.6 ^B	-8.3 ± 0.6 ^A	-20.2 ± 1.5 ^A
	4	0.5	9.6 ± 5.0 ^C	3.0 ± 0.7 ^A	8.7 ± 5.4 ^C	-25.6 ± 4.6 ^A
	5	0.5	8.6 ± 2.6 ^C	3.4 ± 0.4 ^A	0.5 ± 2.4 ^B	-19.3 ± 3.1 ^A
C3	3	0.3	-1.9 ± 0.3 ^A	17.2 ± 0.3 ^B	-9.5 ± 0.3 ^A	-30.4 ± 0.4 ^{AB}
	3	0.5	4.2 ± 0.3 ^A	4.3 ± 0.4 ^A	-3.3 ± 0.3 ^B	-24.4 ± 0.9 ^B
	4	0.5	2.9 ± 0.3 ^A	9.6 ± 1.0 ^{AB}	-0.4 ± 0.6 ^{BC}	-29.9 ± 0.3 ^{AB}
	5	0.5	4.2 ± 4.2 ^A	11.1 ± 5.9 ^{AB}	3.7 ± 4.3 ^C	-31.4 ± 4.4 ^A
C4	3	0.3	-4.8 ± 6.4 ^{AB}	16.8 ± 3.2 ^A	-8.8 ± 8.0 ^A	-37.0 ± 5.0 ^B
	3	0.5	-4.8 ± 0.6 ^{AB}	20.4 ± 0.7 ^A	-8.5 ± 0.4 ^A	-37.3 ± 0.7 ^B
	4	0.5	1.6 ± 1.0 ^B	16.7 ± 0.6 ^A	-2.7 ± 1.6 ^A	-30.3 ± 0.6 ^C
	5	0.5	-7.8 ± 0.3 ^A	16.5 ± 0.6 ^A	-7.1 ± 0.3 ^A	-44.6 ± 0.9 ^A
C5	3	0.3	-7.8 ± 0.6 ^A	14.9 ± 0.4 ^B	-19.0 ± 0.4 ^A	-32.8 ± 0.7 ^A
	3	0.5	-1.1 ± 0.8 ^{AB}	15.0 ± 0.1 ^A	-11.6 ± 1.0 ^{AB}	-26.8 ± 0.7 ^A
	4	0.5	-0.2 ± 6.9 ^{AB}	12.1 ± 1.4 ^A	-8.3 ± 7.4 ^B	-28.2 ± 6.5 ^A
	5	0.5	6.6 ± 1.8 ^B	20.4 ± 0.6 ^C	1.7 ± 1.8 ^C	-24.6 ± 2.0 ^A
C6	3	0.3	-9.8 ± 0.3 ^B	17.1 ± 0.7 ^B	-16.6 ± 0.5 ^{BC}	-39.1 ± 0.4 ^{AB}
	3	0.5	-8.1 ± 1.1 ^B	15.1 ± 2.4 ^{AB}	-16.1 ± 1.0 ^C	-36.4 ± 2.3 ^C
	4	0.5	-9.3 ± 1.0 ^B	13.1 ± 0.5 ^A	-18.1 ± 1.4 ^B	-36.7 ± 0.8 ^{BC}
	5	0.5	-12.5 ± 0.2 ^A	15.0 ± 0.1 ^{AB}	-20.7 ± 0.5 ^A	-40.5 ± 0.2 ^A
C7	3	0.3	-3.8 ± 4.6 ^B	17.3 ± 1.2 ^A	-11.0 ± 2.3 ^B	-32.8 ± 6.8 ^B
	3	0.5	-3.7 ± 5.3 ^B	18.8 ± 0.6 ^B	-9.4 ± 5.1 ^B	-34.2 ± 5.5 ^B
	4	0.5	-7.3 ± 2.1 ^B	20.9 ± 0.5 ^C	-11.4 ± 2.1 ^B	-39.5 ± 2.1 ^B
	5	0.5	-16.4 ± 0.0 ^A	21.6 ± 0.4 ^C	-21.0 ± 0.2 ^A	-48.0 ± 0.2 ^A
C8	3	0.3	-1.8 ± 0.1 ^C	19.8 ± 0.3 ^C	-6.9 ± 0.4 ^C	-32.8 ± 0.7 ^B
	3	0.5	0.2 ± 0.4 ^D	20.1 ± 0.4 ^C	-6.3 ± 0.4 ^C	-29.5 ± 0.5 ^C
	4	0.5	-6.4 ± 0.3 ^B	17.5 ± 0.0 ^B	-14.5 ± 0.4 ^A	-34.4 ± 0.3 ^B
	5	0.5	-9.1 ± 0.5 ^A	9.9 ± 0.8 ^A	-12.2 ± 0.4 ^B	-42.2 ± 1.0 ^A

Note:

^a¹⁵N net isotopic effect;

^b¹⁸O net isotopic effect;

^c C1, organosolv lignin; C2, 4-hydroxybenzoic acid (H unit); C3, 4-hydroxy-3-methoxybenzoic acid (G unit); C4, 4-hydroxy-3,5-dimethoxybenzoic acid (S unit); C5, 4-hydroxybenzaldehyde (H unit); C6, 4-hydroxy-3-methoxybenzaldehyde (G unit); C7, 4-hydroxy-3,5-dimethoxybenzaldehyde (S unit); C8, alkali lignin;

^d Capital letters represent the significant differences ($P < 0.05$) between different pH and NO₂⁻ concentration according to one-way ANOVA.

Decarboxylation, nitrosation, and cleavage of aromatic rings are involved in the formation of CO₂ and N₂O from reactions of NO₂⁻ with lignin-derived aromatic compounds. For example, in the case of 4-hydroxybenzoic acid, the carboxyl group is firstly replaced by a nitroso group with the formation of CO₂ and an oxime, which reacts further with another nitrous acid molecule, leading to the formation of a quinone and N₂O (Reaction [II.1]) (Stevenson, 1995; Thorn and Mikita, 2000).

When there is enough nitrous acid, the quinone can be further oxidized, resulting in the cleavage of the aromatic ring and formation of N₂, N₂O, and CO₂ (Reaction [II.2]) (Austin, 1961). When nitrous acid concentration is very low, traces of nitroxyl (HNO) could be formed by intramolecular interaction (Reaction [II.3]) (Austin, 1961), which can quickly dimerize to *cis*-hyponitrous acid (*cis*-HON=NOH) or *trans*-hyponitrous acid (*trans*-HON=NOH) which can further decompose to N₂O (Reaction [II.3]) (Fehling and Friedrichs, 2011). The N₂O should be formed through similar pathways in the other reactions of NO₂⁻ with lignin derivatives, namely the oxime pathway (Reaction [II.1]), the breakup of the aromatic ring (Reaction [II.2]), and dimerization of HNO as shown in Reaction [II.3]. The existence of methoxy groups in the G and S lignin units increases the electron density of the aromatic ring, hence facilitates the electrophilic attack by the nitrosonium ion with the formation a nitroso group. The nitroso group can not only lead to the production of N₂O but also NO. However, the nitroso group is also more easily eliminated to form NO from 4-nitroso-3-methoxyphenol and 4-nitroso-3,5-dimethoxyphenol than 4-nitrosophenol, which might explain the lower N₂O production in the 4-hydroxy-3-methoxybenzoic acid and 4-hydroxy-3,5-dimethoxybenzoic acid treatments compared to the 4-hydroxybenzoic acid treatment. On the contrary, the aldehydes could not undergo decarboxylation before being oxidized to acids, while the methoxy groups promote the oxidation of the aldehydes and furthermore facilitate N₂O production, which might explain the higher N₂O production in 4-hydroxy-3,5-dimethoxybenzaldehyde and 4-hydroxy-3-methoxybenzaldehyde treatments than 4-hydroxybenzaldehyde. Since the amount of NO₂⁻ was much less than organic substances in our experiment (0.5–2.5 of μmol NO₂⁻ vs 60 μmol of organic substances), the oxime pathway (Reaction [II.1]) might have dominated N₂O production, accompanied by trace N₂O formation through the breakdown of aromatic rings (Reaction [II.2]) and dimerization of HNO (Reaction [II.3]).

Table II.2. Pearson correlation coefficients of isotopic signatures of N₂O (n = 41).

	$\Delta^{15}\text{N}^{\text{bulk}}$ vs air-N ₂ ^a	$\Delta^{18}\text{O}$ vs VSMOW ^b	$\delta^{15}\text{N}^{\alpha}$ vs air-N ₂	$\delta^{15}\text{N}^{\beta}$ vs air-N ₂
$\Delta^{18}\text{O}$	-0.073			
$\delta^{15}\text{N}^{\alpha}$ vs air-N ₂	0.926 **	-0.020		
$\delta^{15}\text{N}^{\beta}$ vs air-N ₂	0.920 **	-0.118	0.703 **	
site preference	0.049	0.124	0.424 **	-0.346 *

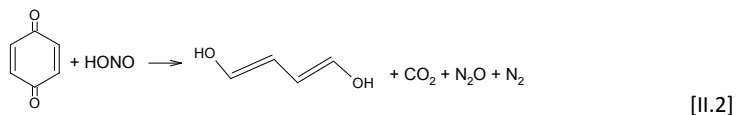
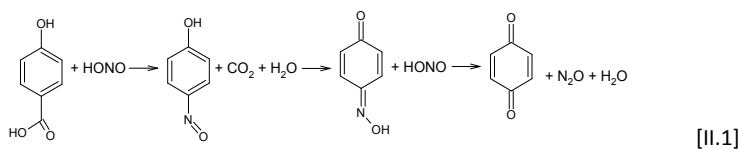
Note:

^a ¹⁵N net isotopic effect;

^b ¹⁸O net isotopic effect;

^c ¹⁵N site preference of N₂O;

** significant at 0.01 level, * significant at 0.05 level.



II.4.2 N₂O isotopic signatures

According to the isotope kinetic effect, the SP of N₂O from *cis*-hyponitrous acid decomposition is around 40 ‰, but -14 ‰ for the decomposition of *trans*-hyponitrous acid (Fehling, 2012). The kinetics of N₂O formation through the dimerization of HNO and decomposition of hyponitrous acid were pH dependent, involving an acid-base equilibrium of hyponitrous acid and hyponitrite (Bringas et al., 2016), hence pH might affect the SP value of N₂O from hyponitrous acid decomposition. On the other hand, the electronegativity of the aromatic compounds is also influenced by pH, which further acts on the processes of decarboxylation and nitrosation in Reaction [II.1] (Beaudoin and Wuest, 2016), and finally affects N₂O formation and its isotopic signature. Except for pH, the structure of organic substances, especially the number of methoxy groups, is another important factor influencing significantly the N₂O SP values (Table II.1, Fig. II.3a). The methoxy group can increase the electron density of the aromatic rings, thereby affecting the SP value of N₂O according to Reaction [II.1] in a similar way as pH. Above all, the reactions of NO₂⁻ with lignin derivatives are simultaneously influenced by the structure of organic substances and pH of the solution. However, the influence of NO₂⁻ concentration on SP, δ¹⁵N, and δ¹⁸O was only tested between 0.3 and 0.5 mM NO₂⁻ in this study, which was much lower than the concentration of lignin compounds. Therefore, a much wider NO₂⁻ concentration range should be explored in further studies.

The reduction of N₂O to N₂ can lead to ¹⁵N enrichment in N₂O (δ¹⁵N^{bulk}) by 5–26 ‰ as well as higher SP values (Toyoda et al., 2015). But neither strong chemical catalysts nor biological enzymes, that can catalyze the reduction of N₂O to N₂, were involved in the reactions here, so N₂O reduction was negligible. The SP value (11.9–37.4 ‰) of N₂O from chemodenitrification in this study covers the previously reported chemodenitrification sources of chemical NO₂⁻ reduction by ferrous iron (10–22 ‰) (Jones et al., 2015), the reaction of NO₂⁻ with trimethylamine borane (30 ‰) (Toyoda et al., 2005), the reaction of NO₂⁻ with SOM fractions (20–26 ‰) (Wei et al., 2017a), and the reaction of

NO₂⁻ with NH₂OH (34 ‰) (Heil et al., 2014). While the SP range in this study was absolutely not comparable with that of the abiotic N₂O source in the Antarctic Don Juan Pond (-45 to 4 ‰) (Samarkin et al., 2010), there could be another unknown chemodenitrification pathway that produces N₂O with low SP values. In addition, the observed SP values in this study are also comparable with the biotic N₂O sources of nitrification (27–37 ‰) (Sutka et al., 2006) and fungal denitrification (34 to 40 ‰) (Sutka et al., 2008), which makes it hard to separate the biotic and abiotic N₂O sources with SP (Fig. II.4).

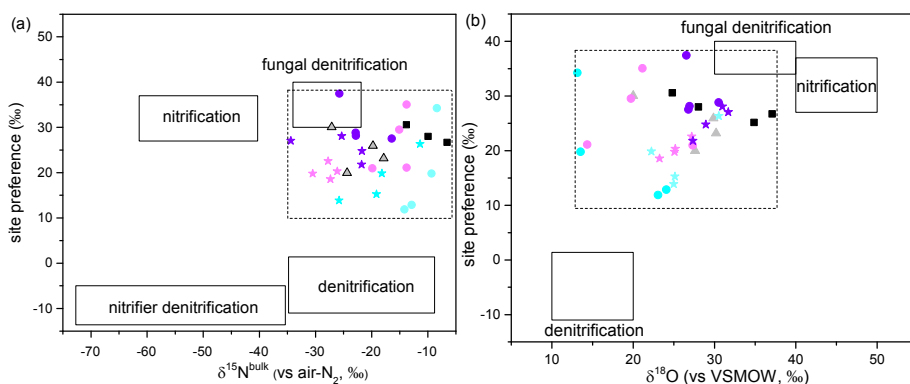


Fig. II.4. End-member maps of SP vs $\delta^{15}\text{N}^{\text{bulk}}$ (a) and $\delta^{18}\text{O}$ (b). The area in the dashed line represents chemodenitrification (SP values of 10 to 37 ‰, $\delta^{15}\text{N}^{\text{bulk}}$ values of -34 to -3 ‰, and $\delta^{18}\text{O}$ values of 13 to 35 ‰, data in this study and previously reported chemical assays) (Jones et al., 2015; Toyoda et al., 2005; Wei et al., 2017a). Nitrification is represented by SP values of 27 to 37 ‰, $\delta^{15}\text{N}^{\text{bulk}}$ values of -61 to -40 ‰, and $\delta^{18}\text{O}$ values of 40 to 50 ‰ (Sutka et al., 2006), fungal denitrification by SP values of 34 to 40 ‰, $\delta^{15}\text{N}^{\text{bulk}}$ values of -34 to -21.9 ‰, and $\delta^{18}\text{O}$ values of 30 to 40 ‰ (Sutka et al., 2008), bacterial denitrification by SP values of -11 to 1.4 ‰, $\delta^{15}\text{N}^{\text{bulk}}$ values of -34.8 to -8.8 ‰, and $\delta^{18}\text{O}$ values of 10 to 20 ‰ (Toyoda et al., 2005; Zou et al., 2014), and nitrifier denitrification by SP values of -13.6 to -5 ‰ and $\delta^{15}\text{N}^{\text{bulk}}$ values of -73 to -35 ‰ (Sutka et al., 2003). Black square, organosolv lignin; gray triangle, alkali lignin; blue symbols, H units; pink symbols, G units; violet symbols, S units; solid circles, acids; solid stars, aldehydes.

The $\delta^{15}\text{N}^{\text{bulk}}$ value of N₂O is simultaneously influenced by the $\delta^{15}\text{N}$ value of the precursor (NO₂⁻ in this study) and the net isotopic effect of ¹⁵N during the reduction, namely $\Delta^{15}\text{N}^{\text{bulk}}$. The $\Delta^{15}\text{N}^{\text{bulk}}$ values in this study (-16.4 to 14.1 ‰) were distinct from those of nitrifier denitrification (-39.5 to -31.4 ‰) (Sutka et al., 2003) and nitrification (-46.9 to -11.7 ‰) (Jung et al., 2014; Sutka et al., 2006). On the end-member map of SP vs $\delta^{15}\text{N}^{\text{bulk}}$, chemodenitrification is located in the mixing zone of fungal denitrification and bacterial denitrification, thereby overlapping with part of the fungal denitrification zone, which makes it impossible to quantify or even separate the N₂O sources located

in this area (Fig. II.4a). The significant positive correlations between $\Delta^{15}\text{N}^{\text{bulk}}$ and $\delta^{15}\text{N}^{\alpha}$ values, $\Delta^{15}\text{N}^{\text{bulk}}$ and $\delta^{15}\text{N}^{\beta}$ values, $\delta^{15}\text{N}^{\alpha}$ and $\delta^{15}\text{N}^{\beta}$ values, but negative correlation between SP and $\delta^{15}\text{N}^{\beta}$ values (Table II.2) indicate that $\delta^{15}\text{N}^{\alpha}$ and $\delta^{15}\text{N}^{\beta}$ might shift in a similar trend corresponding to pH and lignin structures, while the higher increase of $\delta^{15}\text{N}^{\beta}$ values than $\delta^{15}\text{N}^{\alpha}$ could be the main reason for the decrease of SP values, and vice versa, the higher decrease of $\delta^{15}\text{N}^{\beta}$ values than $\delta^{15}\text{N}^{\alpha}$ could account for the increase of SP values.

The $\delta^{18}\text{O}$ value of N₂O is affected by the $\delta^{18}\text{O}$ value of its precursor, the net isotopic effect of oxygen, and the oxygen exchange between water and the nitrogenous oxides (Toyoda et al., 2015). Thus, the $\Delta^{18}\text{O}$ value in this study is the combined result of the oxygen net isotopic effect and oxygen exchange. In this study, the $\delta^{18}\text{O}$ values varied from 3.0 to 27.0 ‰ (Table II.1), which was in a similar range as bacterial denitrification (4–27 ‰) (Toyoda et al., 2005). Kool et al. (Kool et al., 2007; Kool et al., 2009) assume that more than 97 % of the N₂O oxygen originates from water through abiotic and biotic oxygen exchange between water and nitrogenous oxides. The oxygen exchange during denitrification is mainly mediated by nitrite reductase (NIR), and fungal NIR could lead to up to 30 ‰ higher $\delta^{18}\text{O}$ value than bacterial NIR (Lewicka-Szczebak et al., 2016). However, the $\delta^{18}\text{O}$ values of N₂O are not distinguishable between NH₂OH oxidation and NO₂⁻ reduction by nitrifiers (Snider et al., 2012). The $\delta^{18}\text{O}$ values of N₂O in this study (13 to 35 ‰) overlap with most of the bacterial denitrification (10 to 20 ‰) and fungal denitrification (30 to 40 ‰) ranges (Sutka et al., 2008; Toyoda et al., 2005; Zou et al., 2014). Similar to the end-member map of SP vs. $\Delta^{15}\text{N}^{\text{bulk}}$, chemodenitrification was also located in the mixing zone of fungal denitrification and bacterial denitrification on the end-member map of SP vs. $\delta^{18}\text{O}$, and overlapped with most of the fungal denitrification zone (Fig. II.4b). Consequently, end-member map analysis appears of only very limited use for N₂O source partitioning in case chemodenitrification accounts for a substantial part of N₂O emission from soil. A more sophisticated model for N₂O source partitioning should be developed, and more basic data about N₂O isotopic signatures from abiotic reactions, microbial cultures, laboratory soil incubations, and field monitoring are needed to develop such a model.

II.5 Conclusions

This study reported simultaneous CO₂ and N₂O emission from chemical reactions of NO₂⁻ with lignin and its derivatives, and the influence of pH and NO₂⁻ concentration on the isotopic signatures (SP, $\delta^{15}\text{N}^{\text{bulk}}$, and $\delta^{18}\text{O}$) of N₂O from these reactions were characterized for the first time. Both N₂O and CO₂ emissions varied largely depending on the structure of the lignin derivatives, pH, and NO₂⁻ concentration, hence the contribution of chemodenitrification to N₂O and CO₂ emissions in the field might be largely influenced by plant litter composition, soil pH, and NO₂⁻ concentration, which needs to be further explored in laboratory and field experiments.

Contrary to the assumption that N₂O SP values remain restricted to a well-defined range for a certain N₂O formation pathway, the SP values of N₂O from chemodenitrification in this study varied largely from 11 to 37 ‰ in the reactions of NO₂⁻ with lignin and its derivatives. pH and the structure of organic substances were two important factors affecting the SP value of N₂O, and the changes of SP values result from the non-synchronous shifts of δ¹⁵N^α and δ¹⁵N^β values. In addition, both δ¹⁵N^{bulk} and δ¹⁸O values of N₂O from chemodenitrification overlap with most of the mixing zone of bacterial denitrification and fungal denitrification, as well as with most of the fungal denitrification zone, on the end-member maps of SP vs δ¹⁵N^{bulk} and δ¹⁸O, respectively. These results provide important new information about the isotopic signatures of N₂O from chemodenitrification, and it is suggested that both SP and end-member maps are only of limited use for N₂O source partitioning when chemodenitrification is involved, and further research is needed to explore a more efficient model to distinguish and quantify different N₂O sources.

III. First real-time isotopic characterization of N₂O from chemodenitrification

Based on:

Wei, J., Ibraim, E., Brüggemann, N., Vereecken, H., Mohn, J., First real-time isotopic characterization of N₂O from chemodenitrification. *Manuscript in preparation.*

III.1 Introduction

Generally, microbial nitrification and denitrification conducted by bacteria, fungi, and archaea are regarded as main N₂O source processes. During nitrification, NH₄⁺ is first oxidized to NH₂OH by NH₄⁺ oxidizers, which is afterwards oxidized to NO₂⁻ catalyzed by hydroxylamine oxidoreductase (HAO), while N₂O is released as a byproduct of the second reaction step (Stein, 2011). In the case of denitrification, including bacterial denitrification, fungal denitrification, and nitrifier denitrification, N₂O is considered as an obligatory product of the reduction of NO by nitric oxide reductase (NOR) (Stein, 2011; Sutka et al., 2008). However, increasing evidence demonstrates that significant N₂O emission could also occur through abiotic pathways, namely the chemical oxidation of NH₂OH and reduction of NO₂⁻ (Heil et al., 2016; Zhu-Barker et al., 2015). Heil et al. (2015) suggested that N₂O from nitrification might be produced from the leakage of the nitrification intermediate NH₂OH with subsequent abiotic reaction with the soil matrix. Ostrom et al. (2016) reported that chemodenitrification, namely the abiotic reduction of NO₂, accounted for 4.11–4.18 nmol L⁻¹ d⁻¹ N₂O emission in the frozen Lake Vida, Victoria Valley, Antarctica. In addition, Venterea (2007) found that the chemical reduction of NO₂⁻ contributed 31–75 % to the total N₂O production in an agricultural soil when NO₂⁻ was applied. In their study, SOM was identified as the main reaction partner of NO₂⁻, and the total carbon content explained 84 % of the total variance in NO₂⁻-related N₂O emission in Waukegan silt loam soils (Venterea, 2007). In acidic spruce forest soils, the fulvic acid acted as the most reactive SOM fraction in chemodenitrification (Wei et al., 2017a). Therefore, the contribution of chemodenitrification, especially the abiotic reaction of NO₂⁻ with SOM, to global N₂O emissions could have been highly underestimated.

Both biotic and abiotic N₂O production vary according to a number of parameters, such as oxygen availability, moisture, and temperature affect biogenic activity, while chemical reactions depend on the diffusion of reactive intermediates, soil pH, and temperature. Hence, N₂O production is heterogeneous in soils, which consequently provides a major challenge and contributes significantly to the uncertainty of global N₂O source partitioning. Stable isotope techniques offer a tool to identify N₂O production pathways in the environment using N₂O isotopic signatures. Both δ¹⁵N^{bulk} and δ¹⁸O of N₂O are affected by fractionation effects and the isotopic signature of the substrate, while δ¹⁸O is additionally influenced by the O exchange of reaction intermediates with water (Kool et al., 2011). The δ¹⁵N^{bulk} values were about -46.5 ‰ when NH₄⁺ was oxidized to N₂O by AOB (Sutka et al., 2006), while it varied from -35 to -13 ‰ for N₂O produced from NH₄⁺ oxidation by archaea (Jung et al., 2014). When NO₂⁻ was reduced to N₂O, δ¹⁵N^{bulk} averaged at about -28 to -23 ‰ for nitrifier denitrification (Sutka et al., 2006; Sutka et al., 2003), but from -25 to -5 ‰ for fungal denitrification (Rohe et al., 2014; Sutka et al., 2008). Comparably, δ¹⁸O values varied from 30 to 40 ‰ and from 11 to 23 ‰ when NO₂⁻ was reduced to N₂O by fungi and bacteria, respectively (Frame and

Casciotti, 2010; Rohe et al., 2014; Sutka et al., 2008; Sutka et al., 2003). Since the two nitrogen atoms are located asymmetrically in the linear N₂O molecule (N^βN^αO), the difference of δ¹⁵N between the α and β position is defined as ¹⁵N site preference (SP): $SP \equiv \delta^{15}N^{\alpha} - \delta^{15}N^{\beta}$ (Toyoda and Yoshida, 1999). Compared with δ¹⁵N^{bulk} and δ¹⁸O, SP is thought to be more specific for the identification of N₂O production pathways because SP from a certain source is supposed to be stable and independent of the substrate (Toyoda and Yoshida, 1999; Toyoda et al., 2002). Microbial sources of nitrification and fungal denitrification, as well as chemical oxidization of NH₂OH feature relatively high SP values of 27 to 40 ‰ (Decock and Six, 2013; Heil et al., 2014; Rohe et al., 2014), while bacterial denitrification and nitrifier denitrification are characterized by low SP values of -11 to 1.4 ‰ (Frame and Casciotti, 2010; Sutka et al., 2006; Sutka et al., 2003; Toyoda et al., 2005). The reduction of N₂O to N₂ decreased δ¹⁵N values by -26 to -5 ‰, meanwhile increasing the SP value by about 5–8 ‰ due to the isotope effect of N-O bond cleavage (Lewicka-Szczebak et al., 2017; Ostrom et al., 2007). Based on these results N₂O isotopic signatures have been widely used to partition N₂O sources on both local and global scales (Bol et al., 2003; Snider et al., 2015; Wolf et al., 2015). End-member maps of SP vs. δ¹⁵N^{bulk} and SP vs. δ¹⁸O, on which different biotic N₂O production pathways are located separately, are regarded as efficient tools for N₂O source partitioning (Decock and Six, 2013; Toyoda et al., 2015). In the last years, end-member maps have been used to estimate the N₂O sources in urban river (Toyoda et al., 2009), agricultural soil (Toyoda et al., 2011), and waste water treatment (Wunderlin et al., 2013).

In spite of the fact that chemodenitrification accounts for significant N₂O emission under certain conditions, it is overlooked in the current end-member map models (Ostrom et al., 2016; Zhu-Barker et al., 2015). Wei et al. (2017a) found that both SP-δ¹⁵N^{bulk} and SP-δ¹⁸O end-member maps failed to identify the N₂O from chemodenitrification, and N₂O source attribution was strongly biased when the two-end-member mixing model was applied to source partitioning. In addition, SP values of N₂O from chemodenitrification varied significantly depending on different reactions and reaction conditions. The SP ranged from 10 to 22 ‰ for the abiotic reduction of NO₂⁻ by Fe²⁺ at neutral pH when oxygen was limiting (Jones et al., 2015), from 20 to 26 ‰ for the chemical reaction of NO₂⁻ with SOM at pH 3.4 (Wei et al., 2017a), around 30 ‰ for the reaction of NO₂⁻ with trimethylamine-borane and NH₂OH at pH 1 (Toyoda et al., 2005), and 34 to 35 ‰ for the chemical reaction of NH₂OH with NO₂⁻ at pH 3–6 (Heil et al., 2014). Interestingly, the SP of N₂O from abiotic reactions of NO₂⁻ with lignin derivatives was pH dependent rather than remaining stable (Wei et al., 2017b). Hence, more research is needed to explore the N₂O production from chemodenitrification and its isotopic composition, and to further explain the mechanisms behind the complicated pattern of variable SP values of N₂O from NO₂⁻-SOM reactions.

In this study the change in the site-specific isotopic composition of N₂O from chemical reactions of NO₂⁻ with SOM, as well as from NO₂⁻-related N₂O emissions from soil was investigated in real-time

by laser spectroscopy. Organosolv lignin and five lignin-derived aromatic acids and aldehydes were chosen as SOM representatives. N₂O concentration and isotopic composition were analyzed and the N₂O site specific isotopic composition was interpreted with respect to the proposed N₂O formation pathways via hyponitrous acid and nitramide.

III.2 Materials and Methods

III.2.1 Laser spectroscopic analysis of N₂O isotopic composition

The laser spectrometer used in this study is a commercially available QCLAS (CW-QC-TILDAS-76-CS; Aerodyne Research Inc., Billerica, USA) that has been customized for simultaneous analysis of the four most abundant N₂O isotopic species, i.e. ¹⁴N¹⁴N¹⁶O, ¹⁴N¹⁵N¹⁶O, ¹⁵N¹⁴N¹⁶O, and ¹⁴N¹⁴N¹⁸O, respectively (Ibraim et al., 2017). The spectrometer comprises a continuous-wave mid-infrared quantum cascade laser source (Alpes Lasers SA, Switzerland) emitting at 2203 cm⁻¹ and an astigmatic multi-pass absorption cell with a path length of 76 m and a cell volume of 0.62 L. Laser control, data acquisition and quantification of the N₂O isotopic species are performed using the TDL Wintel software (Aerodyne Research Inc., Billerica, USA). The spectrometer was operated in a flow-through mode with a temporal resolution of 1 Hz used for data acquisition. The Allan variance precision of the spectrometer for ratios of isotopic species R^α (¹⁴N¹⁵N¹⁶O / ¹⁴N¹⁴N¹⁶O), R^β (¹⁵N¹⁴N¹⁶O / ¹⁴N¹⁴N¹⁶O) and R^{18O} (¹⁴N¹⁴N¹⁸O / ¹⁴N¹⁴N¹⁶O) with 1250 s spectral averaging was less than 0.1 ‰ (one sigma standard deviation) (Werle et al., 1993) (Fig. B1). The gas flow through the QCLAS gas cell was adjusted to 12 ml min⁻¹ and the cell pressure to 26.67 ± 0.01 hPa using a back pressure controller (MKS Instruments, Andover, MA USA). Analyzed isotope ratios of samples, e.g. ¹⁴N¹⁵N¹⁶O/¹⁴N¹⁴N¹⁶O, were corrected using a two point calibration approach with calibration gas 1 (CG1): δ¹⁵N^α = -22.21 ± 0.39 ‰, δ¹⁵N^β = -49.28 ± 0.40 ‰, δ¹⁸O = 26.94 ± 0.23 ‰ and calibration gas 2 (CG2): δ¹⁵N^α = -0.13 ± 0.28 ‰, δ¹⁵N^β = 1.35 ± 0.29 ‰, δ¹⁸O = 38.46 ± 0.15 ‰. Calibration gases were prepared in synthetic air (20 % of O₂, 80 % of N₂, 99.999 % purity, Messer Schweiz AG, Switzerland) as described in Wächter et al. (2008) and calibrated against standard gases which were primarily analyzed by Sakae Toyoda at Tokyo Institute of Technology. For two-point calibration, CG1 and CG2 were diluted to 36 ppm using mass flow controllers (described below). Selection of sample versus calibration gas was conducted by two 3-way solenoid valves (series 9, Parker Hannifin, USA). To account for drift effects of the laser spectrometer CG1, diluted to 35 ppm N₂O, was analyzed every 35 min for 10 min. Nonlinearity effects of N₂O concentration on isotope ratios were determined, before and after each experiment, analyzing CG1 at 12, 25, 36, 45, 54, 68, 82 ppm N₂O and corrected as described below.

III.2.2 Experimental setup

The experimental setup for online N₂O isotopocule measurement is illustrated in Fig. III.1. A

quartz glass chamber with a polytetrafluoroethylene (PTFE) cover plate was used as reaction chamber. To increase the temporal responsivity of the setup, the reactor volume was reduced to 300 ml, inserting a polypropylene hollow cylinder. In addition, a fan was installed at the top of the chamber to ensure that the headspace gas phase was homogeneously mixed. The absence of significant leaks ($< 100 \text{ Pa min}^{-1}$ at 0.1 MPa overpressure) was assured through a leak test before every experiment. Gas flows in the setup were controlled using five mass flow controllers (MFCs, Redy Smart series, Vögtlin Instruments, Switzerland) and a number of two- and three-position solenoid valves (Parker Hannifin Corp., USA). The experimental setup was controlled via a custom-written LabVIEW code (National Instruments Corp., USA), and devices were connected via a 16-port serial-to-ethernet network connector (Etherlite 160, Digi International Inc., USA).

The reactor was continuously purged with $14\text{--}16 \text{ ml min}^{-1}$ synthetic air (20 % of O₂, 80 % of N₂, 99.999 % purity, Messer Schweiz AG, Switzerland) to transfer the liberated process gases (NO, N₂O, CO, CO₂, etc.) towards the spectrometer. The sample gas flow was dehumidified using a Nafion permeation dryer (MD-050-72S-1, Perma Pure, USA) and the overflow, not subjected to laser spectroscopic analysis, was exhausted into the hood. Thereby the pressure of the chamber system was kept constant at ambient pressure. CO₂ was removed from the process gas with a trap containing 13.8 g Ascarite (10–35 mesh, Fluka, Switzerland), bracketed with magnesium perchlorate (Mg(ClO₄)₂, $2 \times 3.5 \text{ g}$, Fluka, Switzerland). Absorbents were separated with glass wool (BGB Analytics AG, Switzerland). Thereafter, carbon monoxide (CO) was removed with a Sofnocat oxidation catalyst (Sofnocat 423, Molecular Products Ltd., United Kingdom), as CO would otherwise induce spectral interferences during QCLAS analysis. For N₂O concentrations in the sample gas above 82 ppm, the sample gas was diluted by adding an additional flow of synthetic air through MFC1 and the (initial) N₂O concentration was calculated by multiplying the measured N₂O concentration with a dilution factor. Since nitric oxide (NO) can also be produced together with N₂O in the reactions, the absence of spectral interferences by NO was assured by a pre-test, where 50 ppm NO were added to a N₂O calibration gas. No significant change in the analyzed N₂O isotopic composition was observed.

III.2.3 Experimental procedure

Sodium nitrite ($\delta^{15}\text{N} = -18.00 \pm 0.08 \text{ ‰}$, $\delta^{18}\text{O} = 10.09 \pm 0.05 \text{ ‰}$, VWR, Germany) was used as the NO₂⁻ source. Organosolv lignin (chemicalpoint, Germany), 4-hydroxybenzoic acid, 4-hydroxy-3-methoxybenzoic acid, 4-hydroxy-3,5-dimethoxybenzoic acid, 4-hydroxy-3-methoxybenzaldehyde, and 4-hydroxy-3,5-dimethoxybenzaldehyde (VWR, Germany) were chosen as model carbon substances. All chemicals were reagent grade or better. Forest soil and grassland soil were sampled from the Oa layer of the Wüstebach catchment (50°30'15"N, 6°18'15"E) and the Rollesbroich grassland (50°37'0"N, 6°26'0"E), respectively, in Eifel National Park, Germany. The sites are part of

the German interdisciplinary program TERENO (Zacharias et al., 2011). Agricultural soil was sampled from the top layer of Achterwehr field (54°19'05"N, 9°58'38"E), Kiel, Germany. The characteristics of all soils are listed in Table B1.

A 100-ml beaker containing 5–26 g carbon substances (or soil) and a stir bar was put into the chamber. Then, the whole setup was flushed using 18 ml min⁻¹ synthetic air until the N₂O mole fraction signal stabilized at around zero. Afterwards a certain amount of NaNO₂ dissolved into 50 ml ultrapure water (18.2 MΩ cm) was injected into the beaker through a rubber septum on top of the chamber. A magnetic stirrer was used to mix the carbon substance or soil with the NaNO₂ solution for 5 min and then allowed to settle for the rest of the experiment. Experimental details for each treatment (amount of carbon substances/soils and NaNO₂, and flow rate of the carrier gas) are listed in Table B2.

III.2.4 Data analysis

N₂O isotopocule ratios R^α, R^β and R^{18O} were calculated based on concentration values obtained with TDL Wintel. Thereafter, R values were converted to the δ-notation using Matlab R2014b (MathWorks, Inc., USA) applying the following formula:

$$\delta_s = \left(\frac{R_s}{R_{c1}} - 1 \right) \times 1000 \times \frac{\delta_{c1} - \delta_{c2}}{\left(\frac{R_{c1}}{R_{c2}} - 1 \right) \times 1000} + \delta_{c1} \quad [\text{III.1}]$$

δ_s, δ_{c1}, and δ_{c2} denote the δ (δ¹⁵N^α, δ¹⁵N^β, and δ¹⁸O) values of sample, CG1, and CG2, respectively, while R_s, R_{c1}, and R_{c2} (R^α, R^β and R¹⁸O) are the isotope ratios of sample, and CG1 and CG2, respectively. Firstly, a drift correction was applied to all data based on regular measurements of CG1 at 36 ppm N₂O. Then, a stepwise regression was used to correct the N₂O concentration dependency of δ¹⁵N^α, δ¹⁵N^β, and δ¹⁸O (Fig. B2). The dependency of δ values (δ¹⁵N^α, δ¹⁵N^β, and δ¹⁸O) on N₂O concentration from 12 to 45 ppm (*f_{low}*) and from 36 to 83 ppm (*f_{high}*) was calculated using a third-order polynomial regression. The R² values were higher than 0.99 for all the *f_{low}* and *f_{high}* and the differences of δ values calculated by *f_{low}* and *f_{high}* at intermediate N₂O concentrations (36 to 45 ppm) were lower than 0.5 ‰ (Fig. B2), which indicates that both *f_{low}* and *f_{high}* were well fitted. N₂O concentration dependency was corrected according to the following equation:

$$\delta_{s-corr} = f(C_{c1}) - f(C_s) + \delta_s \quad [\text{III.2}]$$

In equation [III.2], δ_s is the δ value of the samples as calculated based on eq. III.1, C_{c1} is the average concentration of all the CG1 measurements at around 36 ppm, C_s denotes the N₂O mixing ratio of the samples, and *f* denotes *f_{low}* when C_s is equal to or lower than 36 ppm but *f_{high}* when higher than 36

ppm. The $\delta^{15}\text{N}^{\text{bulk}}$ was calculated as the average of $\delta^{15}\text{N}^{\alpha}$ and $\delta^{15}\text{N}^{\beta}$, namely, $\delta^{15}\text{N}^{\text{bulk}} \equiv (\delta^{15}\text{N}^{\alpha} + \delta^{15}\text{N}^{\beta}) / 2$, while SP was determined using $\text{SP} \equiv \delta^{15}\text{N}^{\alpha} - \delta^{15}\text{N}^{\beta}$. The net N isotopic effect $\Delta^{15}\text{N}$ was calculated by the $\delta^{15}\text{N}$ difference of N₂O and NO₂⁻: $\Delta^{15}\text{N} = \delta^{15}\text{N}^{\text{bulk}}_{\text{N}_2\text{O}} - \delta^{15}\text{N}_{\text{NO}_2^-}$, while net O isotopic effect $\Delta^{18}\text{O}$ was calculated according to: $\Delta^{18}\text{O} = \delta^{18}\text{O}_{\text{N}_2\text{O}} - \delta^{18}\text{O}_{\text{NO}_2^-} - \delta^{15}\text{N}^{\text{bulk}}_{\text{N}_2\text{O}}$. The relative N₂O emission rate $R_{\text{N}_2\text{O}}$ ($\mu\text{g N g}^{-1} \text{NO}_2^- \text{h}^{-1}$) was calculated as follows:

$$R_{\text{N}_2\text{O}} = \frac{\int_{t_0}^t \frac{C_{\text{N}_2\text{O}} \times P \times f}{R \times T}}{(t - t_0) \times M_{\text{NO}_2^-}} \quad [\text{III.3}]$$

$C_{\text{N}_2\text{O}}$, the mixing ratio of N₂O at each time point; P , the pressure in the reaction chamber, equivalent to the ambient laboratory pressure; f , the flow rate of the synthetic air carrier gas; R , ideal gas constant; T , gas phase temperature in the reaction chamber; $M_{\text{NO}_2^-}$, the weight of applied NO₂⁻; t_0 and t , the starting and ending time of the calibrated period, respectively; the intervals of each measurement were estimated by linear regression.

III.3 Results

III.3.1 N₂O emissions and isotopic composition from reactions of NO₂⁻ with lignin derivatives

In the reaction of NO₂⁻ with organosolv lignin, about 8 % of NO₂⁻ was converted to N₂O within 4 h, accounting for the highest relative N₂O emission rate, while the lowest relative N₂O emission rate occurred in the treatment of 4-hydroxy-3-methoxybenzaldehyde (Table III.1). The N₂O emission rate within the first two hours (0–2 h) was much lower than that of 2–4 h in the NO₂⁻ reaction with 4-hydroxybenzoic acid, but higher in the reaction with 4-hydroxy-3,5-dimethoxybenzoic acid, while they were relatively similar with each other in both 4-hydroxy-3,5-dimethoxybenzaldehyde and 4-hydroxy-3-methoxybenzaldehyde treatments (Table III.1). The N₂O mixing ratio peaked at about 0.8 h in 4-hydroxy-3,5-dimethoxybenzoic acid treatment (Fig. III.3a), which was approximately 2 h earlier compared with 4-hydroxy-3,5-dimethoxybenzaldehyde (Fig. III.4a), 1 and 3 h earlier than 4-hydroxy-3-methoxybenzoic acid (Fig. B4) and 4-hydroxybenzoic acid (Fig. B3), respectively.

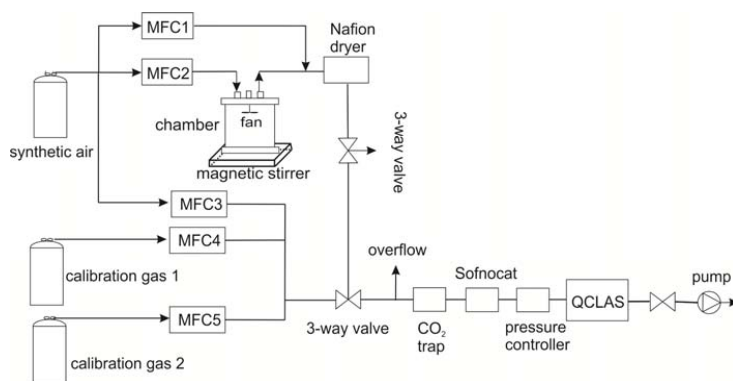


Fig. III.1. Schematic diagram of the setup used for real-time measurements of N_2O isotopic species by QCLAS.

Large variability of SP values (5.6 to 29.0 ‰) was observed in reactions of NO_2^- with different lignin derivatives, and most interestingly, SP of N_2O from the same reaction also changed substantially along time (Table III.1, Fig. III.2–5). In the case of organosolv lignin and 4-hydroxy-3,5-dimethoxybenzaldehyde, SP values increased substantially in 0–4 h (Fig. III.2 and 4). However, the SP of N_2O shifted unregularly in the reaction of NO_2^- with 4-hydroxy-3,5-dimethoxybenzoic acid, where sharp decreases were observed at about 1 and 3 h (Fig. III.3). By contrast, SP remained relatively stable over the reaction period of 1–6 h for the reaction of NO_2^- with 4-hydroxy-3-methoxybenzaldehyde (Fig. B5). The changes of SP values were either caused by opposing trends of $\delta^{15}N^{\alpha}$ and $\delta^{15}N^{\beta}$ or incomparable changes of both parameters, e.g. the increasing SP at 2–6 h in the organosolv lignin treatment resulted from the quicker increase of $\delta^{15}N^{\alpha}$ than $\delta^{15}N^{\beta}$ (Fig. III.2), while the rapidly decreasing SP at 2.5–3 h in the 4-hydroxy-3,5-dimethoxybenzoic acid treatment was caused by a simultaneous decrease and increase in $\delta^{15}N^{\alpha}$ and $\delta^{15}N^{\beta}$, respectively (Fig. III.3). Differences of N_2O concentration-weighted averages of $\delta^{18}O$ values between treatments were slightly smaller than those for SP values (Table III.1). The N_2O concentration-weighted average of $\delta^{18}O$ ranged from 22.7 to 30.0 ‰ between treatments, corresponding with a mean $\Delta^{18}O$ value from 12.6 to 19.9 ‰, while concentration-weighted average SP varied from 14.8 to 24.7 ‰.

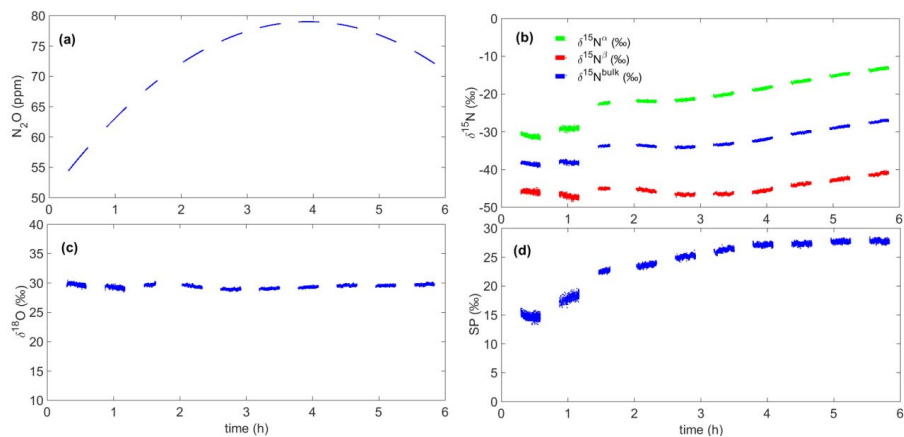


Fig. III.2. Reaction of NO_2^- with organosolv lignin. (a) N_2O mixing ratio, (b) $\delta^{15}N^\alpha$, $\delta^{15}N^\beta$, and $\delta^{15}N^{bulk}$ of N_2O , (c) $\delta^{18}O$ of N_2O , and (d) N_2O ^{15}N site preference.

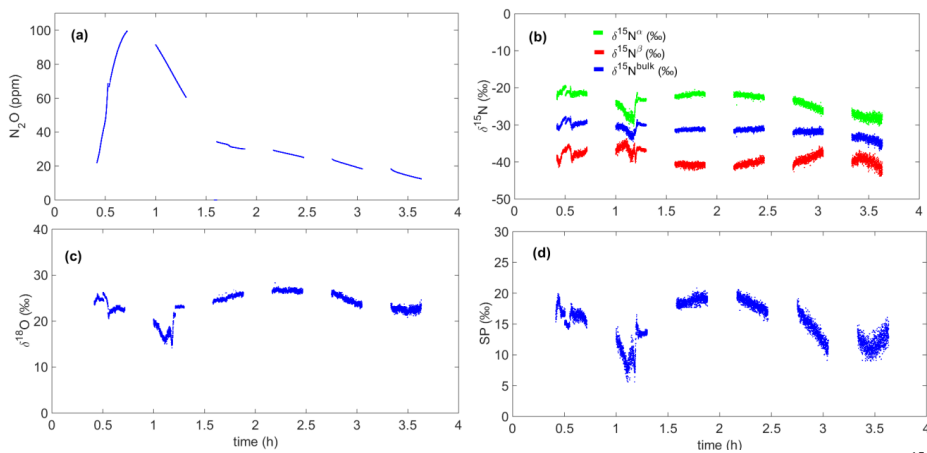


Fig. III.3. Reaction of NO_2^- with 4-hydroxy-3,5-dimethoxybenzoic acid. (a) N_2O mixing ratio, (b) $\delta^{15}N^\alpha$, $\delta^{15}N^\beta$, and $\delta^{15}N^{bulk}$ of N_2O , (c) $\delta^{18}O$ of N_2O , and (d) N_2O ^{15}N site preference.

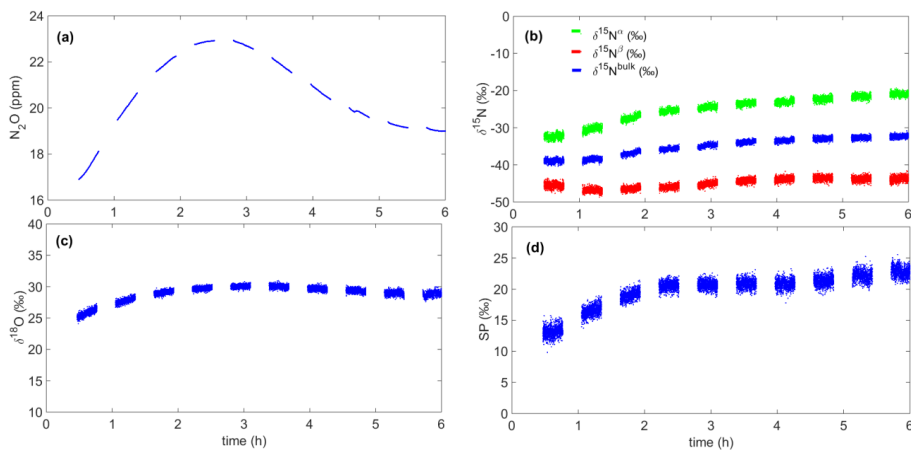


Fig. III.4. Reaction of NO₂⁻ with 4-hydroxy-3,5-dimethoxybenzaldehyde. (a) N₂O mixing ratio, (b) δ¹⁵N^α, δ¹⁵N^β, and δ¹⁵N^{bulk} of N₂O, (c) δ¹⁸O of N₂O, and (d) N₂O ¹⁵N site preference.

Table III.1. δ¹⁵N^{bulk}, δ¹⁸O, and ¹⁵N site preference values of N₂O from the reaction of NO₂⁻ with organics and soils.

Treatment	δ ¹⁵ N ^{bulk} (‰)			δ ¹⁸ O (‰)			SP (‰)			R _{N2O} ^b (μg N g ⁻¹ NO ₂ ⁻ h ⁻¹)	
	Max	Min	Avg. ^a	Max	Min	Avg.	Max	Min	Avg.	0–2 h	2–4 h
Lignin, organosolv	-26.6	-39.4	-32.5	30.5	28.5	29.4	28.5	13.5	24.7	3351	4224
4-hydroxybenzoic acid	-30.2	-40.3	-34.7	27.8	17.9	23.4	27.2	8.9	20.3	16.5	23.0
4-hydroxy-3-methoxybenzoic acid	-28.2	-35.9	-32.1	31.2	20.9	24.2	24.2	10.6	16.4	12.7	15.3
4-hydroxy-3,5-dimethoxybenzoic acid	-27.7	-36.9	-30.8	28.3	14.2	22.7	20.8	5.6	14.8	25.2	8.4
4-hydroxy-3-methoxybenzaldehyde	-32.8	-38.8	-35.2	28.6	23.3	25.2	29.0	12.7	18.8	2.0	2.4
4-hydroxy-3,5-dimethoxybenzaldehyde	-30.9	-40.4	-35.0	30.9	24.1	29.0	25.5	9.8	19.8	4.4	4.4
Agricultural soil	-33.1	-41.8	-35.6	29.6	23.6	27.6	27.5	15.6	22.9	17.3	9.2
Forest soil	-32.2	-36.0	-34.3	32.0	28.2	30.0	22.0	15.9	19.2	31.5	31.2
Grassland soil	-34.1	-44.2	-39.1	29.2	20.2	23.8	22.4	10.9	16.1	13.3	14.4

Note:

^a Average values were concentration-weighted over the complete experimental run.

^b N₂O emissions relative to NO₂⁻ addition.

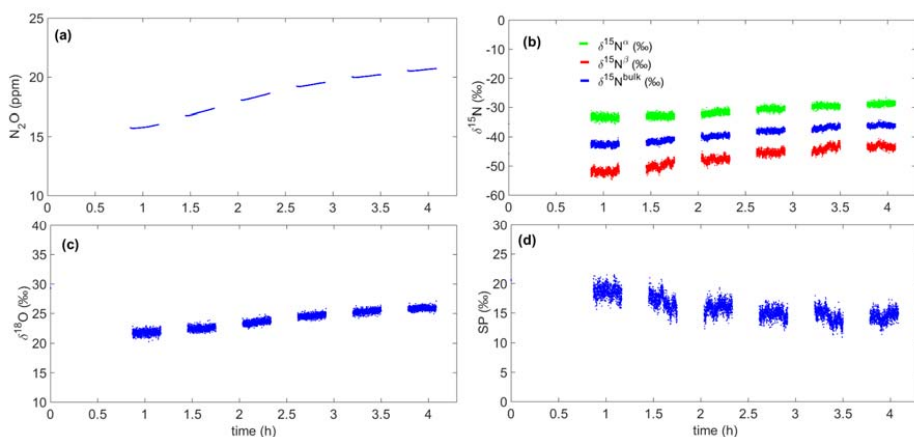


Fig. III.5. N_2O emission and its isotopic composition in grassland soil after NO_2^- application. (a) N_2O mixing ratio, (b) $\delta^{15}N^\alpha$, $\delta^{15}N^\beta$, and $\delta^{15}N^{bulk}$ of N_2O , (c) $\delta^{18}O$ of N_2O , and (d) N_2O ^{15}N site preference.

III.3.2 N_2O emissions and isotopic signature from NO_2^- reactions with soil

The relative N_2O emission rates of both 0–2 and 2–4 h for forest soil were much higher compared with agricultural and grassland soils (Table III.1). The relative N_2O emission rates of all the soil treatments, however, were much lower than that of organosolv lignin, but much higher than that of 4-hydroxy-3-methoxybenzaldehyde and 4-hydroxy-3,5-dimethoxybenzaldehyde. The concentration-weighted averaged SP of N_2O from soils ranged from 16.6–22.9 ‰, which was in the SP range of N_2O from NO_2^- reactions with lignin derivatives. Similarly, $\delta^{18}O$ and $\Delta^{18}O$ of N_2O from soils after NO_2^- application were comparable with data of NO_2^- -lignin derivative reactions. $\delta^{15}N^{bulk}$ and $\Delta^{15}N$ were slightly lower in grassland soil compared with the treatments of lignin derivatives, while values for agricultural and forest soil were similar in magnitude (Table III.1). Changes in N_2O SP values were also found in all the three types of soils. In both forest and grassland soil, SP values of N_2O varied between 10–22 ‰, which was slightly lower than the 15–27 ‰ in agricultural soil (Fig. III.5, B6, B7). In forest soil, $\delta^{18}O$ and $\delta^{15}N^{bulk}$ of N_2O remained relatively stable at around 30 ‰ and -34 ‰, respectively (Fig. B6), while they increased steadily from 20 ‰ to 29 ‰ and from -44 ‰ to -34 ‰, respectively, in grassland soil (Fig. III.5).

III.4 Discussion

III.4.1 Pathways of N_2O formation and impact on N_2O production rate

Two different pathways, a hyponitrous acid pathway or a nitramide pathway (Fig. III.6) (Austin, 1961; Kainz and Huber, 1959), are discussed in relation to NO and N_2O formation of NO_2^- with lignin

derivatives and might therefore explain the shifting SP values and different N_2O production rates. In the reaction of 4-hydroxybenzoic acid with NO_2^- , irrespective of the reaction pathway, the carboxyl group (-COOH) is first substituted by a nitroso group (-NO), associated with the formation of CO_2 and 4-nitrosophenol (compound 1). As 4-nitrosophenol is unstable at acidic pH, it partly decomposes to phenol (compound 4) and nitric oxide (NO), while the other part is transformed to *p*-benzoquinone 4-oxime (compound 2) through rearrangement (Austin, 1961; Stevenson and Swaby, 1964). The formation of NO was confirmed in our experiments by high NO emission in the very beginning of the reactions measured by a chemoluminescence analyzer (Fig. B8). Similarly, 2-methoxyphenol was detected as a product of NO_2^- reaction with 4-hydroxy-3-methoxybenzoic acid (Fig. B9), and 2,6-dimethoxyphenol was observed as a product of the reaction of NO_2^- with 4-hydroxy-3,5-dimethoxybenzoic acid (Fig. B10), which further confirmed the decarboxylation and the following removal of the nitroso group. Subsequently, the phenol can be attacked by another nitrous acid molecule through electrophilic substitution, resulting in the formation of 2-nitrosophenol (compound 5) which can rearrange to compound 6.

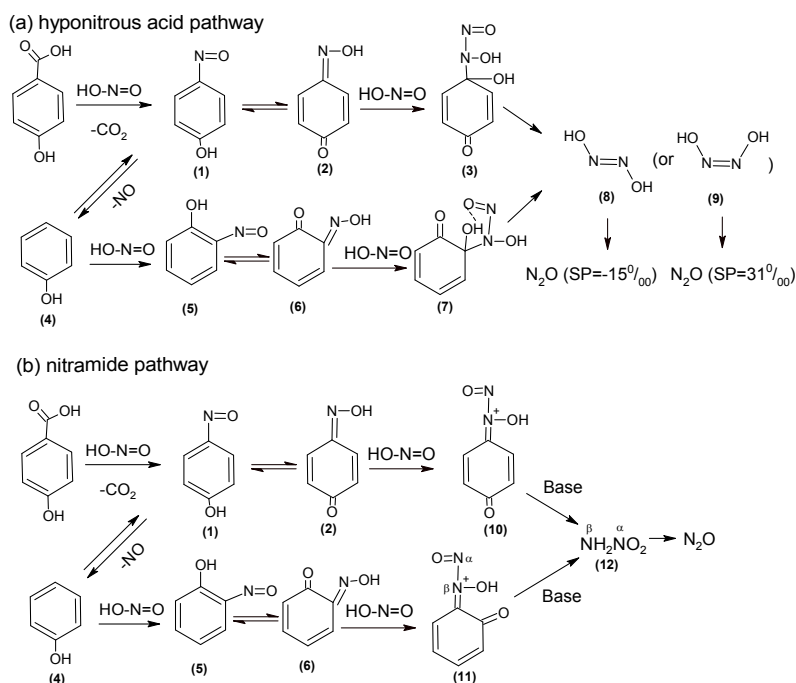


Fig. III.6. Proposed hyponitrous acid pathway (a) and nitramide pathway (b) of N_2O formation in the reactions of NO_2^- with lignin products. The reaction of NO_2^- with 4-hydroxybenzoic acid is taken as an example.

In the hyponitrous acid pathway, the C=N double bond of oximes can be subject to electrophilic attack of nitrous acid with a nitroso group being attached to the nitrogen atom while a hydroxyl group binding to the carbon atom, and hydroxyl-nitroso compounds (compound 3 and 7) are consequently formed (Austin, 1961). Hydroxyl-nitroso compounds are very unstable and decompose quickly to hyponitrous acid (compound 8 and 9) and benzoquinones, with hyponitrous acid decomposing to N₂O (Austin, 1961). In the nitramide pathway, electrophilic substitution, instead of electrophilic addition, occurs at the nitrogen atom of the oximes with the production of nitramines (compound 10 and 11), which decompose quickly to benzoquinones and nitramide (compound 12), and further to N₂O (Kainz and Huber, 1959).

The number and position of electrophilic functional groups attached to the aromatic ring can affect the reaction kinetics through mesomeric (+/−M) and inductive (+/−I) effects. For example, the two methoxy groups (−OCH₃) in 4-hydroxy-3,5-dimethoxybenzoic acid enhance the electron density of the aromatic ring, hence facilitating the electrophilic attack by nitrous acid and finally accelerating the NO and N₂O formation. This could explain the much higher R_{N₂O} at 0–2 h of 4-hydroxy-3,5-dimethoxybenzoic acid treatment than that of 4-hydroxybenzoic acid treatment (Table III.1). Even though the methoxy group in 4-hydroxy-3-methoxybenzoic acid can also increase the aromatic electron density, its steric effect also hinders the formation of oximes to some extent, which could be the reason why R_{N₂O} did not increase in 4-hydroxy-3-methoxybenzoic acid treatment compared with 4-hydroxybenzoic acid. In the case of 4-hydroxy-3-methoxybenzaldehyde and 4-hydroxy-3,5-dimethoxybenzaldehyde, the aldehyde group has to be first oxidized to a carboxyl group, and then undergo subsequent decarboxylation, formation of oxime, hyponitrous acid, and nitramide. Therefore, R_{N₂O} was much lower in 4-hydroxy-3-methoxybenzaldehyde and 4-hydroxy-3,5-dimethoxybenzaldehyde treatments compared with the benzoic acid treatments (Table III.1).

III.4.2 Differences in ¹⁵N SP of N₂O depending on reaction conditions

A large variability of N₂O SP values (11.9–30 ‰) in NO₂[−]-lignin derivative reactions at pH 3 was also found in an off-line study, where incubation experiments of 24 h were conducted and collective gas samples were analyzed for N₂O isotopic signatures by an isotope ratio mass spectrometer (Wei et al., 2017b). In the present study, the N₂O SP values were measured in real-time over 4–6 h, which might explain the even wider range of 5.6–29 ‰. N₂O SP values observed in the present and earlier studies (Wei et al., 2017b) for the NO₂[−]-lignin derivative reaction also covered the range of data detected for the abiotic reactions of NO₂[−] with SOM fractions at pH 3.4 (20–26 ‰) (Wei et al., 2017a) and the chemical reduction of NO₂[−] by ferrous iron at pH 7 under anaerobic condition (10–22 ‰) (Jones et al., 2015), as well as the reaction of NO₂[−] with trimethylamine-borane and NH₂OH at pH 1 (~30 ‰) (Toyoda et al., 2005). In the following, the N₂O isotopic composition will be discussed with

respect to N₂O production pathways. Isotope effects of N₂O reduction will not be discussed, since N₂O is very unlikely to be further reduced during chemodenitrification.

According to the above proposed N₂O production pathways (Fig. III.6), hyponitrous acid and nitramide are supposed to be the direct precursors of N₂O in reactions of NO₂⁻ with lignin derivatives. For the symmetric hyponitrous acid molecule, isotope effects during its decomposition are the key factor controlling N₂O SP values. Theoretical calculations using density functional theory calculations (DFT) predict formation of both *cis*- and *trans*-hyponitrous acid (Fehling and Friedrichs, 2011), and substantially different N₂O SP values for N₂O formation from *trans*-hyponitrous acid (-15 ‰) as compared to *cis*-hyponitrous acid decomposition (31 ‰) (Fehling, 2012). Therefore, the share of N₂O formation through *trans*- and *cis*-hyponitrous acid could be responsible for the differences in SP values between treatments and for one treatment over time. To be more precise, an increase in N₂O SP should be related to a decreased proportion of *trans*-hyponitrous acid-derived N₂O, vice versa, a decrease in N₂O SP should be related to an increasing proportion of *trans*-hyponitrous acid-derived N₂O. In principal, the formation of *trans*-hyponitrous acid from hydroxyl-nitroso compounds is favored due to steric effects, however, *trans*-hyponitrous acid could be isomerized to *cis*-hyponitrous acid through a fast acid-base equilibrium which generally dominates under strongly acidic conditions (Bringas et al., 2016; Fehling and Friedrichs, 2011). This isomerization could explain the increase of N₂O SP at about 0–2 h in the treatments of organosolv lignin, 4-hydroxybenzoic acid, and 4-hydroxy-3,5-dimethoxybenzaldehyde (Fig. III.2, B3, III.4). Methoxy and hydroxyl groups could also act on the formation of *trans*-/*cis*-hyponitrous acid through steric and electronic effects, but the mechanisms involved are still unknown till now.

Hyponitrous acid is also proposed as the key precursor in microbial N₂O production. During the oxidation of NH₂OH to N₂O by HAO, a NH₂OH molecule is first bound to the HAO, then a second NH₂OH molecule attacks the N atom of the first one with the formation of a *cis*-hyponitrous acid-like N-N bond, finally N₂O with the SP of 30–36 ‰ is generated through the removal of the OH group of the first NH₂OH molecule (Yamazaki et al., 2014). The NO reduction by fungal NOR to N₂O is similar to the NH₂OH oxidation by HAO, as two NO molecules are sequentially bound to NOR and form a *cis*-hyponitrite-like compound which decomposes quickly to N₂O with a SP of 35–37 ‰ (Obayashi et al., 1998; Rohe et al., 2014; Sutka et al., 2008). By contrast, two NO molecules are simultaneously bound to the bacterial NOR and a *trans*-hyponitrite-like compound is formed, which further decomposes to N₂O with the SP of around zero during bacterial denitrification (Watmough et al., 2009).

In the nitramide pathway, the N atoms of the firstly and secondly bound nitroso group act as the outer (N^β) and central (N^α) nitrogen atoms of the N₂O molecule, respectively. Therefore, kinetic isotope effects during nitramide formation are supposed to dominate the N₂O isotopic composition. In addition, incomplete nitramide decomposition might cause fractionation effects. It is speculated

that the isotope effects of both the formation of the N-N bond of nitramines and the cleavage of the N=O bond of nitramide favors higher $\delta^{15}\text{N}^{\alpha}$, so the SP value of N₂O from the nitramide pathway should be significantly higher than zero, and the formation of nitramines could be the rate-limiting step. More research is needed to explore the SP value of N₂O from nitramide decomposition and factors influencing the formation and decomposition of nitramide. In addition, factors controlling the relative contribution of the hyponitrous acid and nitramide pathways to N₂O formation from NO₂⁻-lignin reactions are currently not known.

III.4.3 Nitrite-related N₂O formation in soil

As an intermediate of both nitrification and denitrification, NO₂⁻ is substantially and simultaneously released and consumed in soil. Russow et al. (2009) reported that nitrification and denitrification were responsible for 88 % and 12 % of the total NO₂⁻ production in aerobic soils, respectively, while denitrification accounted for 100 % of NO₂⁻ production in anaerobic soils. Nitrite is very reactive and has a high turnover rate in soils, so it is generally thought that NO₂⁻ accumulation does not occur in unfertilized soils. However, alkaline pH (Shen et al., 2003), fertilizer application (Shen et al., 2003), low soil temperature (Tyler et al., 1959), low soil moisture (Justice and Smith, 1962), and low soil buffer capacity (Hauck and Stephenson, 1965) can lead to the accumulation of NO₂⁻ up to several mg N g⁻¹ soil. Even though the significant correlation of N₂O emission and NO₂⁻ concentration in soils was revealed decades ago (Firestone et al., 1979), less attention was paid to the role of NO₂⁻ in N₂O emission, and neither were NO₂⁻ concentrations widely measured in the field due to its mostly low content. However, the central role of NO₂⁻ in the soil N cycle and N₂O emission has recently been emphasized again with more and more evidence revealed. Maharjan and Venterea (2013) reported that nitrite alone explained more than 44 % of the N₂O emission variance in a fertilized maize soil, which was much higher than the contribution of NH₄⁺ and NO₃⁻. Cai et al. (2016) found that N₂O emissions from a sandy loam soil fertilized with urea was positively and linearly correlated with NO₂⁻ concentration, and the correlation highly depended on oxygen availability. A linear relationship between N₂O emission and NO₂⁻ concentration was also found in an agricultural silt loam soil, and the N₂O emission rate after NO₂⁻ application was affected by soil pH, total nitrogen and carbon content (Venterea, 2007).

Nitrite can be biologically reduced to N₂O through fungal or bacterial denitrification, where NO₂⁻ is first reduced to NO by NIR and then further reduced to N₂O by NOR (Long et al., 2015). Except for biological reduction, NO₂⁻ can also be quickly reduced to N₂O under acidic conditions through chemodenitrification, namely the reduction of NO₂⁻ by transition metals and SOM (Chalk and Smith, 1983). Total carbon content was one of the main factors controlling N₂O emission from agricultural soils where chemodenitrification acted as one of the main N₂O sources (Venterea, 2007). When NO₂⁻

was applied to a spruce forest soil, N₂O from chemodenitrification accounted for 19.5–42.3 % of the total emission, while fungal denitrification and bacterial denitrification explained the rest (Wei et al., 2017a). In this study, the NO₂⁻-derived N₂O from agricultural, forest and grassland soils could be produced through the chemical reduction of NO₂⁻ by ferrous iron and SOM, fungal denitrification, and bacterial denitrification. The SP values of 10.9 to 27.5 ‰ were within the ranges of both NO₂⁻-SOM reactions and combined bacterial/fungal denitrification, while the instability of N₂O SP could result from the heterogeneous N₂O production from various pathways and the variability of SP values from NO₂⁻-SOM reactions.

III.4.4 The application of N₂O isotopic species in source partitioning

Even though SP is widely used for N₂O source partitioning, it still remains an open question whether it is sufficiently reliable. Heil et al. (2014) reported that the SP of N₂O from the chemical oxidation of NH₂OH by NO₂⁻ and ferric iron remained stable around 34 ‰ independent of pH during the whole reaction. However, Yang et al. (2014) found that the SP value of N₂O increased from 15 to 29 ‰ along the reduction of NO by purified P450nor from *Histoplasma capsulatum*. In the present study, both SP and δ¹⁵N^{bulk} values shifted largely with reaction time, which makes it even harder to distinguish chemodenitrification from other N₂O sources. In chemical assays, SP, δ¹⁵N^{bulk}, and δ¹⁸O values of N₂O from chemodenitrification ranged from 5.6 to 37.4 ‰, from -39.1 to -3.9 ‰, and from 13 to 44.6 ‰, respectively (Jones et al., 2015; Toyoda et al., 2005; Wei et al., 2017b), which is clearly distinct from isotopic signatures of bacterial denitrification (SP: -11 to 1.4 ‰, δ¹⁵N^{bulk}: -34.8 to -8.8 ‰, δ¹⁸O: 10 to 20 ‰) (Toyoda et al., 2005; Zou et al., 2014) (Fig. III.7). However, more than half of fungal denitrification area (SP: 34 to 40 ‰, δ¹⁵N^{bulk}: -34 to -21.9 ‰, δ¹⁸O: 30 to 40 ‰) (Sutka et al., 2008) is overlapped with that of chemodenitrification (Fig. III.7). Moreover, the N₂O isotopic composition of chemodenitrification is even overlapped with a small part of nitrification (SP: 27 to 37 ‰, δ¹⁵N^{bulk}: -61.4 to -40.3 ‰, δ¹⁸O: 40 to 50 ‰) (Sutka et al., 2006) (Fig. III.7).

Consequently, the application of N₂O isotopic species in source partitioning failed in Lake Vida, Victoria Valley, Antarctica, where chemodenitrification acted as the main N₂O source but N₂O isotopic species were not distinguishable from microbial production (Ostrom et al., 2016; Zhu-Barker et al., 2015). Similarly, the N₂O was assumed to originate from chemodenitrification in the Don Juan Pond, Antarctica, while its SP varied greatly from -45 to 4 ‰, which overlapped with the range of N₂O from bacterial denitrification (Samarkin et al., 2010). In addition, even though chemodenitrification accounted for most of N₂O emission within a pond in the Labyrinth, Lake Vanda and Lake Bonney, the SP values encompassed the ranges of microbial nitrification (33–37 ‰) and denitrification (-10 to 0 ‰) (Peters et al., 2014). Thus, one can conclude that additional constraints, such as clumped-isotope analysis of N₂O and combination of isotope measurements and modelling, are needed for N₂O source

partitioning due to the great variability of N₂O isotopic signatures from chemodenitrification and the large uncertainty associated with it.

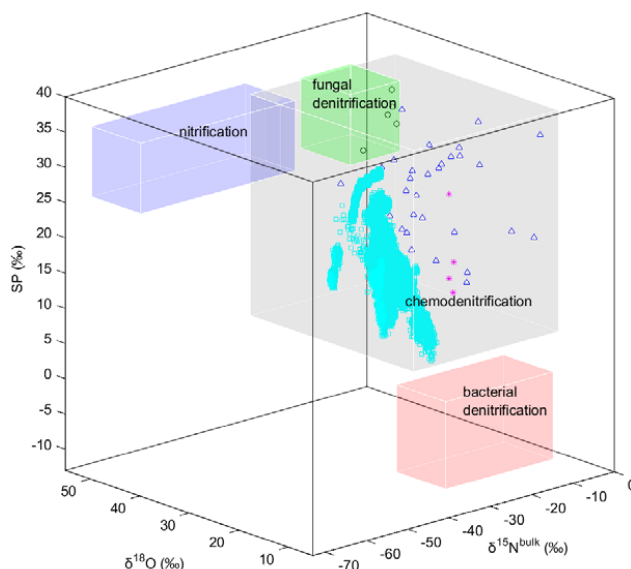


Fig. III.7. Three dimensional end-member map of SP vs. $\delta^{15}\text{N}^{\text{bulk}}$, $\delta^{18}\text{O}$. Pink asterisks represent N₂O from chemical NO₂⁻ reduction by Fe²⁺ (Jones et al., 2015); black circles represent N₂O from the reaction of NO₂⁻ with trimethylamine-borane and NH₂OH (Toyoda et al., 2005); blue triangles are delta values of N₂O from reactions of NO₂⁻ with lignin products at pH 3–5 for 24 h (Wei et al., 2017b); cyan squares denote N₂O isotope deltas measured in this study.

III.5 Conclusions

In this study, the isotopic signatures of N₂O from chemodenitrification in both chemical assays and soils was investigated with QCLAS in real-time for the first time. Lignin, 4-hydroxybenzoic acid, 4-hydroxy-3-methoxybenzoic acid, 4-hydroxy-3,5-dimethoxybenzoic acid, 4-hydroxy-3-methoxybenzaldehyde, and 4-hydroxy-3,5-dimethoxybenzaldehyde were chosen as SOM representatives, and three types of typical soils (agricultural, spruce forest, and grassland soils) in Germany were used to test the NO₂⁻-derived N₂O generation and isotopic signatures at the same time. In contrast to the common assumption that the ¹⁵N SP of N₂O from a certain pathway remains constant over time, the SP of N₂O from chemodenitrification in the present study shifted largely from 5.6 to 29.0 ‰ with elapsing reaction time. The SP values of N₂O from soils after NO₂⁻ application varied substantially between 10.9 and 27.5 ‰. Furthermore, the wide range of N₂O SP of chemodenitrification makes it hard to disentangle N₂O sources in the field by using the current end-member maps of SP vs. $\delta^{15}\text{N}^{\text{bulk}}$ and $\delta^{18}\text{O}$.

Chemodenitrification is always accompanying the release and consumption of NO₂⁻, hence it

acts as a key step of coupled biotic-abiotic N₂O emissions in soils. This laboratory study provides the first real-time information about the isotopic signatures of N₂O from chemodenitrification, showing perspectives for an increased understanding of the application of SP and end-member maps in N₂O source partitioning. Despite the fact that SP has been regarded as a powerful tool to distinguish different N₂O sources and sinks, it is highly limited when chemodenitrification is taken into account. Above all, more investigation on the intramolecular distribution of N₂O isotopes from different sources is needed, and the reliability of SP as a tool to source-partition N₂O emissions still remains an open question.

IV. N₂O and NO_x emissions by reactions of nitrite with soil organic matter of a Norway spruce forest

Based on:

Wei, J., Amelung, W., Lehndorff, E., Schloter, M., Vereecken, H., Brüggemann, N. (2017a). N₂O and NO_x emissions by reactions of nitrite with soil organic matter of a Norway spruce forest. *Biogeochemistry*, 132 325–342.

IV.1 Introduction

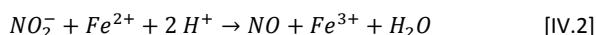
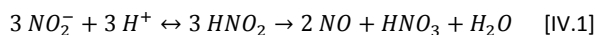
Several biotic processes of N₂O release, such as autotrophic nitrification, heterotrophic nitrification, denitrification, nitrifier denitrification, and co-denitrification, have been identified and quantified (Müller et al., 2014; Spott et al., 2011; Stein, 2011; Zhang et al., 2015c). As an important intermediate in both nitrification and denitrification, NO₂⁻ can accumulate in soil up to several mg per g soil under specific conditions, such as alkaline pH, high NH₄⁺ content, low temperature and soil moisture (Justice and Smith, 1962; Yoo et al., 1999). Due to its high chemical reactivity, accumulated NO₂⁻ can participate in a range of abiotic reactions in soil, especially at acidic pH. Even though biotic N₂O sources are prevalent in many soils, abiotic sources, such as chemodenitrification of NO₂⁻, may account for 31–75 % of the total N₂O production at elevated NO₂⁻ concentrations (Venterea, 2007; Zhu-Barker et al., 2015). According to the ¹⁵N-enrichment study by Ostrom et al. (2016), chemodenitrification accounted for most of the N₂O emission (4.11–4.18 nmol L⁻¹ d⁻¹) in the frozen Lake Vida. Maharjan and Venterea (2013) reported that the intensity of NO₂⁻ in a soil planted with maize was highly positively correlated with N₂O emission and explained about 44 % of the N₂O variability. However, more studies are needed to further explore the magnitude, mechanisms and factors of NO₂⁻-related N₂O emission from soil (Maharjan and Venterea, 2013).

Isotopic signatures of N₂O, such as δ¹⁵N^{bulk}, δ¹⁸O, and ¹⁵N site preference (SP), which is the difference of ¹⁵N abundance at the central (α) and terminal (β) position within the N₂O molecule (SP ≡ δ¹⁵N^α - δ¹⁵N^β), have been used for source identification (Heil et al., 2014). The SP value of N₂O from a certain source remains constant even if δ¹⁵N and δ¹⁸O values of original substrates are changing, which makes it an efficient and sensitive indicator for the different sources (Toyoda and Yoshida, 1999). Decock and Six (2013) classified the SP values of N₂O into a high level of 32.8 ‰, which represents N₂O sources of NH₂OH oxidation, fungal denitrification and N₂O production by AOA, and a low level of -1.6 ‰, which indicates N₂O production through denitrification and nitrifier denitrification. Thereafter, a two end-member mixing model including a high SP level for bacterial denitrification and a low SP level for bacterial nitrification has been used to calculate the N₂O sources (Wu et al., 2017; Zou et al., 2014), regardless of the fact that SP of N₂O from chemodenitrification was overlooked. Since chemodenitrification accounts for large or even most of the N₂O emission under a certain condition (Ostrom et al., 2016; Venterea, 2007; Zhu-Barker et al., 2015), basic data for the SP values of N₂O from chemodenitrification are needed to improve these N₂O source models. Jones et al. (2015) reported a wide range of SP values of 10–22 ‰ from the chemical reduction of NO₂⁻ by Fe²⁺, which was neither within the range of nitrification nor denitrification SP values. However, until now no studies are available that report the isotopic signature of N₂O from chemodenitrification of NO₂⁻ by SOM.

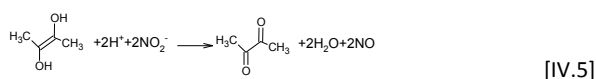
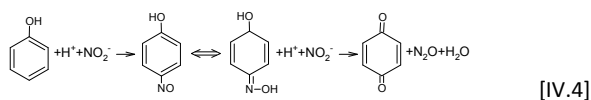
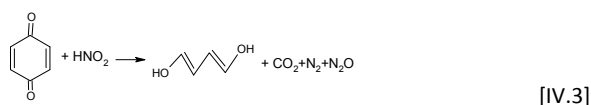
Nitric oxide (NO) and nitrogen dioxide (NO₂), combined as NO_x, are highly reactive due to the

unpaired electron in their molecules and play an essential role in atmospheric chemistry (Pilegaard, 2013). As the main source of atmospheric NO_x, NO is quickly oxidized to NO₂ in the atmosphere. A positive relationship of atmospheric hydroxyl (OH) radical concentration and soil NO emission has been found, indicating that NO could be involved in the production of OH (Steinkamp et al., 2009). Furthermore, NO is an important ozone-depleting compound in the stratosphere, while it is the main precursor of ozone in the troposphere (Pilegaard, 2013). Soils act as the main source as well as the main sink of NO_x, with NO_x exchange between the atmosphere and ecosystems being variable in space and time. Soil NO_x emissions amount to 20–24 Tg N yr⁻¹, including sources from nitrification, denitrification, and chemodenitrification (Medinets et al., 2015).

Nitrite is critical for NO_x emission from soil. Under acidic soil conditions, NO₂⁻ takes up a proton (H⁺), leading to the formation of nitrous acid which further decomposes to NO (Reaction [IV.1]). In addition, NO₂⁻ can also be rapidly reduced to NO by transition metals in soil (Reaction [IV.2]).



Evidence is rising that SOM plays an important role in the abiotic reactions of NO₂⁻ through nitrosation reactions, during which the NO group is incorporated into the organic moiety with the formation of nitroso compounds (Stieglmeier et al., 2014). In NO₂⁻-amended soil, the content of SOM was positively related with N₂O production (Nelson, 1967). Nitric oxide and N₂O were found to be the gaseous products of SOM nitrosation, while the reaction of NO₂⁻ with lignin and its derivatives resulted in the formation of both N₂O and CO₂ (Stevenson and Swaby, 1964). Porter (1969) found that NO is the primary product from the reaction of NO₂⁻ with oximes at pH 5–6. The proposed pathways for the formation of CO₂, NO and N₂O during the reaction of NO₂⁻ with SOM are shown in the following reactions (Austin, 1961):



Hence, SOM quality, namely the reactive component of SOM, could be the key factor of abiotic N₂O and NO_x emission. Lignin, which is composed of guaiacyl (G, also called vanillyl), syringyl (S), and *p*-hydroxyphenyl (H, also called cinnamyl) units, is the most abundant aromatic compound on earth and contributes to the recalcitrant SOM pool due to its high resistance to decomposition (Bahri et al., 2008). During decomposition, lignin derivatives are oxidized from aldehyde to acid form, therefore, the ratios of aldehyde to acid of G and S units are regarded as indicators of lignin degradation (Hedges et al., 1988). Since the reactivity of each lignin unit differs according to its structure and shifts during decomposition, SOM quality is affected by the lignin input and its degree of decomposition.

This study was aimed at elucidating the role of the aforementioned chemical processes in the formation of N₂O and NO from NO₂⁻ in acidic forest soil. It was hypothesized that (1) abiotic processes do not only control most of the NO₂⁻-related NO_x emissions, but also abiotic N₂O production in acidic forest soil, (2) the magnitude of these abiotic reaction pathways depend on SOM quality, and (3) N₂O source models based on SP alone could bias N₂O source attribution without considering abiotic NO₂⁻-driven N₂O production. To address these questions, N₂O and NO_x emissions were monitored after the application of NO₂⁻ to soil samples from a Norway spruce forest, quantified their emissions from reactions of NO₂⁻ with different SOM fractions, and evaluated the suitability of SP to identify N₂O sources.

IV.2 Materials and methods

IV.2.1 Soil sampling and analysis

Five independent Cambisol soil samples were randomly taken from the Oa layer at the Norway spruce (*Picea abies*) dominated Wüstebach catchment (50°30'15"N, 6°18'15"E), Eifel National Park, Germany (Fig. C1). After sampling, soils were immediately transferred to the laboratory, freeze-dried, sieved to 2 mm, and stored at 4 °C for further usage. Half of the soil was sterilized through γ irradiation with a dose of 11 kGy. Chemical parameters were analyzed in three replicates by the Central Institute for Analytics of Forschungszentrum Jülich. Nitrate and NH₄⁺ were extracted with 1 M potassium chloride (KCl) at a ratio of 1:10 (w/v), and measured with ion chromatography (DX-500, Dionex, USA). The total N content (TN) was determined using an elemental analyzer (vario EL Cube, Elementar Analysensysteme GmbH, Hanau, Germany). The total organic carbon (TOC) was determined by a multiphase carbon and hydrogen/moisture analyzer (RC612, LECO Instrumente GmbH, Mönchengladbach, Germany). The contents of iron (Fe), manganese (Mn), aluminum (Al) and phosphate (P) were determined by inductively coupled plasma optical emission spectroscopy (ICP-OES, iCA 7600, Thermo Fisher Scientific, Oberhausen, Germany). Soil pH was determined with a pH meter (multi 340i, WTW GmbH, Germany) according to the ISO 10390 method (ISO, 2005), 1 M KCl

solution at the ratio of 1:5 (w/v) was used. Lignin derivatives, i.e. G units (vanillin, acetovanillone, and vanillic acid), S units (acetosyringone, syringaldehyde, and syringic acid), and H units (*p*-cumaric acid and ferulic acid), were quantified according to the cupric oxide oxidation method (Amelung et al., 1997), and total lignin content was calculated as their sum. Lignin degradation was calculated from the sum of acids to aldehydes of G and S units, respectively (Hedges et al., 1988). Characteristics of the five soil samples are shown in Table C1.

IV.2.2 Soil organic matter fractionation

Due to the high NO_x and N₂O emissions, as well as its high degree of humification, soil from subsite 2 was selected for fractionation into four SOM fractions according to their solubility (Stevenson, 1995). For this purpose, freeze-dried soil was mixed with 1 M KCl solution at the ratio of 1:10 (w/v) on a shaker at 200 rpm and 20 °C for 1 h, centrifuged at 9600 *g* for 10 min. The supernatant contained the DOM fraction and was decanted slowly into a clean beaker. Then, 0.5 M sodium hydroxide (NaOH) solution was added to the residue at a ratio of 1:5 (w/v) in a glove box filled with argon. This mixture was shaken for 12 h, and then centrifuged at 3500 *g* for 10 min. This procedure was repeated for two times with 1 h of shaking each time. The insoluble part was the humin (HN) fraction. The supernatants were mixed and adjusted to pH 1 with 3 M chloride acid (HCl). The humic acid (HA) fraction precipitated overnight, while the fulvic acid (FA) fraction remained dissolved in the acid. All four soil fractions were freeze-dried and stored at 4 °C until usage.

IV.2.3 NO_x and N₂O emissions

A combined system of a dual quantum cascade laser trace gas monitor (QCLAS, DUAL CWRT-QC-TILDA-76, Aerodyne Research, Inc., Billerica, MA, USA) and a chemoluminescence analyzer (CLD, AC32M, Ansyco GmbH, Karlsruhe, Germany) was used for the measurement of N₂O and NO_x emission dynamics, respectively, with high time resolution (Fig. C2). Five grams of soil, or equivalent SOM fractions of 5 g dry weight, were put into a 100-ml beaker in a reaction chamber of 2 L volume, and 1 N NaOH or HCl were used to adjust the pH of SOM fractions to the original soil pH of 3.4. The headspace of the reaction chamber was purged with 3 L min⁻¹ of synthetic air (20 % oxygen and 80 % N₂) till the N₂O and NO_x signals had decreased under 0.1 ppb. NO_x and N₂O concentrations were recorded every 5 s and 1 s, respectively, following the application of 10 ml of 0.25 mM NaNO₂ (VWR, Germany) solution to the soil samples or SOM fractions. For sterilized soil, a 0.2 μm PTFE sterile filter was installed into the gas line to clean the carrier gas. Pure NaNO₂ treatment at pH 3.4 was used as control treatment to compare the difference of NO_x emission from NO₂⁻-SOM reactions and NO₂⁻ self-decomposition. Each treatment was measured in triplicate.

Due to the low N₂O signal monitored by the QCLAS in the dynamic mode, additional batch incubation experiments were conducted in triplicate to quantify the N₂O emission with a gas

chromatography equipped with an electron capture detector (GC-ECD, Clarus 580, PerkinElmer, Rodgau, Germany). The same amount of soil or soil fractions and sodium NaNO₂ solution were mixed in 1 L glass serum bottles with butyl rubber septum caps, 22.5-ml of headspace air were withdrawn with a syringe at time intervals 10, 20, 30, 40, 50, 60, 80, 100, 120, 150, 180, and 240 min, and transferred to 22.5-ml pre-evacuated glass vials sealed with butyl rubber septa. To keep the pressure constant, the same volume of synthetic air was injected into the glass serum bottles after each sampling.

IV.2.4 Isotopic N₂O analysis

For the determination of N₂O isotope composition, 1 g of soil sample or SOM fractions was weighed into 100-ml serum bottles in triplicate. The headspace was evacuated and flushed with a mixture of helium and oxygen (80:20, v/v), then 2 ml of aqueous 0.25 mM NaNO₂ solution (N content = 19.5 ± 0.1 %, δ¹⁵N = -18.00 ± 0.08 ‰, δ¹⁸O = 10.09 ± 0.05 ‰) was injected into the bottles. After incubation for 24 h at 20 °C, N₂O in the headspace was analyzed with an isotope ratio mass spectrometer (IsoPrime 100, Elementar Analysensysteme, Hanau, Germany) coupled to an online pre-concentration unit (TraceGas, Elementar Analysensysteme). The mass-to-charge (m/z) ratios of N₂O at 44 (¹⁴N¹⁴N¹⁶O), 45 (¹⁴N¹⁵N¹⁶O, ¹⁵N¹⁴N¹⁶O, and ¹⁴N¹⁴N¹⁷O), and 46 (¹⁴N¹⁴N¹⁸O), as well as NO⁺ at 30 (¹⁴N¹⁶O⁺) and 31 (¹⁵N¹⁶O⁺) were used to calculate the δ¹⁵N, δ¹⁸O, and SP values of N₂O (Kaiser, 2002). Pure N₂O (99.999 %, Linde, Munich, Germany) was used as reference gas for isotope analysis, while a tertiary working standard (δ¹⁵N^α = 3.18 ± 0.23 ‰, δ¹⁵N^β = 1.42 ± 0.21 ‰, δ¹⁵N^{bulk} = 2.30 ± 0.20 ‰, δ¹⁸O = 39.35 ± 0.27 ‰), calibrated against two secondary standard gases (Ref 1: δ¹⁵N^α = 15.70 ± 0.31 ‰, δ¹⁵N^β = -3.21 ± 0.37 ‰, δ¹⁵N^{bulk} = 6.24 ± 0.11 ‰, SP = 18.92 ± 0.66 ‰, δ¹⁸O = 35.16 ± 0.35 ‰; Ref 2: δ¹⁵N^α = 5.55 ± 0.21 ‰, δ¹⁵N^β = -12.87 ± 0.32 ‰, δ¹⁵N^{bulk} = -3.66 ± 0.13 ‰, SP = 18.42 ± 0.50 ‰, δ¹⁸O = 32.73 ± 0.21 ‰) provided by EMPA (Dübendorf, Switzerland), was used for calibration of δ¹⁵N, δ¹⁸O, and SP.

IV.2.5 Statistical analysis

The NO_x emission was calculated by integrating the NO_x concentration-time curves obtained from the CLD, while N₂O emission was calculated according to the accumulated N₂O concentration obtained by GC-ECD based on the ideal gas law (supporting information). Both accumulated NO_x and N₂O emissions were fitted with the Hill Equation (Goutelle et al., 2008) in Igor Pro 6.22A (WaveMetrics, Portland, OR, USA):

$$E_t = E_0 + \frac{E_{max} - E_0}{1 + \left[\frac{t_{1/2}}{t}\right]^n} \quad [IV.6]$$

E_t —NO_x or N₂O emission at time t , ng N g⁻¹ soil; E_0 —NO_x or N₂O emission at time zero, ng N g⁻¹ soil; E_{max} —total NO_x or N₂O emission, ng N g⁻¹ soil; $t_{1/2}$ —time needed to reach half of E_{max} , min; n —the indicator for the increase of NO_x or N₂O emission rate, unitless.

The maximum NO_x and N₂O emission ($NO_{x,max}$ and N_2O_{max}) and the time needed to reach half of the maximum emission ($t_{1/2}$) were calculated according to Equation [IV.6]. The initial emission rate of NO_x (R_{NOx}) and N₂O (R_{N2O}) was calculated as a first approximation by dividing half of the maximum emission by $t_{1/2}$. Also the ratios of maximum NO_x (S/U_{NOx}) and N₂O (S/U_{N2O}) emission in sterilized to that in unsterilized soils were calculated. Recoveries of NO_x and N₂O were calculated by dividing NO_x-N and N₂O-N by the total NO₂⁻-N application, respectively.

The SP of N₂O from biotic sources was calculated according to a binary mixing model:

$$SP_b = \frac{SP_t \times N_2O_t - SP_a \times N_2O_a}{N_2O_t - N_2O_a} \quad [IV.7]$$

SP_b , SP_a , and SP_t are SP values of N₂O from biotic, abiotic, and total emission, respectively; N_2O_t and N_2O_a are the amount of total and abiotic N₂O emission, respectively. In this binary mixing model, the N₂O emission in unsterilized soil was regarded as the sum of biotic and abiotic N₂O emission, that in sterilized soil was considered abiotic N₂O emission alone, and their difference was the biotic N₂O emission. End-member maps with SP as a function of $\delta^{15}N^{bulk}$ and $\delta^{18}O$, as well as a two-end-member mixing model (equation [IV.7]) were used for N₂O source partitioning (Zhang et al., 2016; Zou et al., 2014).

A paired t -test was conducted with Origin 8.0 (Originlab Corporation, Wellesley Hills, MA, USA) to compare the differences of NO_x and N₂O emissions, as well as the N₂O isotope signatures from sterilized and unsterilized soils. Canoco for Windows 5.0 (Microcomputer Power, Ithaca, NY, USA) was used to conduct redundancy analysis (RDA) to analyze the NO_x and N₂O emissions across gradients of lignin units, soil pH, Fe, Mn, Al, P, NO₃⁻, NH₄⁺, TN, and TOC.

IV.3 Results and discussion

IV.3.1 Soil NO_x and N₂O emissions

IV.3.1.1 NO_x emission from soil

A large amount of NO_x was emitted immediately after the addition of NO₂⁻ from both sterilized and unsterilized soil (Fig. C3). NO_x emissions peaked quickly within 10 min following NO₂⁻ addition, decreased rapidly 30 min later, and then disappeared slowly within the following 2.5 h. The NO_x emission from soil could be well represented by the Hill equation, with residuals less than 100 ng N g⁻¹ soil (Fig. IV.1). Most of the NO_x was rapidly emitted in the first 30 min after NO₂⁻ application, with

$t_{1/2}$ equal to or smaller than 20 min (Fig. IV.1). When NO_2^- was added to the soil, 17.0 to 51.6 % of N was recovered as NO_x , and $\text{NO}_{x\text{-max}}$ ranged from 1188 to 3613 ng N g^{-1} soil with more than 88 % being NO. No significant difference ($P > 0.05$) in total NO_x emission and NO/ NO_x ratio was found between sterilized and unsterilized soil (Fig. IV.2a and e), which indicates that abiotic NO formation was the main source of NO_x emissions, as suggested for acidic soil with high NO_2^- concentration (Pilegaard, 2013). The NO emission rate at a NO_2^- concentration of 7 $\mu\text{g NO}_2^- \text{N g}^{-1}$ soil in this study is equivalent to about 0.6 mg N $\text{m}^{-2} \text{d}^{-1}$ of NO flux in a 5 cm thick band, which is similar with the NO emission rate (608.9 $\mu\text{g N m}^{-2} \text{d}^{-1}$) from the Höglwald spruce forest (Schindlbacher et al., 2004). Generally, the NO_x production in sterilized soil results from the reduction or decomposition of NO_2^- (Medinets et al., 2015), as illustrated in Reactions IV1, IV2, and IV5. Regardless of the similar $\text{NO}_{x\text{-max}}$, the initial emission rate of NO_x (R_{NO_x}) was significantly ($P < 0.05$) higher in sterile soil than in unsterile soil (Fig. IV.2c). In unsterilized soil, NO_2^- can be transformed to NO_3^- by NO_2^- -oxidizing bacteria, which could be potentially reduced to NO_x , N_2O and N_2 through denitrification and nitrifier denitrification (Maharjan and Venterea, 2013). The consumption of NO_2^- by microorganisms in unsterile soil could be the main reason for the lower R_{NO_x} in unsterile than in sterile soils.

IV.3.1.2 N₂O emission from soil

The emission of N_2O occurred 15–60 min later than NO_x emission, peaked within the following 30 min, and then decreased to almost zero slowly within 3 h. In sterilized soil, N_2O peaks were much lower than those in unsterilized soil (Fig. C3). The N_2O emission could also be fitted very well with the Hill equation, with residues of less than 20 ng N g^{-1} soil. $\text{N}_2\text{O}_{\text{max}}$ was significantly ($P < 0.05$) higher in unsterile than in sterile soil (Fig. IV.2b and 3). In unsterilized soils, 3.3 to 7.1 % of applied $\text{NO}_2^- \text{-N}$ was transformed into N_2O , while in sterilized soil significantly ($P < 0.05$) less $\text{NO}_2^- \text{-N}$ (0.9–2.6 %) was converted to N_2O . The $R_{\text{N}_2\text{O}}$ was significantly ($P < 0.05$) lower in sterilized soil than unsterilized soils (Fig. IV.2d). Abiotic processes contributed 19.5–42.3 % of N_2O emission (Fig. IV.2f).

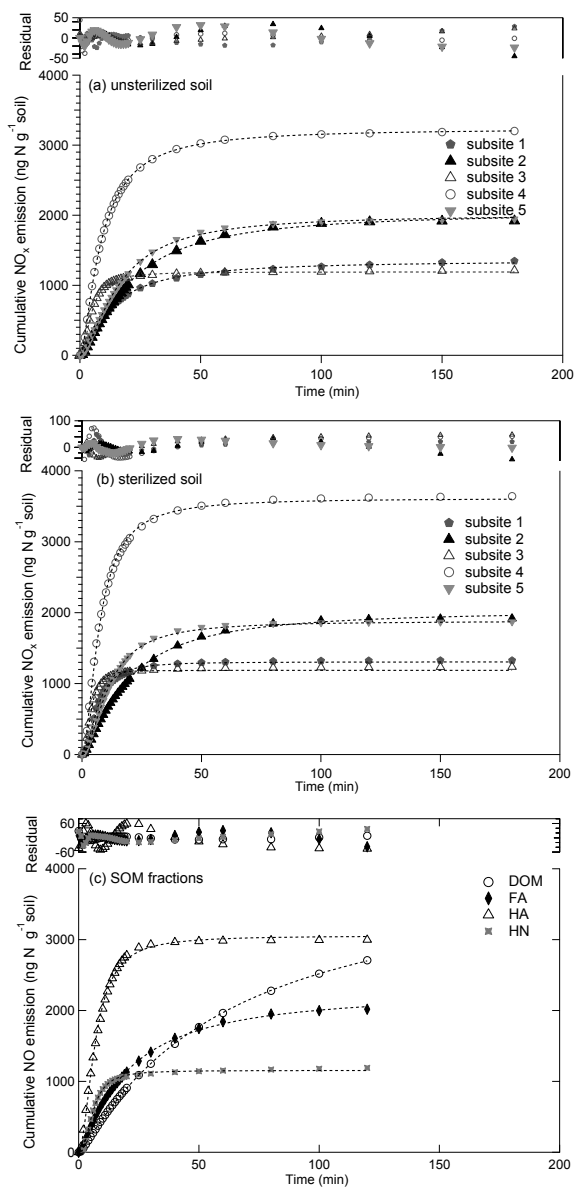


Fig. IV.1. Cumulative NO_x emission from unsterilized soil (a), sterilized soil (b), and NO emission from SOM fractions (c) after application of NO₂⁻. DOM, dissolved organic matter fraction; FA, fulvic acid fraction; HA, humic acid fraction; HN, humin fraction. Lines are the fitting results of the Hill equation; each point is the mean value of three replicates; residues are the differences between the true values and calculated values.

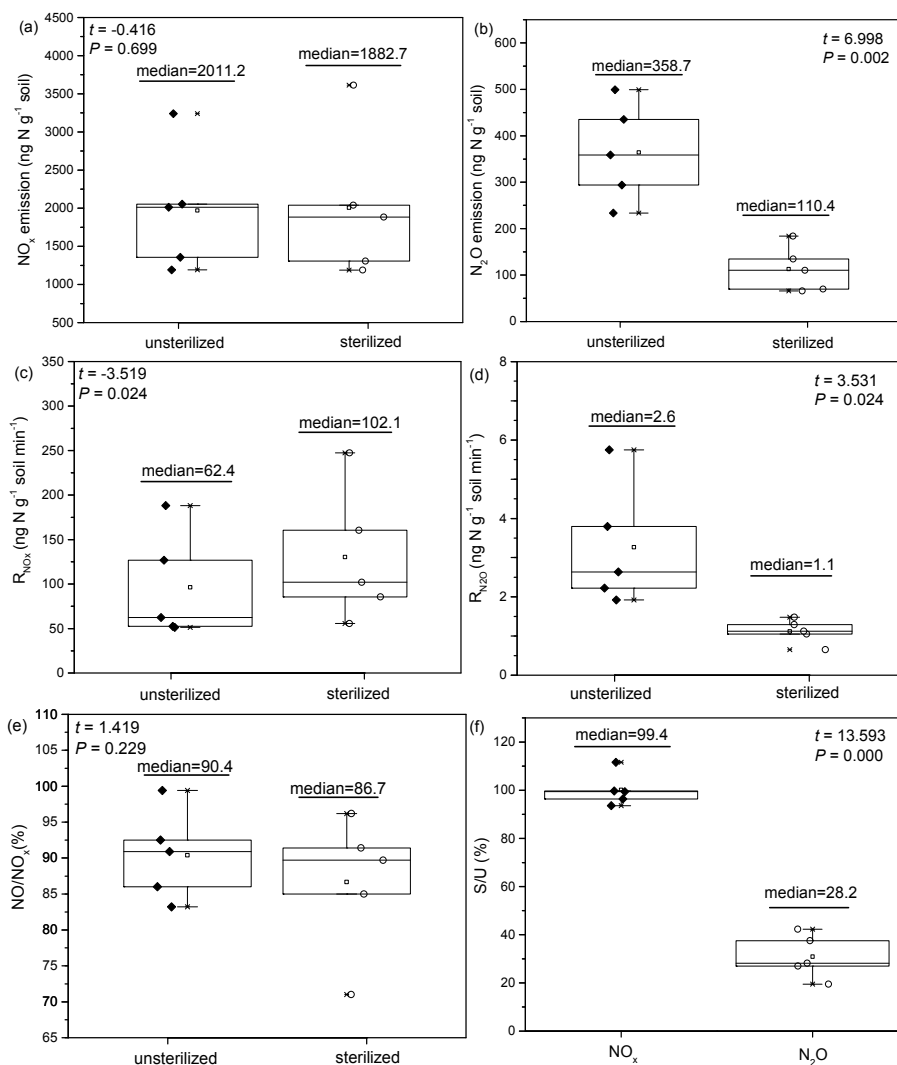


Fig. IV.2. Paired *t*-test of NO_x emission (a), N₂O emission (b), initial NO_x emission rate (c), initial N₂O emission rate (d), NO/NO_x (e), and S/U (f). The box indicates the range of the 25 and 75 percentiles of the data, the line in the box is the median, and the notch lines indicate the 1.5 interquartile range. Each point is the mean value of three replicate, *t* and *P* values represent the results of a paired *t*-test. *R*_{NO_x}, initial NO_x emission rate, calculated by half of *NO_xmax* divided by *t*_{1/2}; *R*_{N₂O}, initial N₂O emission rate, calculated by half of *N₂Omax* divided by *t*_{1/2}; S/U, the ratio of *NO_xmax* or *N₂Omax* of sterilized soil to that of unsterilized soil; NO/NO_x, the proportion of NO in NO_x.

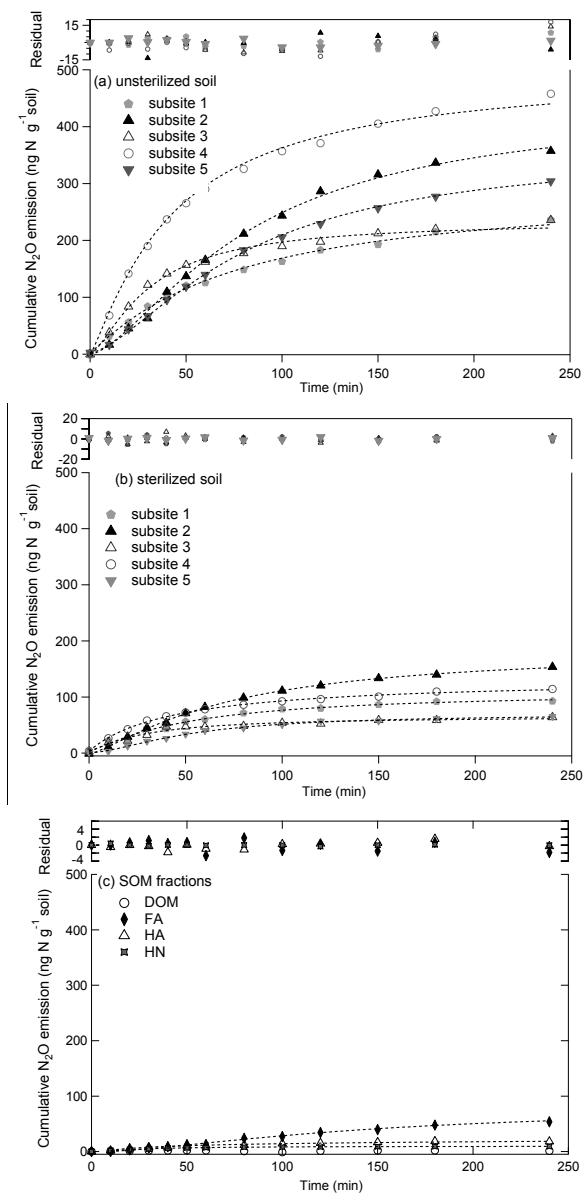


Fig. IV.3. Cumulative N₂O emission from unsterilized soil (a), sterilized soil (b), and SOM fractions (c) after NO₂⁻ application. DOM, dissolved organic matter fraction; FA, fulvic acid fraction; HA, humic acid fraction; HN, humin fraction. Lines are the fitting results of the Hill equation; each point is the mean value of three replicates; residues are the differences between the true values and calculated values.

The abiotic N₂O peak occurred 10–40 min earlier than the biotic one from the same soil (Fig. C4). The delay in the N₂O peak from biotic sources could be caused by the time that soil microbes needed to reactivate after soil rewetting (Lado-Monserrat et al., 2014). While the abiotic N₂O peak decreased

to zero slowly after about one hour, the biotic N₂O emission became the main N₂O source (Fig. C4). Beside the chemical reactions of NO₂⁻ with SOM (e.g., Reactions [IV3] and [IV4]), the reduction of NO₂⁻ by transition metals in soil, such as manganese and iron oxide minerals, can also result in rapid N₂O emission (Jones et al., 2015; Nelson, 1967). In addition, NO₂⁻ is also capable of reacting with other nitrogen compounds, such as NH₂OH and oximes, associated with the production of N₂O (Porter, 1969). Venterea (2007) reported that abiotic NO₂⁻-derived N₂O accounted for 31–75 % of the total N₂O emission in a silt loam agricultural soil, which is much higher than in this study (19–41 %), while the N₂O emission rate was about 5 times lower than in our experiment, which could be explained by the higher SOM content and lower pH of the forest soil in this experiment. In this study, the N₂O emission rate was equivalent to about 107 μg N m⁻² d⁻¹ from a 5 cm thick band, which is slightly lower than the 171.7 ± 42.2 μg N m⁻² d⁻¹ reported for another German spruce forest (Schindlbacher et al., 2004).

IV.3.1.3 N₂O isotopic signatures

The δ¹⁵N^{bulk} of N₂O from unsterilized soil was significantly ($P < 0.05$) lower than in sterilized soil (Fig. IV.4c). Correspondingly, the ¹⁵N net isotopic effect (Δ¹⁵N), i.e., the difference in δ¹⁵N^{bulk} values of the applied NO₂⁻ and the N₂O formed, was 1.39 ‰ ($P < 0.05$) lower in unsterilized soil than that in sterilized soil (Fig. IV.4a). The δ¹⁸O of N₂O was significantly lower ($P < 0.01$) in unsterilized than in sterilized soil (Fig. IV.4f). Factors influencing the δ¹⁵N and δ¹⁸O of N₂O include the isotope signatures of soil native N and soil water, N substrates applied, as well as isotope fractionation effects. Buchwald and Casciotti (2010) found that during bacterial NO₂⁻ reduction, water incorporation altered the δ¹⁸O of N₂O by about 12.8–18.2 ‰ in pure culture incubations. For AOA, N₂O is very likely produced through coupled biotic enzymatic pathway and abiotic reaction of microbe-derived N-oxide intermediates (Kozłowski et al., 2016). The δ¹⁸O and δ¹⁵N values of N₂O produced by archaeal ammonia (NH₃) oxidation are higher than that produced by AOB (Santoro et al., 2011). However, Heil et al. (2014) reported that the ¹⁵N and ¹⁸O isotope effects were not constant during abiotic reactions involving NH₂OH and NO₂⁻, but that they varied with reaction conditions. Hence, although significant differences in δ¹⁸O and δ¹⁵N values of N₂O from unsterile and sterilized soil samples were found in this study, it cannot be anticipated if this will hold true for a range of different soils and reaction conditions.

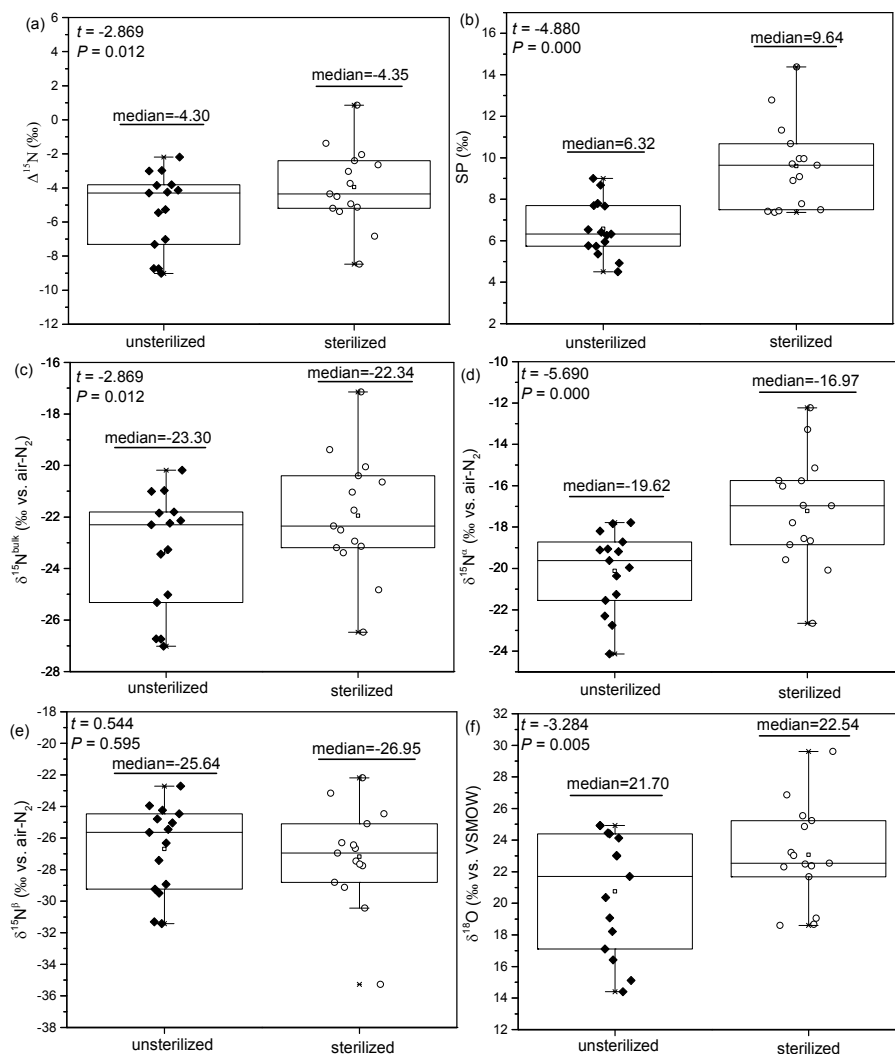


Fig. IV.4. Paired *t*-test of isotope signatures of N₂O between sterilized and unsterilized soil. The box indicates the range of the 25 to 75 percentiles of the data, the line in the box indicates the median value, and the notch lines indicate the 1.5 interquartile range; *t* and *P* values represent the results of a paired *t*-test. $\Delta^{15}\text{N}$ is the ¹⁵N isotopic difference between the applied NO₂⁻ and the $\delta^{15}\text{N}^{\text{bulk}}$ of the N₂O produced; $\delta^{15}\text{N}^{\alpha}$ and $\delta^{15}\text{N}^{\beta}$ are the ¹⁵N values at the central and terminal position of N₂O, respectively; $\delta^{18}\text{O}$ is the ¹⁸O isotopic signature of the N₂O produced, and SP is the ¹⁵N site preference ($\text{SP} \equiv \delta^{15}\text{N}^{\alpha} - \delta^{15}\text{N}^{\beta}$).

The SP of N₂O from unsterilized soil was significantly (*P* < 0.01) lower than of N₂O from sterilized soil (Fig. IV.4b). Interestingly, there was a significant difference in $\delta^{15}\text{N}^{\alpha}$, but not in $\delta^{15}\text{N}^{\beta}$, between sterilized and unsterilized soil (Fig. IV.4d and e), revealing that the changes in SP were caused by the shift in $\delta^{15}\text{N}^{\alpha}$. In contrast to $\delta^{15}\text{N}^{\text{bulk}}$ and $\delta^{18}\text{O}$, SP has been increasingly used as indicator of N₂O

production processes (Decock and Six, 2013). Wunderlin et al. (2013) demonstrated that N₂O from the reduction of NO₂⁻ through nitrifier denitrification had a SP value of -5.8 to 5.6 ‰. In contrast, N₂O from NO₂⁻ reduction through fungal denitrification has a SP value of 36.9 to 37.1 ‰ (Sutka et al., 2008). Even though the SP value of N₂O produced via denitrification is generally assumed to be around -1.6 ‰ (Decock and Six, 2013; Sutka et al., 2006), Toyoda et al. (2005) found that it could be as low as -5.1 ‰ for *Paracoccus denitrificans* (ATCC 17741). The SP value of N₂O from abiotic NO₂⁻ reduction by trimethylamine-borane and NH₂OH was constant at about 30 ‰ (Toyoda et al., 2005), while it was around 10–22 ‰ for the reduction of NO₂⁻ by iron oxide minerals (Jones et al., 2015).

End-member maps of SP with δ¹⁵N and δ¹⁸O were used to identify the NO₂⁻-related N₂O sources (Fig. IV.5a and IV.5b). In addition to the abiotic N₂O production, NO₂⁻-related biotic N₂O production include fungal denitrification, denitrification, and nitrification performed by bacteria, fungi, and archaea. The value ranges of SP, δ¹⁵N^{bulk}, and δ¹⁸O were defined from 27 to 37 ‰, -61.4 to -40.3 ‰, 40 to 50 ‰ for pure nitrification (Sutka et al., 2006), from 34 to 40 ‰, -34 to -21.9 ‰, 30 to 40 ‰ for pure fungal denitrification (Sutka et al., 2008; Wu et al., 2017), and from -11 to 1.4 ‰, -34.8 to -8.8 ‰, 10 to 20 ‰ for pure denitrification (Toyoda et al., 2005; Zou et al., 2014), respectively. The end-member map of SP–δ¹⁸O showed that biotic N₂O emission can be explained by a combination of fungal denitrification-denitrification or nitrification-denitrification (Fig. IV.5b). According to the SP–δ¹⁵N^{bulk} end-member map, the SP values of both the biotic and abiotic N₂O are in the mixing zone of fungal denitrification and denitrification (Fig. IV.5a), while only part of the biotic N₂O SP values was in the mixing zone of nitrification and denitrification. Therefore, fungal denitrification and denitrification were identified as the two main biotic N₂O sources after NO₂⁻ application in this study.

A two-end-member mixing model was used to quantify the contribution of fungal denitrification and denitrification to N₂O production:

$$SP_s = f_{fd}SP_{fd} + (1 - f_{dn})SP_{dn} \quad [IV.8]$$

Therein, SP_s is the SP value of measured N₂O from the samples, SP_{fd} (37 ‰) and SP_{dn} (-2 ‰) are the average SP values of N₂O from fungal denitrification and denitrification, respectively, and f_{fd} is the proportion of N₂O from nitrification.

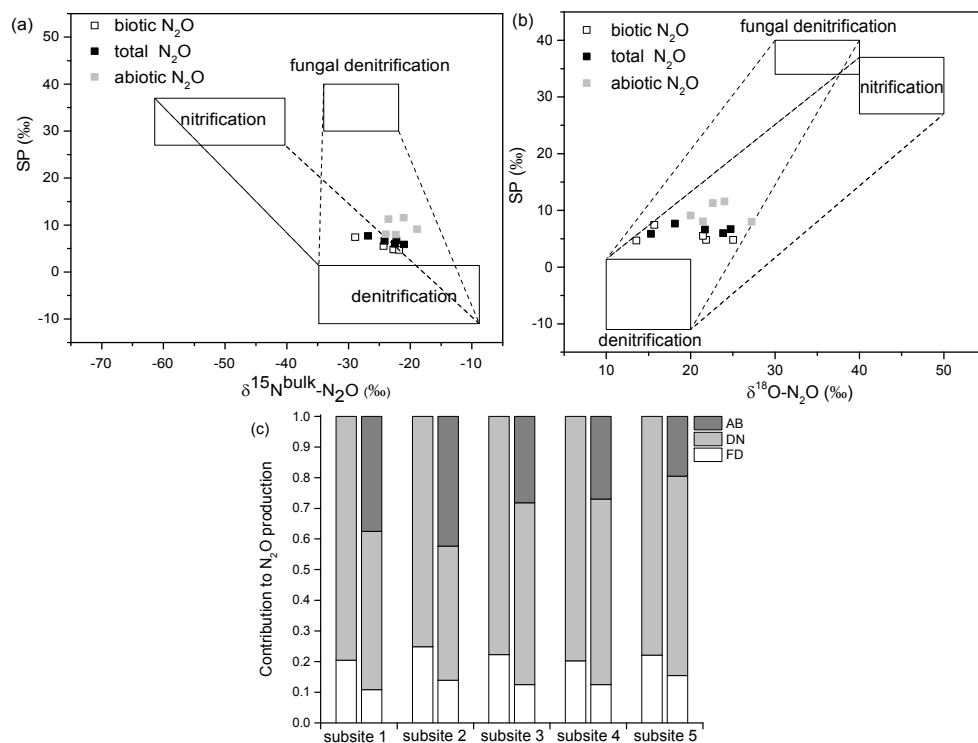


Fig. IV.5. End-member map of SP vs. $\delta^{15}\text{N}^{\text{bulk}}\text{-N}_2\text{O}$ (a) and $\delta^{18}\text{O}\text{-N}_2\text{O}$ (b), and contribution of abiotic N_2O production (AB), fungal denitrification (FD) and denitrification (DN) to N_2O production calculated with a two-end-member mixing model (c). The left bars in (c) show the contribution of FD and DN when AB is neglected, while the right bars represent the relative contribution of all three sources.

If abiotic N_2O was not taken into account in the two-end-member mixing model, fungal denitrification and denitrification contributed 20.4–24.8 % and 75.2–79.8 % of the total N_2O emission, respectively (left bars in Fig. IV.5c). However, fungal denitrification and denitrification contributed only 10.8–15.5 % and 43.8–65.0 % of the total N_2O production, respectively, when the 19.5–42.3 % of abiotic N_2O production was considered (Fig. IV.5c). In this study, the SP values of 8.0–11.6 ‰ from abiotic N_2O emission, which could not be explained by the two end-member model, could be easily misinterpreted as the combined contribution of fungal denitrification and denitrification. In addition, Ostrom et al. (2016) reported a significant linear relationship of $\delta^{15}\text{N}\text{-N}_2\text{O}$ with time in the $^{15}\text{N}\text{-NO}_2^-$ and HgCl_2 treatment, while the SP values of chemically produced N_2O were not distinct from that of microbial N_2O production. Hence, N_2O source apportionment could have been biased in the former studies in which two-end-member mixing models were used without considering abiotic N_2O emission.

Reduction of N_2O not only leads to the enrichment of ^{15}N and ^{18}O , but also to increases in SP values of the residual N_2O by a fractionation factor of -5 ‰ (Lewicka-Szczebak et al., 2015). Since the

main biotic N₂O production pathways were fungal denitrification and denitrification in this study, the measured SP values of N₂O in unsterilized soil should be higher than that of produced N₂O due to N₂O reduction. All in all, end-member maps can help to approximately identify N₂O sources, while a third, i.e. abiotic, N₂O pathway should be included. Since the abiotic N₂O emission and its isotopic characteristics are not completely understood at present, more related studies should be conducted in the future.

IV.3.1.4 Factors controlling N gas emission in soils

The results of the RDA analysis regarding soil characteristics are displayed in Fig. IV.6. RDA 1 and RDA 2 represent the two main components explaining the variability of N₂O and NO_x emission among samples. They explained 72.9 % and 23.2 % of the total variance, respectively (Fig. IV.6). The distance between each sample point represents the similarity of N₂O and NO_x emission, while the angle between the response vector (N₂O or NO_x vector) and the variable vector (soil characteristic vector) represents their linear correlation. Sterilized and unsterilized soils are clearly separated due to their distinct N₂O emission. Lignin-derived H and S units, soil pH, the acid-to-aldehyde ratio of the S unit (Ad/Al)_S, Al, P, Mn, and Fe content were positively correlated with the total NO_x emission, while total lignin, TN, TOC, NH₄⁺, NO₃⁻, lignin-derived G unit, and the acid-to-aldehyde ratio of the G unit (Ad/Al)_G were negatively correlated with the total NO_x emission. In addition, the total N₂O emission was positively correlated with Mn, Fe, P, soil pH, lignin-derived S units, and (Ad/Al)_G, but negatively correlated with total lignin, TN, NH₄⁺, and TOC. In the narrow range of 2.9–3.4, pH was positively correlated with N₂O and NO_x emission. The possible reason could be that nitrous acid becomes more reactive to SOM at lower pH, resulting in higher N retention. In contrast, the reduction of NO₂⁻ to N₂O and NO_x by microorganisms and transition metals was less influenced in this narrow pH range.

Transition metals in soil can reduce NO₂⁻ to NO directly or catalyze the reduction of NO₂⁻ by SOM indirectly under both neutral and acidic conditions (Jones et al., 2015; Pilegaard, 2013), which can explain the strong positive correlation of NO_x emission and Mn, Fe, and Al contents in this study. However, how P content in soil affects N gas emission is not clear until now. The negative correlation of total lignin, TOC and N₂O emission was also demonstrated for agricultural soils with relatively high soil pH (Garcia-Ruiz and Baggs, 2007; Millar and Baggs, 2004). Garcia-Ruiz and Baggs (2007) also reported the strongly negative correlation of N₂O emission with lignin and total organic carbon (TOC) content during the simultaneous application of N fertilizer and plant residues to a silt loam soil at pH 7.1. The possible reason why higher lignin and TOC content decreased N gas emission could be that phenolic compounds derived from lignin decomposition can incorporate NO₂⁻-N into organic compounds, thereby reducing N gas emission and increasing N retention in soil (Lewis and Kaye, 2012; Rousseau and Rosazza, 1998; Thorn and Mikita, 2000). For example, NO₂⁻ was incorporated

into α -naphthol with the formation of nitrogenous aromatic compounds in buffered grassland soil suspensions at pH 6.5 (Azhar et al., 1989); nitroso and heterocyclic N compounds were formed from the reaction of NO_2^- with ferulic acid at pH 2 (Rousseau and Rosazza, 1998); and amides and oximes were produced during the NO_2^- fixation into humic substances at pH 3 and 6 (Thorn and Mikita, 2000). The range of pH and soil types in the different studies demonstrate that the reaction of SOM with NO_2^- is not limited to acidic forest soil but occur widely in grassland and agricultural soils.

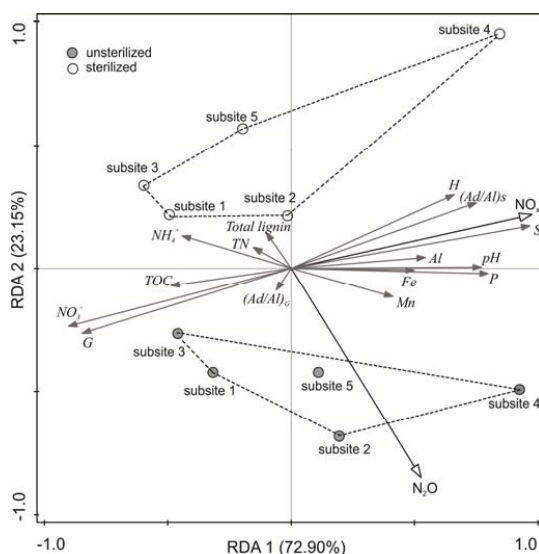


Fig. IV.6. Redundancy analysis (RDA) based on total N_2O and NO_x emission, and characteristics of sterilized and unsterilized soils. TOC, total organic carbon; TN, total nitrogen; P, phosphate; G, guaiacyl units of lignin; S, syringyl units of lignin; H, *p*-hydroxyphenyl units of lignin; $(\text{Ad}/\text{Al})_G$, acid-to-aldehyde ratio of vanillyl units; $(\text{Ad}/\text{Al})_S$, acid-to-aldehyde ratio of syringyl units. $(\text{Ad}/\text{Al})_G$ and $(\text{Ad}/\text{Al})_S$ are indicators of the degree of lignin degradation.

In this study, lignin S and H units contributed to both NO_x and N_2O emissions, while G unit led to less N gas emission. Therefore, application of plant residues with higher lignin and G unit content could help to reduce NO_2^- -related N_2O emission under acidic conditions. Plant litters are widely used to reduce N_2O emission in agricultural management, while lignin structure was never considered as a governing factor of N_2O emission (Millar and Baggs, 2004). It would help to choose suitable N_2O -reducing plant litter for agricultural management if the rule of lignin structure in N_2O emission is also confirmed in agricultural soil in the future. Both $(\text{Ad}/\text{Al})_S$ and $(\text{Ad}/\text{Al})_G$ are lignin degradation indicators (Hedges et al., 1988), however, $(\text{Ad}/\text{Al})_S$ was positively correlated with both NO_x and N_2O emission, while $(\text{Ad}/\text{Al})_G$ was positively correlated with N_2O emission, but negatively related with NO_x emission. At present, there is no clear explanation for this divergence, but the effect of lignin

degradation on N trace gas emission could be related to the N immobilization and re-release dynamics of NO₂⁻-lignin interactions.

IV.3.2 NO_x and N₂O emissions from SOM fractions

IV.3.2.1 NO_x emission from SOM fractions

The real-time NO_x emissions after NO₂⁻ addition to the four SOM fractions are illustrated in Fig. C5. The amount of NO produced was approximately equal to that of NO₂ in both the DOM fraction and the NO₂⁻ control, while the NO fraction was much higher in the FA, HA, and HN fractions. In addition, both NO/NO_x ratio and $t_{1/2}$ decreased greatly in the following order: DOM > FA > HA > HN, according to the pattern that the heavier the SOM molecular weight, the faster the initial NO_x emission. Considering the fact that NO accounted for most of the NO_x emission in soil samples, NO emission was calculated and fitted with the Hill equation (Fig. IV.1c). Total NO emission (NO_{max}) was the lowest in the HN fraction (1154 ng N g⁻¹ soil), which had the fastest initial NO emission, while NO_{max} was highest in the DOM fraction (4048 ng N g⁻¹ soil), which had the slowest initial NO emission.

Previous studies have demonstrated that NO_x and N₂O are the main N gas products from abiotic NO₂⁻ reactions with lignin, lignin derivatives, and humic acid (Azhar et al., 1989; Nelson, 1967; Nelson and Bremner, 1970; Thorn and Mikita, 2000). This study compared the N trace gas emission from NO₂⁻ reactions with different SOM fractions for the first time. The similar NO and NO₂ emissions from the DOM fraction and the NO₂⁻ control indicate that NO_x emission from the DOM fraction originates mainly from the self-decomposition of NO₂⁻, which is a chemical disproportionation reaction leading to equal amounts of NO and NO₂. The significant increase of relative NO_x emission rate and higher NO proportion in FA, HA, and HN fractions indicates that the reductive ability of the FA, HA, and HN fractions was significantly higher than in DOM fraction.

As the main SOM compounds, solid soil humic substances contain a high level of pH-dependent stable organic free radicals (about 10¹⁸ per gram), which could be semiquinones and quinhydrones resulting from lignin degradation (Baehrle et al., 2015). These organic free radicals enable solid SOM to act as efficient electron donor for redox reactions in soil and could facilitate its reaction with NO₂⁻. The amount of NO emission decreased significantly in the order of DOM > HA > FA > HN, which could be the result of N fixation through nitrosation of NO₂⁻ with organic macromolecules in the FA, HA, and HN fractions. Furthermore, it has been shown that NO₂⁻ can be incorporated into humic substances with the formation of stable organic N in soil (Thorn and Mikita, 2000).

IV.3.2.2 N₂O emission from soil fractions

A sharp N₂O peak was found for both the HN and HA fraction, while a broad N₂O peak was found for the FA fraction, however, no obvious N₂O peak was observed for the DOM fraction (Fig. C6).

Fitting of N₂O emissions with the Hill equation revealed that total N₂O emission was saturated at 80.3 ng N g⁻¹ soil in the FA fraction, followed by the HA and HN fractions (Fig. IV.3c). The results clearly showed that SOM quality matters for both the rate and total amount of N₂O produced from NO₂⁻.

Since extremely strong base and acid were used for soil fractionation, it can be assumed that the microorganisms had been killed and that abiotic reactions accounted for most of the N₂O and NO_x emission in the FA, HA, and HN fractions. The combined N₂O emissions from the FA, HA, and HN fractions amounted to 68.4 % of the total abiotic N₂O emission from sterilized soil of subsite 2, while the FA fraction alone made up 43.6 % of the abiotic N₂O release. This result indicates that SOM, especially the FA fraction, favors abiotic N₂O emission from NO₂⁻ in acidic soils. The different N₂O and NO_x emissions from different SOM fractions could result from their individual chemical composition and structures. It is assumed that carbohydrate structures dominate in the FA fraction, while there are much more alkyl carbon and aromatic structures in the HA fraction, whereas the HN fraction mainly contains plant-derived lignin structures (Kögel-Knabner et al., 1988). Other potential reaction partners are semiquinones, and associated transition metals like manganese (Zhang et al., 2014). Aromatic compounds, for example semiquinones, contains large amount of free organic radicals that can facilitate the electron transfer in abiotic redox reactions (Zhang et al., 2014). Humic and humic acid contain much more aromatic radicals than fulvic acid (Ghosh and Schnitzer, 1980; Zhang and Katayama, 2012), which could explain the much higher N₂O and NO_x emission rates in HN and HA treatments. However, it is not clear how the carbohydrate structures react with NO₂⁻ to form N₂O until now. Further studies are needed to explain the detailed mechanisms.

Compared with the N₂O from soil, both δ¹⁵N^{bulk} (-13.82 to -11.03 ‰) and SP (20.27 to 26.14 ‰) of N₂O from SOM fractions were much higher (Table IV.1). In addition, the δ¹⁸O of N₂O from the SOM fractions ranged from 33.20 to 41.48 ‰, which was also much higher than that from soil. The higher δ¹⁵N^{bulk} and δ¹⁸O indicate much stronger fractionation during the reaction with NO₂⁻, which resulted in much higher SP values. During the SOM fractionation, the SOM structure, for example SOM–metal complexes and SOM radicals, must have been disturbed by the concentrated acid and alkali. In addition, the SP values of N₂O from NO₂⁻–SOM reactions depend greatly on the pH and SOM structure instead of staying stable (Chapter II and III), which makes it more complicated to identify N₂O sources when much N₂O emission comes from the NO₂⁻–SOM reactions.

This study demonstrates that NO₂⁻–SOM reactions are important abiotic N₂O and NO_x sources in acidic forest soils. For the first time data are provided on N trace gas emissions from different SOM fractions, revealing the humin fraction as the fraction with the lowest NO_x emission potential and the fulvic acid fraction as the fraction with the highest NO₂⁻-to-N₂O conversion potential. While there is reasonable dispute that during fractionation, SOM structure could slightly change so that the obtained SOM fractions may not exist as such in nature (Stevenson, 1995), the data presented here

nevertheless clearly show that different parts of SOM play a different role in abiotic N₂O and NO_x release.

Table IV.1. Isotopic signatures of N₂O from NO₂⁻-SOM fraction reactions

	$\delta^{15}\text{N}^{\text{bulk}}$ (‰ vs. air-N ₂)	$\delta^{15}\text{N}^{\text{a}}$ (‰ vs. air-N ₂)	$\delta^{15}\text{N}^{\text{b}}$ (‰ vs. air-N ₂)	$\delta^{18}\text{O}$ (‰ vs. VSMQW)	SP ^d (‰)
FA ^a	-11.03 ± 0.21	-0.89 ± 0.02	-21.16 ± 0.39	41.48 ± 0.37	20.27 ± 0.37
HA ^b	-13.82 ± 0.44	-1.23 ± 0.44	-26.42 ± 1.34	35.75 ± 0.44	25.20 ± 1.77
HN ^c	-12.54 ± 0.03	0.52 ± 0.18	-25.61 ± 0.25	33.20 ± 1.63	26.14 ± 0.43

Note:

^a fulvic acid;

^b humic acid;

^c humin;

^d ¹⁵N N₂O site preference.

^e N₂O from DOM fraction was not measured due to its low emission rate.

IV.4 Conclusions

In the present study, NO₂⁻-driven NO_x and N₂O emissions were measured for the first time in real-time with a combination of chemoluminescence analyzer and quantum cascade laser spectrometer. 17–51 % and 3.3–7.1 % of the added NO₂⁻ was quickly transformed to NO_x and N₂O, respectively, when NO₂⁻ was applied to acidic spruce forest soils. Compared with the DOM, humin, and humic acid fractions, the fulvic acid fraction contributed the most to abiotic N₂O emission. The SP values of N₂O from abiotic pathways were not distinguishable from biotic pathways, and application of a two-end-member mixing model biased N₂O source apportioning when abiotic N₂O emissions were not considered. This study suggests that abiotic reactions of NO₂⁻ with SOM could be an additional N₂O source that has been highly underestimated before, and further study is needed to identify and quantify their contribution to soil N₂O emission in various soils.

V. Abiotic nitrite retention in soils revealed by solid-state ¹⁵N-NMR structure analysis

Based on:

Wei, J., Knicker, H., Brüggemann, N., Abiotic nitrite retention in soils revealed by solid-state ¹⁵N-NMR structure analysis. *Manuscript in preparation.*

V.1 Introduction

Nitrogen retention in soils highly depends on the prevalent inorganic N compounds, e.g. the retention of NH_4^+ and NO_3^- largely depends on the biological uptake by microbes and plants, while abiotic reactions with SOM contribute the most to the retention of NO_2^- (Lewis and Kaye, 2012). Nitrite is highly chemically reactive to transition metals and SOM in soils, especially at acidic pH. Isobe et al. (2012) found that 17.8 % of NO_2^- was incorporated into DOM within 4 h when applied to a forest soil. One of the typical products of abiotic NO_2^- reactions with SOM is heterocyclic N compounds, which are receiving more and more interest due to their resistance to decomposition (Leinweber et al., 2009). Heterocyclic N compounds have been detected in various natural humic substances (Thorn and Cox, 2009), and the content of heterocyclic N increased during humification (Abe et al., 2005). Therefore, abiotic reactions of NO_2^- with SOM could play an important role in the long-term N retention in soils.

Nitrite is an intermediate of both nitrification and denitrification, and it occurs widely in terrestrial ecosystem. Generally, NO_2^- is regarded as the direct precursor of both biotic and abiotic production of nitric oxide (NO), and its contribution to abiotic N_2O emission has also been receiving more attention recently (Venterea, 2007). Under acidic conditions, NO_2^- combines with a proton to form nitrous acid (HNO_2), which can further react with SOM through N-, C-, or O-nitrosation to form NO, N_2O , and nitrogenous organic compounds (Austin, 1961). Nitrosophenol, *p*-diazquinone, and *o*-diazquinone were identified in the reaction of NO_2^- with phenol under mildly acidic conditions (Kikugawa and Kato, 1988). Nitrosonaphthol and nitronaphthol were also found as the products of abiotic reaction of NO_2^- with naphthol in soil suspensions at pH 6.5 (Azhar et al., 1989). Rousseau and Rosazza (1998) found that NO_2^- -N was incorporated into 7-hydroxy-6-methoxy-1,2(4*H*)-benzoxazin-4-one in the reaction with ferulic acid at pH 2.

As a key participant in abiotic N retention, SOM is a complex substance constituted of both simple molecules and macro polymers. Except for some low-molecular-weight compounds, such as simple acids, sugars, and amino acids, most of the SOM molecules are not yet chemically identified till now (Stevenson, 1995). According to ¹³C-NMR analysis, O-alkyl-C assigned to amides and polysaccharides dominates in SOM, followed by alkyl-C and C/O-substituted alkyl-C, which correspond to chain aliphatic C from lipids and aromatic C from lignin, respectively (Fontaine et al., 2007). It has been confirmed that aromatic C as well as methylene C and N are reactive sites for nitrosation in the reaction of SOM with NO_2^- (Thorn and Mikita, 2000). Thorn and Mikita (2000) reported the formation of nitrophenol, imine, and indophenol from the reactions of fulvic and humic acid with NO_2^- through ¹⁵N-NMR analysis. Nevertheless, it is still an open question whether these reactions occur in natural soils or not, and if so, how much they contribute to N retention in natural soils. Therefore, more research is needed to bridge the gap between reactions in chemical assays and

N retention in natural soils.

In this study, abiotic N retention as a result of NO_2^- -SOM reactions was investigated in three types of soils (forest, grassland, and agricultural soils) with different soil pH and carbon content. Solid-state CP/MAS ¹⁵N-NMR was used for structure analysis of immobilized N. Influence of microbes on abiotic NO_2^- -SOM reactions was also explored by introducing soil suspension with living soil microbes into the reaction microcosms.

V.2 Materials and Methods

V.2.1 Soils

Forest soil (Cambisol, pH = 3.6 ± 0.0 , Total N = 1.5 ± 0.0 %, Total C = 30.1 ± 0.8 %) was sampled from the top 20 cm of the Wüstebach catchment ($50^\circ 30' 15''\text{N}$, $6^\circ 18' 15''\text{E}$) which is a field site of the German interdisciplinary program TERENO (Zacharias et al., 2011). Grassland soil (Cambisol, pH = 5.1 ± 0.0 , Total N = 1.3 ± 0.0 %, Total C = 4.6 ± 0.0 %) and agricultural soil (Luvisol, pH = 6.0 ± 0.2 , Total N = 0.1 ± 0.0 %, Total C = 1.3 ± 0.0 %) were sampled from the top 20 cm of the Achterwehr field ($54^\circ 19' 05''\text{N}$, $9^\circ 58' 38''\text{E}$) and the Rollesbroich grassland ($50^\circ 37' 0''\text{N}$, $6^\circ 26' 0''\text{E}$), Germany, respectively. Soil samples were air-dried, then sieved at 2 mm mesh size and finally homogeneously mixed.

V.2.2 Abiotic nitrite retention in soils

Five gram of rewetted soil sample was put into 22.5-ml glass vials and autoclaved for 30 min at 121°C and 201.3 kPa. When autoclaved soils had cooled down to room temperature, 5 ml of 5 mM NaNO_2 (10 % atom ¹⁵N, VWR, Germany) solution was applied to the soils. Sodium nitrite solution was sterilized by passing through a 0.2 μm syringe filter. After the application of NaNO_2 , glass vials were immediately closed to avoid any microbial contamination, and soils were incubated in a clean bench at room temperature for 4 d.

After incubation, soil samples were transferred under sterile conditions to sterilized centrifuge tubes, and the remaining NO_2^- , NH_4^+ , and NO_3^- were removed by washing the soils with 20 ml of 1 M KCl (VWR, Germany) solution three times. Before usage, the KCl solution was passed through a 0.2 μm syringe filter to avoid introducing microbes to the soils during washing. After washing, soil samples were immediately freeze-dried and stored at room temperature till analysis. The remaining ¹⁵N in soils was regarded as ¹⁵N immobilized as soil organic nitrogen (SON). As blank control, water instead of NaNO_2 solution was applied to soils, and all treatments were prepared in triplicate. To confirm that no microbial contamination occurred during the whole procedure, 0.1 μl of KCl solution after washing was plated on agar plates, and no bacterial colony was observed after 7 d of incubation at room temperature.

To remove the mineral fractions, soils were stepwise treated with 1 M HCl, 32 % of HCl, a

mixture of 10 % HCl and 10 % HF, and finally 50 % HF. Fulvic acid in the HCl solution was recovered by solid phase extraction (Bond Elut-PPL, 500 mg, 6 ml). All chemicals for this procedure were obtained from VWR (Germany). The remaining humus (OM) fraction after HF treatment was washed with deionized water to pH 3–4, and then freeze-dried.

The ¹⁵N content of soils, fulvic acid, and humus was analyzed with an isotope-ratio mass spectrometer (IRMS, Isoprime 100, Elementar Analysensysteme, Langenselbold, Germany), and N retention was calculated as the proportion of ¹⁵N immobilized in SON of the total applied ¹⁵N-NO₂⁻.

V.2.3 Solid-state ¹⁵N-NMR spectroscopy

To enhance the ¹⁵N-NMR signals, forest humus (FOM) and grassland humus (GOM) were amended with Na¹⁵NO₂ (99 % atom ¹⁵N, VWR, Germany) a second time. For this, 0.4 g of FOM or GOM was mixed with 0.2 g of Na¹⁵NO₂ dissolved in 10 ml of sterilized water in sterilized 25-ml centrifuge tubes, and incubated in a clean bench for 6 d at room temperature. After incubation, the mixture was centrifuged at 4000 *g* for 20 min, and the liquid phase was carefully decanted into another tube. Both liquid and solid phase were freeze-dried for ¹⁵N-NMR analysis. To test the effect of soil microbes on abiotic N immobilization, soil suspension with living microbes instead of sterilized water was used for the incubation.

The solid-state ¹⁵N-NMR spectra were obtained with a Bruker Avance III HD 400 MHz Wideboard (Bruker, Billerica, Massachusetts, United States) operating at a ¹⁵N resonance frequency of 40.56 MHz. Samples were placed into zirconium rotors of a diameter of 7 mm with KEL-F-caps. The cross polarization magic angle spinning (CP/MAS) technique was applied with a spinning speed of the rotor at 6 kHz and a pulse delay of 200 ms. A ramped ¹H-pulse was used during a contact time of 1 ms in order to circumvent spin modulation of Hartmann-Hahn conditions. A contact time of 1 ms and a 90° ¹H-pulse with a width of 3.5 μs were used for all spectra. The ¹⁵N chemical shifts were calibrated against nitromethane (= 0 ppm) with glycine (-346.7 ppm). Depending on the ¹⁵N content of the samples, between 50,000 and 1,900,000 scans were accumulated. The relative intensities of the peaks were obtained by integration of the specific chemical shift ranges with an integration routine with MestreNova 10 (Mestrelab research, Santiago de Compostela, Spain).

V.2.4 Statistical analysis

One-way analysis of variance (ANOVA) was conducted using OriginPro 8.0 (Originlab Corporation, Wellesley Hills, MA, USA) to test if the differences of N retention and ¹⁵N-enrichment between each treatment were significant.

V.3 Results and discussion

V.3.1 Abiotic retention of NO₂⁻

After 4 d of incubation under sterilized conditions, 6.3–7.6 % of NO₂⁻ was immobilized by SON, and there was no significant difference ($P < 0.05$) in the three types of soils (Fig. V.1a). The N retention of NO₂⁻ in this study is comparable to the 10 % in a Canton soil (Dail et al., 2001), but dramatically lower than the 20 % in a sandy loam at pH 3.8–4.0 (Islam et al., 2008) and the 65–80 % in an Inceptisol at pH 3.4–3.9 (Fitzhugh et al., 2003a). The SOC content and pH are generally regarded as main factors controlling the chemical immobilization of NO₂⁻ in soils (Dail et al., 2001). Under acidic conditions, NO₂⁻ can be protonated to nitrous acid (HNO₂) which is highly reactive to SOM and transition metals, hence it is thought that chemical NO₂⁻ immobilization is favored by acidic pH (Riordan et al., 2005). Islam et al. (2008) found no more abiotic NO₂⁻ immobilization when pH was increased to 8. In addition, as the participator into abiotic NO₂⁻-SOM reactions, the SOC content carbon was found to be significantly positively correlated with the chemical N retention in various soils (Fitzhugh et al., 2003b). However, the N retention in forest soil was not significantly higher compared with agricultural and grassland soils in spite of its markedly lower pH and higher carbon content in the present study. Thus, there must be other factors, such as the content of transition metals, that also affect the retention of NO₂⁻-N in soils, and more research is needed to further explore the detailed mechanisms involved.

Even though the recovered fulvic acid fraction made up only 0.5–2 % of the total SOC, its $\delta^{15}\text{N}$ value was 2–3 times higher than for the corresponding humus fraction and the soil before HF treatment (Fig. V.1b), which indicates that fulvic acid is highly reactive to NO₂⁻. Wei et al. (2017a) also found that fulvic acid was the SOM fraction most reactive to NO₂⁻ compared with DOM, humic acid, and humin, and it accounted for most of the abiotic soil N₂O emissions. Fulvic acid is composed of aromatic macro-polymers with lower molecular weight and aromaticity compared with humic acid and humin (Stevenson, 1995). In addition, fulvic acid is generally characterized by relatively higher C/N ratio, more alkyl-C and carboxyl-C than humic acid (Gondar et al., 2005; Weber and Wilson, 1975). These characteristics could be the reason why fulvic acid is much more reactive to NO₂⁻ compared with humus.

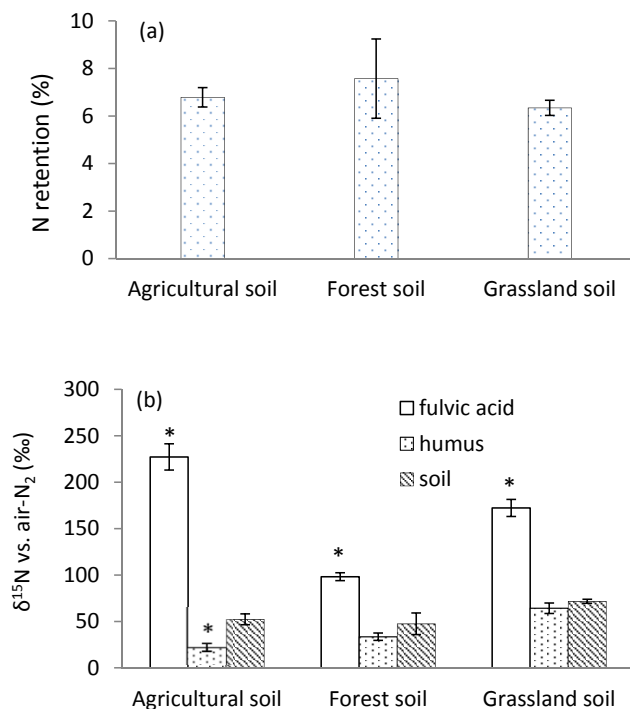


Fig. V.1. Abiotic N retention of NO_2^- in agricultural, forest, and grassland soil (a) and $\delta^{15}\text{N}$ values of soil, fulvic acid, and humus in $^{15}\text{NO}_2^-$ amended soils (b). Stars indicate the $\delta^{15}\text{N}$ value is significantly ($P < 0.05$) different from the soil before HF treatment.

V.3.2 Structure of immobilized N

The solid-state CP/MAS ^{15}N -NMR spectra of forest humus are shown in Fig. V.2. The major peaks occurred between -50 and 50 ppm, and -180 to -320 ppm, representing 10–30 % and 49–66 % of the total N, respectively (Table V.1). The downfield shoulder from 50 to 10 ppm could represent the monoximes derived from their corresponding tautomer of nitrosophenols (Reaction [V.1]) (Thorn and Mikita, 2000). The peak at -2 ppm could denote NO_3^- which was formed through the oxidation of NO_2^- (Reaction [V.2]). The peak between 50 and -50 ppm could originate from ketoxime and nitro compounds from the nitrosation of activated methylene carbons (Reaction [V.3]) and the oxidation of nitroso compounds (Reaction [V.4]), respectively (Thorn and Mikita, 2000). The frequency from -50 to -180 ppm is assigned to pyridines and nitriles, whereas the range from -180 to -230 ppm is characteristic for pyrroles (Knicker, 2011a). No pyridine was found in any treatment of the present study, while a nitrile peak from -100 to -160 ppm was found in the solid phase of forest humus treated with $^{15}\text{NO}_2^-$ (Fig. V.2). Nitriles could be formed through Beckmann fragmentation of Ketoximes and quinone monoximes (Reactions [V.5–6]) (Thorn et al., 1992; Thorn and Mikita, 2000).

The downfield peak between -180 and -230 ppm overlaps with the frequency of substituted pyrroles (Knicker, 2011a), which could be formed through Knorr pyrrole synthesis (Thorn and Mikita, 1992). The peak between -230 and -285 ppm, with the maximum at -270 ppm in NO₂⁻-treated humus, corresponds with amides, which result from the hydrolysis of nitriles (Reaction [V.7]) or the Beckmann rearrangement of oximes (Reaction [V.8]) (Thorn and Cox, 2016). The peak of microbial amides also ranged from -230 to -285 ppm in natural humus, but centered at -257 ppm. The downfield peak from -285 to -320 ppm could be finally assigned to amino N (Knicker, 2011a).

Table V.1. Peak areas as percentage of total ¹⁵N for CP/MAS ¹⁵N-NMR spectra.

Treatment	50 to 50 ppm (nitro/oxime/NO ₃ ⁻ , %)	-100 to -180 ppm (nitrile, %)	-180 to -230 ppm (pyrrole, %)	-230 to -285 ppm (amide, %)	-285 to -320 ppm (amino, %)
GOM+ ¹⁵ NO ₂ ⁻ (S) ^a	22	8	8	51	8
GOM+ ¹⁵ NO ₂ ⁻ +M (L) ^b	14	5	9	65	4
GOM+ ¹⁵ NO ₂ ⁻ +M (S) ^c	26	6	7	51	8
FOM+ ¹⁵ NO ₂ ⁻ (S) ^d	30	3	9	49	7
FOM+ ¹⁵ NO ₂ ⁻ (L) ^e	10	6	9	66	6

Note:

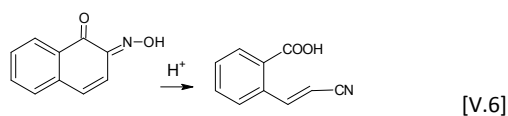
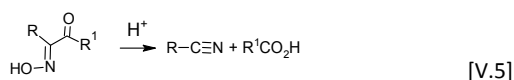
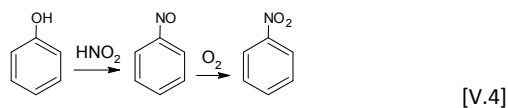
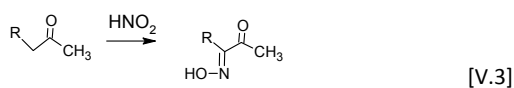
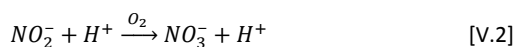
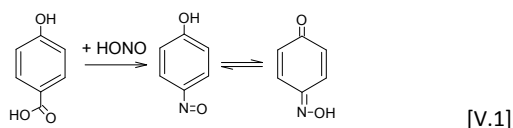
^a Solid phase of NO₂⁻-amended grassland humus without microbial inoculant;

^b Liquid phase of NO₂⁻-amended grassland humus with microbial inoculant;

^c Solid phase of NO₂⁻-amended grassland humus with microbial inoculant;

^d Solid phase of NO₂⁻-amended forest humus without microbial inoculant;

^e Liquid phase of NO₂⁻-amended forest humus without microbial inoculant.



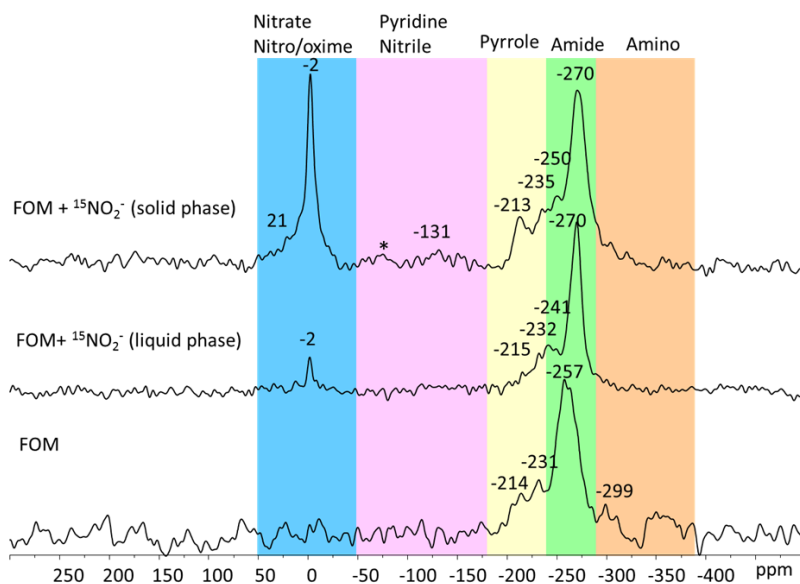
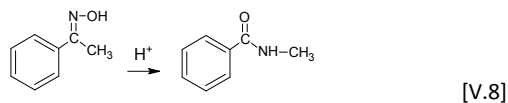


Fig. V.2. Solid-state CP/MAS ^{15}N -NMR spectra of forest humus (FOM) with or without $^{15}\text{NO}_2^-$ amendment under sterilized conditions. * signifies spinning side band.

The spectra of $^{15}\text{NO}_2^-$ -treated GOM were similar to those of $^{15}\text{NO}_2^-$ -treated FOM, and peaks of nitro/oxime, nitrile, pyrrole, amide, and amino N were found in both sterilized and unsterilized treatments (Fig. V.3). After $^{15}\text{NO}_2^-$ amendment, the liquid phase contained 12–20 % less nitro/oxime and 14–17 % more amide compared with the solid phase, while the contents of other products were similar in the two phases (Table V.1). Notably, neither the forms of abiotic products nor their quantification were affected by the microbial inoculation (Fig. V.3 and Table V.1). Generally, the abiotic $^{15}\text{NO}_2^-$ -SOM reactions occurred much quicker than the microbial transformation of $^{15}\text{NO}_2^-$, so it is very likely that NO_2^- has been incorporated into SOM before it could be used by the microbes. On the other hand, high concentration of NO_2^- is toxic to microbes (Bollag and Henninger, 1978), so it could also be possible that the microbial activity was inhibited by the high NO_2^- concentration during the incubation.

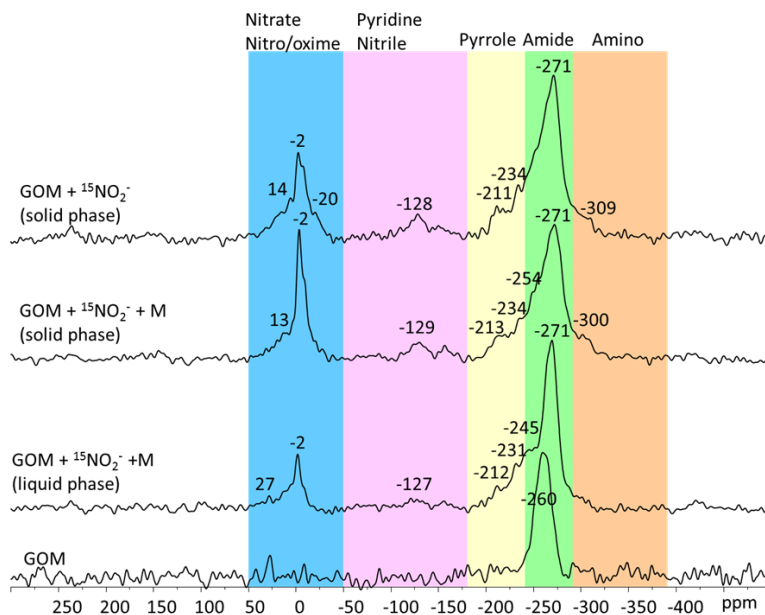


Fig. V.3. Solid-state ^{15}N -NMR spectra of grassland humus (GOM), GOM amended with $^{15}\text{NO}_2^-$ and microbial inoculant (GOM+ NO_2^- +M), and GOM amended with $^{15}\text{NO}_2^-$ under sterilized conditions (GOM+ NO_2^-).

Thorn and Mikita (2000) investigated the reaction of NO_2^- with International Humic Substance Society peat humic acid using liquid-phase ACOUSTIC ^{15}N -NMR, and found that nitrosophenol and oxime N made up 76 % of the total products, while amides only accounted for about 7 %. In the present study, the samples were reacted for 6 d, which was much longer than the 24 h used in the former study, so there was enough time for oximes to go through the following Beckmann rearrangement, Beckmann fragmentation, and hydrolysis to finally form amides. This could explain the much higher content of amides in this study. In addition, nitro compounds instead of nitroso compounds were prevalent in this study, because nitroso compounds are not stable and can be easily oxidized to nitro compounds or transformed to amides at acidic pH. By contrast, Rousseau and Rossazza (1998) reported the formation of 2-methoxy-4,6-dinitrophenol and 2-methoxy-6-nitrophenol from the reaction of NO_2^- with ferulic acid, originating from the oxidation of their corresponding nitrosophenols.

The formation of oximes is the key step for N incorporation not only in the reactions of SOM with NO_2^- , but also with NH_2OH and nitric acid, while nitriles and amides are the products of the following Beckmann rearrangement or fragmentation. Therefore, similar products were found in the reactions of humic substances (fulvic acid and humic acid) with inorganic N compounds (NO_2^- , NH_3 , and nitric acid) (Thorn et al., 1992; Thorn and Cox, 2016; Thorn and Mikita, 1992). By contrast, the

major products were heterocyclic N compounds, such as indoles and pyrroles, instead of oximes and amides, for reactions of fulvic and humic acids with NH₃ (Thorn and Mikita, 1992). It was proposed that pyrroles were produced through the polymerization of amino N (Thorn and Mikita, 1992), which could also explain the formation of pyrroles in this study.

In natural soils and humic substances, amides are the most abundant N compounds, and amide N could be directly bonded to aromatic rings through abiotic reactions when SOM is rich in lignin-derived residues (Schmidt-Rohr et al., 2004). Generally, amides are regarded as typical biological N compounds, however, it was demonstrated in the present study that abiotic reactions of NO₂⁻ and SOM under natural conditions could also lead to substantial formation of amides. In addition, heterocyclic N was also found in the fulvic acids of Elliot Soil and Florida Pahokee Peat, and humic acids of Florida Pahokee Peat, Summit Hill soil, and Leonardite (Thorn and Cox, 2009). According to the study of Leinweber et al. (2009), all changes of SON were related to heterocyclic N compounds in long-term incubated soils. Abe et al. (2005) also found that the proportion of heterocyclic N compounds was positively correlated with the aromaticity of SOM and increased during humification. On the contrary, nitro-aromatic compounds were found in the rhizosphere of pea, where aromatic compounds decreased (Gillespie et al., 2009). Therefore, abiotic N retention could be much more prevalent than previously thought. However, more research is needed to further explore the role of abiotic reactions in N cycling and the factors affecting these processes.

V.4 Conclusions

The abiotic N retention by NO₂⁻-SOM reactions was studied in forest, grassland, and agricultural soils. About 6 % of NO₂⁻-N was immobilized by SOM within 4 d, and there was no significant difference between the three types of soil. Interestingly, fulvic acid showed a drastically higher reactivity compared with other humic substances. What is more, nitro and amide N were the dominant products of abiotic NO₂⁻-N retention according to the solid-state CP/MAS ¹⁵N-NMR analysis. In conclusion, abiotic NO₂⁻-SOM reactions do contribute to N immobilization in soils, and further study is needed to explore the contribution of abiotic N retention to total N retention in soils, and to characterize the controlling factors.

VI. Effect of lignin content and composition of organic soil amendments on nitrogen partitioning in agricultural soil

Based on:

Wei, J. Reichel, R., Islam, M. S., Wissel, H., Amelung, W., Brüggemann, N., Effect of lignin content and composition of organic soil amendments on nitrogen partitioning in agricultural soil. *Manuscript in preparation.*

VI.1 Introduction

Nitrogen is one of the most important, essential elements for all living organisms on earth, and has usually been a growth-limiting nutrient in natural and agricultural ecosystems. Since 1920s, industrial N fertilizers, such as urea, NH_4^+ , and NO_3^- , have been widely applied to promote agricultural food production, and the global consumption of N fertilizers exceeded 173 million tons in 2013 (FAO, 2015). However, the recovery of applied fertilizer-N in crops is generally less than 65 %, and the rest is immobilized as SON, or emitted to the atmosphere as N_2O and NO, or leached into water systems as NO_3^- (Zhu and Chen, 2002). Global fertilizer-associated N_2O and NO emissions represent 6.8–7.3 % and 0.1–0.4 % of the applied fertilizer-N, respectively (IFA, 2001). Consequently, the global atmospheric N_2O concentration increased to 328 ppb in 2015, which is about 121 % of the pre-industrial level (WMO, 2016). Therefore, it is currently the primary task to improve the N use efficiency (NUE) in agriculture.

It has been proposed that combined application of N fertilizer and organic soil amendment (OSA) could enhance NUE and raise soil fertility by strongly promoting N retention (Baggs et al., 2000). However, the influence of OSA on fertilizer-associated N_2O emission and N retention depends to a great extent on the chemical composition of the applied soil amendments. Mooshammer et al. (2014) stressed that NUE increases linearly with increasing carbon-to-nitrogen (C/N) ratio in C-limited soils until it reaches the maximum when the SOC content exceeds a threshold. In a tropical agroforestry ecosystem with a C/N ratio of about 10, N_2O emission was significantly negatively correlated with the C/N ratio of applied OSA (Millar et al., 2004). Except for C/N ratio, the chemical composition of OSA also plays an essential role in NUE and N_2O emission (Frimpong and Baggs, 2010; Millar and Baggs, 2004). The (lignin + polyphenol)-to-N ratio of legume material exerted a significant negative effect on N_2O emission when applied to a silt loam with a C/N ratio of about 9.5 (Garcia-Ruiz and Baggs, 2007). In addition, a significant negative correlation of N_2O emission with the lignin content of applied OSA was also found in a clay with a C/N ratio of about 9 (Millar and Baggs, 2004). In spite of differential effects of OSA on N_2O emission depending on their chemical composition, they generally reduce the mineral N content in various soils by promoting N retention in organic matter (Gentile et al., 2008). However, the influence of lignin composition on N_2O emission and N partitioning in soils has never been studied till now.

As an important source of stable SOC, lignin is widely distributed in walls of plant cells and accounts for 10–30 % of lignocellulose (Bugg et al., 2011b). Lignin is formed by radical polymerization of lignin G, S, and H units from their precursor coniferyl alcohol, sinapyl alcohol, and *p*-coumaryl alcohol, respectively (Stevenso et al., 1970). The composition of lignin varies between plant species, for example, softwoods mainly contain lignin G units, while hardwoods are comprised of a mixture of

lignin G and S units, whereas grass lignin is composed of mainly G and H units (Faix, 1991; Stevenson, 1995). It has been reported that derivatives of different lignin units show distinct reactivity to NO_2^- and could play discriminating roles in abiotic N_2O emission and N retention (Wei et al., 2017b). The relationship of N_2O and NO emissions with lignin units was first tested in acidic spruce forest soils, and N_2O emission was positively correlated with the proportion of lignin S units, but negatively with the proportion of lignin G units (Wei et al., 2017a). Therefore, it is assumed that the lignin composition of OSA could play an important role in soil N_2O emission and N partitioning, and further affect NUE in fertilized soils.

To test this assumption, a laboratory incubation study was conducted with a sandy loam sampled from an agricultural site in Kiel, Germany, which was amended with three types of OSA whose lignin content and composition were completely different from each other, before ^{15}N -labeled fertilizer was applied. Fertilizer-associated N_2O emission, NH_4^+ and NO_3^- concentration, as well as N retention in SOM were monitored for 114 d and their dependencies on lignin content and composition of OSA were further analyzed.

VI.2 Materials and Methods

VI.2.1 Materials

Soil (sandy loam, $\text{pH} = 6.0 \pm 0.1$, total C = 1.3 ± 0.1 %, total N = 0.15 ± 0.01 %) was sampled from the top layer of the Achterwehr field ($54^\circ 19' 05''\text{N}$, $9^\circ 58' 38''\text{E}$), Kiel, Germany, for the laboratory incubation experiment. After sampling, soils were air-dried and sieved at 2 mm mesh size for homogenization. Ammonium sulfate ($(\text{NH}_4)_2\text{SO}_4$, ^{15}N atom% = 2.648 %, VWR, Germany) was used as N fertilizer in this study.

Wheat straw (total C = 44.4 ± 0.1 %, total N = 0.28 ± 0.02 %) was obtained from the Hohenschulen experimental farm close to Kiel, Germany, and spruce sawdust (Art. Nr. 823 Siebgut fein, total C = 45.8 ± 0.2 %, total N = 0.06 ± 0.01 %) was obtained in 2015 from Holz Ruser (Bornhöved, Germany). They were ground to < 1 mm in a rotary mill before usage. Alkali lignin (total C = 61.6 ± 0.1 %, total N = 0.43 ± 0.01 %) was obtained from VWR, Germany. Its soluble minerals and micro-particles were removed by precipitation in deionized water, and then it was freeze-dried for usage.

VI.2.2 Experimental setup

Three treatments with the combined application of N fertilizer with wheat straw (SWF), or spruce sawdust (SSF), or alkali lignin (SLF) were established. Blank control (S), in which neither fertilizer nor OSA was applied, and fertilizer control (SF), in which N fertilizer instead of organic material was applied, were set up. All treatments were prepared in triplicate.

The experiment was established in soil columns (30 cm × 20 cm) made of stainless steel. The columns were customer-made by the workshop of Forschungszentrum Jülich, Germany, and each of them was equally divided into 6 sections with equally spaced plastic clapboards which were glued together in the center of the column to avoid mixing between the different sections. About 8 kg of soil mixed with or without OSA was filled into all sections of the soil columns. The soil was compacted to field bulk density with a tool that had the same shape (segment of a circle) as each single soil column section. OSA were applied at a rate of 1.5 g C kg⁻¹ soil, 90% of which had been mixed with the soil homogeneously before filling of the soil columns. Litter bags made of 0.2 µm nylon mesh containing the remaining 10 % of the respective organic material applied to each column section were buried horizontally in the soil at a depth of 2 cm at the beginning of the pre-incubation. Afterwards, the soil was rewetted to 40 % of its water holding capacity (WHC) and pre-incubated for two weeks. Then, N fertilizer dissolved in deionized water was applied at a rate of 50 mg N kg⁻¹ soil to the pre-incubated soils. The final soil moisture was about 60 % of WHC. Soil columns were incubated at room temperature for 114 d after the application of N fertilizer from 22nd November 2016 to 16th March 2017. The mean temperature during the whole experiment was about 21 °C, and deionized water was supplied every week to keep the soil moisture at about 50–60 % of WHC during the incubation.

VI.2.3 Gas sampling and analysis

N₂O and CO₂ fluxes, as well as N₂O isotopic composition, were regularly measured 2–3 times per week. For gas sampling, a PVC chamber (20 cm × 20 cm) with one inlet and one outlet was installed gas-tight on the top of the soil column. The outlet was closed with a screwcap with septum, and the inlet was equipped with a rubber tube closed with a clamp. The gas-tightness of the columns was checked with a helium detector before the experiment. As soon as the chamber was installed, 35 ml of headspace gas was sampled through the septum with a syringe and transferred to a 22.5-ml pre-evacuated gas chromatography vial, thereby creating an overpressure in the vial. During gas sampling, the clamp on the inlet tube was opened to allow ambient air to flow into the chamber for pressure equilibration. The sampling procedure was repeated three times in 20–40 min intervals. Afterwards, the mixing ratios of N₂O and CO₂ were measured with a gas chromatography equipped with an electron capture detector and a flame ionization detector (GC-ECD/FID, Clarus 580, PerkinElmer, Rodgau, Germany). The N₂O and CO₂ fluxes were calculated from the increase of their mixing ratios during the total sampling time and related to the surface area of the columns. After the different soil sampling events (see section VI.2.4), the decrease in soil surface area was accounted for.

For N₂O isotope measurements, a gas sample of 120 ml was sampled at the end of each regular

gas sampling and injected into a 100-ml pre-evacuated glass bottle. N₂O isotopic composition was analyzed with an isotope ratio mass spectrometer (IRMS, IsoPrime 100, Elementar Analysensysteme, Hanau, Germany) coupled to an online pre-concentration unit (TraceGas, Elementar Analysensysteme). Fertilizer-derived N₂O was calculated according to a two-end-member mixing model based on the ¹⁵N-enrichment of the fertilizer and the N₂O.

VI.2.4 Soil sampling and analysis

Soils in each section were separately and destructively sampled at different time intervals, and appropriately shaped plastic blocks were used to refill the empty sections after soil sampling. The first soil sampling in the first section of each soil column was performed 6 d before N fertilizer application, and remaining soil in the 2nd to 6th sections were sampled 8, 22, 50, 78, and 114 d after fertilizer application, respectively. After sampling, soils were immediately freeze-dried and stored at room temperature till analysis. Litter bags were sampled together with soils in each section and immediately freeze-dried.

Freeze-dried litter bags were carefully cleaned with a brush, and remaining organic material was weighed. The decomposition of organic material was calculated according to the decrease in weight. Soil pH was determined according to the ISO 10390 method (ISO, 2005). For this, 1 M KCl solution was mixed with soil at a ratio of 1:5 (w/v) for 2 h, and then pH was measured with a pH meter (multi 340i, WTW GmbH, Germany). Soil and organic material were washed three times with 1 M KCl solution at a ratio of 1:5 (w/v) to remove water-soluble nitrogen compounds, such as NH₄⁺, NO₃⁻, and dissolved organic nitrogen (DON), and then freeze-dried. The remaining immobilized ¹⁵N was measured using an IRMS (Delta V plus, Thermo Fisher Scientific, Bremen, Germany). Retention of fertilizer-N was calculated as the ratio of immobilized N to the initially applied fertilizer-N.

Content of NH₄⁺ and NO₃⁻, as well as their ¹⁵N-enrichment, was sequentially measured through micro-diffusion and liquid-liquid extraction methods (Huber et al., 2012; Mulvaney et al., 1997): 80 ml of 1M KCl solution (pre-treated by ignition for 16 h at 550°C to minimize background NH₄⁺) was mixed with 8–9 g of soil, the mixture was shaken for 1 h at 200 rpm and then centrifuged for 20 min at 3000 rpm and filtered through 2–3 µm paper filter; 60 ml of KCl extractive was removed to 100-ml polypropylene (PP) bottles and adjusted to pH ~12 with 1M NaOH solution to deprotonate NH₄⁺ to NH₃, NH₃ was evaporated at room temperature for 7 d and collected with 2 × 15 µl of saturated oxalic acid pipetted onto quartz glass filter disk, afterwards filter disks were dried in a desiccator over silica gel for 24 h and samples were packed in Sn capsules (10 x 10 mm) and analysed using an Elemental Analysis-Isotope Ratio Mass Spectrometry (EA-IRMS, Flash EA 2000; Delta V Plus; Thermo Fisher Scientific, Bremen, Germany); after micro-diffusion, remaining KCl extractive was dried at around 65°C and resolved into 3 ml of 1M NaOH, and then mixed with 37 ml of acetone for 30 s, the

mixture was centrifuged for 20 min at 3000 rpm and the supernatant acetone phase containing NO_3^- was transferred into a glass beaker and dried at 30–40°C, dried matter was re-dissolved into ~5 ml of deionized water, freeze-dried, packed in Sn capsules (5 x 9 mm), and analysed with an EA-IRMS.

Nitrite concentration in soils was determined according to an improved colorimetric method (Colman, 2010; Homyak et al., 2015). To be precise, 5 g of fresh soil was extracted with 25 ml of 0.012 M NaOH solution. The extract was filtered with a 0.45 μm PTFE syringe filter, and NO_2^- in the extract was reacted with the color reagents of sulfanilamide and N-(1-naphthyl)-ethylenediamine in diethylenetriaminepentaacetic acid buffer, and then the colored product was measured with a DU-800 Spectrophotometer (Beckman Coulter, Fullerton, USA) at 560 nm.

Lignin in soil samples was characterized according to the cupric oxide oxidation method (Amelung et al., 1997; Hedges and Ertel, 1982), and lignin derivatives, i.e. vanillin, acetovanillone, vanillic acid, acetosyringone, syringaldehyde, syringic acid, and *p*-cumaric acid, were quantified. Total lignin G units were calculated as the sum of vanillin, acetovanillone, vanillic acid, and ferulic acid, while total lignin S units were represented by the sum of acetosyringone, syringaldehyde, and syringic acid. Finally, *p*-cumaric acid and ferulic acid was the representative of lignin H units.

VI.2.5 Statistical analysis

Origin 8.0 (Originlab Corporation, Wellesley Hills, MA, USA) was used to conduct one-way analysis of variance (ANOVA), Pearson correlations, and linear regression. Canoco for Windows 5.0 (Microcomputer Power, Ithaca, NY, USA) was used for redundancy analysis (RDA).

VI.3 Results

VI.3.1 Soil N_2O and CO_2 emissions

Rewetting of soils induced substantial N_2O and CO_2 emissions in all treatments (Fig. VI.1a and b). According to Pearson correlation analysis, N_2O and CO_2 emissions were significantly ($P < 0.01$) positively correlated with each other (Table D1). From day 0 to 30, CO_2 emission was significantly higher in soils amended with wheat straw compared with the other treatments, while it was the highest in spruce soils amended with spruce sawdust from day 75 to 113 (Fig. VI.1a). By contrast, total N_2O emission was always much higher in wheat-amended treatments than in lignin-amended soils and fertilizer control during the whole experiment (Fig. VI.1b). Large N_2O emissions occurred immediately after fertilizer application (Fig. VI.1c), while the highest contribution of fertilizer-N to N_2O emission was observed about 15 d later (Fig. VI.1d). Compared with the fertilizer control, combined application of fertilizer and wheat straw or spruce sawdust increased fertilizer-derived N_2O emission greatly, while lignin only enhanced fertilizer-associated N_2O emission in the first 18 d after fertilizer addition (Fig. VI.1c). At the end of the experiment, accumulated fertilizer-derived N_2O was

about 126, 157, 341, and 275 $\mu\text{g N kg}^{-1}$ soil in SF, SLF, SWF, and SSF treatments, respectively. Even though the total N_2O emission rate was significantly ($P < 0.01$) positively correlated with that of fertilizer-derived N_2O (Table D1), the highest contribution of fertilizer-derived to total N_2O emission was only about 40 %, and stayed relatively stable at 5–20 % beyond 50 d after the application of nitrogen fertilizer (Fig. VI.1d).

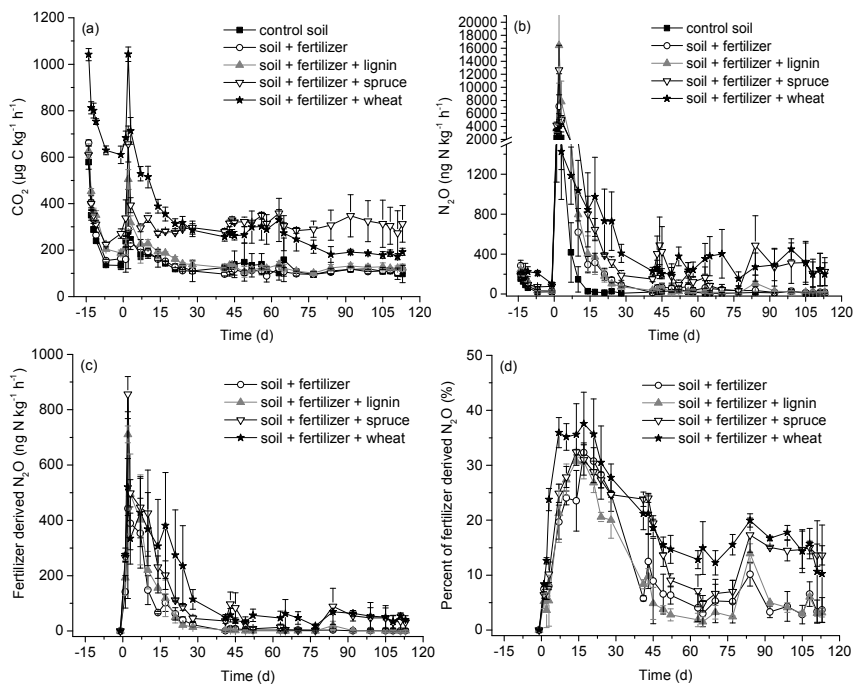


Fig. VI.1. Total CO_2 flux (a), total N_2O flux (b), fertilizer-derived N_2O flux (c), and contribution of fertilizer- N_2O to total N_2O flux (d). Nitrogen fertilizer was applied at day 0.

VI.3.2. Nitrogen partitioning in soils

When applied to soils, NH_4^+ was rapidly oxidized to NO_3^- , only approximately 20–25 % of the initial $^{15}\text{N-NH}_4^+$ was left at day 8, whereas 23–31 % and 9–15 % were transformed to $^{15}\text{N-NO}_3^-$ and $^{15}\text{N-SON}$, respectively (Fig. VI.2). More than 90 % of the fertilizer-derived NH_4^+ had disappeared about three weeks after fertilizer application, and almost all of it was gone 78 d later (Fig. VI.2b). Both total and fertilizer- NH_4^+ disappeared quickly during the first weeks of the experiment, and they were strongly positively correlated with each other (Table D2). On day 8 after fertilizer addition, the contribution of fertilizer- NH_4^+ to total NH_4^+ was about 70 %, and there was no significant ($P > 0.05$) difference in the four treatments with fertilizer application. However, it decreased most rapidly in the SLF treatment and most slowly in the SSF treatment (Fig. VI.2c). In addition, NH_4^+ content was significantly ($P < 0.01$) positively correlated with N_2O emission and N retention, but negatively

correlated with NO_3^- content in soils (Table D2).

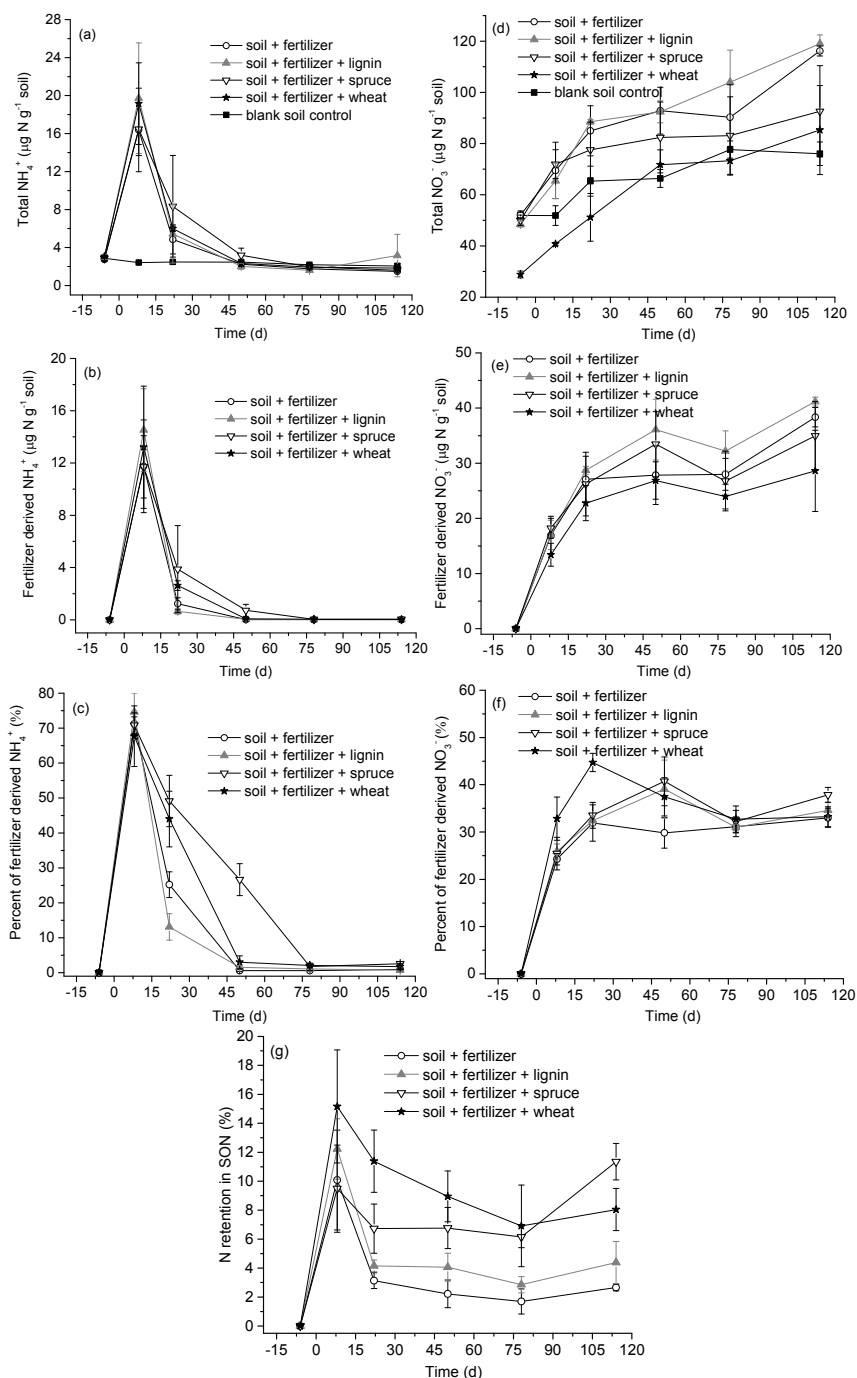


Fig. VI.2. Total and fertilizer-derived NH_4^+ (a–c) and NO_3^- (d–f), and fertilizer-N retention in the form of soil organic nitrogen (SON) (g) in the different treatments during the experiment. Nitrogen fertilizer was

applied at day 0.

Contrary to the quick decrease of NH_4^+ , total NO_3^- increased steadily from about 30–50 to 80–120 $\mu\text{g N g}^{-1}$ soil, and fertilizer-derived NO_3^- from 0 to approximately 30–40 $\mu\text{g N g}^{-1}$ soil during the whole incubation period (Fig. VI.2d and e). Total NO_3^- in the blank control soil also increased over time and was even slightly higher than in the SWF treatment at the beginning of the experiment (Fig. VI.2d). Even though fertilizer-derived NO_3^- only accounted for less than 50 % of the total soil NO_3^- , a significant ($P < 0.01$) positive correlation between them was observed (Table D2). The highest and fastest increase of fertilizer-derived NO_3^- was found in lignin-amended soil, while the slowest occurred in the wheat-amended soil (Fig. VI.2e). Interestingly, fertilizer-derived NO_3^- continued to increase the following 80 d, and its relative ratio to the total NO_3^- also increased slightly although almost all fertilizer-derived NH_4^+ had already disappeared (Fig. VI.2e). The largest contribution of fertilizer-derived NO_3^- to total NO_3^- was found on day 22 in the SWF treatment, but on day 50 in the SSF and SLF treatments (Fig. VI.2f). Moreover, both total and fertilizer-derived NO_3^- contents were significantly ($P < 0.01$) correlated with N_2O emission (Table D2).

After fertilizer addition, a substantial amount (about 9–15 %) of fertilizer-N was immobilized in the form of SON within 8 d, while the fraction of immobilized N decreased steadily during the following weeks (Fig. VI.2g). Nitrogen retention in SON was much higher in wheat- and spruce-amended soils compared with lignin-amended soils and fertilizer control (Fig. VI.2g). From day 78 to 114, the fraction of fertilizer-N immobilized in SON increased again in all organic amendment treatments, with the largest increase in the SSF treatment (Fig. VI.2g). Pearson correlation analysis revealed that N retention in SON was significantly ($P < 0.01$) positively correlated with N_2O emission and NH_4^+ content, but negatively related to NO_3^- in soils (Table D2).

Nitrogen partitioning of fertilizer-N based on N retention, N_2O emission, and mineral N data (NH_4^+ and NO_3^-) in the SF, SLF, SSF, and SWF treatments is shown in Fig. VI.3. Interestingly, nitrogen partitioning differed strongly in response to the application of the different OSA. Nitrogen partitioning of fertilizer-N in lignin-amended soils was characterized by relatively high mineral N content, but lower N_2O emission and N retention. By contrast, wheat-amended soils were characterized by relatively low mineral N content but higher N_2O emission and N retention, whereas the pattern of N partitioning in spruce-amended soils was in the middle of the SWF and SLF treatments. Nitrogen retention was the lowest in fertilizer control compared with the combined application of fertilizer and OSA.

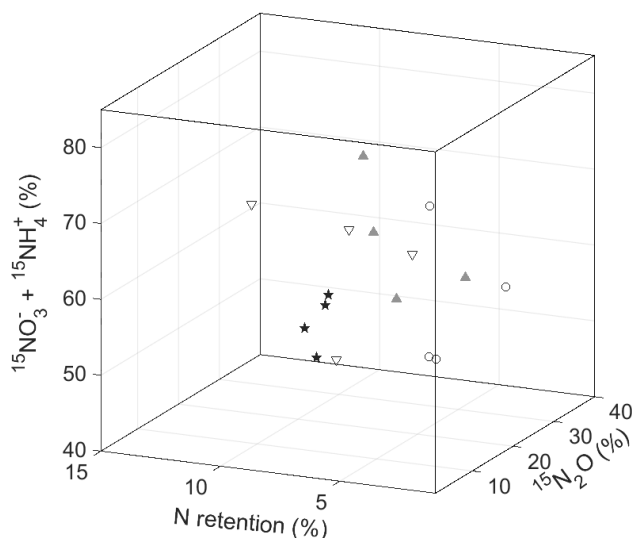


Fig. VI.3. Nitrogen partitioning in soil amended with wheat straw (black stars), spruce sawdust (downward triangles), lignin (upward triangles), and fertilizer control (circles). X, Y, and Z axes denote N retention, the contribution of fertilizer-derived N_2O to total N_2O , and the proportion of mineral N ($\text{NH}_4^+ + \text{NO}_3^-$) to total fertilizer-N, respectively.

VI.3.3 Influence of lignin content and composition on decomposition of OSA

The decomposition rate of OSA decreased in the order: wheat straw > spruce sawdust > lignin (Table D3), linearly related to their total lignin content (Fig. D1). Lignin G units, which accounted for 45–70 % of the total lignin, exerted a negative effect on the decomposition of OSA, while lignin S and H units, amounting to 27–47 % and 3.5–8.5 % of the total lignin, respectively, were positively correlated with the decomposition of OSA (Fig. VI.4a–c). Soil amended with wheat straw was characterized by the highest content of lignin S and H units, but the lowest content of lignin G units. On the contrary, lignin-amended soils were characterized by the highest content of lignin G units and lowest content of lignin S and H units (Fig. VI.4d). The lignin content and composition in soil amended with spruce sawdust was in an intermediate position between wheat straw and lignin amended soil (Fig. VI.4d).

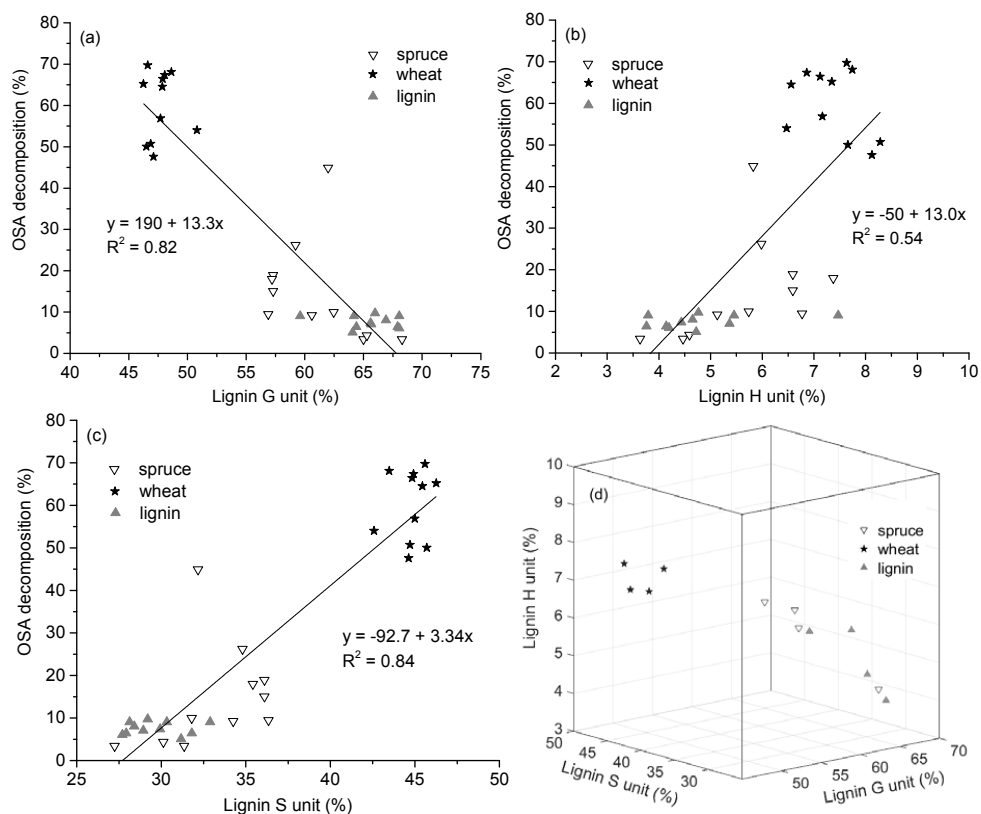


Fig. VI.4. Dependency of decomposition of organic soil amendments (OSA) on the content of lignin G units (a), H units (b), and S units (c) ($n = 36$), and the lignin composition of soil amended with spruce sawdust, wheat straw, or lignin (d).

The immobilization of fertilizer-N in wheat straw was significantly higher ($P < 0.01$) than in spruce sawdust and lignin (Table D3). Total fertilizer-N retained in wheat straw was highest on day 28 after fertilizer addition and decreased steadily afterwards. The immobilized fertilizer-N, however, continued to increase during the whole experiment (Table D3). By contrast, the immobilization of fertilizer-N in lignin started to decrease on day 28, which indicates that N immobilized in lignin started to be released again 28 d after fertilizer addition (Table D3). The fertilizer-N immobilized in spruce sawdust was much higher than in lignin, but lower than in wheat straw, and both the total and immobilized fertilizer-N were increasing continuously during the whole incubation period (Table D3). The N content of OSA increased linearly with proceeding decomposition of the organic materials (Fig. D2), which could have resulted from the recalcitrance of indigenous or newly formed organic N compounds, the continued N immobilization by the remaining organic material, or both. Furthermore, OSA decomposition was also significantly ($P < 0.01$) positively correlated with

immobilized N in OSA, which was significantly ($P < 0.05$) positively correlated with N retention in soils (Table VI.1).

VI.4 Discussion

VI.4.1 Transformation of fertilizer-N in soils

Autotrophic nitrification dominated in all the treatments with fertilizer application in the first period (0–50 d) of the experiment, but the net NH_4^+ consumption rate decreased from 5.01–5.48 $\mu\text{g N g}^{-1}\text{soil d}^{-1}$ (0–8 d) to 0.18–0.29 $\mu\text{g N g}^{-1}\text{soil d}^{-1}$ (22–50 d) corresponding with the decrease in NH_4^+ concentration. However, the net NH_4^+ consumption rate was slightly lower compared with the net NO_3^- production rate (maximum 9.81 $\mu\text{g N g}^{-1}\text{soil d}^{-1}$ for 0–8 d). On the other hand, fertilizer-derived SON and DON decreased from 4.74–7.58 to 1.33–5.67 $\mu\text{g N g}^{-1}\text{soil}$ and from 5.64–8.66 to 3.51–5.60 $\mu\text{g N g}^{-1}\text{soil}$, respectively, from day 8–114 parallel to the increase of fertilizer-derived NO_3^- (Fig. VI.2 and D3). Therefore, heterotrophic nitrification, namely the oxidation of organic N to NO_3^- , could have been another pathway of NO_3^- production (Zhang et al., 2015c). In the second period (50–78 d), concentrations of fertilizer-derived NO_3^- , DON and SON decreased, indicating that denitrification and heterotrophic nitrification could have been the dominant processes of N transformation in the soil during this period. Bol et al. (2003) also demonstrated that autotrophic nitrification dominated in the first phase after N fertilizer application to a grassland soil, before denitrification replaced autotrophic nitrification as the dominant N_2O source. In contrast, from day 78 to 114 both SON and NO_3^- contents increased again in the present study, which indicates that N immobilization and heterotrophic nitrification might have dominated in this period.

In the present study, the total fertilizer-N recovery in soil averaged approximately 77–88 %, and accumulated N_2O emission accounted for about 0.25–0.68 % of the fertilizer-N. The total fertilizer-N recovery in lignin-amended soils (~88 %) was significantly ($P < 0.05$) higher than in the fertilizer control (~77 %), but there were no significant differences to and between the other treatments. However, it should be noted that only less than 15 % of fertilizer-N was immobilized as SON, and most of the rest prevailed in the form of NO_3^- , which could be used by crops or leached to water or reduced to N_2 in case of heavy rains or flooding (Zhu and Chen, 2002). Therefore, further work is needed to explore the consumption of mineral N by crops before one can say if the combined application of lignin and fertilizer could enhance NUE in agriculture or not.

Compared with the fertilizer control (SF), the combined application of fertilizer and OSA increased N retention by about 2–9 %, and much higher N retention was found in the SWF and SSF treatments compared with SLF (Fig. VI.3). However, the amount of mineral N (NH_4^+ and NO_3^-) was the lowest in the SWF treatment, but the highest in SLF (Fig. VI.3). It is generally thought that labile C, which can be quickly and easily consumed by soil microbes as C source, is very efficient in reducing

mineral N content in the short term by promoting biological N uptake (Burke et al., 2013). So the higher N retention but lower mineral N content in wheat-amended soils could be explained by the more labile C content in wheat straw compared with spruce sawdust and lignin. Similarly, Cucu et al. (2014) found that the application of rice straw to both flooded and unflooded paddy soils promoted N retention to a large extent.

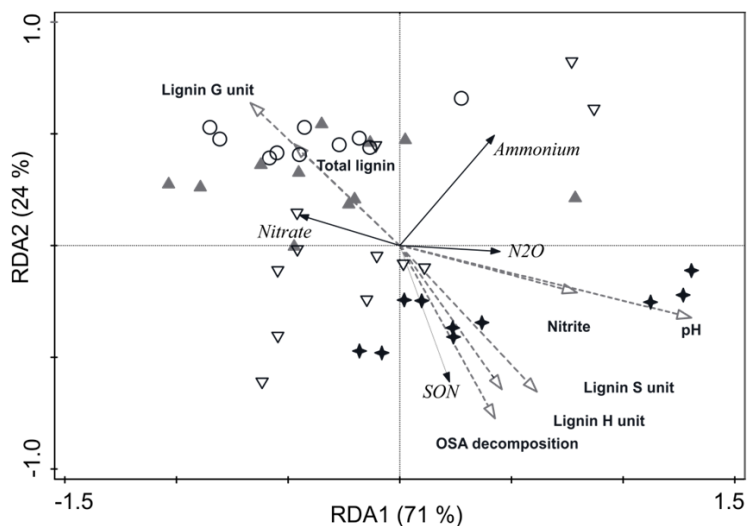


Fig. VI.5. Redundancy analysis (RDA) to explain the effect of total lignin content, content of lignin G/S/H units, NO_2^- content, soil pH, and organic soil amendment (OSA) decomposition rate on fertilizer-N partitioning into NH_4^+ , NO_3^- , soil organic nitrogen (SON), and N_2O . Circles, upward triangles, downward triangle and stars represent fertilizer control, soil + lignin + fertilizer, soil + spruce + fertilizer, and soil + wheat + fertilizer treatments, respectively.

According to redundancy analysis (RDA), 71 % and 24 % of the distinct N partitioning in different treatments can be explained by the first (RDA1) and second (RDA2) components, respectively (Fig. VI.5). Nitrate content was significantly ($P < 0.01$) negatively related to pH, NO_2^- content, content of lignin S and H units, and OSA decomposition rate, but positively correlated with lignin G unit content (Fig. VI.5 and Table VI.2). During nitrification, NO_2^- can be produced and released into soils. Nitrite is chemically reactive to SOM, to forming NO , N_2O and SON (Austin, 1961). Kholdebarin and Oertli (1994) reported that phenols can consume NH_4^+ and NO_2^- and further inhibit the production of NO_3^- via nitrification. Since the reactivity of NO_2^- increases with decreasing soil pH, and since polyphenols can be formed during OSA decomposition (Bremner and Führ, 1966), the strong negative correlation between NO_3^- and NO_2^- , soil pH, and OSA decomposition could be explained by the chemical fixation of NO_2^- by lignin-derived polyphenols.

VI.4.2 Effect of lignin content and composition on N₂O emission

Considering the pathways of N transformation in soils, possible N₂O sources include autotrophic nitrification, heterotrophic nitrification, denitrification and chemodenitrification. The significant ($P < 0.01$) negative correlation of fertilizer-derived N₂O with fertilizer-derived NO₃⁻ and the positive correlation of fertilizer-derived N₂O with fertilizer-derived NH₄⁺ (Table VI.2) could be an indicator for autotrophic nitrification as N₂O source. By contrast, the significant ($P < 0.01$) positive correlation of N₂O emission with SON (Table VI.2) could be an indicator of heterotrophic nitrification as N₂O source. Application of OSA can stimulate microbial respiration by supplying C for soil microbes, including both nitrifiers and denitrifiers, hence promote N₂O emission (Chen et al., 2013). On the other hand, enhanced microbial respiration will further accelerate oxygen consumption, which consequently fosters denitrification (Chen et al., 2013). Thus, the substantial N₂O emission in the SWF and SSF treatments could be explained by the stimulatory effect of labile C from wheat straw and spruce sawdust on nitrifiers and denitrifiers. Significant promotion of N₂O emission by plant residues was also found in a Ferric Luvisol from Ghana (Frimpong and Baggs, 2010), a typical arable surface soil (García-Ruiz et al., 2012), a silt loam soil (Garcia-Ruiz and Baggs, 2007), and in a humid tropics (Millar et al., 2004). Since lignin-C was recalcitrant, microbial N₂O emission could be hardly promoted in SLF treatment, which could explain the much lower N₂O emission in SLF than in SWF and SSF treatments.

Nitrogen content and C/N ratio of applied OSA are generally regarded as key factors controlling N₂O emission from soils (Frimpong and Baggs, 2010; Rezaei Rashti et al., 2016). Millar et al. (2004) found that N₂O emission in soil (total C 1.3 %, total N 0.12 %) amended with six crop residues was significantly ($P < 0.05$) positively correlated with the N content of the residues. Huang et al. (2004) found that N₂O emission decreased linearly with increasing C/N ratio in soils (total C 2.0 %, total N 0.16 %) amended with five crop residues. Although the soil used in this study had a C/N ratio similar to the previously reported studies by Millar et al. (2004) and Huang et al. (2004), no significant correlation between cumulative N₂O emission and N content or C/N ratio of applied residues was found (Fig. D4a and b). However, the cumulative fertilizer-derived N₂O emission decreased linearly with increasing lignin content of the OSA (Fig. D4c). This result is in accordance with the previous study by Garcia-Ruiz and Baggs (2007) with a silt loam where NO₃⁻-fertilizer and ground weed material were applied. Similarly, N₂O emission was significantly ($P < 0.05$) negatively correlated with lignin content in a clay soil (total C 1.5 %, total N 0.16 %) of an improved-fallow agroforestry system when ammonium nitrate (NH₄NO₃) was used as fertilizer (Millar and Baggs, 2004), and with (lignin + polyphenol)/N ratio in reddish brown sandy loam soil (total C 1.1 %, and total N 0.07 %) when NH₄NO₃ was used as N fertilizer and cowpea, *Mucuna*, and *Leucaena* were used as plant residues (Frimpong and Baggs, 2010). On the contrary, Rezaei Rashti et al. (2016) found that the lignin content of crop residues was positively correlated with N₂O emission in a black Vertisol (total C 1.54 %, total

N 0.11 %) where urea and plant residues of six crop species were applied. Soil properties and plant characteristics, such as redox potential, soil microbial community, and lignin composition, could be the reason for this inconsistency.

Lignin composition of OSA could act on N_2O emission biologically by affecting the activity of soil microbes or chemically by influencing reactions of NO_2^- with SOM. Lignin is extremely recalcitrant compared with other forms of organic carbon, such as sugar and cellulose. Thus, higher lignin content leads to slower OSA decomposition rates and lower C supply to soil microbes (Hadas et al., 2004; Rahman et al., 2013). It was confirmed in this study that the decomposition of OSA decreased linearly with increasing lignin content (Fig. D1). Interestingly, in addition to the total lignin content, the lignin composition also greatly affected the degradation of organic materials (Fig. VI.4). Therefore, both total lignin content and lignin composition could affect the activity of soil microbes and hence also biotic N_2O emission. On the other hand, lignin and its derivatives are chemically reactive to NO_2^- , and their reactions could lead to N_2O and SON production (Stevenson et al., 1970; Thorn and Mikita, 2000). Nevertheless, N_2O production from the reactions of NO_2^- with lignin products varies greatly with their composition, and lignin G units are associated with a lower potential for N_2O production compared with lignin S and H units (Wei et al., 2017b). This could explain why N_2O emission was significantly ($P < 0.05$) positively correlated with the proportion of lignin S and H units, but negatively correlated with the proportion of lignin G units (Table VI.2). Also in spruce forest soils, negative correlation between N_2O emission and the proportion of lignin G units, but positive correlation with the proportion of lignin S units were observed according to RDA analysis (Wei et al., 2017a).

VI.4.3 Effect of lignin content and composition on mineral N content and N retention

Lignin content and composition could affect N retention and mineral N content through both microbial and chemical processes. The lignin-containing complex in plant cell walls acts as a natural barrier hindering microbial access to labile C in the cell, so biological decomposition of plant residues is in general negatively correlated with their lignin content (Pauly and Keegstra, 2008). On the other hand, higher lignin content means less available C for soil microbes, so plant residues with lower lignin content could be more efficient to stimulate soil microbial activity and promote biotic N immobilization (Burke et al., 2013). Furthermore, compared with lignin G units, lignin S and H units are more susceptible to biotic decomposition due to their lower abundance of aryl-aryl bonds and lower redox potential (Nierop and Filley, 2007; Vane et al., 2003, 2006). This could help to explain why OSA decomposition was significantly ($P < 0.01$) negatively correlated with total lignin content and proportion of lignin G units, but positively with the proportion of lignin S and H units (Fig. D1 and VI.4). Higher OSA decomposition rate is generally associated with higher C availability for soil

microbes and hence higher microbial activity, so microbial N retention in soils would be increased by a higher proportion of S and H units, but reduced by higher lignin content and a higher proportion of lignin G units. This could explain the significant ($P < 0.01$) positive correlation between N retention and proportion of lignin S and H units, but negative correlation between N retention and proportion of lignin G units and lignin content (Fig. VI.6 and D5). The significant correlations between OSA decomposition, proportion of lignin units, and NO_3^- content could be indicative for microbial N immobilization (Table VI.2).

Table VI.1. Pearson correlations between immobilization of fertilizer-N in soil organic amendments (OSA), total fertilizer-N in OSA, degree of OSA decomposition, and N retention in soil ($n = 45$).

	Total fertilizer-N in OSA (μg)	OSA decomposition (%)	N retention in soil
OSA decomposition	0.89**		
N retention in soil	0.50**	0.31*	
Immobilized fertilizer-N in OSA	0.98**	0.93**	0.39**

Note:

* Significantly correlated at $P < 0.05$;

** Significantly correlated at $P < 0.01$.

Table VI.2. Pearson correlations between NO_2^- content, soil pH, lignin composition, soil organic amendments (OSA) decomposition, and contents of fertilizer-derived NO_3^- , NH_4^+ , N_2O , and SON ($n = 36$).

	Fertilizer- NO_3^- ($\mu\text{g N g}^{-1}$ soil)	Fertilizer- NH_4^+ ($\mu\text{g N g}^{-1}$ soil)	Fertilizer- N_2O ($\text{ng N kg}^{-1} \text{h}^{-1}$)	Fertilizer-SON ($\mu\text{g N g}^{-1}$ soil)
Fertilizer- N_2O ($\text{ng N kg}^{-1} \text{h}^{-1}$)	-0.43**	0.58**		
Fertilizer-SON ($\mu\text{g N g}^{-1}$ soil)	-0.29	0.29	0.63**	
NO_2^- ($\mu\text{g N g}^{-1}$ soil)	-0.37*	0.26	0.44**	0.36*
pH	-0.72**	0.35*	0.62**	0.54**
Lignin G units (%)	0.48**	0.07	-0.39*	-0.60**
Lignin S units (%)	-0.49**	-0.06	0.38*	0.58**
Lignin H units (%)	-0.39*	-0.08	0.36*	0.58**
OSA decomposition (%)	-0.45**	-0.14	0.32	0.56**

Note:

* Significantly correlated at $P < 0.05$;

** Significantly correlated at $P < 0.01$.

Except for biotic N retention, the chemical reaction of lignin derivatives with NO_2^- is another pathway of N retention in soils. The degradation of lignin leads to the production of phenolic compounds (Have and Teunissen, 2001), which have a strong capability of retaining N substances (Smolander et al., 2012). Both nitrification and denitrification can release NO_2^- to soils, which is highly chemically reactive to SOM and lignin derivatives to form SON (Wei et al., 2017a). Therefore, lignin content could be positively related to N retention in a certain range if biotic N retention remained relatively stable, which was the case for the study of Garcia-Ruiz et al. (2012), in which

(lignin + polyphenols)/N ratio was positively correlated to N retention in a silt loam (total C 1.9 %, total N 0.2 %) amended with weed residues in a narrow range of C/N ratios and lignin content. In the present study, the significant ($P < 0.05$) positive correlation between NO_2^- and fertilizer-derived SON could be an indicator for abiotic N retention (Table VI.2).

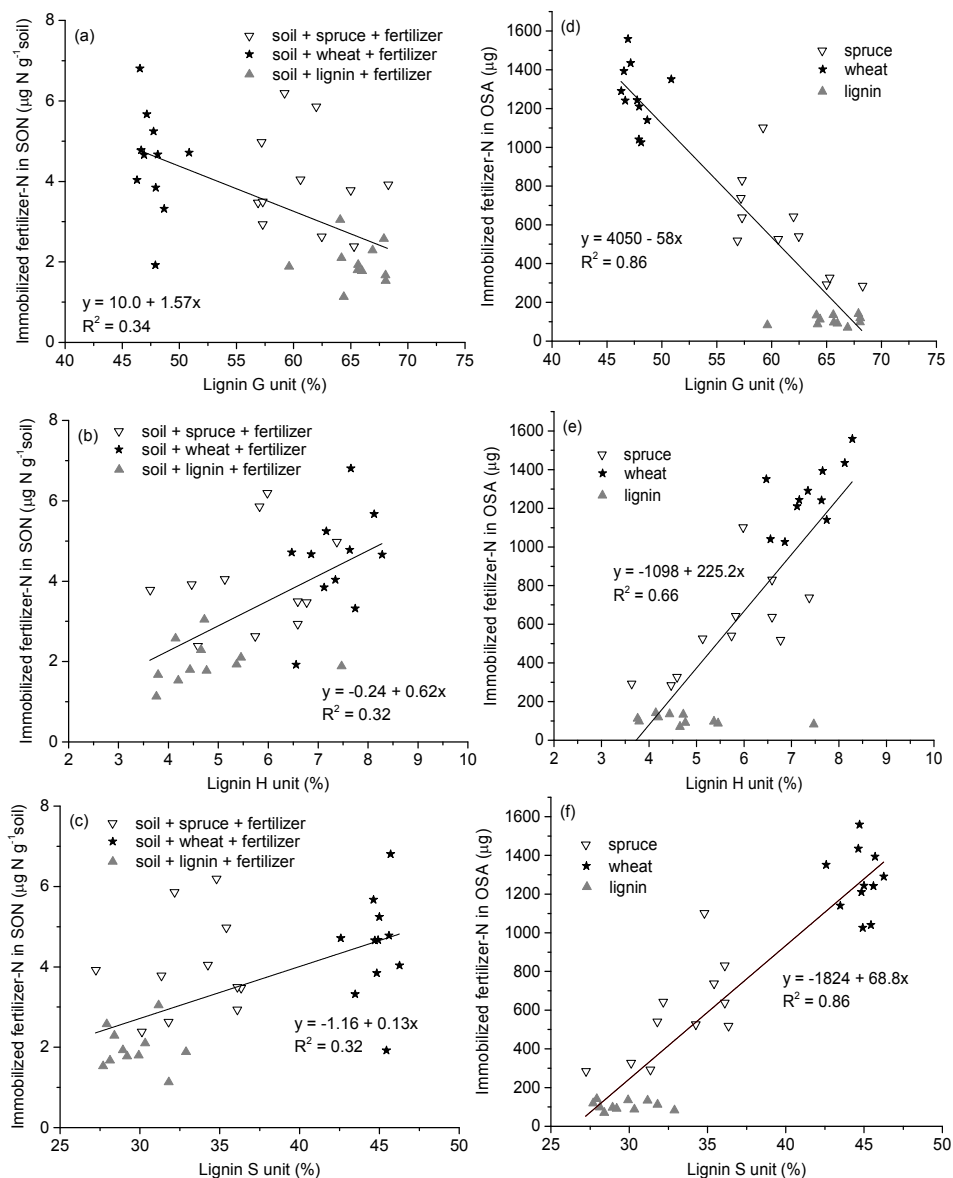


Fig. VI.6. Correlations between lignin composition and immobilized fertilizer-N ($n = 36$) in SON (a–c), and immobilized fertilizer-N in organic soil amendments (OSA) (e–f).

The combined application of fertilizer and wheat straw or spruce sawdust increased N retention

and decreased mineral N content compared with the fertilizer control (Fig. VI.3). Gentile et al. (2008) also reported that mineral N content was reduced by the combined application of crop residues and urea in different soils, most likely by promoting microbial N uptake. By contrast, the combined application of lignin and fertilizer increased N retention but did not reduce the mineral N content of the soil (Fig. VI.3). Since lignin is recalcitrant to soil microbial degradation, but reactive to NO_2^- , the N retention in the SLF treatment could be caused by chemical reactions instead of microbial N immobilization, which could also be the reason why mineral N did not decrease significantly in spite of the increase of N retention.

VI.5 Conclusions

The effect of lignin content and composition on fertilizer-N partitioning in agricultural soil was tested in the present study. The decomposition of three OSA (wheat straw, spruce sawdust, and lignin) with a wide range of C/N ratios was strongly affected by their lignin content and composition. Lignin content exerted a significant negative effect on N retention and decomposition of OSA. Both N_2O emission and N retention were significantly ($P < 0.05$) positively correlated with NO_2^- content and proportion of lignin S and H units, but negatively correlated with the proportion of lignin G units. For the first time, it is proved that lignin content and composition regulate the N partitioning of NH_4^+ fertilizer in a sandy loam, which could provide useful information about the use of combined application of fertilizer and OSA to improve NUE and reduce N_2O emission in agriculture. To further confirm these lignin effects, more soils with different texture, redox potential and pH, as well as OSA with various C/N ratios and chemical composition should be test in the future.

VII. Open-pump theory of biotic–abiotic C–N interactions in soil

VII.1 Introduction

Nitrogen and carbon (C) are two fundamental elements in ecosystems that determine ecosystem functions and structure in a concerted way. Anthropogenic activities have changed their cycles significantly and, hence, they have become the dominating elements of global change. For example, global N deposition increased from 34 Tg N yr⁻¹ in 1860 to 100 Tg N·yr⁻¹ in 1995 (Galloway et al., 2008), and global averaged atmospheric CO₂ and N₂O concentrations increased by 143 % and 121 % in 2015, respectively, compared with the pre-industrial level (WMO, 2016). Elevated N deposition has adversely affected many ecosystems by delaying the decomposition of organic matter (Dias et al., 2013), changing the biochemical composition of SOM (Gillespie et al., 2014), altering soil biota (Eisenlord and Zak, 2010), as well as modifying plant physiology (Langley and Megonigal, 2010). On the other hand, SOC is the main C source for heterotrophic microbes, including most of the nitrifiers, denitrifiers and ammonifiers, hence its quality affects the biological transformation of N compounds in soils.

Even though it has been challenging to quantify the contribution of abiotic processes to C–N interactions in soils till now, it has been demonstrated that chemical reactions between reactive N and C compounds do occur in soils, resulting in the emission of N₂O and NO_x (Heil et al., 2016; Wei et al., 2017a). In NH₂OH-amended agricultural soil, abiotic reactions accounted for about 50 % of the total N₂O emission (Heil et al., 2015), while in acidic spruce forest soils, abiotic processes contributed to almost 100 % of nitric oxide (NO) emission and 20–40 % of N₂O emission, respectively, after addition of NO₂⁻ (Wei et al., 2017a). In addition, abiotic N₂O emission from NO₂⁻ accounted for 31–75 % of the total production in a silt loam soil under aerobic conditions (Venterea, 2007). On the other hand, chemical reactions of C and N compounds could also form nitrogenous organic compounds like nitroso and heterocyclic compounds (Heil et al., 2016; Thorn and Mikita, 2000). Nitrogen K-edge X-ray absorption near edge structure (XANES) spectroscopy analysis revealed that pyridinic N and its oxidized derivatives, which are most likely the products of abiotic C–N reactions, accounted for 20–30 % of the total N in Suwannee River, peat, and soil humic substances of the International Humic Substances Society and various marine sediments in Shelter Island, NY (Vairavamurthy and Wang, 2002). Schmidt-Rohr et al. (2004) also reported that more than 40 % of the total N in the humic acid fraction of a lignin-rich rice soil was anilide-like N bonded to aromatic carbon, most of which came from abiotic C–N reactions. Hence, biotic and abiotic C–N interactions are always co-occurring, and abiotic processes could have been highly underestimated until now.

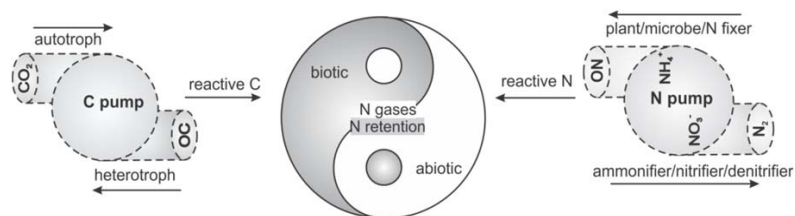


Fig. VII.1. Open-pump theory of combined abiotic and biotic C–N interactions in soils. N pump refers to biological N transformation driven by N fixers, nitrifiers, denitrifiers, ammonifiers, and N-assimilating plants and microbes, while C pump refers to the synthesis and decomposition of organic carbon driven by autotrophs and heterotrophs.

Here, the open pump theory is proposed to interpret the combined biotic and abiotic C–N interactions in soils (Fig. VII.1). In this open-pump theory, C and N flows are driven by various organisms with their extracellular and intracellular enzymes. For example, nitrifiers and denitrifiers drive the N flow in the case of nitrification and denitrification, respectively. However, biotic pumps are not isolated, continuous mass exchanges between pumps and soils are occurring through assimilation and excretion everywhere in terrestrial systems. Here, the C and N pump are defined as the biotic C and N flows, respectively. The C pump, accounting for C flows through photosynthesis, chemosynthesis, and C mineralization, is driven by autotrophs and heterotrophs. Reactive C compounds are released by the C pump, e.g., lignin degradation leads to the formation of polyphenols, which are highly reactive to NO_2^- , NH_4^+ , NH_2OH , and amines (Stevenson, 1995). By contrast, the biological N flow, including N fixation, nitrification, denitrification, N assimilation, and ammonification, are representing the N pump. Reactive N intermediates, such as NO_3^- , NO_2^- , NH_2OH , NH_4^+ , amino sugars, amino acids, and peptides are leaking into the soil from the N pump (Stevenson, 1995). Once these reactive N and C compounds have leaked into the soil, they react quickly with each other, leading to nitrogenous gas emissions and N retention. All in all, C–N interactions are in fact the combination of simultaneously interacting biotic and abiotic processes in soils. Till now, biotic processes have been widely studied, whereas abiotic C–N interactions have hardly received attention in the last decades. Therefore, the aim of this chapter is to focus on the formation and release of reactive C and N compounds, as well as their chemical reactions in soils.

VII.2 Soil N pump

Organic nitrogen (ON) accounts for more than 90 % of the total N in soils, while the remaining N exists in the form of inorganic nitrogen (IN), mainly as NH_4^+ and NO_3^- (Schulten et al., 1995). Biological N flow in soils includes N fixation, N assimilation, ammonification, nitrification, and denitrification (Fig. VII.2). Although IN only accounts for less than 10 % of the total N in soils, it plays a key role in N gas emissions and N retention. This section focuses on the biotic N flow via the soil N

pump, as well as the release of reactive N to the soil.

VII.2.1 Drivers of the soil N pump

Atmospheric N_2 is converted to NH_3 by N fixers through N fixation, thereafter NH_3 is quickly protonated to NH_4^+ in the soil (Cleveland et al., 1999). About 100–290 T $N\ yr^{-1}$ N_2 is fixed as NH_4^+ through N fixation in terrestrial ecosystems (Cleveland et al., 1999). Typical N fixers include symbiotic diazotrophs, such as *Rhizobia* and *Frankia* (Gubry-Rangin et al., 2013), and non-symbiotic diazotrophs, such as *Azotobacter chroococcum*, *Azotobacter vinelandii*, *Clostridium spp.*, and *Azospirillum spp.* (Kennedy et al., 2004). It is generally thought that symbiotic diazotrophs are 100 times more efficient in N fixing than non-symbiotic diazotrophs, however, free-living N-fixing strains could be the dominant diazotrophs in some forest stands (Cleveland et al., 1999). Nitrogenase composed of a Fe and MoFe protein is responsible for the catalysis of N fixation (Hoffman et al., 2013), and it is encoded by the *nifH* gene, whose abundance is positively correlated with the SOC content in forest and agricultural soils (Morales et al., 2010).

Under aerobic conditions, NH_4^+ quickly undergoes nitrification (Fig. VII.2): NH_4^+ is firstly oxidized to NH_2OH by ammonia monooxygenase (AMO), afterwards NH_2OH itself is oxidized to NO_2^- by HAO, and NO_2^- is finally oxidized to NO_3^- by NOR (Abeliovich, 2006; Heil et al., 2016). Ammonia-oxidizing bacteria and AOA are responsible for the biotic oxidation of NH_4^+ . *Nitrosomonas sp.*, *Nitrosococcus sp.*, and *Nitrospira sp.* are the most abundant AOB which have been discovered till now (Purkhold et al., 2000). The first isolated AOA, *Nitrosopumilus maritimus*, was discovered in ocean water in 2005, followed by the discoveries of *Thaumarchaeota*, *Crenarchaeota*, and *Euryarchaeota* (Stahl and de la Torre, 2012). Ammonia-oxidizing archaea and bacteria both contain AMO, encoded by the *amoA* gene which is generally used to characterize the diverse ammonia-oxidizing community (Levy-Booth et al., 2014). In contrast to AOB, HNO instead of NH_2OH is proposed as the product of NH_3 oxidation by AOA, which is further oxidized to NO_2^- (Reigstad et al., 2008). The oxidation of NH_4^+ is the rate-limiting step of nitrification, and it is affected by soil pH, temperature, fertilization, and soil moisture (Alves et al., 2013; Ouyang et al., 2016).

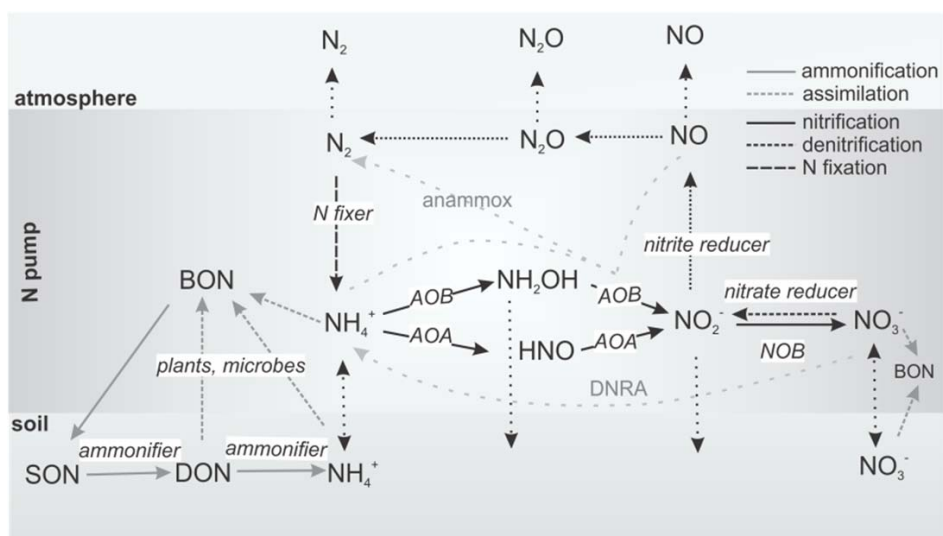


Fig. VII.2 Biotic drivers and reactive nitrogen intermediates of the soil N pump. AOB, ammonia-oxidizing bacteria; AOA, ammonia-oxidizing archaea; NOB, NO_2^- -oxidizing bacteria; anammox, anaerobic ammonium oxidation; DNRA, dissimilatory NO_3^- reduction to NH_4^+ ; BON, biological organic nitrogen in organisms; SON, soil organic nitrogen; DON, dissolved organic nitrogen.

Under anaerobic conditions, NO_3^- is quickly reduced through denitrification by NO_3^- and NO_2^- reducers (Fig. VII.2): NO_3^- is firstly reduced to NO_2^- by nitrate reductase (NAR) encoded by the genes *nas*, *nar*, and *nap* (Stolz and Basu, 2002), then NO_2^- is stepwise reduced to NO , N_2O , and N_2 by NIR, NOR, and nitrous oxide reductase (*nosZ*), respectively (Long et al., 2015). Both NO_3^- and NO_2^- reducers are ubiquitous in a wide range of bacteria, archaea, and fungi, and they account for 0.5–5 % of the total soil microbial biomass (Giles et al., 2012).

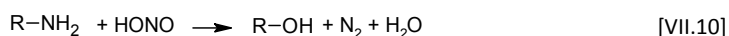
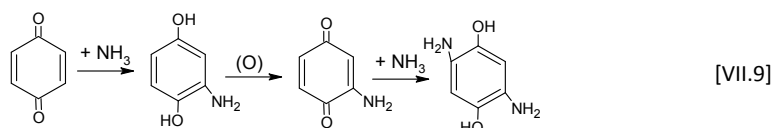
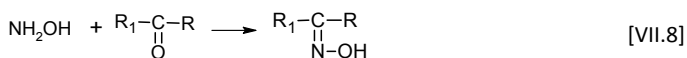
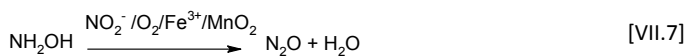
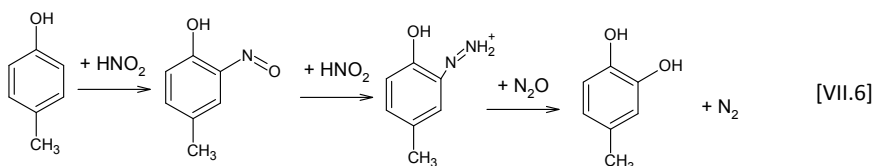
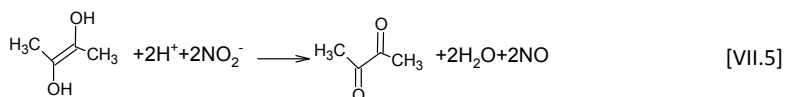
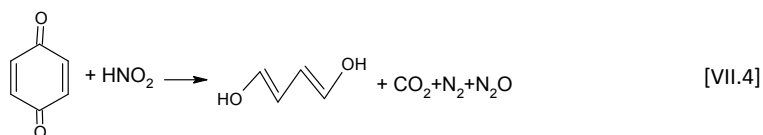
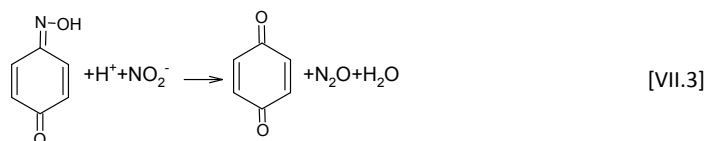
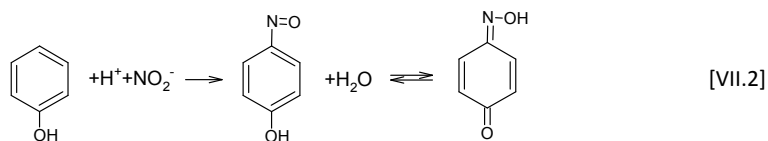
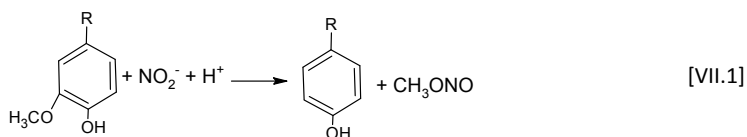
Both NH_4^+ and NO_3^- can be taken up by plants and soil microbes as nutrients and then assimilated to biological organic nitrogen (BON) compounds. In addition, some DON including amino acids, amino sugars, peptides, and even low-molecular-weight proteins can also be assimilated directly by plants, especially mycorrhizal plants (Vranova et al., 2012). When plant or microbial cells die, BON enter the soils and are transformed to SON, which will be firstly decomposed to DON and finally to NH_3/NH_4^+ through ammonification. Common DON contains amino acids, amino sugars, and simple peptides. The most abundant BON, protein, it is firstly attacked by proteases to produce peptides and amino acids, then the amino groups are removed through deamination to form NH_3 (Stevenson, 1995). Ammonification of SON, i.e. the release of NH_4^+ , is conducted by most of the heterotrophic microbes and usually accompanied by the mineralization of SOC (Wolińska et al., 2016).

VII.2.2 Reactive N intermediates in the soil

Nitrate, NH_4^+ , NO_2^- , and NH_2OH can be released to the soil from biological nitrification and denitrification. Nitrate and NH_4^+ are the most abundant IN compounds released from the soil N pump, their contents range heterogeneously from a few to a thousand mg N kg^{-1} soil (Cruz et al., 2008). Nitrate is chemically relatively stable, but it was proposed that NO_3^- can be reduced to NO_2^- by ferrous iron and then incorporated into SON through the so called “ferrous wheel” mechanism proposed by Davidson et al. (2003). In contrast, NH_4^+ can be transformed to NH_3 through deprotonation and then react with quinones to form SON (Reaction [VII.9]) (Stevenson, 1995), therefore the abiotic reaction of NH_4^+ with SOM is favored by alkaline pH and associated with the consumption of oxygen (Broadbent, 1960).

As the key intermediate of both nitrification and denitrification, NO_2^- can also be continuously released to the soil. Because of its high reactivity, NO_2^- cannot be accumulated over 1 mg N kg^{-1} soil under normal soil conditions, however, an alkaline environment, low temperature, free NH_3 and NH_2OH facilitate the accumulation of NO_2^- up to several mg N kg^{-1} soil (Shen et al., 2003). Nitrite can combine with a proton to form nitrous acid (HNO_2) under acidic conditions, and the acid dissociation constant (pK_a) for this equilibrium is 3.27 at 298 K (Riordan et al., 2005). Nitrous acid reacts rapidly with lignin and lignin-derived aromatic compounds. Considerable amounts of N_2 , N_2O , NO_x , methyl nitrite (CH_3ONO), and CO_2 were produced from the abiotic reactions of NO_2^- with lignin and lignin derivatives at acidic and neutral pH in both chemical assays and soils (Nelson and Bremner, 1970; Stevenco et al., 1970; Stevenson and Harrison, 1966; Stevenson and Swaby, 1964; Wei et al., 2017b). N_2O and CO_2 emissions from these reactions are affected greatly by both pH and NO_2^- concentration (Wei et al., 2017b).

Nitrite could enhance the cleavage of C–O bonds in aromatic ethers through O-demethylation, resulting in the removal of a methoxyl group from the molecule (Reaction [VII.1]) (Sobolev, 1961). It was found that the methoxyl ($-\text{OCH}_3$) groups of lignin and humic acid decreased after their reaction with NO_2^- under acidic conditions (Steen and Stojanovic, 1971). In the reaction with SOM, HNO_2 transfers a nitroso group ($-\text{N}=\text{O}$) to an aromatic ring by replacing a hydrogen atom to form nitroso ($\text{C}-\text{N}=\text{O}$) and oxime ($\text{C}=\text{NOH}$) compounds (Reaction [VII.2]), which can subsequently react with excess HNO_2 to form N_2O and quinones (Reaction [VII.3]) (Austin, 1961). Nitrous acid can further react with quinones, resulting in the cleavage of aromatic rings and production of N_2 , N_2O , and CO_2 (Reaction [VII.4]) (Austin, 1961). Furthermore, the chemical reaction of reductones with NO_2^- under acidic conditions is an abiotic NO source (Reaction [VII.5]), and N_2 can also be produced through the formation of diazo-compounds (Reaction [VII.6]) (Austin, 1961).



Except for N gases, the reaction of NO_2^- with SOM could lead to the formation of organic N

compounds. The development of analysis techniques, such as coupled gas chromatography-mass spectrometry (GC-MS) and nuclear magnetic resonance (NMR) spectroscopy has helped to identify the organic N compounds from NO_2^- -SOM reactions. Nitrosophenol, *p*-diazquinone, and *o*-diazquinone were identified in the reaction of NO_2^- with phenol under mildly acidic conditions (Kikugawa and Kato, 1988). GC-MS analysis also revealed nitrosonaphthol and nitronaphthol from abiotic reaction of NO_2^- with naphthol in soil suspensions at pH 6.5 (Azhar et al., 1989). Rousseau and Rosazza (1998) found in ^1H - and ^{13}C -NMR spectral analyses that NO_2^- was incorporated into 7-hydroxy-6-methoxy-1,2(4*H*)-benzoxazin-4-one when reacting with ferulic acid at pH 2.

Even though the release of NH_2OH from biological cells is still not proved directly, several $\mu\text{g N kg}^{-1}$ soil of NH_2OH has been extracted from spruce forest soil (Liu et al., 2014). Hydroxylamine is a very unstable N compound with a pK_a of 5.94 (Politzer and Murray, 2008), and it can be easily oxidized to N_2O by oxygen, NO_2^- , ferric iron, and manganese dioxide (Reaction [VII.7]) (Heil et al., 2015; Heil et al., 2016). Under alkaline conditions, NH_2OH also reacts with aldehydes, ketones, acetyl halides and esters, resulting in the formation of aldoximes, ketoximes, and hydroxamic acids, respectively (Reaction [VII.8]) (Politzer and Murray, 2008). Since oximes and hydroxamic acids are important precursors of chemically formed nitriles, amides, xazoles, oxazolines, isocyanides, and since lactams and carbonyl groups are abundant in SOM, these reactions could be prevalent in soils and contribute significantly to N retention where NH_2OH is released in substantial amounts (Heil et al., 2015).

Amides are the most abundant biologically formed organic N species, which accounts for more than 50 % of SON, followed by amines, which contribute about 3 % to SON (Thorn and Cox, 2009; Vairavamurthy and Wang, 2002). Amino acids and amino sugars have been identified from DON, while the remaining compounds are still unknown (Stevenson, 1995). The free amino group in both amides and amines is reactive to NO_2^- , forming N_2 during the abiotic reaction, also known as the Van Slyke reaction (Reaction [VII.10]) (Chalk and Smith, 1983). Amines can be transformed to imines and amides through reactions with carbonyl and carboxyl groups, respectively, while secondary amides can react with NO_2^- in acidic soils to form N-nitroso groups (Austin, 1961). The fixation of amino nitrogen, including glycine and cyanamide was observed in spruce humus (Nömmik, 1970). In addition, Schmidt-Rohr et al. (2004) confirmed the existence of anilides in soil humic substances through advanced NMR analysis, which could come from the abiotic reactions of amino acids with phenols. Hence, organic N intermediates from ammonification could be another key player in abiotic C–N reactions.

VII.3 Soil C pump

VII.3.1 Drivers of the soil C pump

The amount of C stored as SOC is much larger than the total amount of atmospheric CO₂ and biological organic carbon (BOC); about 2,344 Gt C are stored as SOC in the top 3 m of terrestrial soils (Fontaine et al., 2007). The C flow in soils is driven by plants, autotrophs and heterotrophs through assimilation and mineralization (Fig. VII.3). Almost all the heterotrophs take part in the C mineralization in soils. During C mineralization, macropolymers, such as lignin and polysaccharides, are depolymerized to relatively simple organic molecules of dissolved organic carbon (DOC), which are further oxidized to CO₂. The C mineralization rate ranges largely from 0.7 μg C kg⁻¹ d⁻¹ to 2.5 mg C kg⁻¹ d⁻¹, and is strongly influenced by fresh C input, the structure of organic C, and soil conditions (Davidson and Janssens, 2006; Fontaine et al., 2007; Mutuo et al., 2006). As the most abundant aromatic polymer on earth, lignin constitutes about 30 % of the total organic carbon in the biosphere and is regarded as the main source of stable SOC and reactive C in soils (Bahri et al., 2008). Thus, the decomposition of lignin will be discussed in detail in this section.

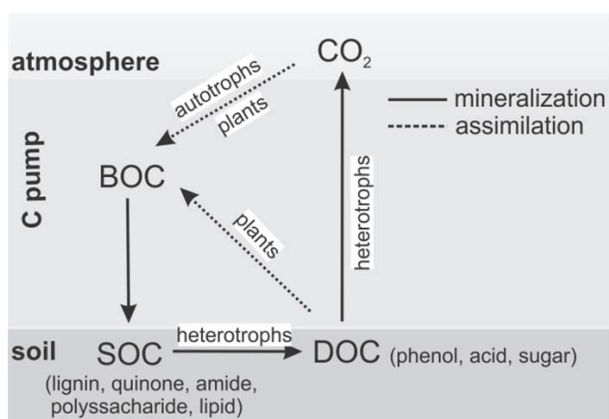


Fig. VII.3 Drivers of the soil C pump and C intermediates released. BOC, biologic organic carbon; SOC, soil organic carbon; DOC, dissolved organic carbon.

Lignin is formed by radical polymerization of G, S, and H units through C-O-C and C-C bonds (Fig. VII.4) (Bugg et al., 2011a). Generally, the lignin G unit is the main constituent of softwood, while a mixture of lignin G and S units account for most of the hardwood lignin, and lignin G and H units make up most of the grass lignin (Faix, 1991; Stevenson, 1995). Aerobic filamentous fungi, including *Basidiomycetes*, *Ascomycetes*, and *Deuteromycetes*, are the main known lignin decomposers in soils (Dashtban et al., 2010). As lignin cannot act as the sole C source for microorganisms, its decomposition is accompanied by co-metabolism with other labile organic C compounds. Lignin

peroxidases (LiP, EC 1.11.1.14), Manganese peroxidases (MnP, EC 1.11.1.13), and laccase (Lac, EC 1.10.3.2) are the most common extracellular oxygenases that catalyze lignin degradation (Hernandez-Ortega et al., 2012). During the decomposition of lignin, highly reactive polyphenols and aromatic compounds are formed and released to the soil. For example, vanillin and vanillic acid are formed during the degradation of lignin G units, and they can be be further oxidized to 3,4-dioxocyclohexa-1,5-diene-1-carboxylic acid, which is reactive to NH_3 and amino groups to form quinone amines that condense to humic substances (Bugg et al., 2011a).

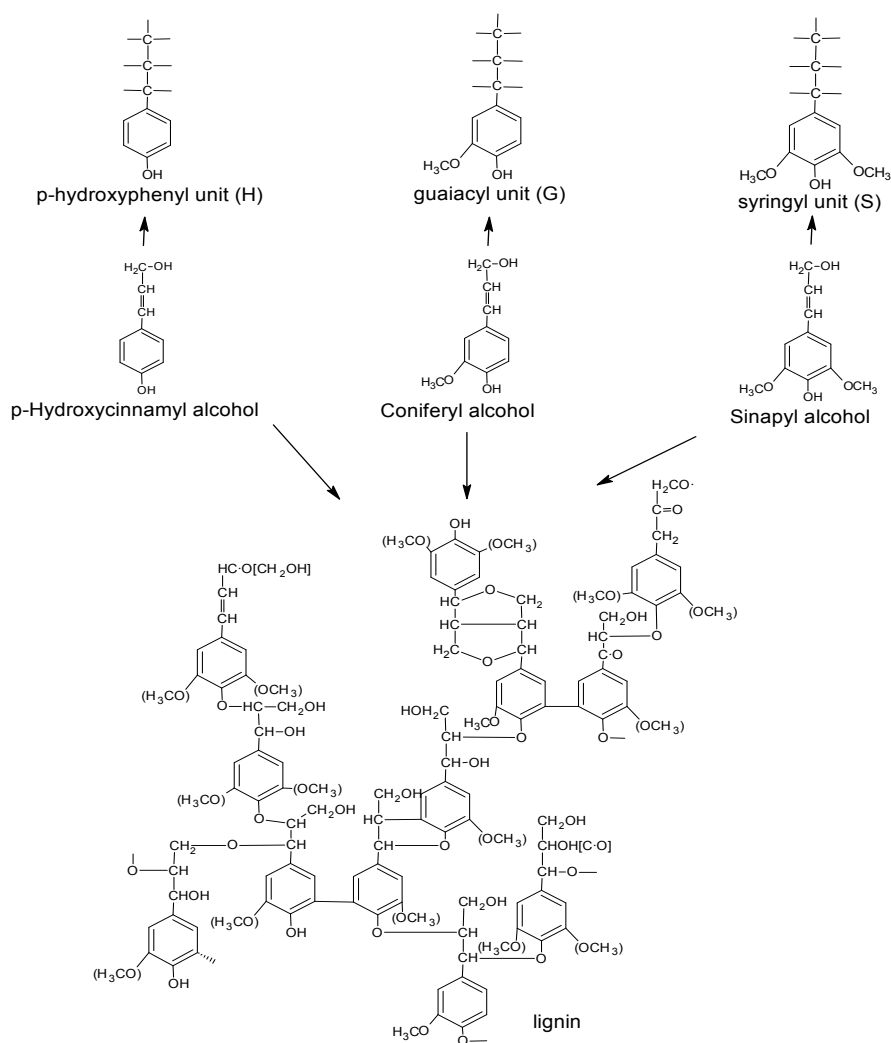


Fig. VII.4 The structure of lignin with guaiacyl (G), syringyl (S), and *p*-hydroxyphenyl (H) units.

VII.3.2 Reactive C intermediates in soil

According to solubility, SOC is divided into four fractions: DOC, which is soluble in water; fulvic acid, which is insoluble in water but soluble in both acid and base; humic acid, which is only soluble in base; and humin, which is insoluble in both acid and base. Except for simple acids, sugars, and amino acids, most of the DOC compounds are not yet chemically identified (Kalbitz et al., 2000). Both humic and fulvic acids are aromatic macropolymer, that differ in distribution of unsaturated aliphatic, N-alkyl methoxyl, carbohydrate, aromatic, –COOH and ketone moieties (Stevenson, 1995). Humin is carbonaceous and heterogeneous material, which might account for more than 50 % of the SOC, and it is abundant in various functional groups, such as carbonyl (C=O), unsaturated hydrocarbon (C=C), hydroxyl (OH), and aromatic hydrocarbon moieties (Zhang et al., 2015a). According to ¹³C-NMR analysis, O-alkyl-C assigned to amide and polysaccharide C dominates in soils, followed by the alkyl-C and C-/O-substituted alkyl-C which corresponds to chain aliphatic C from lipids and aromatic C from lignin, respectively (Fontaine et al., 2007).

Most of the –C=O, –C=C–, and –OH groups, as well as aromatic hydrocarbons, are reactive to NO₂[–], NH₂OH, NH₃, and amino-N under natural soil conditions. Gases including N₂, N₂O, NO, and CO₂ were observed from the reactions of NO₂[–] with humic and fulvic acids (Stevenson et al., 1970), while the N₂O and NO production rates depended greatly on their specific structures (Wei et al., 2017a). Except for N gases, nitrophenols, amides, imines, and indophenols were identified as the reaction products of NO₂[–] with fulvic acid by ¹⁵N-NMR analysis (Davidson et al., 2003; Thorn and Mikita, 2000). It is thought that the incorporation of NO₂[–]-N into organic substances occurs through C-nitrosation and further cyclization (Thorn and Mikita, 2000). In addition, ¹³C- and ¹⁵N-NMR studies have proven the formation of oximes and hydroxamic acid from reactions of NH₂OH with humic and fulvic acids, as well as their rearrangement products nitriles and amides (Thorn et al., 1992). Thorn and Mikita (1992) explored the NH₄⁺ fixation by peat and Leonardite humic acids, and Suwannee River fulvic acid with ¹⁵N- and ¹³C-NMR. They found that fulvic acid fixed the most NH₄⁺, thereby increasing its N content by 2.29 %, and the products were indole, pyrrole, pyridine, pyrazine, amide, and aminohydroquinone.

VII.3.3 Free organic radicals

Electron paramagnetic resonance (EPR) studies have shown that lignin, lignin preparations, fulvic acid, humic acid, and humin contain stable organic radicals in the order of 1×10^{17} – 8×10^{19} spins g^{–1}, and these free organic radicals are very likely hydroquinone and quinone moieties, co-existing with semiquinones (Senesi and Schnitzer, 1977; Steelink, 1964). Interestingly, the content of stable organic radicals increases in the order: lignin < lignin derivatives < fulvic acid < humic acid (Steelink, 1964), indicating that these organic radicals might be formed from lignin products during

humification. It is proposed that methoxyl groups in subunits of lignin can be oxidized during the decomposition of lignin with the formation of semiquinone radicals (SQ), while SQ can be deprotonated to the semiquinone radical anion (SQA) upon basification, or disproportionate to a hydroquinone (HQ) and a quinone (Q) (Baehrle et al., 2015).

Oxygen and pH are two important factors affecting the content of free stable organic radicals. Fitzpatrick and Steelink (1969) found that benzosemiquinone was formed from benzoquinone under exposure to oxygen in aqueous sodium hydroxide solution, and its intensity increased when pH increased from 10 to 13, while it was destroyed by exposure to excess oxygen. By contrast, Senesi and Schnitzer (1977) found that the abundance of organic radicals increased to a maximum in the first 70 min after fulvic acid was added to alkaline solutions, and then decreased to 0.25×10^{-17} 28 d later. Redox potential also exerts a great effect on the abundance of organic radicals. Chemical reducers, such as NaBH_4 and SnCl_2 , increased the abundance of organic radicals in fulvic acid by more than 60 times in a short time (Senesi and Schnitzer, 1977). In addition, the abundance of organic radicals in lignin and fulvic acid could also be increased by ultraviolet germicidal irradiation (Baur and Easteal, 2014; Senesi and Schnitzer, 1977). Except for humic substances, organic pollutants with aromatic rings can also form organic radicals in soils. Dela Cruz et al. (2011) found that the abundance of persistent free organic radicals was about 30 times higher in pentachlorophenol-contaminated soil than in the non-contaminated soil.

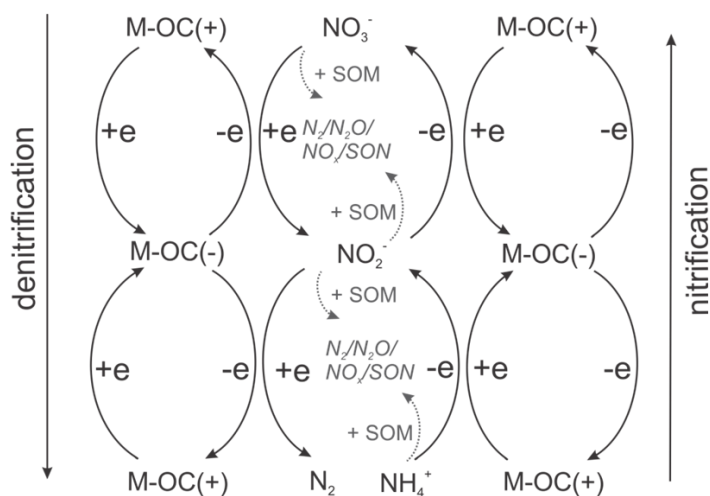


Fig. VII.5 The M-OC wheel hypothesis, explaining the combined biotic and abiotic production of nitrogenous gases and soil organic nitrogen. Gray dotted arrows indicate abiotic reactions; M-OC, the complex of metal and organic radicals; SOM, soil organic matter; SON, soil organic nitrogen.

Organic radicals can act as electron donors as well as acceptors in both acidic and alkaline

solutions (Van der Zee and Cervantes, 2009). It has been reported that humin acted as electron mediator during the microbial reduction of Fe^{3+} to Fe^{2+} , microbial reduction of NO_3^- , and microbial dechlorination of pentachlorophenol (Zhang et al., 2015a; Zhang et al., 2015b). The bonding of metals with humic substances shifts the quinone-semiquinone-hydroquinone equilibria and decreases the abundance of organic radicals (Christoforidis et al., 2010; Jerzykiewicz et al., 2002). However, the complex of Fe and humic acid acts as a more efficient electron shuttle than humic acid itself (Zhang et al., 2014). Considering the excellent electron-transferring ability of the metal–OC complex (M–OC), here a M–OC wheel hypothesis is proposed explaining the combined biotic and abiotic formation of N gases and SON (Fig. VII.5). In the M–OC wheel, the M–OC complex acts as the electron carrier to facilitate microbial nitrification and denitrification and catalyze the abiotic reactions of N and C intermediates. Mahieu et al. (2000) found that the accumulation of heterocyclic N compounds responded positively to the abundance of free organic radicals in three agricultural soils, which could be a proof of the participation of organic radicals in the abiotic formation of heterocyclic N.

VII.4 Role of abiotic C–N interactions in N trace gas formation and N retention

VII.4.1 N_2O and NO_x emissions

Recently, more and more evidence has been provided that abiotic NO_2^- –SOM reactions significantly contribute to N_2O and NO_x emission and N retention in various soils (Table VII.1). Nitrite is regarded as the direct precursor of both biotic and abiotic NO emission in soils (Medinets et al., 2015). Islam et al. (2008) found that 47–57 % of NO_2^- was chemically decomposed to NO in 2.5 h in two acidic pasture soils. Wei et al. (2017a) also found that NO_2^- was rapidly transformed to NO in acidic forest soils, and the reaction rate of NO_2^- with humin was the highest compared with other SOM fractions. Li et al. (2000) developed a process-oriented model to predict N_2O and NO emission in forest soils, in which the abiotic NO_2^- –SOM reactions were considered for NO production. But the influences of SOM quality, free organic radicals, and transition metals were not considered in this model, and its validation was only tested for temperate forest soils (Stange et al., 2000).

Nitrite is also an important precursor of N_2O emission. Maharjan and Venterea (2013) found that N_2O emission from maize soils amended with urea was significantly positively correlated with NO_2^- content. A kinetic study proved that the N_2O emission rate was linearly correlated with NO_2^- concentration in a pH range of 4.8–5.7 in sterilized soils, and 84 % of the variance in N_2O emission rate was explained by total C content of the soil (Venterea, 2007). In addition, the reaction of NO_2^- with fulvic acid accounted for a much higher N_2O production in acidic forest soils compared with dissolved organic matter, humic acid, and humin (Wei et al., 2017a). However, the abiotic N_2O emission from NO_2^- –SOM reactions has been overlooked so far in both N_2O emission models and

N₂O source-partitioning models. The ¹⁵N site preference (SP) of N₂O, which has been generally assumed constant for a certain N₂O source, is regarded as an efficient tool to partition N₂O sources (Toyoda and Yoshida, 1999). Nevertheless, Wei et al. (2017b) found that the SP of N₂O varied largely in the reactions of NO₂⁻ with lignin derivatives, and this variation was affected by both pH and the structure of the organic substances. The N₂O source partitioning was biased when SP was used for N₂O source partitioning and N₂O production from abiotic C–N interactions was neglected (Wei et al., 2017a).

Table VII.1. N₂O loss, NO_x loss, and N retention in various soils after N application.

	Soil	Soil pH	Total C (%)	N ₂ O loss (%)		NO _x loss (%)		N retention (%)		Reference
				Non-sterile	sterile	Non-sterile	sterile	Non-sterile	sterile	
NO ₂ ⁻	Cambisol	2.9–3.4	19–39	3–7	1–3	17–46	17–52	–	–	(Wei et al., 2017a)
	silty loam	5.1–5.2	2.5–2.6	0.7	0.5	–	–	–	–	(Venterea, 2007)
	silty loam	5.3–5.4	3.0–3.1	1	0.6	–	–	–	–	
	silty loam	5.5–5.6	6.3–7.0	7.7	2.7	–	–	–	–	
	clay	8.1	7.1	–	–	–	–	0	0	(Islam et al., 2008)
	sandy loam	4.8	6.2	–	–	–	–	21	20	
	sandy loam	5.0	6.8	–	–	–	–	20	19	(Fitzhugh et al., 2003b)
	Inceptisol	3.4–3.9	42–84	–	–	–	–	20–40	65–80	
Canton	3.8–4.0	25	–	–	–	–	5–6	10	(Dail et al., 2001)	
NH ₂ OH	Cambisol	2.9–3.4	14–46	0.7–6	0.4–4	–	–	–	–	(Heil et al., 2015)
	Cambisol	4.9	2.9	23	0.7–20	–	–	–	–	
	Luvisol	6.4	1.1	28	21–25	–	–	–	–	
NH ₄ ⁺	Inceptisol	3.4–3.9	42–84	–	–	–	–	20–60	7–10	(Fitzhugh et al., 2003b)
	loam	3.5–4.0	38–49	–	–	–	–	–	5–30	(Corre et al., 2007)
	loam	3.5–3.7	3–6	–	–	–	–	–	4–23	
NO ₃ ⁻	Inceptisol	3.4–3.9	42–84	–	–	–	–	8–18	6–10	(Fitzhugh et al., 2003b)
	Canton	3.8–4.0	25	–	–	–	–	40–50	10–30	(Dail et al., 2001)
	loam	7.2	4.8	–	–	–	–	8	14	(Torres-Canabate et al., 2008)
	sandy loam	5.7	9.3	–	–	–	–	6	11	(Corre et al., 2007)
	loam	3.5–4.0	38–49	–	–	–	–	–	0–5	
loam	3.5–3.7	3–6	–	–	–	–	–	0		

Hydroxylamine is a direct N₂O precursor in both biotic and abiotic pathways, while the N₂O production from abiotic reactions of NH₂OH is inhibited by high SOM content, as found, e.g., for acidic forest soil (Heil et al., 2015). The SP of N₂O from abiotic oxidation of NH₂OH is around 34–36 % (Heil et al., 2014), which is similar to the SP values for N₂O assigned to biotic NH₂OH oxidation. Hence, it is hard to distinguish biotic and abiotic N₂O sources in the field at present, as more sophisticated methods and models are needed to quantify abiotic and biotic N₂O emissions.

VII.4.2 Nitrogen retention

The reported immobilization of NO_2^- , NH_4^+ , and NO_3^- in various soils is listed in Table VII.1. The immobilization of NH_4^+ in soils has been reported decades ago, and the amount of fixed NH_4^+ -N is positively correlated with SOC content (Opuwariboi and Odu, 1975). When urea was applied to a Swedish organic soil containing 36.62 % of soil carbon at pH 6.9, 9.7 % of the urea-N was incorporated into SOM as non-extractable N after 10 d (Johansson, 1998). Even though NH_4^+ immobilization is facilitated by alkaline pH, it was also found that NH_4^+ was incorporated into SON in acidic soils (Corre et al., 2007; Fitzhugh et al., 2003b). In contrast, the structure of chemically immobilized NH_4^+ has been rarely reported (Thorn and Mikita, 1992).

Abiotic NO_3^- immobilization in organic N compounds was observed in a German spruce forest (Corre et al., 2007), an American mixed hardwood forest (Dail et al., 2001), and two *Abies pinsapo* fir forest soils (Torres-Canabate et al., 2008). However, the validity of the hypothesis that the reduction of NO_3^- to NO_2^- by ferrous iron and the reaction of NO_2^- with SOM are too slow to lead to NO_3^- fixation is discussed controversially (Colman et al., 2007, 2008). Incubation conditions, soil pH, intensity of N application, and analysis methods are the main reasons of this controversy (Bosatta and ÅGren, 1995).

As an N intermediate whose reactivity is much higher than that of NH_4^+ and NO_3^- , NO_2^- can quickly react with SOC in general, and DOC in particular, resulting in the formation of nitro-aromatic compounds and heterocyclic N (Rousseau and Rosazza, 1998; Thorn and Mikita, 2000). When NO_2^- was applied into a forest soil, 17.8 % of it was incorporated into dissolved organic matter within 4 h (Isobe et al., 2012). Since the reactivity of NO_2^- is highly dependent on pH, soil pH is a key factor controlling the abiotic NO_2^- -SOM reactions. Islam et al. (2008) found that abiotic NO_2^- immobilization did not occur any more when the pH increased to 8. As one of the key determinants of abiotic C–N reactions, the SOC content was found to be significantly positively correlated with chemical N retention (Fitzhugh et al., 2003b). Heterocyclic and nitro-aromatic compounds are common organic N compounds resulting from abiotic C–N reactions, and they have received increasing interest in the last years due to their resistance to decomposition (Leinweber et al., 2009). Heterocyclic compounds like pyrroles and pyridines, pyrazines, nitriles, and imines have been detected in various natural humic substances (Thorn and Cox, 2009), and the content of heterocyclic N was found to increase during humification (Abe et al., 2005). Gillespie et al. (2009) also found that nitro-aromatic compounds do exist in the rhizosphere of pea, accompanied by a decrease of aromatic C compounds. This suggest that abiotic C–N reactions do occur in natural soils, and that long-term N retention could be caused by the increase of heterocyclic and nitro-aromatic N compounds in soil (Thorn and Cox, 2009).

VII.5 Conclusions

The newly proposed open-pump theory is designed to explain the simultaneous and multiply interacting biotic and abiotic C–N processes in soils. Soil microbes and plants act as drivers of N and C flows, during which reactive intermediates, such as NH_3 , NO_2^- , NH_2OH , amino acids, amino sugars, phenols, organic acids, and organic radicals, are released to the soil, and various abiotic C–N reactions occur once the reactive intermediates get in contact with each other. It has been proven that abiotic C–N reactions do contribute to N gas emission from and N retention in soils. However, it is still an open question how much these abiotic C–N reaction contribute to the whole soil C and N cycling. At present, sterilization is a widely used method to investigate abiotic N gas emission and N retention in soils. Since the continuous release of reactive N and C intermediates is inhibited after sterilization and externally applied N intermediates are quickly consumed, it is very difficult to exactly quantify the magnitude of these abiotic reactions. Therefore, advanced techniques, such as determination of the net isotopic effect of the various processes and clumped isotope analysis, are needed to identify, disentangle and quantify the biotic–abiotic C–N interactions.

VIII. Synopsis

VIII.1 Summary

Although NO_2^- is highly chemically reactive to various prevalent soil organic compounds, the effect of abiotic processes on N cycling has been scantily studied for decades. In this thesis, the chemical reactions of NO_2^- with SOM were systematically investigated in both chemical assays and soils to explore their role in N trace gas emissions and N retention in soil.

The influences of pH and NO_2^- concentrations on N_2O and CO_2 emissions, as well as N_2O isotopic signatures, were investigated in chemical reactions of NO_2^- with two types of lignin and six lignin derivatives in Chapter II. Both pH and NO_2^- concentrations affected N_2O and CO_2 emissions nonlinearly, and the reductive lignin S unit (4-hydroxy-3,5-dimethoxybenzaldehyde) was the most reactive lignin derivative, which indicates that NO_2^- -SOM reactions in soil could be facilitated by acidic pH, higher NO_2^- concentration, and higher content of lignin S units. Most interestingly, it was found for the first time that the ^{15}N SP of N_2O varied largely with pH and structure of lignin derivatives instead of staying relatively stable, which challenges to the common assumption that the ^{15}N SP of N_2O remains stable for a certain N_2O source, independent of environmental factors and the substrate.

To further explore the mechanisms involved in the shift of ^{15}N SP values of N_2O from NO_2^- -SOM reactions, N_2O isotopic signatures were characterized in real-time using a QCLAS that has been customized for simultaneous analysis of the four most abundant $^{14}\text{N}^{14}\text{N}^{16}\text{O}$, $^{14}\text{N}^{15}\text{N}^{16}\text{O}$, $^{15}\text{N}^{14}\text{N}^{16}\text{O}$, and $^{14}\text{N}^{14}\text{N}^{18}\text{O}$ in Chapter III. Also in these experiments it was found that ^{15}N SP changed during the reactions of NO_2^- with lignin derivatives, which could be explained by a shift of the ratio of N_2O precursors, i.e. *trans*-hyponitrous acid-to-(*cis*-hyponitrous acid + nitramide). Chemodenitrification was located in a three-dimensional end-member map of $\text{SP}-\delta^{15}\text{N}^{\text{bulk}}-\delta^{18}\text{O}$, using data of previously reported studies and this thesis. Instead of being isolated from other N_2O sources, the isotopic signature of chemodenitrification overlapped partly with that of fungal denitrification, and was mostly located in the mixing zone of nitrification and denitrification, which makes it impossible to distinguish chemodenitrification from biotic N_2O sources with end-member maps. Therefore, the use of end-member maps in N_2O source partitioning could bias N_2O source apportioning without consideration of chemodenitrification.

The contribution of abiotic NO_2^- -SOM reactions to N_2O and NO_x emissions in Spruce forest soil was explored in Chapter IV with a coupled chemoluminescence analyzer and QCLAS system. Abiotic processes contributed 19.5–42.3 % and more than 88 % to N_2O and NO_x emissions, respectively. Among the four SOM fractions, i.e. DOM, fulvic acid, humic acid, and humin, the reaction of fulvic acid with NO_2^- was associated with the highest abiotic N_2O emission. Redundancy analysis revealed that N_2O emission was negatively correlated with total lignin content, but positively correlated with the proportion of lignin S units. In addition, just as it was suggested in Chapter III, end-member maps

failed to distinguish abiotic from biotic N₂O emission, and a two-end-member mixing model overestimated fungal and bacterial denitrification when chemodenitrification was neglected.

Beside N₂O and NO_x, SON was another product of NO₂⁻-SOM reactions, hence abiotic NO₂⁻ immobilization and the structure of immobilized N were investigated in Chapter V using the ¹⁵N-labelling technique and solid-state ¹⁵N-NMR analysis. About 7 % of NO₂⁻ was immobilized by SOM to form SON, and there was no significant difference of N retention between forest, grassland, and agricultural soils. About 50 % of immobilized N existed as amides, and the other half consisted of nitrile-N, amino-N, pyrrole-N, and nitro-/oxime/nitrate-N. Notably, ¹⁵N-entichment in fulvic acid was dramatically higher compared with the remaining humus after HF treatment, which demonstrated again that fulvic acid was much more reactive to NO₂⁻ than other SOM fractions (cf. Chapter IV, where fulvic acid contributed the most to N₂O emission among SOM factions).

Since it has been shown in Chapter II–V that lignin composition and SOM quality affect abiotic N₂O emission and N retention, lignin content and composition could very likely play an important role in fertilizer-N partitioning and NUE in agriculture. Therefore, the effect of lignin content and composition of OSA on N partitioning was studied in a 114-d laboratory incubation experiment in Chapter VI. Wheat straw, spruce sawdust, and lignin were chosen as three types of OSA with different lignin content and composition, and fertilizer-associated N₂O emission, N retention, and mineral N content were monitored after the combined application of N fertilizer and OSA. Both N retention and N₂O emission were promoted by OSA in the order: wheat straw > spruce sawdust > lignin, while the highest content of mineral N was found in lignin amended treatment. In accordance with Chapter IV, N₂O emission was positively correlated with the proportion of lignin S units. Furthermore, lignin composition correlated linearly with OSA decomposition and N retention.

These results suggest that abiotic NO₂⁻-SOM reactions play an important role in both N trace gas emission and N retention in soil depending on soil pH, transition metals, and SOM quality. Finally, the biotic release of reactive N and C compounds into soil, their reactions in soil, as well as the role of abiotic C-N interactions in N₂O and NO_x emissions and N retention, were reviewed in Chapter VII. It is suggested that biotic and abiotic processes occur and interact with each other simultaneously in soil, and that both, especially their interactions, should be regarded in N cycling studies and models instead of focusing on only one. Till now, ample evidence has been found that abiotic processes act an important part in N cycling, however, further studies are still needed to explore effective methods to identify and quantify biotic and abiotic N₂O emissions and N retention, and to bridge the gap between laboratory experiments and global models.

VIII.2 Synthesis

VIII.2.1 N₂O emission and N₂O isotopic signatures

Various N₂O production pathways, such as nitrification, bacterial denitrification, fungal denitrification, nitrifier denitrification, abiotic NH₂OH oxidation, and chemodenitrification, have been revealed till now (Butterbach-Bahl et al., 2013). However, it remains an open question how to identify and quantify precisely the contribution of each pathway to global N₂O emission and to propose more effective N₂O mitigation strategies accordingly. Since ¹⁵N SP of N₂O was first defined, it has been regarded as a reliable tool for N₂O source partitioning (Toyoda and Yoshida, 1999). According to the N₂O isotopic signatures of different N₂O sources, end-member maps in which biotic N₂O sources such as nitrification, fungal denitrification, and bacterial denitrification are located separately, have been used to identify and quantify N₂O sources (Toyoda et al., 2015). However, it was found in this thesis for the first time that SP of N₂O from chemodenitrification was neither stable nor distinguishable from biotic N₂O sources, and end-member mixing model analysis biased N₂O source apportionment by overlooking chemodenitrification. Therefore, the applicability of currently used N₂O isotopic techniques for N₂O source partitioning should be reconsidered, and an explanation should be found for the reason why SP stayed stable in abiotic NH₂OH oxidation (Heil et al., 2014) but shifted in NO₂⁻-SOM reactions (current study). Once the mechanisms involved in stable or shifting N₂O ¹⁵N SP values are revealed, it could be promising to propose a more effective method for N₂O source partitioning.

VIII.2.2 N sequestration

Recently, “black N”, i.e. heterocyclic aromatic N including pyrroles, pyridines etc., has been receiving more and more attention due to their riddling sources and recalcitrance to biological consumption. Fire obvious can induce the formation of pyrroles (Knicker, 2011b), while abiotic C–N reactions during humification could be another formation mechanism (Mahieu et al., 2000). According to the results in Chapter V of this thesis, pyrroles can be formed from NO₂⁻-SOM reactions, while more than 50 % of chemically immobilized N was amide-N. Amides resulting from chemical reactions could also be recalcitrant to mineralization if the amide-N is directly bonded to aromatic rings like it is mostly the case (Schmidt-Rohr et al., 2004). It has been reported that heterocyclic N could also be decomposed by soil microbes (De la Rosa and Knicker, 2011; De la Rosa et al., 2013), while knowledge is still limited about the relative degradation rates of heterocyclic N compared with amides and other SON compounds. All in all, abiotic N retention does act a part in total soil N sequestration, while it still needs to be answered in the further to which extent abiotic processes affect N sequestration in soil, what factors are influencing these processes, and which C and N compounds contribute the most to N sequestration.

VIII.2.3 Role of lignin in N cycling

Lignin and its derivatives are important participants in NO_2^- -SOM reactions, which has been shown in Chapter II–IV, and lignin composition of OSA affected N partitioning of fertilizer both biologically and chemically in agricultural soil (Chapter VI). It was also reported in previous studies that lignin and polyphenols influenced N_2O emission (Garcia-Ruiz and Baggs, 2007; Millar and Baggs, 2004). In this thesis, it was further demonstrated that the proportion of lignin S units was the most easily degradable and most reactive to NO_2^- . Generally, C/N ratio is regarded as the main factor controlling fertilizer NUE (Mooshammer et al., 2014), while the role of lignin content and composition in soil N cycling has been neglected. Thus, except for C/N ratio, the latter should also be considered when assessing the influence of combined application of N fertilizer and OSA on soil N gas emission and soil N retention.

VIII.3 Perspectives

According to the pathways of NO_2^- -SOM reactions, *trans*-/*cis*-hyponitrous acid and nitramide were proposed as possible N_2O precursors in chemodenitrification, and the change of their ratios could be the reason for the observed shift in ^{15}N SP values of N_2O . Further studies should be conducted to test this hypothesis, especially the *trans*-/*cis*-hyponitrous acid pathway, which is quite similar to the biotic N_2O production pathways for which high SP values were found for *cis*-hyponitrous acid-derived N_2O , but low SP value for *trans*-hyponitrous acid-derived N_2O (Toyoda et al., 2015). Since the current N_2O isotopic methods fail to partition N_2O sources if chemodenitrification is involved, a more precise N_2O source-partitioning approach is needed. For example, it could be promising to modify the current N_2O source-partitioning approach by taking into account environmental factors affecting the formation of *trans*- and *cis*-hyponitrous acid if *trans*-/*cis*-hyponitrous acid are indeed the precursors of both abiotic and biotic N_2O production as proposed in Chapter III. On the other hand, clumped isotope analysis of N_2O could be a promising alternative to characterize N_2O production pathways.

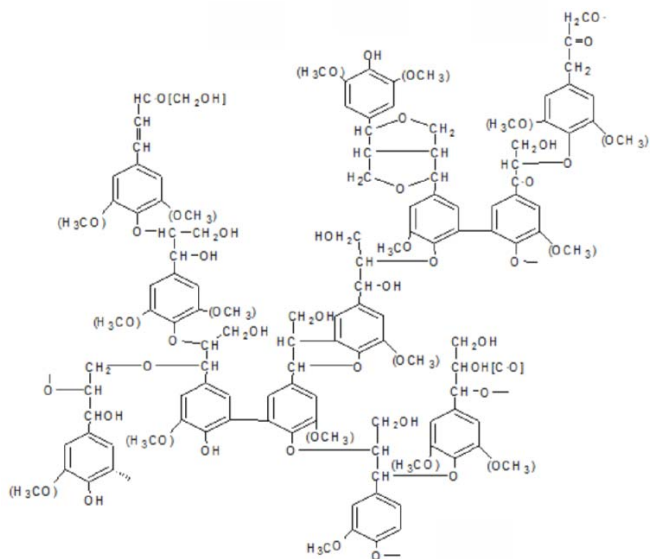
In this thesis, it was found that fulvic acid and humin accounted for the largest and fastest N_2O emission, respectively, when reacting with NO_2^- compared with the other SOM fractions. It has been proposed that $-\text{C}=\text{O}$, $-\text{C}=\text{C}-$, $-\text{OH}$, and $-\text{NH}_2$ could be the functional groups reactive to NO_2^- , and the M-OC wheel could catalyze abiotic interactions (cf. Chapter VII). However, knowledge is still too limited to explain the reason. Therefore, further studies are needed to confirm these hypotheses and explore quantitative and kinetic effects of these functional groups on N trace gas emission and N retention.

Solid-state ^{15}N -NMR analysis revealed that amide-N was the dominant form of N in SON resulted from abiotic NO_2^- immobilization in Chapter V. Amides from abiotic and biotic sources are not

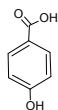
sufficiently distinguishable from each other which could be partly a reason why abiotic N retention is often overlooked in natural soils. Abiotic formation of pyrrole-N, nitro-N, oxime-N, and nitrile-N from NO_2^- -SOM reactions was also confirmed in this thesis. However, it needs to be further studied how resilient these compounds are to the degradation by soil microbes and what role these compounds play in long-term N sequestration in soil. In addition, it was also demonstrated in the present thesis that lignin content and composition of OSA played an important role in fertilizer-associated N_2O emission and N retention in agriculture. Hence, besides C/N ratio, lignin content and composition of OSA should also be considered in agricultural management to improve NUE and reduce N_2O emission. More studies in various soils under different environmental conditions should be conducted, though, to further assess this lignin effect.

IX. Appendix

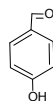
Appendix A: supplementary information for chapter II



H units:

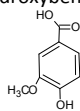


(b) 4-hydroxybenzoic acid

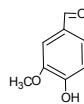


(c) 4-hydroxybenzaldehyde

G units:

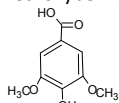


(d) 4-hydroxy-3-methoxybenzoic acid

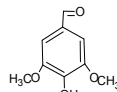


(e) 4-hydroxy-3-methoxybenzaldehyde

S units:



(f) 4-hydroxy-3,5-dimethoxybenzoic acid



(g) 4-hydroxy-3,5-dimethoxybenzaldehyde

Fig. A1. The structures of lignin and lignin derivatives.

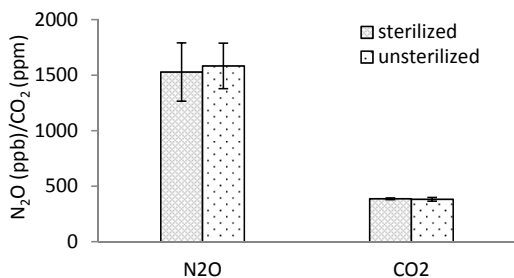


Fig. A2. N_2O and CO_2 emissions from the reaction of 0.01 g organosolv lignin and 5 ml of 0.5 mM NO_2^- solution in water for 24 h. For sterilized treatment, the vials were sterilized at 170 °C for 6 h in an oven, and NO_2^- solution was sterilized by passing through a 0.2 μm filter. There was no significant difference ($P > 0.05$) between sterilized and unsterilized treatments.

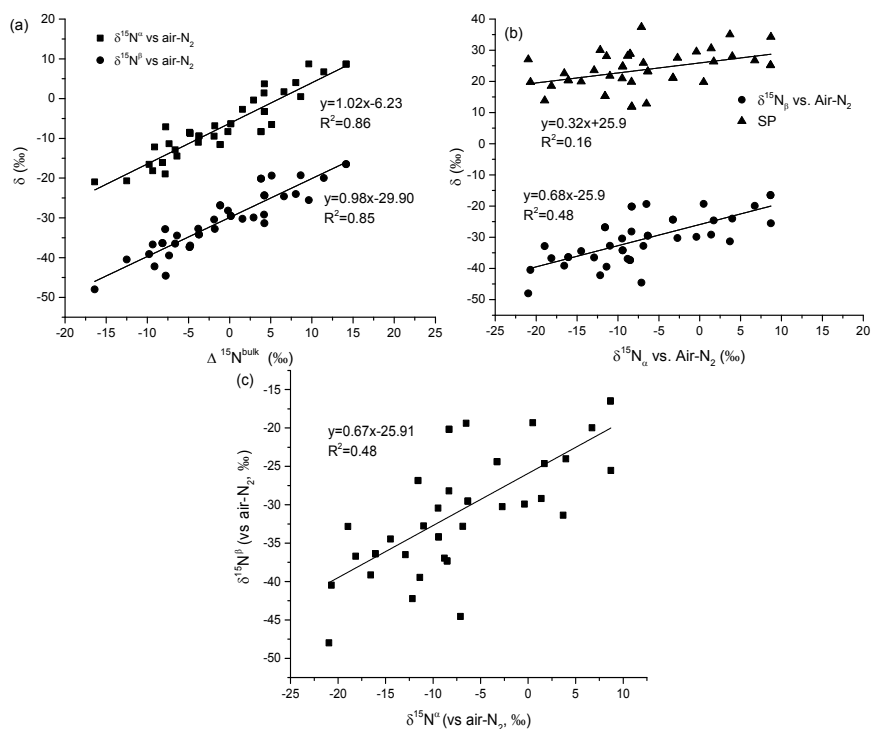


Fig. A3. Linear regression of $\Delta^{15}\text{N}^{\text{bulk}}$ with $\delta^{15}\text{N}^{\alpha}$ and $\delta^{15}\text{N}^{\beta}$ (a), $\delta^{15}\text{N}^{\alpha}$ with site preference and $\delta^{15}\text{N}^{\beta}$ (b), and $\delta^{15}\text{N}^{\alpha}$ with $\delta^{15}\text{N}^{\beta}$ (c) ($n = 41$).

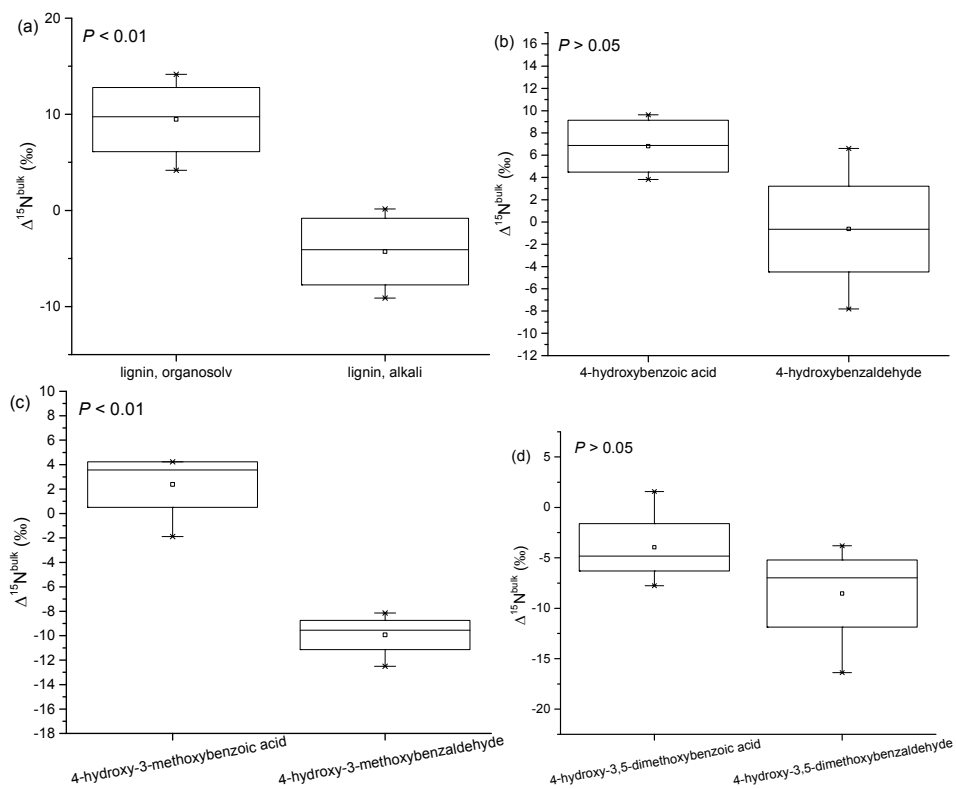


Fig. A4. Paired t test to compare the differences of $\Delta^{15}\text{N}^{\text{bulk}}$ between organosolv and alkali lignin (a), 4-hydroxybenzoic acid and 4-hydroxybenzaldehyde (b), 4-hydroxy-3-methoxybenzoic acid and 4-hydroxy-3-methoxybenzaldehyde (c), and 4-hydroxy-3,5-dimethoxybenzoic acid and 4-hydroxy-3,5-dimethoxybenzaldehyde (d). The *box* indicates the range of the 25 and 75 percentiles of the data, the *line in the box* is the median, and the notch lines indicate the 1.5 interquartile rang.

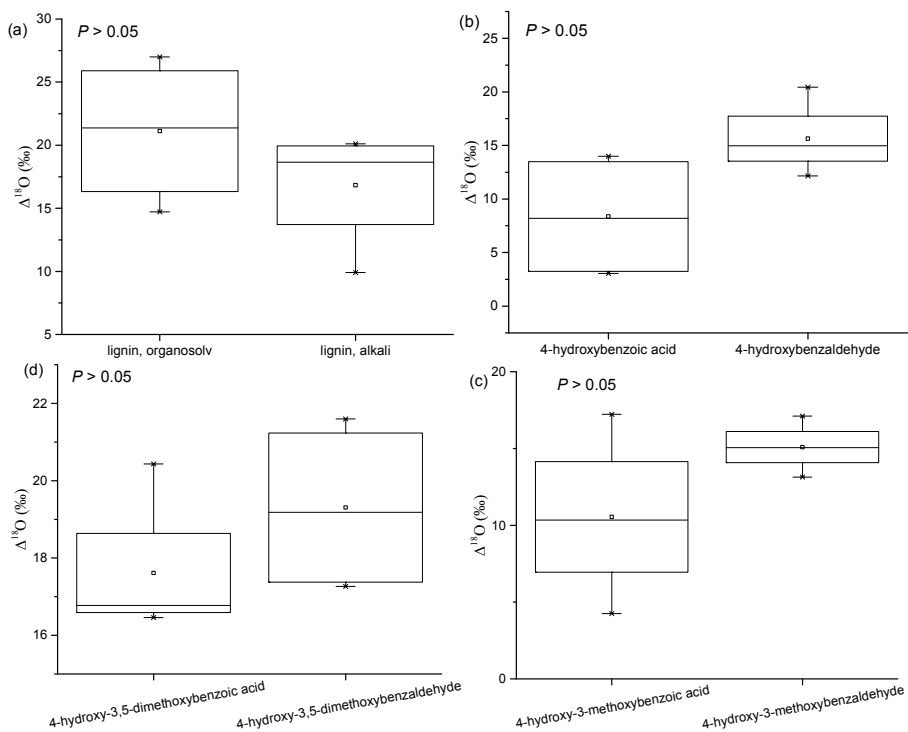


Fig. A5. Paired t test to compare the differences of $\Delta^{18}\text{O}$ between organosolv and alkali lignin (a), 4-hydroxybenzoic acid and 4-hydroxybenzaldehyde (b), 4-hydroxy-3-methoxybenzoic acid and 4-hydroxy-3-methoxybenzaldehyde (c), and 4-hydroxy-3,5-dimethoxybenzoic acid and 4-hydroxy-3,5-dimethoxybenzaldehyde (d). The *box* indicates the range of the 25 and 75 percentiles of the data, the *line in the box* is the median, and the *notch lines* indicate the 1.5 interquartile rang.

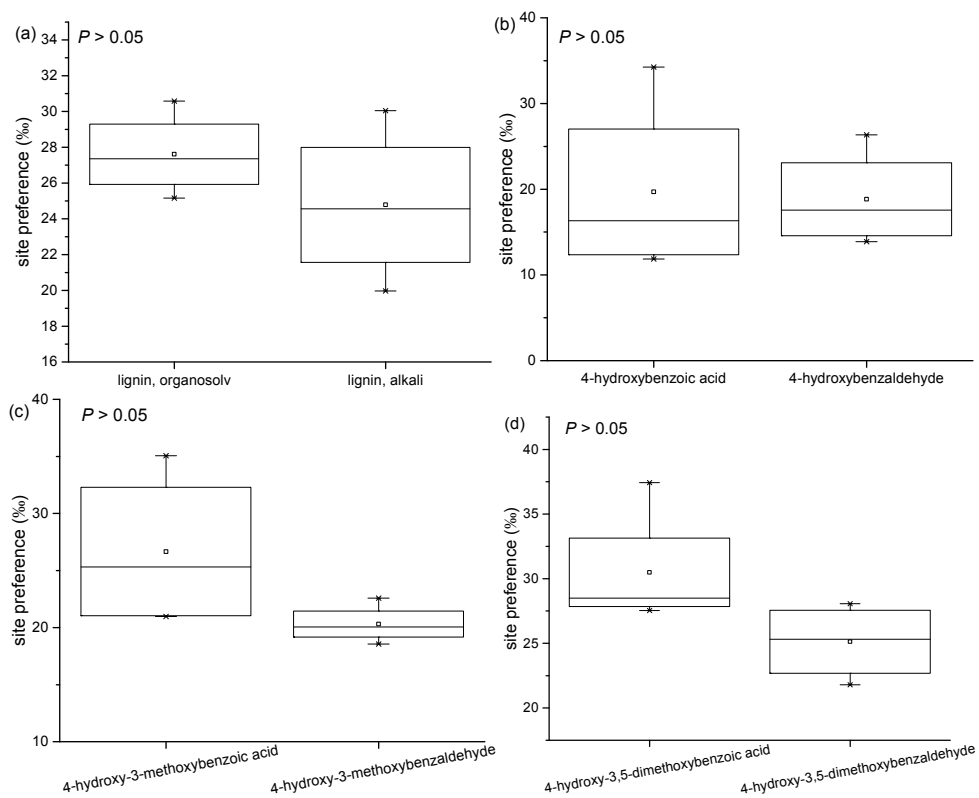


Fig. A6. Paired t test to compare the differences of site preference between organosolv and alkali lignin (a), 4-hydroxybenzoic acid and 4-hydroxybenzaldehyde (b), 4-hydroxy-3-methoxybenzoic acid and 4-hydroxy-3-methoxybenzaldehyde (c), and 4-hydroxy-3,5-dimethoxybenzoic acid and 4-hydroxy-3,5-dimethoxybenzaldehyde (d). The *box* indicates the range of the 25 and 75 percentiles of the data, *the line in the box* is the median, and the notch lines indicate the 1.5 interquartile rang.

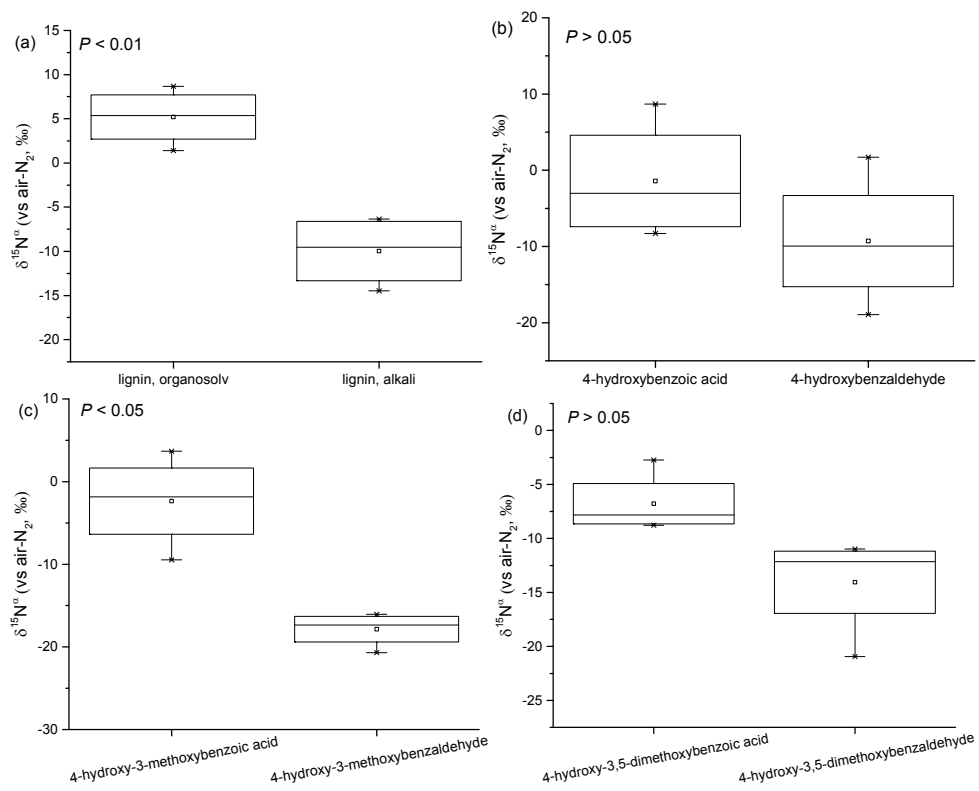


Fig. A7. Paired t test to compare the differences of $\delta^{15}\text{N}^{\alpha}$ between organosolv and alkali lignin (a), 4-hydroxybenzoic acid and 4-hydroxybenzaldehyde (b), 4-hydroxy-3-methoxybenzoic acid and 4-hydroxy-3-methoxybenzaldehyde (c), and 4-hydroxy-3,5-dimethoxybenzoic acid and 4-hydroxy-3,5-dimethoxybenzaldehyde (d). The *box* indicates the range of the 25 and 75 percentiles of the data, the *line in the box* is the median, and the notch lines indicate the 1.5 interquartile range.

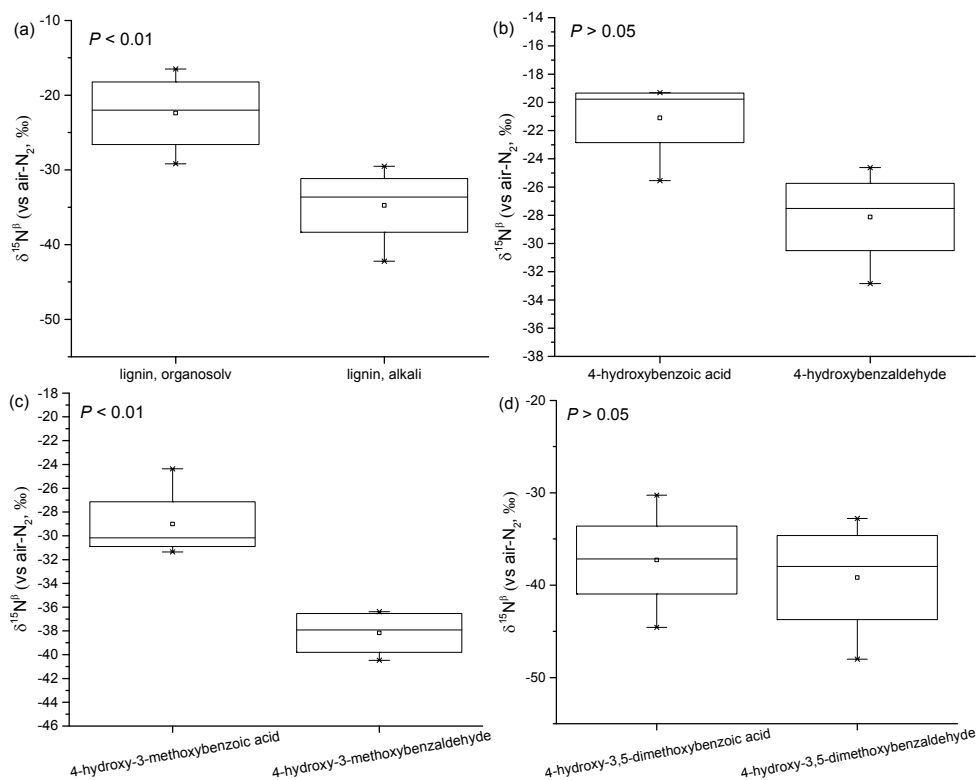


Fig. A8. Paired t test to compare the differences of $\delta^{15}\text{N}^{\beta}$ between organosolv and alkali lignin (a), 4-hydroxybenzoic acid and 4-hydroxybenzaldehyde (b), 4-hydroxy-3-methoxybenzoic acid and 4-hydroxy-3-methoxybenzaldehyde (c), and 4-hydroxy-3,5-dimethoxybenzoic acid and 4-hydroxy-3,5-dimethoxybenzaldehyde (d). The *box* indicates the range of the 25 and 75 percentiles of the data, the *line in the box* is the median, and the *notch lines* indicate the 1.5 interquartile range.

Table A1. Parameters of the mathematical equations for response surfaces of N₂O emission from NO₂⁻ reactions with lignin and lignin derivatives.

	pH	C _{nit}	pH×C _{nit}	pH ²	C _{nit} ²	pH ² ×C _{nit}	pH×C _{nit} ²	pH ³	R ² ^b	Adj R ² ^c	Pred R ² ^d
Lignin, organosolv ^a	-3.198	42.371	-13.849	-0.143	-16.108	1.140	3.179	-0.007	0.993	0.991	0.988
Lignin, alkali	-6.448	26.587	-7.850	-1.030	-7.8608	0.553	1.473	0.078	0.996	0.995	0.993
4-hydroxybenzoic acid	13.234	-26.819	8.586	1.836	35.277	-0.764	-4.897	-0.128	0.964	0.954	0.940
4-hydroxybenzaldehyde	-1.133	0.735	-1.363	-0.144	6.592	0.152	-1.048	0.010	0.994	0.992	0.989
4-hydroxy-3-methoxybenzoic acid	3.399	-2.853	-3.412	0.697	-11.796	0.171	2.433	-0.051	0.898	0.867	0.824
4-hydroxy-3-methoxybenzaldehyde	-5.847	4.048	-4.159	-0.927	-7.564	0.231	1.499	0.070	0.994	0.992	0.989
4-hydroxy-3,5-dimethoxybenzoic acid	1.883	-1.236	0.911	0.290	2.924	-0.083	-0.313	-0.022	0.920	0.897	0.864
4-hydroxy-3,5-dimethoxybenzaldehyde	-90.245	65.500	18.600	-14.989	59.240	-1.540	-11.82	1.095	0.913	0.887	0.853

Note:

^a the equation of response surface of N₂O emission from NO₂⁻ organosolv lignin reactions is $-3.198+1.750 \times \text{pH}+42.371 \times \text{C}_{\text{nit}}-13.849 \times \text{pH} \times \text{C}_{\text{nit}}-0.143 \times \text{pH}^2-16.108 \times \text{C}_{\text{nit}}^2+1.140 \times \text{pH}^2 \times \text{C}_{\text{nit}}+3.179 \times \text{pH} \times \text{C}_{\text{nit}}^2-0.007 \times \text{pH}^3$, the same for the other treatments;

^b R² is the measure of the amount of variation around the mean explained by the model;

^c Adj R², adjusted R², is the measure of the amount of variation around the mean explained by the model, adjusted for the number of terms in the model;

^d Pred R², predicted R², is the measure of the amount of variation in new data explained by the model.

Table A2. Parameters of the mathematical equations for response surface of CO₂ emission from NO₂⁻ reactions with lignin and lignin derivatives.

	pH	C _{nit}	pH × C _{nit}	pH ²	C _{nit} ²	pH ² × C _{nit}	pH × C _{nit} ²	pH ³	R ² ^b	Adj R ² ^c	Pred R ² ^d
Lignin, organosolv ^a	-41.052	180.986	-65.622	-6.367	-80.213	5.369	22.119	0.445	0.941	0.924	0.901
Lignin, alkali	14.126	159.322	-52.389	3.924	-86.575	4.240	19.585	-0.404	0.961	0.950	0.935
4-hydroxybenzoic acid	164.520	-81.194	79.490	33.200	46.607	-9.516	-19.868	-2.805	0.997	0.996	0.995
4-hydroxybenzaldehyde	70.773	45.007	-17.708	14.250	-47.851	1.415	14.138	-1.188	0.938	0.919	0.888
4-hydroxy-3-methoxybenzoic acid	369.321	-236.558	129.112	63.018	181.397	-12.309	-50.336	-4.975	0.994	0.992	0.990
4-hydroxy-3-methoxybenzaldehyde	58.665	42.887	-2.993	7.508	-102.676	-0.991	23.192	-0.505	0.951	0.936	0.916
4-hydroxy-3,5-dimethoxybenzoic acid	588.732	-403.204	233.658	92.646	200.220	-25.032	-60.745	-6.981	0.992	0.989	0.986
4-hydroxy-3,5-dimethoxybenzaldehyde	-310.732	341.728	-90.887	-49.432	-178.863	5.120	36.441	3.521	0.983	0.978	0.970

Note:

^a the equation of response surface of CO₂ emission from NO₂⁻-organosolv lignin reactions is $26.04 - 48.39 \times \text{pH} + 24.99 \times \text{C}_{\text{nit}} - 52.47 \times \text{pH} \times \text{C}_{\text{nit}} + 30.90 \times \text{pH}^2 + 14.48 \times \text{C}_{\text{nit}}^2 + 25.41 \times \text{pH}^2 \times \text{C}_{\text{nit}} - 4.11 \times \text{pH} \times \text{C}_{\text{nit}}^2 - 5.33 \times \text{pH}^3$, the same for the other treatments;

^b R² is the measure of the amount of variation around the mean explained by the model;

^c Adj R², adjusted R², is the measure of the amount of variation around the mean explained by the model, adjusted for the number of terms in the model;

^d Pred R², predicted R², is the measure of the amount of variation in new data explained by the model.

Appendix B: supplementary information for chapter III

Methods

Simultaneous analysis of N₂O and NO_x emissions: A dual quantum cascade laser trace gas monitor (QCLAS, DUAL CWRT-QC-TILDAS-76, Aerodyne Research, Inc., Billerica, MA, USA) coupled with a chemoluminescence analyzer (CLD, AC32 M, Ansyco GmbH, Karlsruhe, Germany) was used to simultaneously measure the N₂O and NO_x emissions (Wei et al., 2017a). In the respective experiments, 0.5 g of lignin or 0.3 mmol of lignin derivatives was placed into a 100-mL beaker in a 2 L of reaction chamber. Then 3 L min⁻¹ of synthetic air (20% oxygen and 80% nitrogen) was used to purge the system till both N₂O and NO_x signals decreased under 0.1 ppb. Finally, 100 mL of 1 mM NaNO₂ (VWR, Germany) solution was injected into the reaction beaker. The headspace of the reaction chamber was continuously flushed with 3 L min⁻¹ of synthetic air, and the mixing ratios of NO_x and N₂O were recorded with 5 s and 1 s temporal resolution, respectively.

Results

Table B1 Characteristics of the soil samples. The indicated precision is the standard deviation for replicate sample measurements (n = 3).

Soil sample	Soil pH	Total N (%)	Total C (%)	C/N	WHC (%)
Forest soil	3.56 ± 0.00	1.46 ± 0.00	30.1 ± 0.8	20.6 ± 0.6	137.0 ± 0.1
Grassland soil	5.13 ± 0.00	1.28 ± 0.01	4.62 ± 0.02	3.6 ± 0.1	80.0 ± 1.2
Agricultural soil	6.03 ± 0.15	0.14 ± 0.01	1.28 ± 0.01	9.1 ± 0.2	35.0 ± 4.2

Table B2. Experimental details for individual treatments.

Lignin derivative/soil sample	Lignin derivative/soil (g)	NO ₂ ⁻ (g)	Water (ml)	Flow rate (ml min ⁻¹)
organosolv lignin	5.0	0.02	50	16
4-hydroxybenzoic acid	8.0	1.70	50	16
4-hydroxy-3-methoxybenzoic acid	10.0	2.00	50	16
4-hydroxy-3,5-dimethoxybenzoic acid	8.0	2.37	50	16
4-hydroxy-3-methoxybenzaldehyde	25.7	6.07	50	14
4-hydroxy-3,5-dimethoxybenzaldehyde	6.2	5.00	50	16
forest soil	10.0	1.61	50	16
grassland soil	10.0	1.50	50	16
agricultural soil	10.0	1.70	50	16

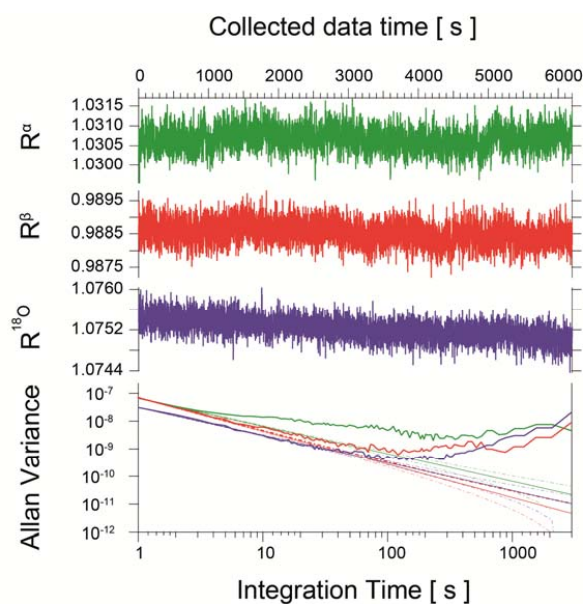


Fig. B1. Allan variance plot for N₂O isotopologue ratios R^α (green lines), R^β (red lines) and R^{18O} (purple lines) at 35 ppm of N₂O mixing ratio. R^α, R^β, and R^{18O} correspond to ¹⁴N¹⁵N¹⁶O / ¹⁴N¹⁴N¹⁶O, ¹⁵N¹⁴N¹⁶O / ¹⁴N¹⁴N¹⁶O and ¹⁴N¹⁴N¹⁸O / ¹⁴N¹⁴N¹⁶O, respectively.

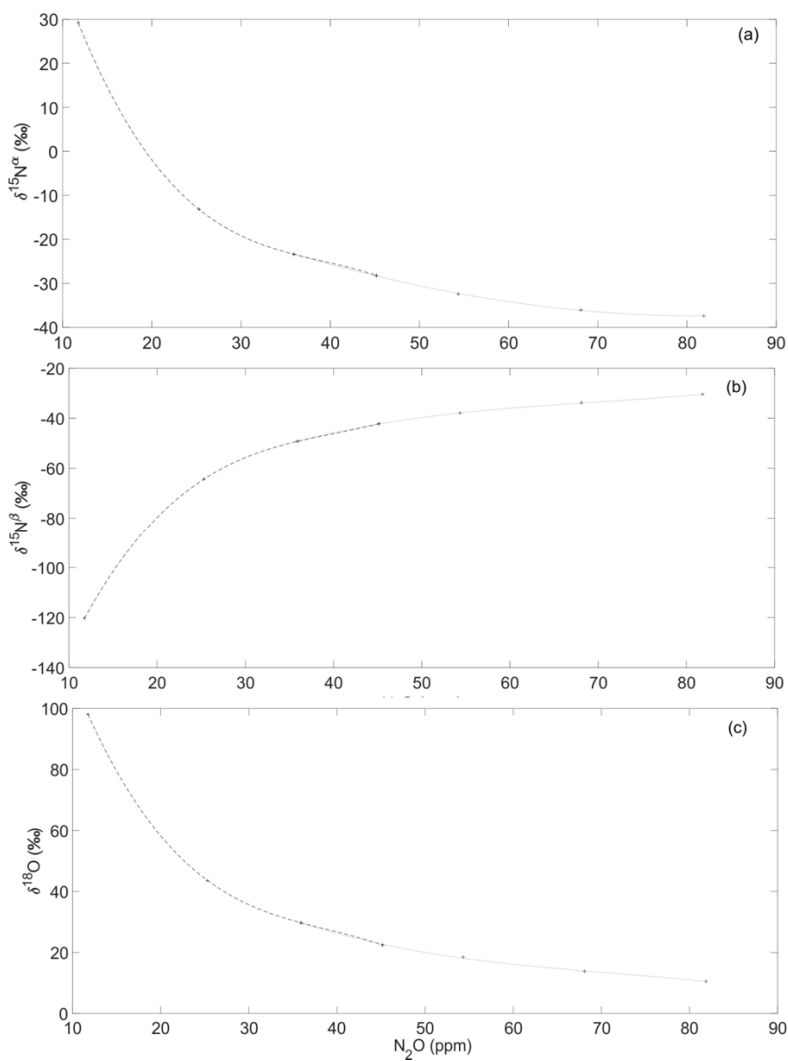


Fig. B2. Stepwise regression of $\delta^{15}N^\alpha$ vs N_2O concentration (a), $\delta^{15}N^\beta$ vs N_2O concentration (b), and $\delta^{18}O$ vs N_2O concentration (c) for 12 to 45 ppm N_2O (dashed line) and 36 to 82 ppm N_2O (dotted line). The R^2 values were higher than 0.99 for all the f_{low} and f_{high} .

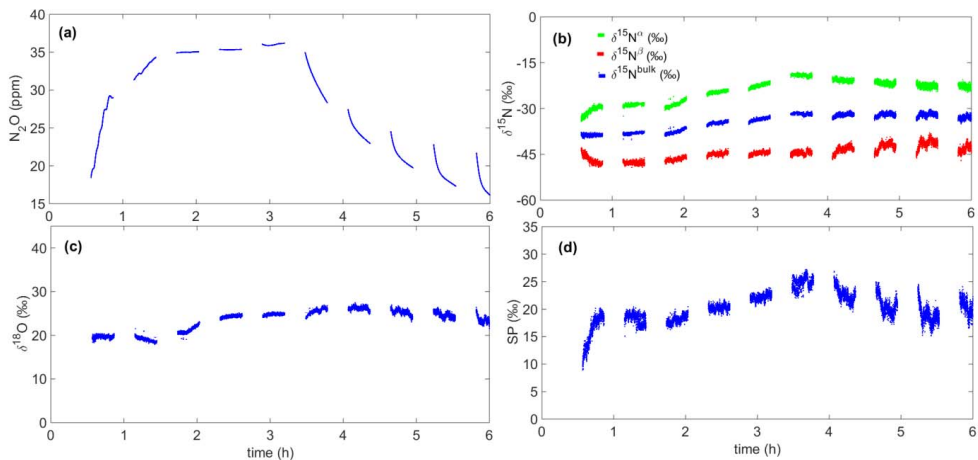


Fig. B3. Reaction of NO_2^- with 4-hydroxybenzoic acid. (a) N_2O mixing ratio, (b) $\delta^{15}\text{N}^\alpha$, $\delta^{15}\text{N}^\beta$, and $\delta^{15}\text{N}^{\text{bulk}}$ of N_2O , (c) $\delta^{18}\text{O}$ of N_2O , and (d) ^{15}N site preference of N_2O .

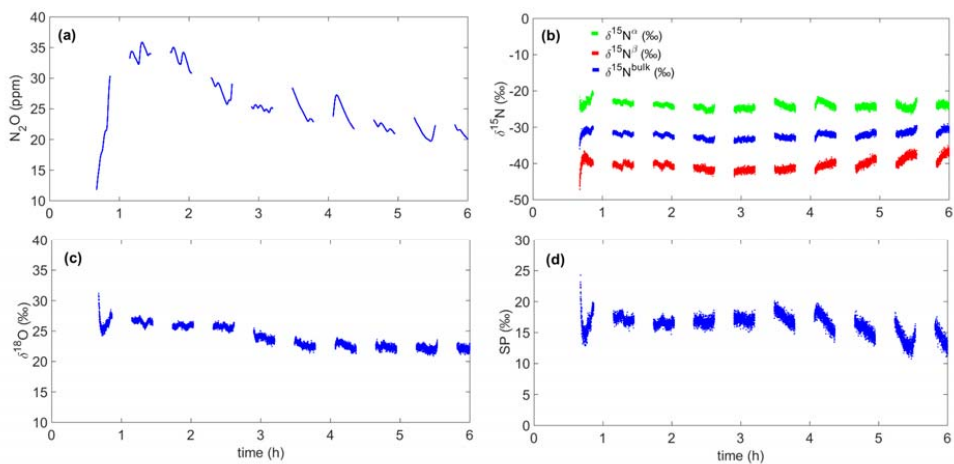


Fig. B4. Reaction of NO_2^- with 4-hydroxy-3-methoxybenzoic acid. (a) N_2O mixing ratio, (b) $\delta^{15}\text{N}^\alpha$, $\delta^{15}\text{N}^\beta$, and $\delta^{15}\text{N}^{\text{bulk}}$ of N_2O , (c) $\delta^{18}\text{O}$ of N_2O , and (d) ^{15}N site preference of N_2O .

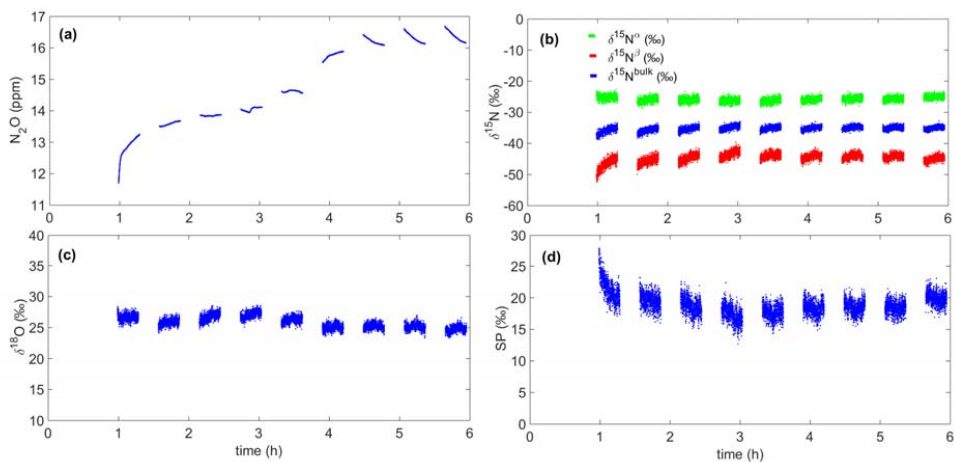


Fig. B5. Reaction of NO_2^- with 4-hydroxy-3-methoxybenzaldehyde. (a) N_2O mixing ratio, (b) $\delta^{15}\text{N}^\alpha$, $\delta^{15}\text{N}^\beta$, and $\delta^{15}\text{N}^{\text{bulk}}$ of N_2O , (c) $\delta^{18}\text{O}$ of N_2O , and (d) ^{15}N site preference of N_2O .

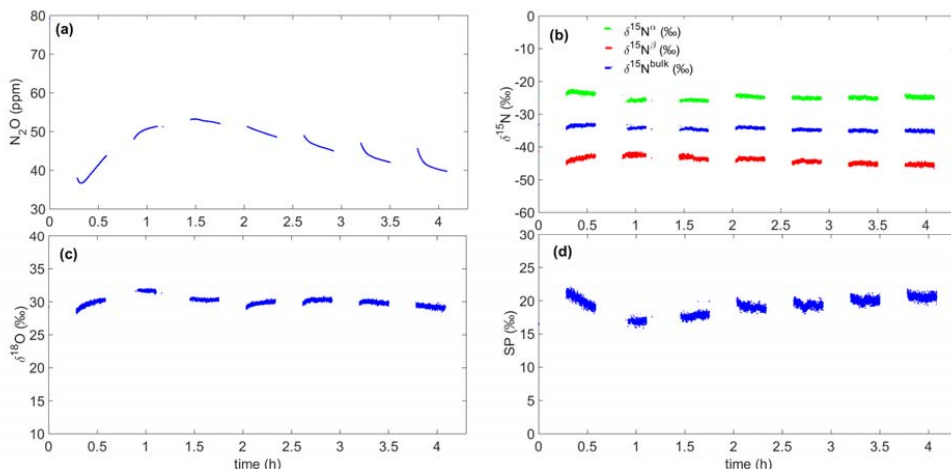


Fig. B6. N_2O emission and its isotopic composition in forest soil after NO_2^- application. (a) N_2O mixing ratio, (b) $\delta^{15}\text{N}^\alpha$, $\delta^{15}\text{N}^\beta$, and $\delta^{15}\text{N}^{\text{bulk}}$ of N_2O , (c) $\delta^{18}\text{O}$ of N_2O , and (d) ^{15}N site preference of N_2O .

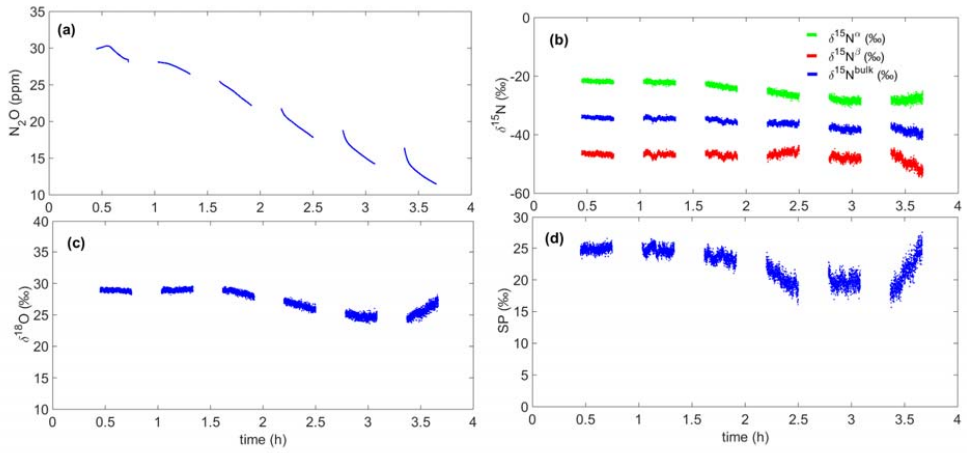


Fig. B7. N₂O emission and its isotopic composition in agricultural soil after NO₂⁻ application. (a) N₂O mixing ratio, (b) δ¹⁵N^α, δ¹⁵N^β, and δ¹⁵N^{bulk} of N₂O, (c) δ¹⁸O of N₂O, and (d) ¹⁵N site preference of N₂O.

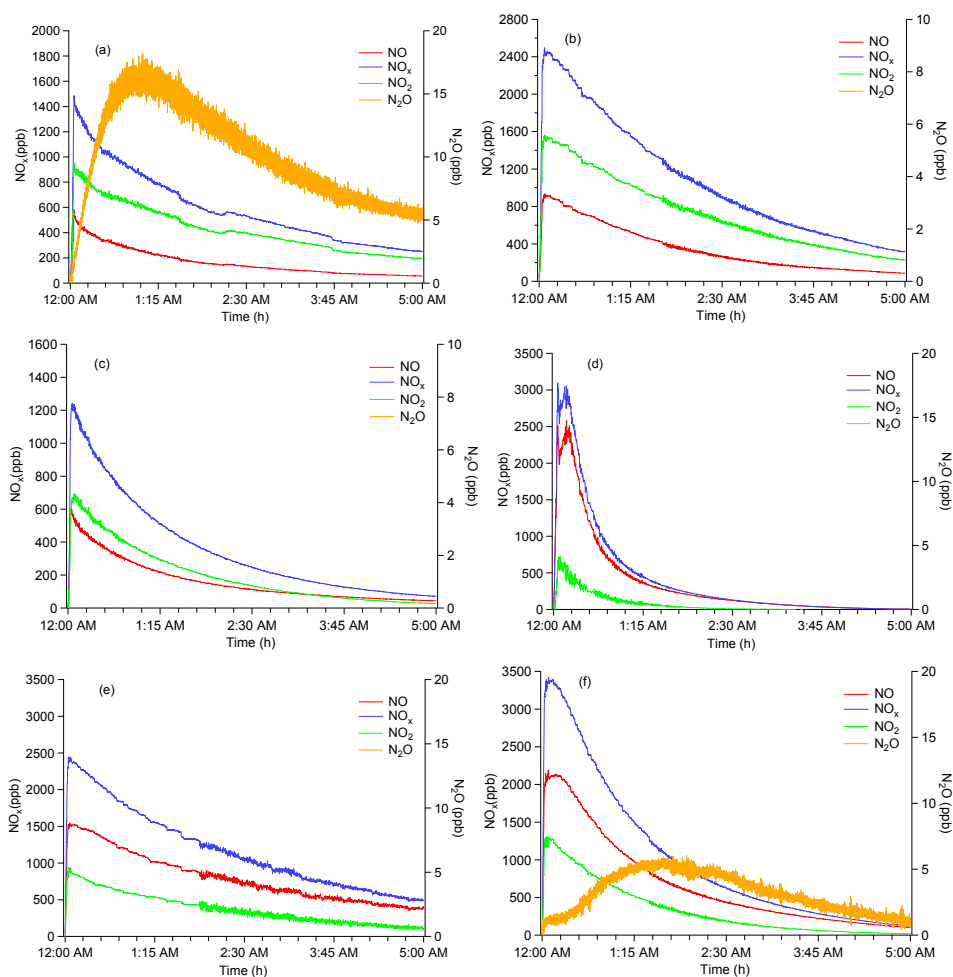


Fig. B8. NO_x (NO and NO₂) and N₂O emissions from the reactions of NO₂⁻ with organosolv lignin (a), 4-hydroxybenzoic acid (b), 4-hydroxy-3-methoxybenzoic acid (c), 4-hydroxy-3,5-dimethoxybenzoic acid (d), 4-hydroxy-3-methoxybenzaldehyde (e), 4-hydroxy-3,5-dimethoxybenzaldehyde (f). Sodium nitrite solution was injected into the reaction chamber at 12:00 AM. The N₂O signal of 4-hydroxybenzoic acid, 4-hydroxy-3-methoxybenzoic acid, 4-hydroxy-3,5-dimethoxybenzoic acid, and 4-hydroxy-3-methoxybenzaldehyde treatments was below the detection limit of 0.1 ppb.

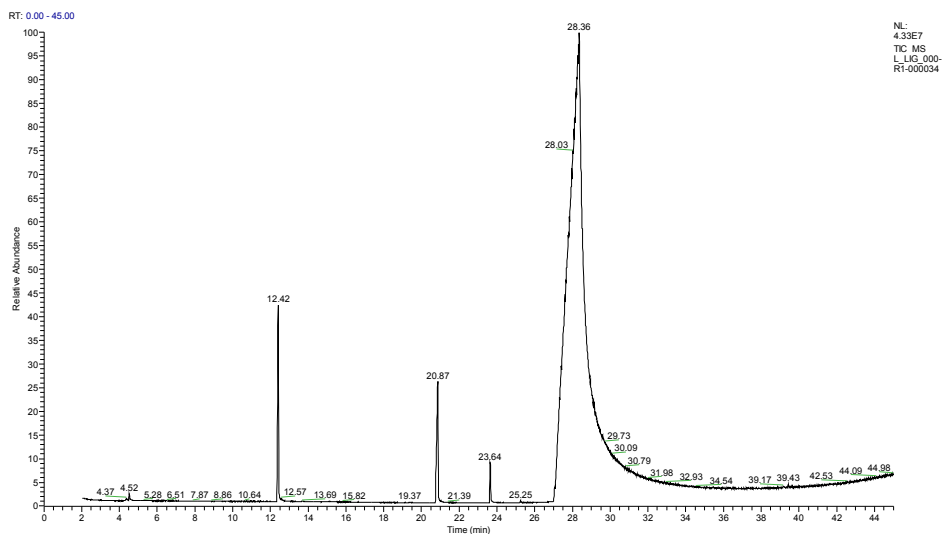


Fig. B9. Gas chromatography–mass spectrometry spectrum of the products from the reaction of NO_2^- with 4-hydroxy-3-methoxybenzoic acid. Three main products including 2-methoxyphenol (retention time: 12.42 min), vanillin (retention time: 20.87 min), and methyl vanillate (retention time: 23.64 min) were detected. The broad peak between 27–32 min denotes the reactant 4-hydroxy-3-dimethoxybenzoic acid.

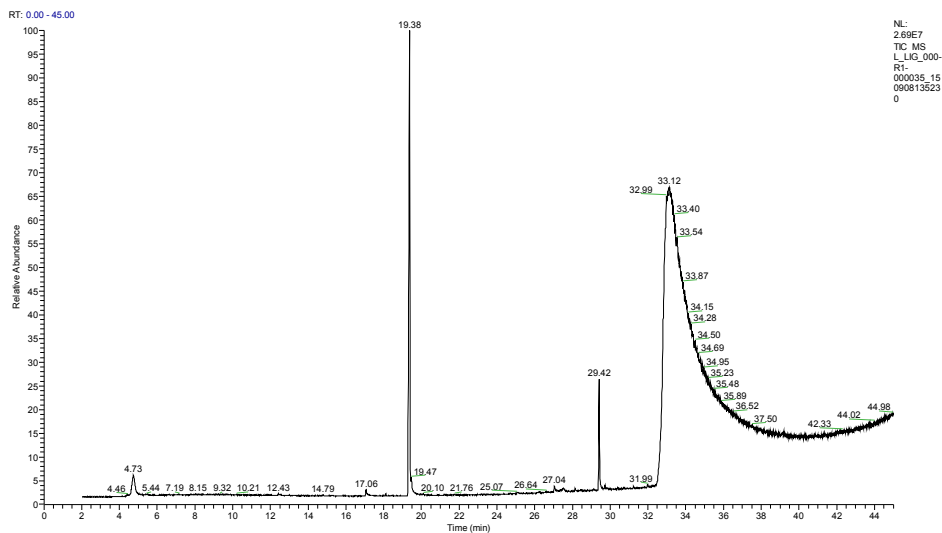


Fig. B10. Gas chromatography–mass spectrometry spectrum of the products from the reaction of NO_2^- with 4-hydroxy-3,5-dimethoxybenzoic acid. Two main products including 2,6-dimethoxyphenol (retention time: 19.38 min) and 4-hydroxy-3,5-dimethoxybenzohydrazide (retention time: 29.42 min) were detected. The broad peak between 32–36 min denotes the reactant 4-hydroxy-3,5-dimethoxybenzoic acid.

Appendix C: supplementary information for chapter IV

CO₂ emission

The CO₂ peak was identified at first 15 min in both sterilized and unsterilized soils, and disappeared quickly. There were no significant differences between sterilized and unsterilized treatments, as well as among soils from different sampling sites. Therefore, this CO₂ peak should originate from the physical release of CO₂ accumulated in soil pores. This suggests that at least a part of CO₂ emission from the Birch effect could be related to former physical entrapment.

NO_x and N₂O emission

The NO_x emission was calculated by integrating the NO_x concentration time curves obtained by CLD based on the ideal gas law:

$$E = \int_0^t \left(\frac{101325 \times F \times M}{8.314 \times T \times 1000 \times m} \right) \frac{dc}{dt} \quad (C1)$$

E —total NO_x emission in three hours, ng N·g⁻¹ soil; T —operating temperature, 293.15 K; F —flow rate, 3 L·min⁻¹; c —real-time NO_x concentration, ppb; t —the total time for measurement, 180 min for soil samples and 120 min for SOM fractions; M —molar weight of N, 14 g·mole⁻¹; m —weight of soil samples, 5 g.

The N₂O emission was calculated according to the accumulated N₂O concentration obtained by GC-ECD based on the ideal gas law:

$$E = \frac{101325 \times C \times V \times M \times 2}{8.314 \times T \times 1000 \times m} \quad (C2)$$

E —total N₂O emission in three hours, ng N·g⁻¹ soil; T —operating temperature, 293.15 K; C —N₂O concentration, ppb; V —volume of the glass bottle for incubation, 1 L; M —molar weight of N, 14 g·mole⁻¹; m —weight of soil samples, 5 g.

Table C1. Characteristics of five soil samples from the Wüstebach test sites

Sampling sites	Soil pH	NH ₄ ⁺ (µg g ⁻¹)	NO ₃ ⁻ (µg g ⁻¹)	Fe (mg g ⁻¹)	Mn (µg g ⁻¹)	Al (mg g ⁻¹)	P (mg g ⁻¹)	TOC ^a (%)	TN ^b (%)
Subsite 1	2.9 ± 0.0	19.2 ± 0.7	8.9 ± 0.4	13.3 ± 0.1	92 ± 3	14.5 ± 0.2	1.09 ± 0.02	38.5 ± 0.1	1.77 ± 0.01
Subsite 2	3.4 ± 0.0	15.1 ± 0.6	6.5 ± 0.4	25.9 ± 0.4	2130 ± 50	41.6 ± 0.4	1.64 ± 0.02	22.7 ± 0.7	0.98 ± 0.03
Subsite 3	2.9 ± 0.0	40.8 ± 1.8	6.8 ± 0.3	16.3 ± 0.2	217 ± 5	25.0 ± 0.4	0.98 ± 0.02	30.1 ± 0.8	1.46 ± 0.00
Subsite 4	3.3 ± 0.0	20.5 ± 0.5	2.9 ± 0.1	20.7 ± 0.3	400 ± 6	34.8 ± 0.6	1.57 ± 0.02	24.1 ± 0.1	1.49 ± 0.01
Subsite 5	3.2 ± 0.0	23.4 ± 0.3	5.7 ± 0.4	24.5 ± 0.3	220 ± 10	39.8 ± 0.4	1.19 ± 0.02	18.9 ± 0.4	1.04 ± 0.04

Note:

^a TOC, total organic carbon;^b TN, total nitrogen;^c each value is presented as the mean value of three replicates ± standard deviation.**Table C2.** Fitting results of Hill equation

Sampling sites	NO _{x,max} ^a (ng N g ⁻¹ soil)	NO _{x,t_{1/2}^b (min)}	NO _{x,n}	N ₂ O _{max} ^c (ng N g ⁻¹ soil)	N ₂ O-t _{1/2} ^d (min)	N ₂ O-n	
Subsite 1	unsterilized	1355.9 ± 8.8	12.9 ± 0.2	1.21	294.0 ± 34.5	76.6 ± 18.3	1.07
	sterilized	1306.7 ± 30.7	6.4 ± 0.4	2.08	110.4 ± 9.8	52.5 ± 9.5	0.93
Subsite 2	unsterilized	2052.2 ± 15.9	20.0 ± 0.3	1.39	435.0 ± 18.8	82.5 ± 5.2	1.52
	sterilized	2040.0 ± 14.9	18.3 ± 0.3	1.41	184.0 ± 5.4	71.4 ± 3.6	1.31
Subsite 3	unsterilized	1190.7 ± 3.2	4.7 ± 0.0	1.94	233.7 ± 22.5	30.8 ± 1.3	1.43
	sterilized	1187.7 ± 108.0	3.7 ± 0.6	2.49	65.9 ± 5.8	29.4 ± 6.2	1.23
Subsite 4	unsterilized	3238.2 ± 7.9	8.6 ± 0.1	1.48	499.0 ± 38.1	43.4 ± 5.7	1.18
	sterilized	3613.1 ± 65.5	7.3 ± 0.3	1.75	134.6 ± 5.3	45.4 ± 4.3	1.00
Subsite 5	unsterilized	2011.2 ± 10.8	16.1 ± 0.2	1.58	258.7 ± 19.0	80.7 ± 6.1	1.53
	sterilized	1882.7 ± 139.0	11.0 ± 1.2	1.79	70.0 ± 2.5	53.5 ± 3.0	1.55
DOM ^e	4048.8 ± 58.7	62.2 ± 1.7	–	–	–	1.07	
FA ^f	2290.2 ± 23.6	19.9 ± 0.4	1.58	80.3 ± 3.3	142.7 ± 2.9	1.21	
HA ^g	3054.9 ± 18.8	6.9 ± 0.1	0.47	35.9 ± 7.9	43.7 ± 2.2	1.96	
HN ^h	1154.4 ± 6.2	5.8 ± 0.1	1.36	9.7 ± 0.3	26.2 ± 4.9	2.28	

Note:

^a NO_{x,max} is the maximum NO_x emission estimated from the Hill equation fit;^b NO_{x,t_{1/2}} is the time needed to reach half of NO_{x,max};^c N₂O_{max} is the maximum N₂O emission estimated from the Hill equation fit;^d N₂O-t_{1/2} is the time needed to reach half of the total N₂O emission;^e DOM, dissolved organic matter fraction;^f FA, fulvic acid fraction;^g HA, humic acid fraction;^h HN, humin fraction.

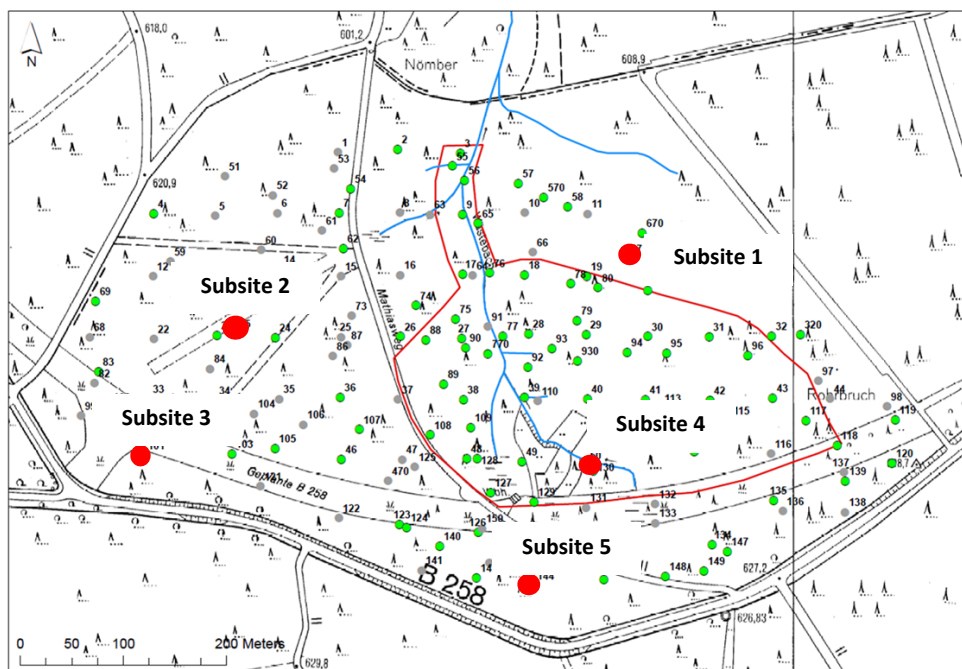


Fig. C1. Sampling sites of Wüstebach catchment. The blue line is the river, the five sampling sites are labelled with red dots.

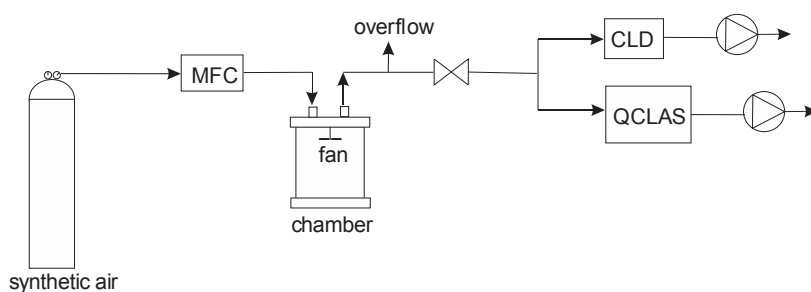


Fig.C2. Schematic diagram of the QCLAS-CLD system for the real-time determination of N_2O and NO_x emission from soils induced by NO_2^- .

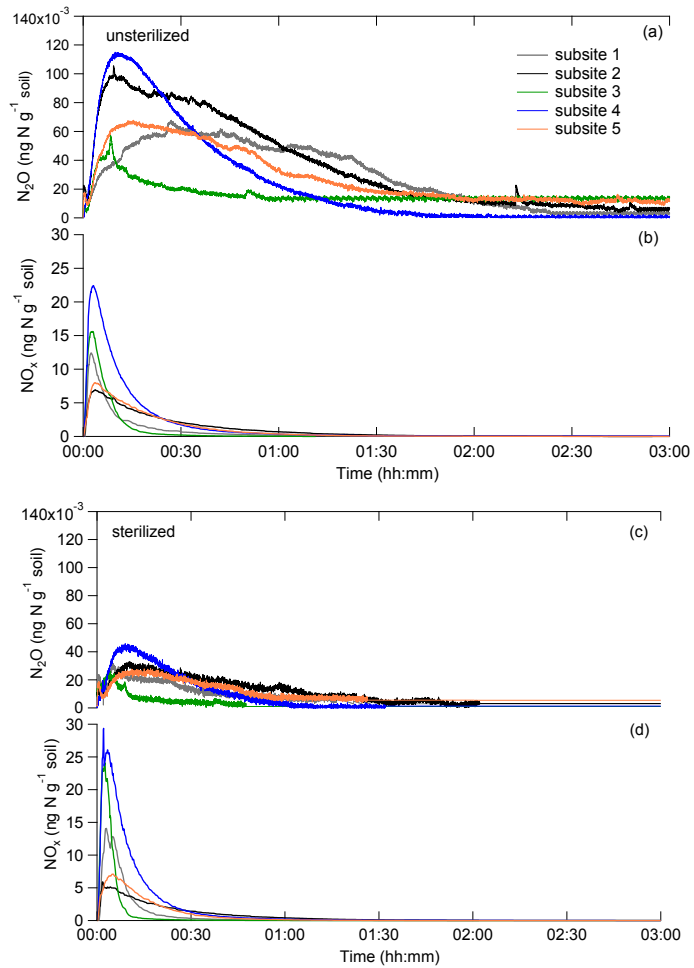


Fig. C3. The real-time measurement of N_2O and NO_x emissions from unsterilized (a, b) and sterilized (c, d) soils.

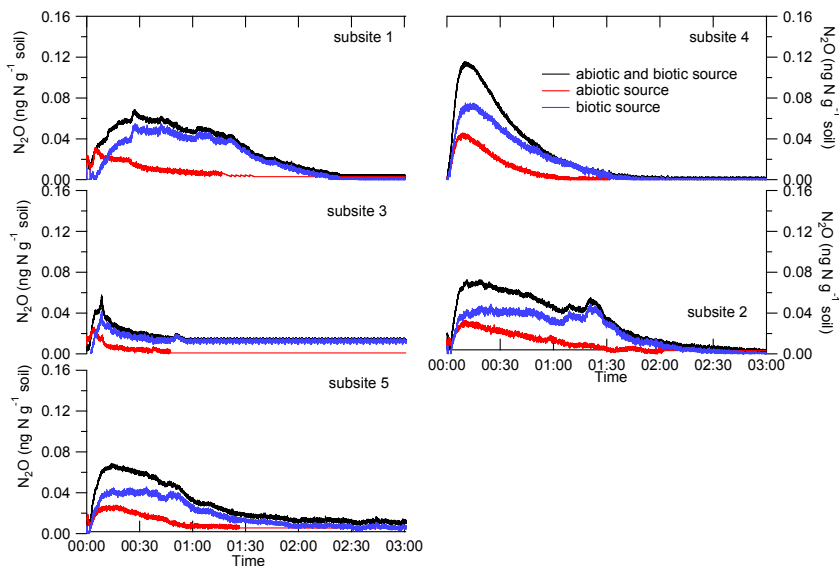


Fig. C4. Real-time N_2O emission from biotic and abiotic sources. The biotic N_2O mixing ratio at each time point was calculated by the N_2O mixing ratio from unsterilized soil minus the N_2O mixing ratio from its corresponding sterilized soil at the same time point.

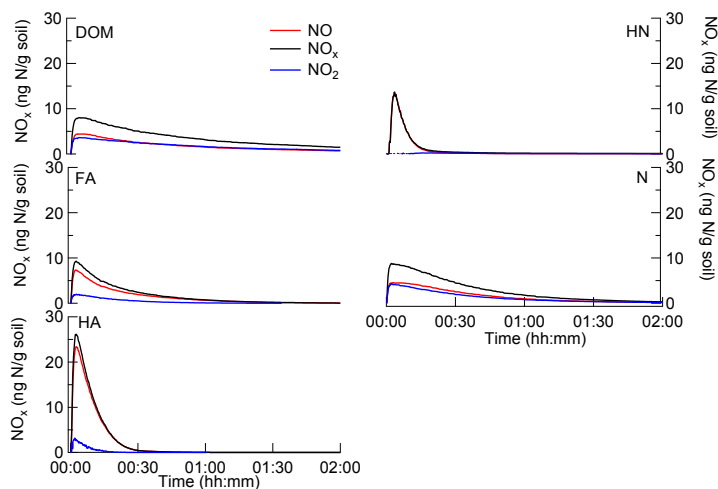


Fig. C5. NO_x emission from different soil organic matter fractions measured in real-time. DOM, dissolved organic matter fraction; FA, fulvic acid fraction; HA, humic acid fraction; HN, humin fraction; N, control treatment of 0.25 M NO_2^- solution at pH 3.4.

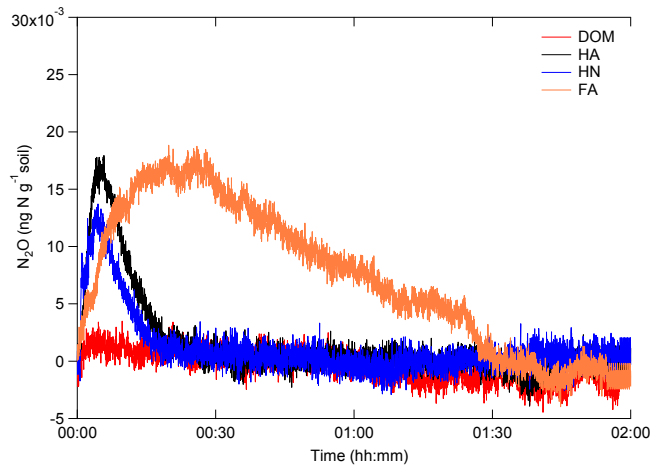


Fig. C6. N_2O emission from the different soil organic matter fractions measured in real-time. DOM, dissolved organic matter fraction; FA, fulvic acid fraction; HA, humic acid fraction; HN, humin fraction.

Appendix D: supplementary information for chapter VI

Table D1. Pearson Correlations among total CO₂ and N₂O emission rates, fertilizer-derived N₂O emission rate, δ¹⁵N-N₂O, and δ¹⁸O-N₂O (n = 141).

	Total CO ₂ flux	Total N ₂ O flux	δ ¹⁵ N-N ₂ O	δ ¹⁸ O-N ₂ O
Total N ₂ O flux	0.47**			
δ ¹⁵ N-N ₂ O	0.31**	-0.01		
δ ¹⁸ O-N ₂ O	0.08	-0.29**	0.82**	
Fertilizer-N ₂ O flux	0.67**	0.81**	0.28**	-0.14

Note:

** Significantly correlated at $P < 0.01$.

Table D2. Pearson Correlations among total N₂O, NH₄⁺, and NO₃⁻, and fertilizer-derived N₂O, NH₄⁺, and NO₃⁻ in soils (n = 90).

	Total NH ₄ ⁺	Fertilizer-NH ₄ ⁺	Total NO ₃ ⁻	Fertilizer-NO ₃ ⁻	Total N ₂ O
Fertilizer-NH ₄ ⁺	0.98**				
Total NO ₃ ⁻	-0.24*	-0.55**			
Fertilizer-NO ₃ ⁻	-0.69**	-0.70**	0.86**		
Total N ₂ O	0.88**	0.90**	-0.53**	-0.66**	
Fertilizer-N ₂ O	0.86**	0.86**	-0.64**	-0.71**	0.94**

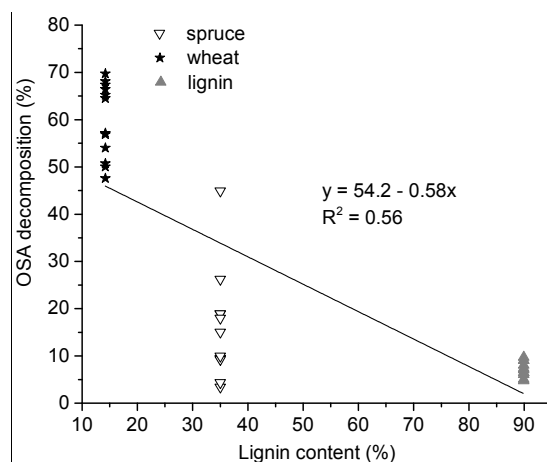
Note:

* Significantly correlated at $P < 0.05$;

** Significantly correlated at $P < 0.01$.

Table D3. Decomposition of organic soil amendment (OSA), total fertilizer-N in OSA, immobilized fertilizer-N in OSA, and immobilized/total fertilizer-N in OSA.

	Date (d)	OSA decomposition (%)	Total fertilizer-N in OSA (μg)	Immobilized fertilizer-N in OSA (μg)	Immobilized/total fertilizer-N in OSA (%)
Spruce	8	2.3 \pm 0.4	242.6 \pm 22.0	116.5 \pm 18.1	48.7 \pm 11.1
	22	3.7 \pm 0.6	301.4 \pm 22.9	175.5 \pm 23.8	58.4 \pm 8.8
	50	9.6 \pm 0.4	528.5 \pm 11.0	316.0 \pm 39.6	59.7 \pm 6.2
	78	17.6 \pm 2.2	703.1 \pm 110.5	475.9 \pm 95.4	67.4 \pm 2.8
	114	29.7 \pm 13.8	827.7 \pm 242.1	515.1 \pm 205.6	61.3 \pm 15.0
Wheat	8	39.7 \pm 1.8	1134.7 \pm 52.4	675.3 \pm 63.1	59.5 \pm 4.9
	22	49.2 \pm 1.6	1457.5 \pm 86.1	1034.8 \pm 89.9	71.0 \pm 3.9
	50	55.8 \pm 1.7	1241.1 \pm 103.9	1035.4 \pm 53.3	83.7 \pm 6.2
	78	65.9 \pm 1.4	1087.6 \pm 102.4	907.8 \pm 143.5	83.2 \pm 5.7
	114	67.5 \pm 2.3	1219.2 \pm 76.9	1065.4 \pm 54.5	87.4 \pm 1.7
Lignin	8	2.1 \pm 1.2	109.2 \pm 20.0	28.1 \pm 3.6	25.9 \pm 1.4
	22	8.6 \pm 0.6	77.4 \pm 8.9	37.2 \pm 3.4	48.3 \pm 4.0
	50	5.9 \pm 1.2	107.7 \pm 26.8	41.9 \pm 9.8	39.1 \pm 3.9
	78	7.0 \pm 1.6	107.2 \pm 10.9	33.2 \pm 2.6	31.1 \pm 0.9
	114	7.3 \pm 2.3	117.4 \pm 25.0	29.8 \pm 4.2	25.8 \pm 3.1

**Fig. D1.** Effect of lignin content on organic soil amendment (OSA) decomposition (n = 36).

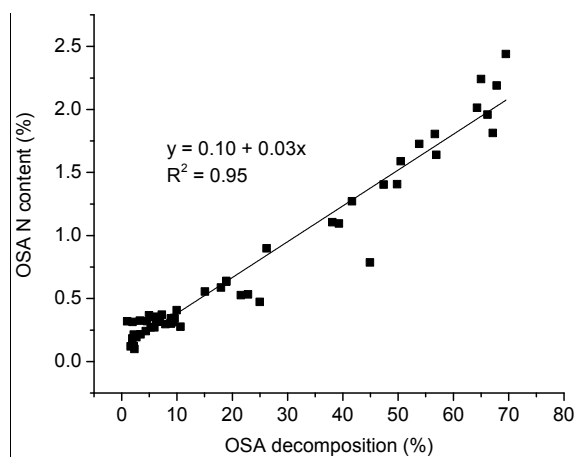


Fig. D2. Linear regression of organic soil amendment (OSA) N content based on OSA decomposition (n = 36).

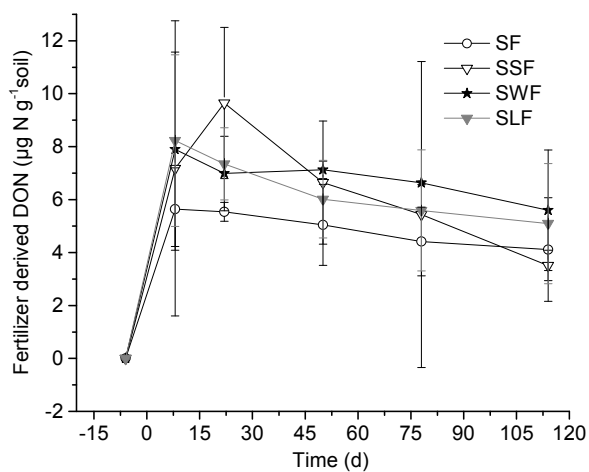


Fig. D3. Concentration of fertilizer-derived DON in different treatments during the experiment. Nitrogen fertilizer was applied at day 0.

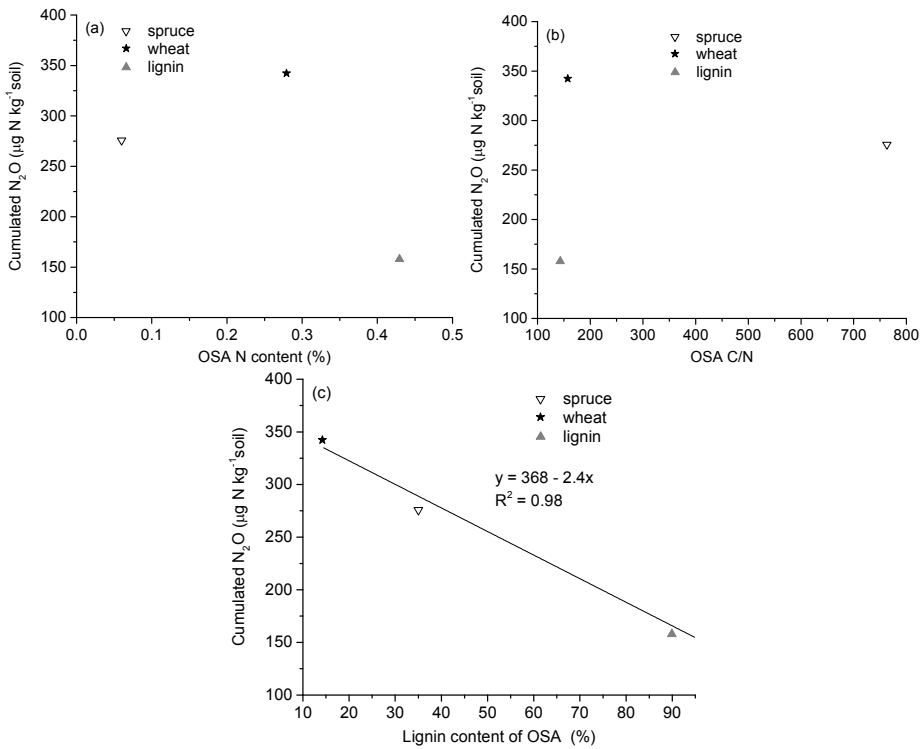


Fig. D4. Effect of N content, C/N ratio, and lignin content of organic soil amendment (OSA) on cumulated N_2O emission.

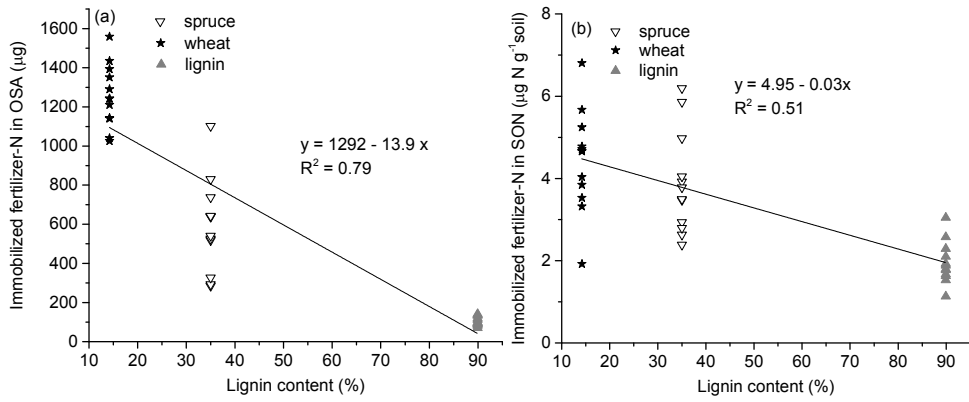


Fig. D5. Effect of lignin content on N immobilization in organic soil amendment (OSA) and soil ($n = 36$).

References

- Abe, T., Maie, N., and Watanabe, A. (2005). Investigation of humic acid N with X-ray photoelectron spectroscopy: Effect of acid hydrolysis and comparison with N-15 cross polarization/magic angle spinning nuclear magnetic resonance spectroscopy. *Organic Geochemistry* 36, 1490-1497.
- Abeliovich, A. (2006). The nitrite oxidizing bacteria. In *The prokaryotes: Volume 5: Proteobacteria: Alpha and beta subclasses*, M. Dworkin, S. Falkow, E. Rosenberg, K.H. Schleifer, and E. Stackebrandt, eds. (New York, NY: Springer New York), pp. 861-872.
- Allison, F.E. (1963). Losses of gaseous nitrogen from soils by chemical mechanisms involving nitrous acid and nitrites. *Soil Science* 96, 404-409.
- Alves, R.J.E., Wanek, W., Zappe, A., Richter, A., Svenning, M.M., Schleper, C., and Urich, T. (2013). Nitrification rates in arctic soils are associated with functionally distinct populations of ammonia-oxidizing archaea. *The ISME Journal* 7, 1620-1631.
- Amelung, W., Zech, W., and Flach, K.W. (1997). Climatic effects on soil organic matter composition in the great plains. *Soil Science Society of America Journal* 61, 115-123.
- Austin, A.T. (1961). Nitrosation in organic chemistry. *Science in Progress XLIX*, 619-640.
- Azhar, E.S., Verhe, R., Proot, M., Sandra, P., and Verstraete, W. (1989). Fixation of nitrite nitrogen during the humification of alpha-naphthol in soil suspensions. *Journal of Agricultural and Food Chemistry* 37, 262-266.
- Baehrle, C., Nick, T.U., Bennati, M., Jeschke, G., and Vogel, F. (2015). High-field electron paramagnetic resonance and density functional theory study of stable organic radicals in lignin: Influence of the extraction process, botanical origin, and protonation reactions on the radical *g* tensor. *Journal of Physical Chemistry A* 119, 6475-6482.
- Baggs, E.M., Watson, C.A., and Rees, R.M. (2000). The fate of nitrogen from incorporated cover crop and green manure residues. *Nutrient Cycling in Agroecosystems* 56, 153-163.
- Bahri, H., Dignac, M.F., Rumpel, C., Rasse, D.P., Chenu, C., and Mariotti, A. (2006). Lignin turnover kinetics in an agricultural soil is monomer specific. *Soil Biology and Biochemistry* 38, 1977-1988.
- Bahri, H., Rasse, D.P., Rumpel, C., Dignac, M.F., Bardoux, G., and Mariotti, A. (2008). Lignin degradation during a laboratory incubation followed by ¹³C isotope analysis. *Soil Biology and Biochemistry* 40, 1916-1922.
- Bateman, E.J., Cadisch, G., and Baggs, E.M. (2004). Soil water content as a factor that controls N₂O production by denitrification and autotrophic and heterotrophic nitrification. In *Controlling nitrogen flows and losses*, Hatch, D.J., Chadwick, D.R., Jarvis, S.C., and Roker, J.A. eds. Wageningen Academic Publishers, Wageningen, The Netherlands, 290-291.

- Baur, S.I., and Easteal, A.J. (2014). ESR studies on the free radical generation in wood by irradiation with selected sources from UV to IR wavelength regions. *Holzforschung* 68, 775-780.
- Beaudoin, D., and Wuest, J.D. (2016). Dimerization of aromatic C-nitroso compounds. *Chemical Reviews* 116, 258-286.
- Blesh, J., and Drinkwater, L.E. (2014). Retention of N-15-labeled fertilizer in an illinois prairie soil with winter rye. *Soil Science Society of America Journal* 78, 496-508.
- Bol, R., Toyoda, S., Yamulki, S., Hawkins, J.M.B., Cardenas, L.M., and Yoshida, N. (2003). Dual isotope and isotopomer ratios of N₂O emitted from a temperate grassland soil after fertiliser application. *Rapid Communications in Mass Spectrometry* 17, 2550-2556.
- Bollag, J.M., and Henninger, N.M. (1978). Effects of nitrite toxicity on soil bacteria under aerobic and anaerobic conditions. *Soil Biology and Biochemistry* 10, 377-381.
- Bosatta, E., and ÅGren, G.I. (1995). Theoretical analyses of interactions between inorganic nitrogen and soil organic matter. *European Journal of Soil Science* 46, 109-114.
- Bremner, J.M., and Führ, F. (1966). Tracer studies of the reaction of soil organic matter with nitrite. *Kernforschungsanlage Jülich, Verlag Jülich*, 388, 10.
- Bringas, M., Semelak, J., Zeida, A., and Estrin, D.A. (2016). Theoretical investigation of the mechanism of nitroxyl decomposition in aqueous solution. *Journal of Inorganic Biochemistry* 162, 102-108.
- Broadbent, F.E.B., W. D.; Nakashima, T. (1960). Factors influencing the reaction between ammonia and soil organic matter. *Transactions of 7th International Congress of Soil Science* 2, 509-516.
- Buchwald, C., and Casciotti, K.L. (2010). Oxygen isotopic fractionation and exchange during bacterial nitrite oxidation. *Limnology and Oceanography* 55, 1064-1074.
- Bugg, T.D.H., Ahmad, M., Hardiman, E.M., and Rahmanpour, R. (2011a). Pathways for degradation of lignin in bacteria and fungi. *Natural Product Reports* 28, 1883-1896.
- Bugg, T.D., Ahmad, M., Hardiman, E.M., and Singh, R. (2011b). The emerging role for bacteria in lignin degradation and bio-product formation. *Current Opinion in Biotechnology* 22, 394-400.
- Burke, I.C., Bontti, E.E., Barrett, J.E., Lowe, P.N., Lauenroth, W.K., and Riggle, R. (2013). Impact of labile and recalcitrant carbon treatments on available nitrogen and plant communities in a semiarid ecosystem. *Ecological Applications* 23, 537-545.
- Butterbach-Bahl, K., Baggs, E.M., Dannenmann, M., Kiese, R., and Zechmeister-Boltenstern, S. (2013). Nitrous oxide emissions from soils: How well do we understand the processes and their controls? *Philosophical Transactions of the Royal Society B-Biological Sciences* 368, 20130122.
- Cai, Z., Gao, S., Hendratna, A., Duan, Y., Xu, M., and Hanson, B.D. (2016). Key factors, soil nitrogen processes, and nitrite accumulation affecting nitrous oxide emissions. *Soil Science Society of America Journal* 80, 1560-1571.
- Cassman, K.G., Peng, S., Olk, D.C., Ladha, J.K., Reichardt, W., Dobermann, A., and Singh, U. (1998).

- Opportunities for increased nitrogen-use efficiency from improved resource management in irrigated rice systems. *Field Crops Research* 56, 7-39.
- Chalk, P.M., and Smith, C.J. (1983). Chemodenitrification. In *Gaseous loss of nitrogen from plant-soil systems*, Developments in Plant and Soil Sciences. J.R. Freney, and J.R. Simpson, eds. Springer, Dordrecht, Netherlands 9, 65-89.
- Chen, H., Li, X., Hu, F., and Shi, W. (2013). Soil nitrous oxide emissions following crop residue addition: A meta-analysis. *Global Change Biology* 19, 2956-2964.
- Christoforidis, K.C., Un, S., and Deligiannakis, Y. (2010). Effect of metal ions on the indigenous radicals of humic acids: High field electron paramagnetic resonance study. *Environmental Science & Technology* 44, 7011-7016.
- Cleveland, C.C., Townsend, A.R., Schimel, D.S., Fisher, H., Howarth, R.W., Hedin, L.O., Perakis, S.S., Latty, E.F., Von Fischer, J.C., Elseroad, A., *et al.* (1999). Global patterns of terrestrial biological nitrogen (N₂) fixation in natural ecosystems. *Global Biogeochemical Cycles* 13, 623-645.
- Colman, B.P. (2010). Understanding and eliminating iron interference in colorimetric nitrate and nitrite analysis. *Environmental Monitoring and Assessment* 165, 633-641.
- Colman, B.P., Fierer, N., and Schimel, J.P. (2007). Abiotic nitrate incorporation in soil: Is it real? *Biogeochemistry* 84, 161-169.
- Colman, B.P., Fierer, N., and Schimel, J.P. (2008). Abiotic nitrate incorporation, anaerobic microsites, and the ferrous wheel. *Biogeochemistry* 91, 223-227.
- Coplen, T.B. (2011). Guidelines and recommended terms for expression of stable-isotope-ratio and gas-ratio measurement results. *Rapid Communications in Mass Spectrometry* 25, 2538-2560.
- Corre, M.D., Brumme, R., Veldkamp, E., and Beese, F.O. (2007). Changes in nitrogen cycling and retention processes in soils under spruce forests along a nitrogen enrichment gradient in germany. *Global Change Biology* 13, 1509-1527.
- Cruz, C., Bio, A.M.F., Jullioti, A., Tavares, A., Dias, T., and Martins-Loução, M.A. (2008). Heterogeneity of soil surface ammonium concentration and other characteristics, related to plant specific variability in a mediterranean-type ecosystem. *Environmental Pollution* 154, 414-423.
- Cucu, M.A., Said-Pullicino, D., Maurino, V., Bonifacio, E., Romani, M., and Celi, L. (2014). Influence of redox conditions and rice straw incorporation on nitrogen availability in fertilized paddy soils. *Biology and Fertility of Soils* 50, 755-764.
- Dail, D.B., Davidson, E.A., and Chorover, J. (2001). Rapid abiotic transformation of nitrate in an acid forest soil. *Biogeochemistry* 54, 131-146.
- Dashtban, M., Schraft, H., Syed, T.A., and Qin, W. (2010). Fungal biodegradation and enzymatic modification of lignin. *International Journal of Biochemistry and Molecular Biology* 1, 36-50.
- Davidson, E.A., Chorover, J., and Dail, D.B. (2003). A mechanism of abiotic immobilization of nitrate in

- forest ecosystems: The ferrous wheel hypothesis. *Global Change Biology* 9, 228-236.
- Davidson, E.A., and Janssens, I.A. (2006). Temperature sensitivity of soil carbon decomposition and feedbacks to climate change. *Nature* 440, 165-173.
- De la Rosa, J.M., and Knicker, H. (2011). Bioavailability of n released from N-rich pyrogenic organic matter: An incubation study. *Soil Biology and Biochemistry* 43, 2368-2373.
- De la Rosa, J.M., Liebner, F., Pour, G., and Knicker, H. (2013). Partitioning of N in growing plants, microbial biomass and soil organic matter after amendment of n-ammonoxidized lignins. *Soil Biology and Biochemistry* 60, 125-133.
- Decock, C., and Six, J. (2013). How reliable is the intramolecular distribution of ^{15}N in N_2O to source partition N_2O emitted from soil? *Soil Biology and Biochemistry* 65, 114-127.
- Dela Cruz, A.L.N., Gehling, W., Lomnicki, S., Cook, R., and Dellinger, B. (2011). Detection of environmentally persistent free radicals at a superfund wood treating site. *Environmental science & technology* 45, 6356-6365.
- Delon, C., Mougín, E., Serça, D., Grippa, M., Hiernaux, P., Diawara, M., Galy-Lacaux, C., and Kergoat, L. (2015). Modelling the effect of soil moisture and organic matter degradation on biogenic no emissions from soils in sahel rangeland (Mali). *Biogeosciences* 12, 3253-3272.
- Dias, T., Oakley, S., Alarcón-Gutiérrez, E., Ziarelli, F., Trindade, H., Martins-Loução, M.A., Sheppard, L., Ostle, N., and Cruz, C. (2013). N-driven changes in a plant community affect leaf-litter traits and may delay organic matter decomposition in a mediterranean maquis. *Soil Biology and Biochemistry* 58, 163-171.
- Eisenlord, S.D., and Zak, D.R. (2010). Simulated atmospheric nitrogen deposition alters actinobacterial community composition in forest soils. *Soil Science Society of America Journal* 74, 1157-1166.
- Faix, O. (1991). Classification of lignins from different botanical origins by FT-IR spectroscopy. In *Holzforchung - International Journal of the Biology, Chemistry, Physics and Technology of Wood*, 21.
- FAO (2015). Current world fertilizer trends and outlook to 2018. Food and Agriculture Organization of the United Nations (FAO), Rome, Italy.
- Fehling, C. (2012). Mechanistic insights from the ^{15}N -site preference of nitrous oxide utilizing high resolution near-infrared cw cavity ringdown spectroscopy and density functional theory calculations. PhD thesis, Kiel University, Germany.
- Fehling, C., and Friedrichs, G. (2011). Dimerization of HNO in aqueous solution: An interplay of solvation effects, fast acid–base equilibria, and intramolecular hydrogen bonding? *Journal of the American Chemical Society* 133, 17912-17922.
- Fillery, I.R.P. (1983). Biological denitrification. In *Gaseous loss of nitrogen from plant-soil systems*, J.R.

- Freney, and J.R. Simpson, eds. Springer, Dordrecht, Netherlands 33-64.
- Firestone, M.K., and Davidson, E.A., eds. (1989). Microbiological basis of NO and N₂O production and consumption in soil. Wiley, New York 47, 7-21.
- Firestone, M.K., Smith, M.S., Firestone, R.B., and Tiedje, J.M. (1979). The influence of nitrate, nitrite, and oxygen on the composition of the gaseous products of denitrification in soil. *Soil Science Society of America Journal* 43, 1140-1144.
- Fitzhugh, R.D., Christenson, L.M., and Lovett, G.M. (2003a). The fate of ¹⁵NO₂⁻ tracer in soils under different tree species of the catskill mountains, new york. *Soil Science Society of America Journal* 67, 1257-1265.
- Fitzhugh, R.D., Lovett, G.M., and Venterea, R.T. (2003b). Biotic and abiotic immobilization of ammonium, nitrite, and nitrate in soils developed under different tree species in the catskill mountains, New York, USA. *Global Change Biology* 9, 1591-1601.
- Fitzpatrick, J.D., and Steelink, C. (1969). Benzosemiquinone radicals in alkaline solutions of hardwood lignins. *Tetrahedron Letters* 10, 5041-5044.
- Fontaine, S., Barot, S., Barre, P., Bdioui, N., Mary, B., and Rumpel, C. (2007). Stability of organic carbon in deep soil layers controlled by fresh carbon supply. *Nature* 450, 277-280.
- Frame, C.H., and Casciotti, K.L. (2010). Biogeochemical controls and isotopic signatures of nitrous oxide production by a marine ammonia-oxidizing bacterium. *Biogeosciences* 7, 2695-2709.
- Frimpong, K.A., and Baggs, E.M. (2010). Do combined applications of crop residues and inorganic fertilizer lower emission of N₂O from soil? *Soil Use and Management* 26, 412-424.
- Galloway, J.N., Townsend, A.R., Erisman, J.W., Bekunda, M., Cai, Z., Freney, J.R., Martinelli, L.A., Seitzinger, S.P., and Sutton, M.A. (2008). Transformation of the nitrogen cycle: Recent trends, questions, and potential solutions. *Science* 320, 889-892.
- Garcia-Ruiz, R., and Baggs, E.M. (2007). N₂O emission from soil following combined application of fertiliser-N and ground weed residues. *Plant and Soil* 299, 263-274.
- García-Ruiz, R., Gómez-Muñoz, B., Hatch, D.J., Bol, R., and Baggs, E.M. (2012). Soil mineral N retention and N₂O emissions following combined application of ¹⁵N-labelled fertiliser and weed residues. *Rapid Communications in Mass Spectrometry* 26, 2379-2385.
- Gentile, R., Vanlauwe, B., Chivenge, P., and Six, J. (2008). Interactive effects from combining fertilizer and organic residue inputs on nitrogen transformations. *Soil Biology and Biochemistry* 40, 2375-2384.
- Ghosh, K., and Schnitzer, M. (1980). Effects of pH and neutral electrolyte concentration on free radicals in humic substances. *Soil Science Society of America Journal* 44, 975-978.
- Giles, M., Morley, N., Baggs, E.M., and Daniell, T.J. (2012). Soil nitrate reducing processes drivers, mechanisms for spatial variation, and significance for nitrous oxide production. *Frontiers in*

- Microbiology 3, 407.
- Gillespie, A.W., Diochon, A., Ma, B.L., Morrison, M.J., Kellman, L., Walley, F.L., Regier, T.Z., Chevrier, D., Dynes, J.J., and Gregorich, E.G. (2014). Nitrogen input quality changes the biochemical composition of soil organic matter stabilized in the fine fraction: A long-term study. *Biogeochemistry* 117, 337-350.
- Gillespie, A.W., Walley, F.L., Farrell, R.E., Leinweber, P., Schlichting, A., Eckhardt, K.U., Regier, T.Z., and Blyth, R.I.R. (2009). Profiling rhizosphere chemistry: Evidence from carbon and nitrogen k-edge XANES and pyrolysis-fims. *Soil Science Society of America Journal* 73, 2002-2012.
- Gondar, D., Lopez, R., Fiol, S., Antelo, J.M., and Arce, F. (2005). Characterization and acid-base properties of fulvic and humic acids isolated from two horizons of an ombrotrophic peat bog. *Geoderma* 126, 367-374.
- Goutelle, S., Maurin, M., Rougier, F., Barbaut, X., Bourguignon, L., Ducher, M., and Maire, P. (2008). The hill equation: A review of its capabilities in pharmacological modelling. *Fundamental & Clinical Pharmacology* 22, 633-648.
- Gruber, N., and Galloway, J.N. (2008). An earth-system perspective of the global nitrogen cycle. *Nature* 451, 293-296.
- Gubry-Rangin, C., Béna, G., Cleyet-Marel, J.C., and Brunel, B. (2013). Definition and evolution of a new symbiovar, sv. *Rigiduloides*, among *Ensifer meliloti* efficiently nodulating *Medicago* species. *Systematic and Applied Microbiology* 36, 490-496.
- Hadas, A., Kautsky, L., Goek, M., and Erman Kara, E. (2004). Rates of decomposition of plant residues and available nitrogen in soil, related to residue composition through simulation of carbon and nitrogen turnover. *Soil Biology and Biochemistry* 36, 255-266.
- Hauck, R.D., and Stephenson, H.F. (1965). Nitrogen sources, nitrification of nitrogen fertilizers. Effect of nitrogen source, size and pH of granule, and concentration. *Journal of Agricultural and Food Chemistry* 13, 486-492.
- Have, R., and Teunissen, P.J. (2001). Oxidative mechanisms involved in lignin degradation by white-rot fungi. *Chemical Reviews* 101, 3397-3413.
- Hedges, J.I., Blanchette, R.A., Weliky, K., and Devol, A.H. (1988). Effects of fungal degradation on the *in situ* oxidation products of lignin: A controlled laboratory study. *Geochimica et Cosmochimica Acta* 52, 2717-2726.
- Hedges, J.I., and Ertel, J.R. (1982). Characterization of lignin by gas capillary chromatography of cupric oxide oxidation products. *Analytical Chemistry* 54, 174-178.
- Heil, J., Liu, S., Vereecken, H., and Brüggemann, N. (2015). Abiotic nitrous oxide production from hydroxylamine in soils and their dependence on soil properties. *Soil Biology and Biochemistry* 84, 107-115.

- Heil, J., Vereecken, H., and Brüggemann, N. (2016). A review of chemical reactions of nitrification intermediates and their role in nitrogen cycling and nitrogen trace gas formation in soil. *European Journal of Soil Science* 67, 23-39.
- Heil, J., Wolf, B., Brüggemann, N., Emmenegger, L., Tuzson, B., Vereecken, H., and Mohn, J. (2014). Site-specific ^{15}N isotopic signatures of abiotically produced N_2O . *Geochimica et Cosmochimica Acta* 139, 72-82.
- Hernandez-Ortega, A., Ferreira, P., and Martinez, A.T. (2012). Fungal aryl-alcohol oxidase: A peroxide-producing flavoenzyme involved in lignin degradation. *Applied Microbiology and Biotechnology* 93, 1395-1410.
- Homyak, P.M., Vasquez, K.T., Sickman, J.O., Parker, D.R., and Schimel, J.P. (2015). Improving nitrite analysis in soils: Drawbacks of the conventional 2 M KCl extraction. *Soil Science Society of America Journal* 79, 1237-1242.
- Huang, Y., Zou, J., Zheng, X., Wang, Y., and Xu, X. (2004). Nitrous oxide emissions as influenced by amendment of plant residues with different C:N ratios. *Soil Biology and Biochemistry* 36, 973-981.
- Huber, B., Bernasconi, S.M., Pannatier, E.G., and Luster, J. (2012). A simple method for the removal of dissolved organic matter and $\delta^{15}\text{N}$ analysis of NO_3^- from freshwater. *Rapid Communications in Mass Spectrometry* 26, 1475-1480.
- Ibrahim, E., Harris, E., Eyer, S., Tuzson, B., Emmenegger, L., Six, J., and Mohn, J. (2017). Development of a field-deployable method for simultaneous, real-time measurements of the four most abundant N_2O isotopocules. *Isotopes in Environmental and Health Studies*, 1-15.
- IFA, F.a. (2001). Global estimates of gaseous emissions of NH_3 , NO and N_2O from agricultural land. and International Fertilizer Industry Association (IFA) and Food and Agriculture Organization of the United Nations (FAO), Rome, Italy.
- IPCC (2013). *Climate change 2013: The physical science basis. Contribution of working group I to the fifth assessment report of the intergovernmental panel on climate change* (Cambridge, United Kingdom and New York, NY, USA: Cambridge University Press).
- Islam, A., Chen, D., White, R.E., and Weatherley, A. (2008). Chemical decomposition and fixation of nitrite in acidic pasture soils and implications for measurement of nitrification. *Soil Biology & Biochemistry* 40, 262-265.
- ISO (2005). *ISO 10390:2005 Soil quality—determination of pH* (International Organization for Standardization).
- Isobe, K., Koba, K., Suwa, Y., Ikutani, J., Kuroiwa, M., Fang, Y., Yoh, M., Mo, J., Otsuka, S., and Senoo, K. (2012). Nitrite transformations in an N-saturated forest soil. *Soil Biology & Biochemistry* 52, 61-63.

- Jerzykiewicz, M., Jezierski, A., Czechowski, F., and Drozd, J. (2002). Influence of metal ions binding on free radical concentration in humic acids. A quantitative electron paramagnetic resonance study. *Organic Geochemistry* *33*, 265-268.
- Johansson, G. (1998). Chemical fixation of ammonia to soil organic matter after application of urea. *Acta Agriculturae Scandinavica, Section B—Soil & Plant Science* *48*, 73-78.
- Johansson, K., Gillgren, T., Winstrand, S., Jarnstrom, L., and Jonsson, L.J. (2014). Comparison of lignin derivatives as substrates for laccase-catalyzed scavenging of oxygen in coatings and films. *Journal of Biological Engineering* *8*, 1.
- Johnson, D.W., Cheng, W., and Burke, I.C. (2000). Biotic and abiotic nitrogen retention in a variety of forest soils. *Soil Science Society of America Journal* *64*, 1503-1514.
- Jones, L.C., Peters, B., Pacheco, J.S.L., Casciotti, K.L., and Fendorf, S. (2015). Stable isotopes and iron oxide mineral products as markers of chemodenitrification. *Environmental Science & Technology* *49*, 3444-3452.
- Jung, M.Y., Well, R., Min, D., Giesemann, A., Park, S.J., Kim, J.G., Kim, S.J., and Rhee, S.K. (2014). Isotopic signatures of N₂O produced by ammonia-oxidizing archaea from soils. *The ISME Journal* *8*, 1115-1125.
- Justice, J.K., and Smith, R.L. (1962). Nitrification of ammonium sulfate in a calcareous soil as influenced by combinations of moisture, temperature, and levels of added nitrogen. *Soil Science Society of America Journal* *26*, 246-250.
- Kainz, G., and Huber, H. (1959). Zur kenntnis der reaktionen, die bei der aminostickstoffbestimmung anomale resultate verursachen. Die anomalie der isonitrosoverbindungen. *Microchimica Acta* *47*, 337-345.
- Kaiser, J. (2002). Stable isotope investigations of atmospheric nitrous oxide. PhD thesis, In Fachbereich Chemie, Johannes Gutenberg-Universität, Mainz, Germany.
- Kaiser, J., Röckmann, T., and Brenninkmeijer, C.A.M. (2003). Complete and accurate mass spectrometric isotope analysis of tropospheric nitrous oxide. *Journal of Geophysical Research: Atmospheres* *108* (D15), 4476.
- Kalbitz, K., Solinger, S., Park, J.H., Michalzik, B., and Matzner, E. (2000). Controls on the dynamics of dissolved organic matter in soils: A review. *Soil Science* *165*, 277-304.
- Kennedy, I.R., Choudhury, A.T.M.A., and Kecskés, M.L. (2004). Non-symbiotic bacterial diazotrophs in crop-farming systems: Can their potential for plant growth promotion be better exploited? *Soil Biology and Biochemistry* *36*, 1229-1244.
- Kholdebarin, B., and Oertli, J.J. (1994). Nitrification: Interference by phenolic compounds. *Journal of Plant Nutrition* *17*, 1827-1837.
- Kiem, R., and Kögel-Knabner, I. (2003). Contribution of lignin and polysaccharides to the refractory

- carbon pool in C-depleted arable soils. *Soil Biology and Biochemistry* **35**, 101-118.
- Kikugawa, K., and Kato, T. (1988). Formation of a mutagenic diazoquinone by interaction of phenol with nitrite. *Food and Chemical Toxicology* **26**, 209-214.
- Knicker, H. (2011a). Solid state cpmas ^{13}C and ^{15}N NMR spectroscopy in organic geochemistry and how spin dynamics can either aggravate or improve spectra interpretation. *Organic Geochemistry* **42**, 867-890.
- Knicker, H. (2011b). Soil organic N - an under-rated player for C sequestration in soils? *Soil Biology and Biochemistry* **43**, 1118-1129.
- Kögel-Knabner, I., Zech, W., and Hatcher, P.G. (1988). Chemical composition of the organic matter in forest soils: The humus layer. *Zeitschrift für Pflanzenernährung und Bodenkunde* **151**, 331-340.
- Kool, D.M., Wrage, N., Oenema, O., Dolfing, J., and Van Groenigen, J.W. (2007). Oxygen exchange between (de)nitrification intermediates and H_2O and its implications for source determination of NO_3^- and N_2O : A review. *Rapid Commun Mass Spectrom* **21**, 3569-3578.
- Kool, D.M., Wrage, N., Oenema, O., Harris, D., and Van Groenigen, J.W. (2009). The ^{18}O signature of biogenic nitrous oxide is determined by O exchange with water. *Rapid Commun Mass Spectrom* **23**, 104-108.
- Kool, D.M., Wrage, N., Oenema, O., Van Kessel, C., and Van Groenigen, J.W. (2011). Oxygen exchange with water alters the oxygen isotopic signature of nitrate in soil ecosystems. *Soil Biology and Biochemistry* **43**, 1180-1185.
- Kozłowski, J.A., Stieglmeier, M., Schleper, C., Klotz, M.G., and Stein, L.Y. (2016). Pathways and key intermediates required for obligate aerobic ammonia-dependent chemolithotrophy in bacteria and thaumarchaeota. *The ISME Journal* **10**, 1836-1845.
- Lado-Monserrat, L., Lull, C., Bautista, I., Lidón, A., and Herrera, R. (2014). Soil moisture increment as a controlling variable of the “birch effect”. Interactions with the pre-wetting soil moisture and litter addition. *Plant and Soil* **379**, 21-34.
- Langley, J.A., and Megonigal, J.P. (2010). Ecosystem response to elevated CO_2 levels limited by nitrogen-induced plant species shift. *Nature* **466**, 96-99.
- Leinweber, P., Walley, F., Kruse, J., Jandl, G., Eckhardt, K.U., Blyth, R.I.R., and Regier, T. (2009). Cultivation affects soil organic nitrogen: Pyrolysis-mass spectrometry and nitrogen k-edge XANES spectroscopy evidence. *Soil Science Society of America Journal* **73**, 82-92.
- Levy-Booth, D.J., Prescott, C.E., and Grayston, S.J. (2014). Microbial functional genes involved in nitrogen fixation, nitrification and denitrification in forest ecosystems. *Soil Biology & Biochemistry* **75**, 11-25.
- Lewicka-Szczebak, D., Augustin, J., Giesemann, A., and Well, R. (2017). Quantifying N_2O reduction to N_2 based on N_2O isotopocules – validation with independent methods (helium incubation and

- ¹⁵N gas flux method). *Biogeosciences* *13*, 711-732.
- Lewicka-Szczebak, D., Dyckmans, J., Kaiser, J., Marca, A., Augustin, J., and Well, R. (2016). Oxygen isotope fractionation during N₂O production by soil denitrification. *Biogeosciences* *13*, 1129-1144.
- Lewicka-Szczebak, D., Well, R., Bol, R., Gregory, A.S., Matthews, G.P., Misselbrook, T., Whalley, W.R., and Cardenas, L.M. (2015). Isotope fractionation factors controlling isotopocule signatures of soil-emitted N₂O produced by denitrification processes of various rates. *Rapid Communications in Mass Spectrometry* *29*, 269-282.
- Lewis, D.B., and Kaye, J.P. (2012). Inorganic nitrogen immobilization in live and sterile soil of old-growth conifer and hardwood forests: Implications for ecosystem nitrogen retention. *Biogeochemistry* *111*, 169-186.
- Li, C., Aber, J., Stange, F., Butterbach-Bahl, K., and Papen, H. (2000). A process-oriented model of N₂O and NO emissions from forest soils: 1. Model development. *Journal of Geophysical Research: Atmospheres* *105*, 4369-4384.
- Liu, C., Yao, Z., Wang, K., and Zheng, X. (2015). Effects of increasing fertilization rates on nitric oxide emission and nitrogen use efficiency in low carbon calcareous soil. *Agriculture, Ecosystems & Environment* *203*, 83-92.
- Liu, S.R., Vereecken, H., and Bruggemann, N. (2014). A highly sensitive method for the determination of hydroxylamine in soils. *Geoderma* *232*, 117-122.
- Long, A., Song, B., Fridley, K., and Silva, A. (2015). Detection and diversity of copper containing nitrite reductase genes (NirK) in prokaryotic and fungal communities of agricultural soils. *FEMS Microbiology Ecology* *91*, 1-9.
- Ma, L., Shan, J., and Yan, X. (2015). Nitrite behavior accounts for the nitrous oxide peaks following fertilization in a fluvo-aquic soil. *Biology and Fertility of Soils* *51*, 563-572.
- Maeda, K., Spor, A., Edel-Hermann, V., Heraud, C., Breuil, M.C., Bizouard, F., Toyoda, S., Yoshida, N., Steinberg, C., and Philippot, L. (2015). N₂O production, a widespread trait in fungi. *Scientific Reports* *5*, 9697.
- Maharjan, B., and Venterea, R.T. (2013). Nitrite intensity explains N management effects on N₂O emissions in maize. *Soil Biology and Biochemistry* *66*, 229-238.
- Mahieu, N., Olk, D.C., and Randall, E.W. (2000). Accumulation of heterocyclic nitrogen in humified organic matter: A ¹⁵N-NMR study of lowland rice soils. *European Journal of Soil Science* *51*, 379-389.
- Medinets, S., Skiba, U., Rennenberg, H., and Butterbach-Bahl, K. (2015). A review of soil NO transformation: Associated processes and possible physiological significance on organisms. *Soil Biology & Biochemistry* *80*, 92-117.

- Millar, N., and Baggs, E.M. (2004). Chemical composition, or quality, of agroforestry residues influences N₂O emissions after their addition to soil. *Soil Biology & Biochemistry* 36, 935-943.
- Millar, N., and Baggs, E.M. (2005). Relationships between N₂O emissions and water-soluble C and N contents of agroforestry residues after their addition to soil. *Soil Biology & Biochemistry* 37, 605-608.
- Millar, N., Ndufa, J.K., Cadisch, G., and Baggs, E.M. (2004). Nitrous oxide emissions following incorporation of improved-fallow residues in the humid tropics. *Global Biogeochemical Cycles* 18, GB1032.
- Mohn, J., Wolf, B., Toyoda, S., Lin, C.T., Liang, M.C., Bruggemann, N., Wissel, H., Steiker, A.E., Dyckmans, J., Szvec, L., *et al.* (2014). Interlaboratory assessment of nitrous oxide isotopomer analysis by isotope ratio mass spectrometry and laser spectroscopy: Current status and perspectives. *Rapid Communications in Mass Spectrometry* 28, 1995-2007.
- Mooshammer, M., Wanek, W., Hämmerle, I., Fuchslueger, L., Hofhansl, F., Knoltsch, A., Schnecker, J., Takriti, M., Watzka, M., Wild, B., *et al.* (2014). Adjustment of microbial nitrogen use efficiency to carbon:nitrogen imbalances regulates soil nitrogen cycling. *Nature Communications* 5, 3694.
- Morales, S.E., Cosart, T., and Holben, W.E. (2010). Bacterial gene abundances as indicators of greenhouse gas emission in soils. *The ISME Journal* 4, 799-808.
- Müller, C., Laughlin, R.J., Spott, O., and Rütting, T. (2014). Quantification of N₂O emission pathways via a ¹⁵N tracing model. *Soil Biology and Biochemistry* 72, 44-54.
- Mulvaney, R.L., Khan, S.A., Stevens, W.B., and Mulvaney, C.S. (1997). Improved diffusion methods for determination of inorganic nitrogen in soil extracts and water. *Biology and Fertility of Soils* 24, 413-420.
- Mutuo, P.K., Shepherd, K.D., Albrecht, A., and Cadisch, G. (2006). Prediction of carbon mineralization rates from different soil physical fractions using diffuse reflectance spectroscopy. *Soil Biology and Biochemistry* 38, 1658-1664.
- Nelson, D.W. (1967). Chemical transformations of nitrite in soils. PhD thesis, Iowa State University, US.
- Nelson, D.W., and Bremner, J.M. (1970). Gaseous products of nitrite decomposition in soils. *Soil Biology and Biochemistry* 2, 203-IN208.
- Nierop, K.G.J., and Filley, T.R. (2007). Assessment of lignin and (poly-)phenol transformations in oak (*Quercus robur*) dominated soils by ¹³C-TMAH thermochemistry. *Organic Geochemistry* 38, 551-565.
- Nömmik, H. (1970). Non-exchangeable binding of ammonium and amino nitrogen by norway spruce raw humus. *Plant and Soil* 33, 581-595.
- Obayashi, E., Takahashi, S., and Shiro, Y. (1998). Electronic structure of reaction intermediate of

- cytochrome p450nor in its nitric oxide reduction. *Journal of the American Chemical Society* *120*, 12964-12965.
- Opuwariboi, E., and Odu, C.T.I. (1975). Fixed ammonium in nigerian soils. *Journal of Soil Science* *26*, 358-363.
- Ostrom, N.E., Gandhi, H., Trubl, G., and Murray, A.E. (2016). Chemodenitrification in the cryoecosystem of Lake Vida, Victoria Valley, Antarctica. *Geobiology* *14*, 575-587.
- Ostrom, N.E., Pitt, A., Sutka, R., Ostrom, P.H., Grandy, A.S., Huizinga, K.M., and Robertson, G.P. (2007). Isotopologue effects during N₂O reduction in soils and in pure cultures of denitrifiers. *Journal of Geophysical Research: Biogeosciences* *112*, G02005.
- Ouyang, Y., Norton, J.M., Stark, J.M., Reeve, J.R., and Habteselassie, M.Y. (2016). Ammonia-oxidizing bacteria are more responsive than archaea to nitrogen source in an agricultural soil. *Soil Biology & Biochemistry* *96*, 4-15.
- Pauly, M., and Keegstra, K. (2008). Cell-wall carbohydrates and their modification as a resource for biofuels. *The Plant journal : for cell and molecular biology* *54*, 559-568.
- Peters, B., Casciotti, K.L., Samarkin, V.A., Madigan, M.T., Schutte, C.A., and Joye, S.B. (2014). Stable isotope analyses of NO₂⁻, NO₃⁻, and N₂O in the hypersaline ponds and soils of the McMurdo Dry Valleys, Antarctica. *Geochimica et Cosmochimica Acta* *135*, 87-101.
- Pilegaard, K. (2013). Processes regulating nitric oxide emissions from soils. *Philosophical Transactions of the Royal Society B-Biological Sciences* *368*, 20130126.
- Politzer, P., and Murray, J.S. (2008). Some intrinsic features of hydroxylamines, oximes and hydroxamic acids: Integration of theory and experiment. In *The chemistry of hydroxylamines, oximes and hydroxamic acids* (John Wiley & Sons, Ltd), pp. 1-27.
- Porter, L.K. (1969). Gaseous products produced by anaerobic reaction of sodium nitrite with oxime compounds and oximes synthesized from organic matter. *Soil Science Society of America Proceedings* *33*, 696-702.
- Prather, M.J., Hsu, J., DeLuca, N.M., Jackman, C.H., Oman, L.D., Douglass, A.R., Fleming, E.L., Strahan, S.E., Steenrod, S.D., Søvde, O.A., *et al.* (2015). Measuring and modeling the lifetime of nitrous oxide including its variability. *Journal of Geophysical Research: Atmospheres* *120*, 5693-5705.
- Purkhold, U., Pommerening-Röser, A., Juretschko, S., Schmid, M.C., Koops, H.P., and Wagner, M. (2000). Phylogeny of all recognized species of ammonia oxidizers based on comparative 16S rRNA and *amoA* sequence analysis: Implications for molecular diversity surveys. *Applied and Environmental Microbiology* *66*, 5368-5382.
- Rahman, M.M., Tsukamoto, J., Rahman, M.M., Yoneyama, A., and Mostafa, K.M. (2013). Lignin and its effects on litter decomposition in forest ecosystems. *Chemistry and Ecology* *29*, 540-553.
- Ravishankara, A.R., Daniel, J.S., and Portmann, R.W. (2009). Nitrous oxide (N₂O): The dominant

- ozone-depleting substance emitted in the 21st century. *Science* *326*, 123-125.
- Reigstad, L.J., Richter, A., Daims, H., Ulrich, T., Schwark, L., and Schleper, C. (2008). Nitrification in terrestrial hot springs of Iceland and Kamchatka. *FEMS Microbiology Ecology* *64*, 167-174.
- Rezaei Rashti, M., Wang, W.J., Reeves, S.H., Harper, S.M., Moody, P.W., and Chen, C.R. (2016). Linking chemical and biochemical composition of plant materials to their effects on N₂O emissions from a vegetable soil. *Soil Biology and Biochemistry* *103*, 502-511.
- Riordan, E., Minogue, N., Healy, D., O'Driscoll, P., and Sodeau, J.R. (2005). Spectroscopic and optimization modeling study of nitrous acid in aqueous solution. *The journal of physical chemistry A* *109*, 779-786.
- Rohe, L., Anderson, T.H., Braker, G., Flessa, H., Giesemann, A., Lewicka-Szczebak, D., Wrage-Mönnig, N., and Well, R. (2014). Dual isotope and isotopomer signatures of nitrous oxide from fungal denitrification – a pure culture study. *Rapid Communications in Mass Spectrometry* *28*, 1893-1903.
- Rousseau, B., and Rosazza, J.P.N. (1998). Reaction of ferulic acid with nitrite: Formation of 7-hydroxy-6-methoxy-1,2(4*H*)-benzoxazin-4-one. *Journal of Agricultural and Food Chemistry* *46*, 3314-3317.
- Russow, R., Stange, C.F., and Neue, H.U. (2009). Role of nitrite and nitric oxide in the processes of nitrification and denitrification in soil: Results from ¹⁵N tracer experiments. *Soil Biology and Biochemistry* *41*, 785-795.
- Said-Pullicino, D., Cucu, M.A., Sodano, M., Birk, J.J., Glaser, B., and Celi, L. (2014). Nitrogen immobilization in paddy soils as affected by redox conditions and rice straw incorporation. *Geoderma* *228*, 44-53.
- Santoro, A.E., Buchwald, C., McIlvin, M.R., and Casciotti, K.L. (2011). Isotopic signature of N₂O produced by marine ammonia-oxidizing archaea. *Science* *333*, 1282-1285.
- Saunders, D.L., and Kalff, J. (2001). Nitrogen retention in wetlands, lakes and rivers. *Hydrobiologia* *443*, 205-212.
- Schindlbacher, A., Zechmeister-Boltenstern, S., and Butterbach-Bahl, K. (2004). Effects of soil moisture and temperature on NO, NO₂, and N₂O emissions from European forest soils. *Journal of Geophysical Research: Atmospheres* *109*, D17302.
- Schmidt-Rohr, K., Mao, J.-D., and Olk, D.C. (2004). Nitrogen-bonded aromatics in soil organic matter and their implications for a yield decline in intensive rice cropping. *Proceedings of the National Academy of Sciences of the United States of America* *101*, 6351-6354.
- Schulten, H.R., Sorge, C., and Schnitzer, M. (1995). Structural studies on soil nitrogen by curie-point pyrolysis-gas chromatography/mass spectrometry with nitrogen-selective detection. *Biology and Fertility of Soils* *20*, 174-184.

- Senesi, N., Chen, Y., and Schnitzer, M. (1977). The role of free radicals in the oxidation and reduction of fulvic acid. *Soil Biology & Biochemistry* 9, 397-403.
- Senesi, N., and Schnitzer, M. (1977). Effects of pH, reaction time, chemical reduction and irradiation on ESR spectra of fulvic acid. *Soil Science* 123, 224-234.
- Shen, Q.R., Ran, W., and Cao, Z.H. (2003). Mechanisms of nitrite accumulation occurring in soil nitrification. *Chemosphere* 50, 747-753.
- Smolander, A., Kanerva, S., Adamczyk, B., and Kitunen, V. (2012). Nitrogen transformations in boreal forest soils-does composition of plant secondary compounds give any explanations? *Plant and Soil* 350, 1-26.
- Snider, D.M., Venkiteswaran, J.J., Schiff, S.L., and Spoelstra, J. (2012). Deciphering the oxygen isotope composition of nitrous oxide produced by nitrification. *Global Change Biology* 18, 356-370.
- Snider, D.M., Venkiteswaran, J.J., Schiff, S.L., and Spoelstra, J. (2015). From the ground up: Global nitrous oxide sources are constrained by stable isotope values. *PLoS ONE* 10, e0118954.
- Sobolev, I. (1961). Lignin model compounds. Nitric acid oxidation of 4-methylguaiacol. *The Journal of Organic Chemistry* 26, 5080-5085.
- Spott, O., Russow, R., and Stange, C.F. (2011). Formation of hybrid N₂O and hybrid N₂ due to codenitrification: First review of a barely considered process of microbially mediated N-nitrosation. *Soil Biology and Biochemistry* 43, 1995-2011.
- Spott, O., and Stange, C.F. (2011). Formation of hybrid N₂O in a suspended soil due to codenitrification of NH₂OH. *Journal of Plant Nutrition and Soil Science* 174, 554-567.
- Stahl, D.A., and de la Torre, J.R. (2012). Physiology and diversity of ammonia-oxidizing archaea. *Annual Review of Microbiology* 66, 83-101.
- Stange, F., Butterbach-Bahl, K., Papen, H., Zechmeister-Boltenstern, S., Li, C., and Aber, J. (2000). A process-oriented model of N₂O and NO emissions from forest soils: 2. Sensitivity analysis and validation. *Journal of Geophysical Research: Atmospheres* 105, 4385-4398.
- Steelink, C. (1964). Free radical studies of lignin, lignin degradation products and soil humic acids. *Geochimica et Cosmochimica Acta* 28, 1615-1622.
- Steen, W.C., and Stojanovic, B.J. (1971). Nitric oxide volatilization from a calcareous soil and model aqueous solutions. *Soil Science Society of America Journal* 35, 277-282.
- Stein, L.Y. (2011). Surveying N₂O-producing pathways in bacteria. *Methods in Enzymology* 486, 131-152.
- Steinkamp, J., Ganzeveld, L.N., Wilcke, W., and Lawrence, M.G. (2009). Influence of modelled soil biogenic NO emissions on related trace gases and the atmospheric oxidizing efficiency. *Atmos Chem Phys* 9, 2663-2677.
- Stevenson, F.J., Harrison, R.M., Wetselaa, R., and Leeper, R.A. (1970). Nitrosation of soil organic

- matter: III. Nature of gases produced by reaction of nitrite with lignins, humic substances, and phenolic constituents under neutral and slightly acidic conditions. *Soil Science Society of America Proceedings* 34, 430.
- Stevenson, F.J. (1995). *Humus chemistry: Genesis, composition, reactions*, second edition, Vol 72 (American Chemical Society).
- Stevenson, F.J., and Harrison, R.M. (1966). Nitrosation of soil organic matter: II. Gas chromatographic separation of gaseous products. *Soil Science Society of America Proceedings* 30, 609.
- Stevenson, F.J., and Swaby, R.J. (1964). Nitrosation of soil organic matter: I. Nature of gases evolved during nitrous acid treatment of lignins and humic substances. *Soil Science Society of American Journal* 28, 773-778.
- Stieglmeier, M., Mooshammer, M., Kitzler, B., Wanek, W., Zechmeister-Boltenstern, S., Richter, A., and Schleper, C. (2014). Aerobic nitrous oxide production through N-nitrosating hybrid formation in ammonia-oxidizing archaea. *The ISME Journal* 8, 1135-1146.
- Stolz, J.F., and Basu, P. (2002). Evolution of nitrate reductase: Molecular and structural variations on a common function. *ChemBiochem* 3, 198-206.
- Sutka, R.L., Adams, G.C., Ostrom, N.E., and Ostrom, P.H. (2008). Isotopologue fractionation during N₂O production by fungal denitrification. *Rapid Communications in Mass Spectrometry* 22, 3989-3996.
- Sutka, R.L., Ostrom, N.E., Ostrom, P.H., Breznak, J.A., Gandhi, H., Pitt, A.J., and Li, F. (2006). Distinguishing nitrous oxide production from nitrification and denitrification on the basis of isotopomer abundances. *Applied and Environmental Microbiology* 72, 638-644.
- Sutka, R.L., Ostrom, N.E., Ostrom, P.H., Gandhi, H., and Breznak, J.A. (2003). Nitrogen isotopomer site preference of N₂O produced by *Nitrosomonas europaea* and *Methylococcus capsulatus* bath. *Rapid Communications in Mass Spectrometry* 17, 738-745.
- Sutka, R.L., Ostrom, N.E., Ostrom, P.H., Gandhi, H., and Breznak, J.A. (2004). Nitrogen isotopomer site preference of N₂O produced by *Nitrosomonas europaea* and *Methylococcus capsulatus* bath. *Rapid Communications in Mass Spectrometry* 18, 1411-1412.
- Thorn, K.A., Arterburn, J.B., and Mikita, M.A. (1992). Nitrogen-15 and carbon-13 NMR investigation of hydroxylamine-derivatized humic substances. *Environmental Science & Technology* 26, 107-116.
- Thorn, K.A., and Cox, L.G. (2009). N-15 NMR spectra of naturally abundant nitrogen in soil and aquatic natural organic matter samples of the international humic substances society. *Organic Geochemistry* 40, 484-499.
- Thorn, K.A., and Cox, L.G. (2016). Nitrosation and nitration of fulvic acid, peat and coal with nitric acid. *Plos One* 11, e0154981.
- Thorn, K.A., and Mikita, M.A. (1992). Humic substances ammonia fixation by humic substances: A

- nitrogen-15 and carbon-13 NMR study. *Science of The Total Environment* **113**, 67-87.
- Thorn, K.A., and Mikita, M.A. (2000). Nitrite fixation by humic substances: Nitrogen-15 nuclear magnetic resonance evidence for potential intermediates in chemodenitrification. *Soil Science Society of America Journal* **64**, 568-582.
- Torres-Canabate, P., Davidson, E.A., Bulygina, E., Garcia-Ruiz, R., and Carreira, J.A. (2008). Abiotic immobilization of nitrate in two soils of relic *Abies pinsapo*-fir forests under Mediterranean climate. *Biogeochemistry* **91**, 1-11.
- Toyoda, S., Iwai, H., Koba, K., and Yoshida, N. (2009). Isotopomeric analysis of N₂O dissolved in a river in the Tokyo metropolitan area. *Rapid Communications in Mass Spectrometry* **23**, 809-821.
- Toyoda, S., Mutobe, H., Yamagishi, H., Yoshida, N., and Tanji, Y. (2005). Fractionation of N₂O isotopomers during production by denitrifier. *Soil Biology & Biochemistry* **37**, 1535-1545.
- Toyoda, S., Yano, M., Nishimura, S.I., Akiyama, H., Hayakawa, A., Koba, K., Sudo, S., Yagi, K., Makabe, A., Tobari, Y., *et al.* (2011). Characterization and production and consumption processes of N₂O emitted from temperate agricultural soils determined via isotopomer ratio analysis. *Global Biogeochemical Cycles* **25**, GB2008.
- Toyoda, S., and Yoshida, N. (1999). Determination of nitrogen isotopomers of nitrous oxide on a modified isotope ratio mass spectrometer. *Analytical Chemistry* **71**, 4711-4718.
- Toyoda, S., Yoshida, N., and Koba, K. (2015). Isotopocule analysis of biologically produced nitrous oxide in various environments. *Mass Spectrometry Reviews* **36**, 135-160.
- Toyoda, S., Yoshida, N., Miwa, T., Matsui, Y., Yamagishi, H., Tsunogai, U., Nojiri, Y., and Tsurushima, N. (2002). Production mechanism and global budget of N₂O inferred from its isotopomers in the western North Pacific. *Geophysical Research Letters* **29**, 7-1-7-4.
- Tyler, K.B., Broadbent, F.E., and Hill, G.N. (1959). Low-temperature effects on nitrification in four California soils. *Soil Science* **87**, 123-129.
- Vairavamurthy, A., and Wang, S. (2002). Organic nitrogen in geomacromolecules: Insights on speciation and transformation with k-edge XANES spectroscopy. *Environmental Science & Technology* **36**, 3050-3056.
- Van der Zee, F.P., and Cervantes, F.J. (2009). Impact and application of electron shuttles on the redox (bio)transformation of contaminants: A review. *Biotechnology Advances* **27**, 256-277.
- Vane, C.H., Drage, T.C., and Snape, C.E. (2003). Biodegradation of oak (*Quercus alba*) wood during growth of the shiitake mushroom (*Lentinula edodes*): A molecular approach. *Journal of Agricultural and Food Chemistry* **51**, 947-956.
- Vane, C.H., Drage, T.C., and Snape, C.E. (2006). Bark decay by the white-rot fungus *Lentinula edodes*: Polysaccharide loss, lignin resistance and the unmasking of suberin. *International Biodeterioration & Biodegradation* **57**, 14-23.

- Venterea, R.T. (2007). Nitrite-driven nitrous oxide production under aerobic soil conditions: Kinetics and biochemical controls. *Global Change Biology* 13, 1798-1809.
- Vranova, V., Zahradnickova, H., Janous, D., Skene, K.R., Matharu, A.S., Rejsek, K., and Formanek, P. (2012). The significance of D-amino acids in soil, fate and utilization by microbes and plants: Review and identification of knowledge gaps. *Plant and Soil* 354, 21-39.
- Watmough, N.J., Field, S.J., Hughes, R.J., and Richardson, D.J. (2009). The bacterial respiratory nitric oxide reductase. *Biochemical Society Transactions* 37, 392-399.
- Weber, J.H., and Wilson, S.A. (1975). The isolation and characterization of fulvic acid and humic acid from river water. *Water Research* 9, 1079-1084.
- Wei, J., Amelung, W., Lehdorff, E., Schloter, M., Vereecken, H., and Brüggemann, N. (2017a). N₂O and NO_x emissions by reactions of nitrite with soil organic matter of a norway spruce forest. *Biogeochemistry* 132, 325–342.
- Wei, J., Zhou, M., Vereecken, H., and Brüggemann, N. (2017b). Large variability of CO₂ and N₂O emissions and of ¹⁵N site preference of N₂O from reactions of nitrite with lignin and its derivatives at different pH. *Rapid Communications in Mass Spectrometry* 31, 1333-1343.
- Werle, P., Mucke, R., and Slemr, F. (1993). The limits of signal averaging in atmospheric trace-gas monitoring by tunable diode-laser absorption-spectroscopy (TDLAS). *Applied Physics B* 57, 131-139.
- WMO (2016). WMO greenhouse gas bulletin: The state of greenhouse gases in the atmosphere based on global observations through 2015 (Geneva: World Meteorological Organization).
- Wolf, B., Merbold, L., Decock, C., Tuzson, B., Harris, E., Six, J., Emmenegger, L., and Mohn, J. (2015). First on-line isotopic characterization of N₂O above intensively managed grassland. *Biogeosciences* 12, 2517-2531.
- Wolińska, A., Szafranek-Nakonieczna, A., Banach, A., Błaszczuk, M., and Stępniewska, Z. (2016). The impact of agricultural soil usage on activity and abundance of ammonifying bacteria in selected soils from poland. *SpringerPlus* 5, 565.
- Wrage, N., Velthof, G.L., van Beusichem, M.L., and Oenema, O. (2001). Role of nitrifier denitrification in the production of nitrous oxide. *Soil Biology and Biochemistry* 33, 1723-1732.
- Wu, D., Senbayram, M., Well, R., Brüggemann, N., Pfeiffer, B., Loick, N., Stempfhuber, B., Dittert, K., and Bol, R. (2017). Nitrification inhibitors mitigate N₂O emissions more effectively under straw-induced conditions favoring denitrification. *Soil Biology and Biochemistry* 104, 197-207.
- Wullstein, L.H., and Gilmour, C.M. (1964). Non-enzymatic gaseous loss of nitrite from clay and soil systems. *Soil Science* 97, 428-430.
- Wunderlin, P., Lehmann, M.F., Siegrist, H., Tuzson, B., Joss, A., Emmenegger, L., and Mohn, J. (2013). Isotope signatures of N₂O in a mixed microbial population system: Constraints on N₂O producing

- pathways in wastewater treatment. *Environmental Science & Technology* **47**, 1339-1348.
- Yamazaki, T., Hozuki, T., Arai, K., Toyoda, S., Koba, K., Fujiwara, T., and Yoshida, N. (2014). Isotopomeric characterization of nitrous oxide produced by reaction of enzymes extracted from nitrifying and denitrifying bacteria. *Biogeosciences* **11**, 2679-2689.
- Yang, H., Gandhi, H., Ostrom, N.E., and Hegg, E.L. (2014). Isotopic fractionation by a fungal p450 nitric oxide reductase during the production of N₂O. *Environmental Science & Technology* **48**, 10707-10715.
- Yoo, H., Ahn, K.H., Lee, H.J., Lee, K.H., Kwak, Y.J., and Song, K.G. (1999). Nitrogen removal from synthetic wastewater by simultaneous nitrification and denitrification (SND) via nitrite in an intermittently-aerated reactor. *Water Research* **33**, 145-154.
- Zacharias, S., Bogen, H., Samaniego, L., Mauder, M., Fuß, R., Pütz, T., Frenzel, M., Schwank, M., Baessler, C., Butterbach-Bahl, K., *et al.* (2011). A network of terrestrial environmental observatories in Germany. *Vadose Zone Journal* **10**, 955-973.
- Zhang, C., and Katayama, A. (2012). Humic acid as an electron mediator for microbial reductive dehalogenation. *Environmental Science & Technology* **46**, 6575-6583.
- Zhang, C., Zhang, D., Li, Z., Akatsuka, T., Yang, S., Suzuki, D., and Katayama, A. (2014). Insoluble Fe-humic acid complex as a solid-phase electron mediator for microbial reductive dechlorination. *Environmental Science & Technology* **48**, 6318-6325.
- Zhang, C., Zhang, D., Xiao, Z., Li, Z., Suzuki, D., and Katayama, A. (2015a). Characterization of humins from different natural sources and the effect on microbial reductive dechlorination of pentachlorophenol. *Chemosphere* **131**, 110-116.
- Zhang, D., Zhang, C., Xiao, Z., Suzuki, D., and Katayama, A. (2015b). Humic acid as an electron donor for enhancement of multiple microbial reduction reactions with different redox potentials in a consortium. *Journal of Bioscience and Bioengineering* **119**, 188-194.
- Zhang, J., Müller, C., and Cai, Z. (2015c). Heterotrophic nitrification of organic N and its contribution to nitrous oxide emissions in soils. *Soil Biology and Biochemistry* **84**, 199-209.
- Zhang, W., Li, Y., Xu, C., Li, Q., and Lin, W. (2016). Isotope signatures of N₂O emitted from vegetable soil: Ammonia oxidation drives N₂O production in NH₄⁺-fertilized soil of North China. *Scientific Reports* **6**, 29257.
- Zhu-Barker, X., Cavazos, A.R., Ostrom, N.E., Horwath, W.R., and Glass, J.B. (2015). The importance of abiotic reactions for nitrous oxide production. *Biogeochemistry* **126**, 251-267.
- Zhu, Z.L., and Chen, D.L. (2002). Nitrogen fertilizer use in China—contributions to food production, impacts on the environment and best management strategies. *Nutrient Cycling in Agroecosystems* **63**, 117-127.
- Zou, Y., Hirono, Y., Yanai, Y., Hattori, S., Toyoda, S., and Yoshida, N. (2014). Isotopomer analysis of

nitrous oxide accumulated in soil cultivated with tea (*Camellia sinensis*) in Shizuoka, Central Japan. *Soil Biology and Biochemistry* 77, 276-291.

Band / Volume 396

Coupled biotic-abiotic mechanisms of nitrous oxide production in soils during nitrification involving the reactive intermediates hydroxylamine and nitrite

S. Liu (2017), xvii, 148 pp

ISBN: 978-3-95806-272-6

Band / Volume 397

Mixed-phase and ice cloud observations with NIXE-CAPS

A. Costa (2017), xviii, 117 pp

ISBN: 978-3-95806-273-3

Band / Volume 398

Deposition Mechanisms of Thermal Barrier Coatings (TBCs) Manufactured by Plasma Spray-Physical Vapor Deposition (PS-PVD)

W. He (2017), ix, 162 pp

ISBN: 978-3-95806-275-7

Band / Volume 399

Carbonyl Sulfide in the Stratosphere: airborne instrument development and satellite based data analysis

C. Kloss (2017), vi, 84, 1-14 pp

ISBN: 978-3-95806-276-4

Band / Volume 400

Lagrangian transport of trace gases in the upper troposphere and lower stratosphere (UTLS)

P. Konopka (2017), 70 pp

ISBN: 978-3-95806-279-5

Band / Volume 401

Numerical Simulation of Plasma Spray-Physical Vapor Deposition

P. Wang (2017), IX, 127 pp

ISBN: 978-3-95806-282-5

Band / Volume 402

The Selective Separation of Am(III) from Highly Radioactive PUREX Raffinate

P. Kaufholz (2017), IV, 173 pp

ISBN: 978-3-95806-284-9

Band / Volume 403

Spatio-Temporal Estimation and Validation of Remotely Sensed Vegetation and Hydrological Fluxes in the Rur Catchment, Germany

M. Ali (2018), xvi, 116 pp

ISBN: 978-3-95806-287-0

Band / Volume 404

**Thermomechanical Characterization of Advanced
Ceramic Membrane Materials**

Y. Zou (2018), xvi, 168 pp
ISBN: 978-3-95806-288-7

Band / Volume 405

**Betrachtung der Kristallinitätsentwicklung in mikrokristallinem
Dünnschicht-Silizium mit in-situ Raman-Spektroskopie**

T. Fink (2018), XI, 166 pp
ISBN: 978-3-95806-289-4

Band / Volume 406

**Institute of Energy and Climate Research
IEK-6: Nuclear Waste Management
Report 2015 / 2016**

Material Science for Nuclear Waste Management
S. Neumeier, H. Tietze-Jaensch, D. Bosbach (Eds.)
(2018), 221 pp
ISBN: 978-3-95806-293-1

Band / Volume 407

Reduction properties of a model ceria catalyst at the microscopic scale

J. Hackl (2018), VIII, 98 pp
ISBN: 978-3-95806-294-8

Band / Volume 408

**Comparative Analysis of Infrastructures:
Hydrogen Fueling and Electric Charging of Vehicles**

M. Robinus, J. Linßen, T. Grube, M. Reuß, P. Stenzel, K. Syranidis,
P. Kuckertz and D. Stolten (2018), VII, 108 pp
ISBN: 978-3-95806-295-5

Band / Volume 409

**Reactions between nitrite and soil organic matter and their role in
nitrogen trace gas emissions and nitrogen retention in soil**

J. Wei (2018), XXII, 160 pp
ISBN: 978-3-95806-299-3

Weitere **Schriften des Verlags im Forschungszentrum Jülich** unter
<http://www.zbw1.fz-juelich.de/verlagextern1/index.asp>

Energie & Umwelt / Energy & Environment
Band / Volume 409
ISBN 978-3-95806-299-3

Mitglied der Helmholtz-Gemeinschaft

